UNIVERSITY OF
NEWCASTLE UPON TYNE

Development of Materials for Handling Hot Glass

by

H. M. Bishop

Materials Division
Department of Mechanical, Materials & Manufacturing Engineering

A Thesis submitted in partial fulfilment
of the requirements for the degree of
Doctor of Philosophy

1991

Contents

PREFACE

This thesis describes original work which has not been submitted for a degree at any other University. The investigations were carried out in the Materials Division of the Department of Mechanical, Materials and Manufacturing Engineering of the University of Newcastle upon Tyne, Great Britain, during the period of October 1987 to October 1990, under the supervision of Dr. H. W. Chandler.

Funding for the project was provided by SERC and Johnson Radley Ltd. Laboratory facilities were provided by Prof R.N.Parkins and Prof T.F.Page at The University of Newcastle upon Tyne.

ABSTRACT

For glass bottles to compete with plastic ones they need to be very much lighter. As their present weight is often constrained by their current strength, the glass they are made from needs to be very much stronger. In its virgin state glass is very strong, but handling bottles during manufacture introduces minute flaws, lowering their strength considerably.

The aim of this work has been to gain a greater understanding of the mechanisms of thermal and mechanical damage and so to improve existing, and develop new hot glass handling materials which will reduce the amount of damage to the glass during hot-end handling

To help gain an understanding of the interaction between thermal and mechanical damage mathematical modelling using finite difference techniques was utilised. Experimental investigations of how controlled contact, including thermal shock, weakened high strength glass were also undertaken. It was concluded from these investigations that the nearest to the ideal a real hot glass handling material could approach would be a material which produces mechanical damage which is limited to such a size that the thermal stresses produced by that material do not exacerbate the damage.

A dimensionless group was identified which helped to assess if a material had a selection of material properties which render it a likely hot glass handling material. Zirconium and Titanium were identified as possible hot glass handling materials.

Carbon based materials proved to be the best handling materials but they have a limited life as they suffer oxidation in use. The oxidation resistance of various Carbon based materials was investigated with thermal gravimetric analysis and a test was designed to assess the strength retention of laminated Carbon-Carbon composites. Various coatings were developed to increase the life of existing hot glass handling materials.

A Titanium/graphite composite was developed in which the Titanium acted as an oxidation resistant skeleton and the graphite provided optimum glass handling ability.

ACKNOWLEDGEMENTS

I would like to thank the following

- Dr Howard Chandler for his advice, encouragment, enthusiasm and support throughout this project.
- All the staff of the Materials Division of The Department of Mechanical, Materials and Manufacturing Engineering, especially Dr.J.T.Evans and Dr.D.P.Thompson for contributions to many informal discussions.
- All those at Johnson Radley Ltd. for sharing their deep knowledge of the glass industry with me and for supplying many of the sample materials.
- All the technicians in the Department especially Dave and Phil for their prompt preparation of apparatus and samples.
- My contemparies, especially Andrew, Brian, Freddie, Jos, Ray, Sarah and Teresa for their friendship over the last four years.
- Sarah again for proof reading this thesis.
- My Parents, Vanessa and Ian for their love and support.
- Robert for his assistance with all aspects of the preparation of this thesis and for always listening when the going got tough.

Chapter 1

INTRODUCTION

In recent years there has been considerable pressure to reduce the weight of glass containers to enable them to compete with other lighter packaging materials such as Aluminium, tinned metal cans, plastics and cardboard cartons. This can only be achieved if the strength of the container glass is increased so that they can be made lighter.

Containers are produced in modern glass works at rates approaching 600 a minute. (LeGood, 1988) They are manufactured on I.S.machines originally by the 'Blow and blow'† technique, which will now be outlined, followed by a review of the developments that have been made since the process was first introduced

1.1 Blow and blow process

Figure 1.1 is a schematic representation of the process. A pre-weighed piece of hot glass known as the 'gob' is dropped into the first 'blank' mould, made of cast iron, where the 'parison' is formed. This preform is then transferred to the 'blow' mould which is also usually made from cast iron. First the parison is reheated and this is followed by a second blow where the final form of the container is produced. The completed bottle is then lifted from the mould by the 'take out tongs' and placed onto the 'dead plate', (see Plate 1.1) from where the bottles are swept onto a conveyor belt. (Plate 1.2 shows the 'sweepout'.) Once on the conveyor the bottles are pushed and jostled, often under rough and dirty conditions (Williams, 1985) towards a tunnel furnace known as the 'lehr' where residual stresses resulting from forming are annealed out. The section of the production line from the take out position to the lehr mouth is known as the 'hot-end' as the container is still at approximately 300°C as it enters the lehr mouth. Figure 1.2 is a schematic representation of the hot end. From the point the bottle leaves the lehr at around

† Definitions of all the glass making terms used here are listed in Appendix A.

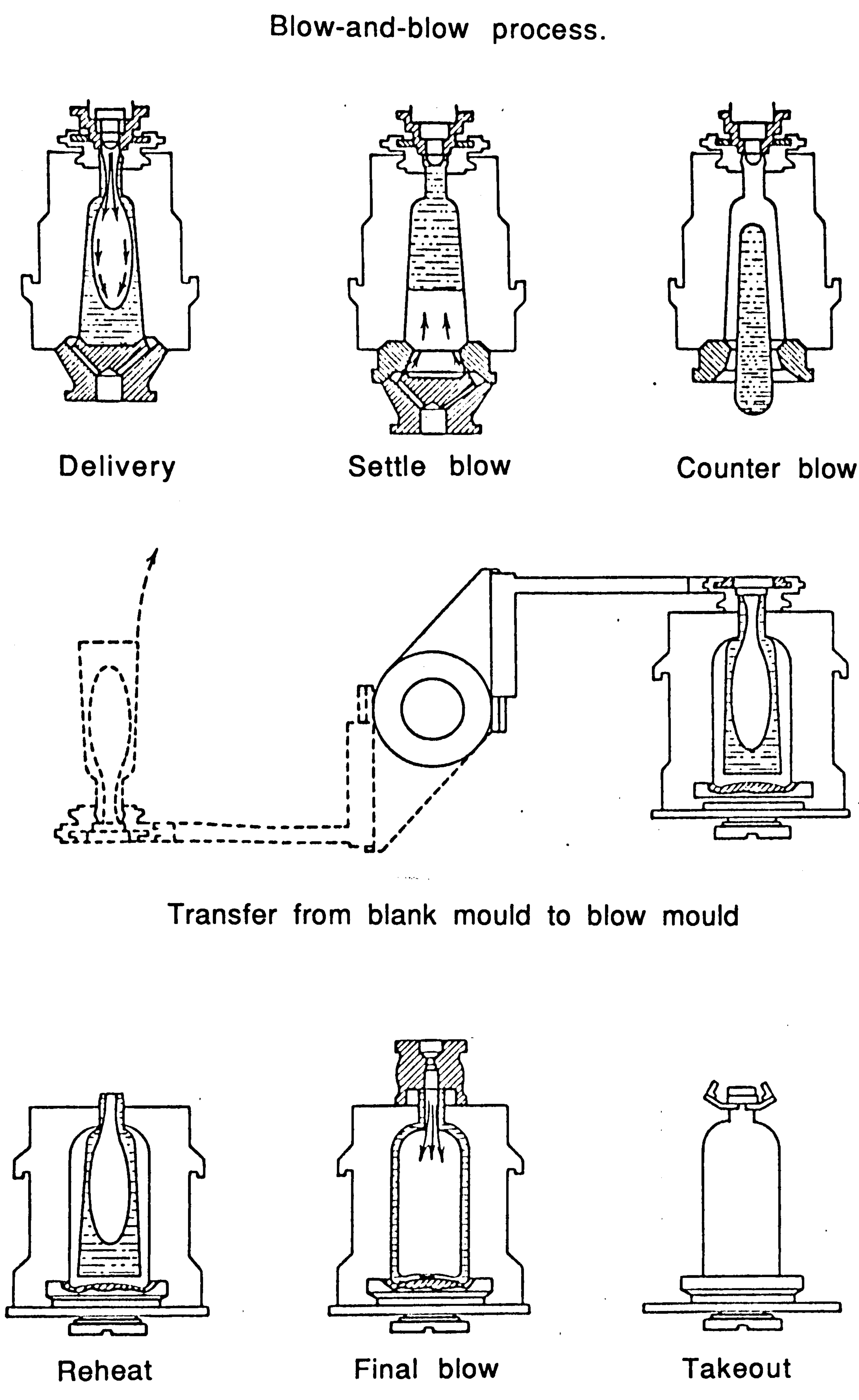

Figure 1.1 Schematic representation of the Blow-and-blow process for the production of glass containers.

Figure 1.2 Schematic representation of the Hot-end of a glass container production line.

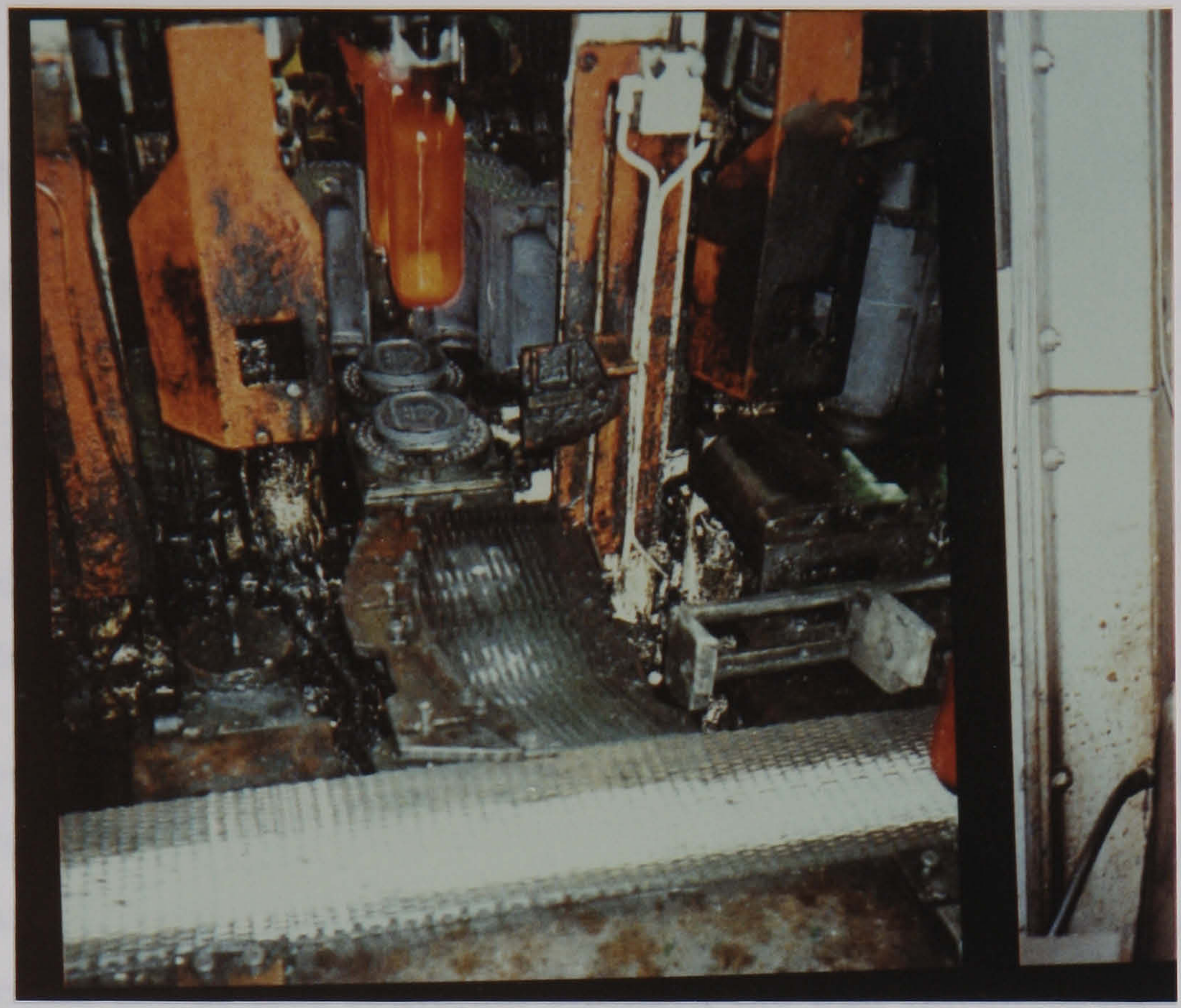

Plate 1.1 This plate shows hot bottles being lifted by take-out tongs from the blow mould on to the dead-plate.

Plate 1.2 This plate shows the sweep-out region where the bottles are 'swept' out onto a conveyer from the dead plate.

50°C to the end of the line is known as the 'cold-end'. The cold-end includes inspection and packing procedures.

1.2 The automated production of lightweight containers

Before automation, manually produced bottles were formed with much thinner walls, because the glass was stronger, so consequently they were lighter (Griffel, 1987). The introduction of automatic I.S.machines in 1928 resulted in a large increase in the production rate although the wall thickness had to be drastically increased. The increase in wall thicknesses can be attributed to two features of automated production.

1. Automation resulted in many points of contact with the glass surface during production, which did not occur whilst hand blowing a container. This resulted in damage to the glass surface so causing strength degradation of the container. To retain the desired container strength the wall thickness had to be increased.

2. Non-uniform reheating of the gob results in the blown bottle having an uneven wall thickness, so that extra glass must be included in the gob to ensure the areas of minimum wall thickness fulfil the container specification. Consequently most sections of the wall are of a much greater thickness than required.

Since the introduction of modifications to I.S.machines which produce better reheating and better overall process control, some reduction in the weights of containers has taken place (Griffel, 1987). But it was in the 1950's that major efforts to reduce the weight of containers originated. At that stage this consisted of a gradual reduction in the wall thickness through better design of the bottles and the use of soluble coatings applied at the cold-end. A typical non-returnable beer bottle was reduced in weight over several years to approximately 75% of its original weight. At the beginning of the 1960's this trend stagnated awaiting further technological developments. These arrived in the form of new designs which incorporated spherical bulbs at the shoulder and heel of the container, to act as contact points, see Figure 1.3. These contact points prevent, or at least greatly reduce, the degree and effects of mechanical damage to the mid-sidewall region by concentrating the damage incurred on filling lines at the shoulder and heel contact points (Southwick, 1985).

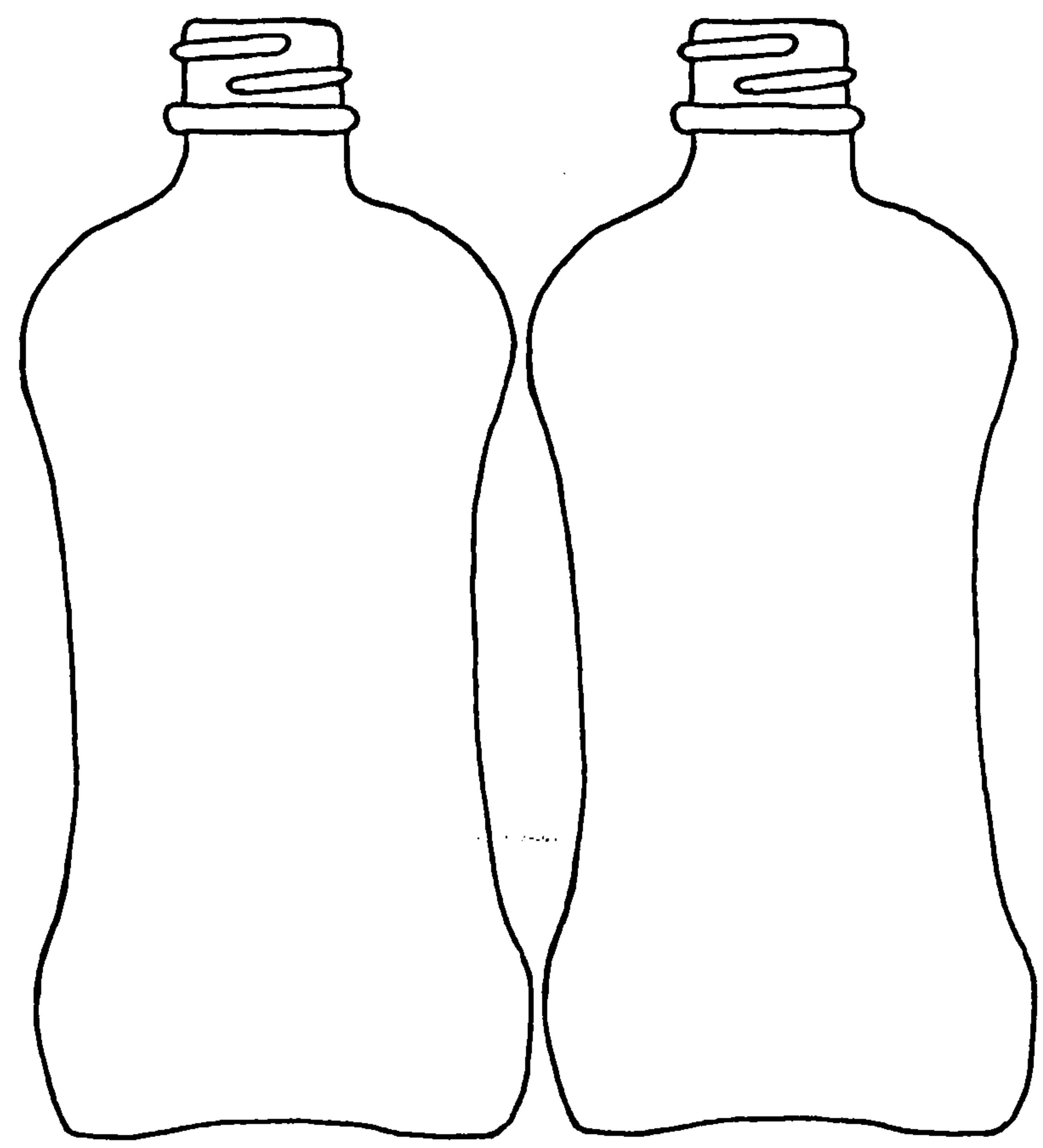

Figure 1.3 Representation of two bottles with spherical bulbs at the shoulders, which act to minimise contact between the-side walls of the bottles.

The most significant development enabling further reduction in the weight of containers was at the beginning of the 1970's with the development of permanent lubricating coatings applied in a two stage application at the hot and cold ends. These act to preserve a greater percentage of the as-moulded glass strength. They help prevent damage during the manufacture, packing and filling of the container (Budd *et al*, 1980). The first stage of this coating is applied as the bottle enters the lehr, after which the the container is protected from further damage on the production line (Bourn *et al*, 1984). However before the container has reached this point it will already have lost a percentage of its as-moulded strength, mainly as a result of damage caused by contact with handling materials at the hot-end (Budd *et al*, 1980. Williams, 1985. and Stewart and Spear, 1984.).

1.2.1 Handling materials at the hot-end

The points at which the materials contact the hot glass are labelled on figure 1.2. These materials have traditionally been cast iron, steel, brass and most commonly asbestos composites. In the mid 1970's work was started to investigate the damage caused by hot-end handling materials and to try to find efficient replacements (Bourne *et al*, 1984. United Glass Research, 1979. Budd, 1980. Stewart and Spear, 1984.). The development of new materials was further instigated by the urgent need to replace asbestos due to the growing awareness of the health hazards it presented.

The on-going development of such materials is the basis of this work. A more detailed review of the development of these materials is undertaken in 1.3.

1.2.2 Press and blow process

One of the most recent developments in the on-going battle to reduce the weight of glass containers is the use of the 'narrow-neck-press-and-blow-process' (figure 1.4). Here the parison is formed by pressing, that is a plunger rather than a blow forms the parison. This has the advantage of producing a very even wall thickness and with careful control of the reheat process this can be maintained in the final blow. This means that little excess glass needs to be included in the gob. A comparison of the two production processes was made by Griffel, (1987). He found, that for the same capacity bottle, a 10% reduction in the container weight

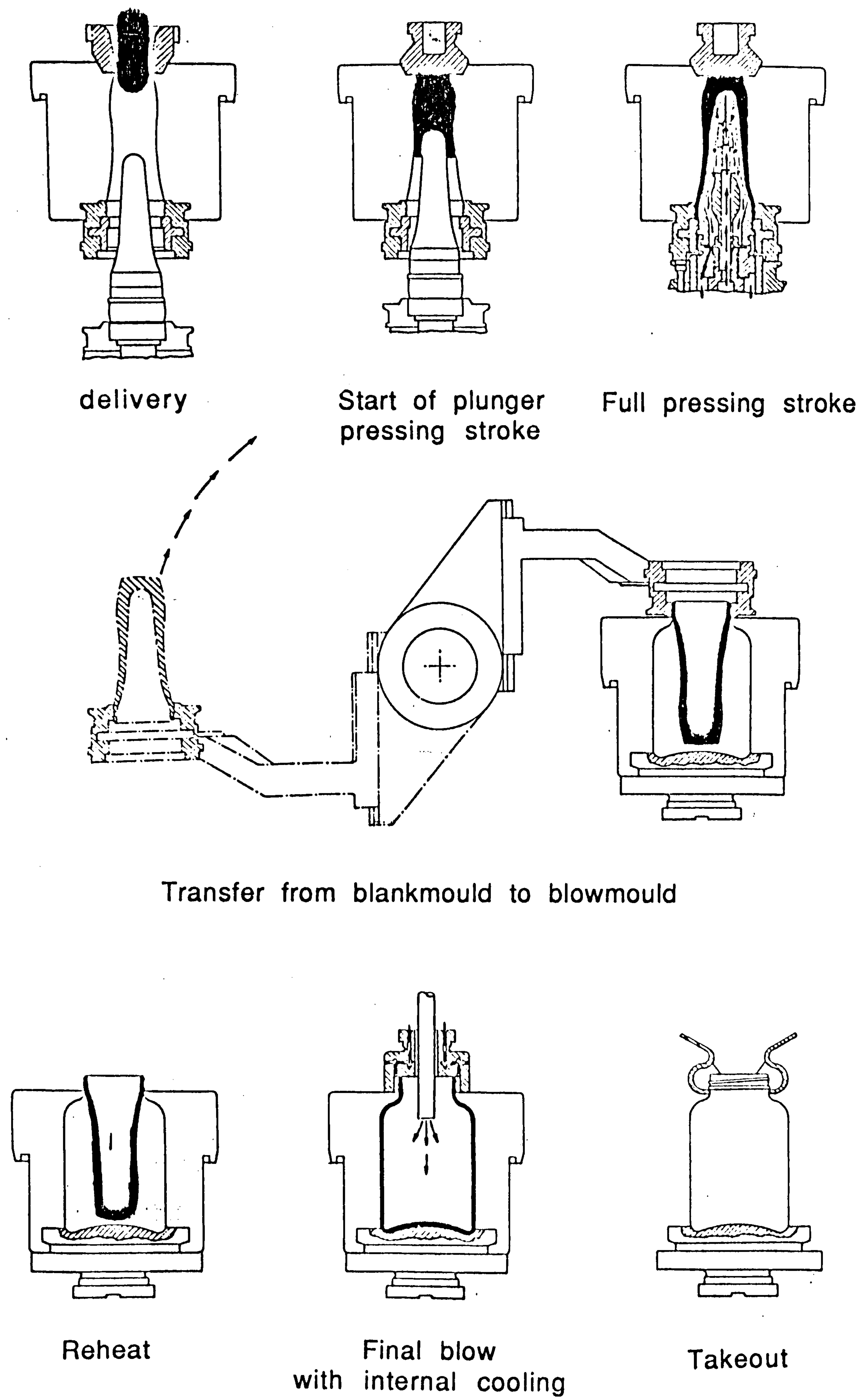

Figure 1.4 Schematic representation of the Press-and-blow process for the production of glass containers.

was achieved by the press and blow process and the mean strength of the bottle was increased.

1.2.3 Pre-Labelling

A method employed to retain the as manufactured strength of the glass containers is the polythene, or polystyrene label (Seidel et al, 1984 and Brungs, 1988) which encapsulates the container so preventing further contact which may damage the bottle. The sleeves are usually decorative and are applied on a separate process line prior to dispatch. The labelling, however incurs a further cost to the production which must be recouped in the price. Although a considerable advantage to customers on high speed filling lines this process in no way strengthens the glass as a material in its own right.

1.3 History of hot glass handling materials

In the past many materials have been used as hot glass handling materials: cast iron; steel; brass and asbestos in the form of woven mats or cemented composites. It is still commonplace to see these materials in use in the Third World (Johnson, 1987). Historically such materials were used as they were not damaged by contact with hot glass, and thus they had a long life. They were also easily shaped and attached to existing handling machinery.

At the beginning of the 1970's researchers at The United Glass Research Centre St. Albans (United Glass Research Group, 1979. Budd, 1980. Budd *et al*, 1980.) realised that the true criteria for the selection of such handling materials should be that they do not damage the glass. They found that although there was an extensive literature on the effects of contact on the strength of glass at ambient temperature they had no knowledge of the effects of contact at elevated temperatures. They investigated such contact by abrading the internal surface of hot bottles produced by the blow and blow process. It was important to use such a surface as it had not been handled and still retained a strength known to be $\geq$ 1GPa. With the glass held at 300°C they found that all the common handling materials caused a dramatic drop in the strength of the glass see table 1.1.

Material	% of strength retained compared with non-contacted containers
Asbestos Composite	27 %
Steel	14 %
Brass	13 %

Table 1.1 The percentage of original strength retained by glass after contact with various materials, while the glass was hot.

They concluded that damage was caused by a combination of mechanical scratching and thermal shock. They tested other materials in an attempt to find ones more suitable for handling glass. They concluded that both graphite and a composite of Carbon-fibre and polyimide caused considerably less damage than the handling materials used at the time. They drew no conclusions as to why this was so. But in later work by Bourne *et al*, (1984) attempts were made to correlate the handling properties of metallic materials to their hardness and thermal conductivity. They concluded that the strength of glass after isothermal contact was inversely proportional to the hardness of the handling material, determined at the appropriate temperature. Deviations from this relationship when the contact material was at ambient temperature and the glass at 300°C were attributed to the high thermal conductivity of the materials in question. These were Copper, Silver and brass. The temperature differences resulted in thermal stresses which very likely caused further damage. They did not however, examine polymers, asbestos, Carbon or other composite materials in this attempt to correlate material parameters with their handling properties.

1.3.1 Specialist materials

Running concurrently with the investigation of what features of a material make it damage hot glass, the group at United Glass were developing a new material specifically for handling hot glass. They set themselves a long list of criteria for such a material (United Glass Research Group, 1979): sufficient thermal stability; reasonable strength; not brittle; lubricious and not damaging to hot glass;

adequate wear resistance; low thermal conductivity; impervious to oil; environmentally safe; readily available and at a reasonable cost. A similar list was set by Stewart and Spear, (1984). Not surprisingly satisfying this extensive list necessitated compromise on some points.

Budd's group discarded all metals and inorganic refractory materials from their investigation and concentrated their efforts on filled polymeric systems. For such systems their first concern was its stability at elevated temperatures.

Polymers
Phenolics
Alkyds
PTFE
Polyphenylene sulphide
Polysulphones
Polyimides
Polybenzoyls

Fillers
Asbetsos
Glass fibre
Graphite powder
Carbon fibre
Minerals

Table 1.2 (A) The polymers and (B) the fillers, which were combined to produce new hot glass handling materials.

They tested materials produced by combining the polymers and fillers listed in Tables 1.2 A and B, by putting them in contact with hot silica rods which were rubbed repeatedly against the sample. They selected for development a composite involving the least compromise, in terms of cost, availability and expected life. This was a polyimide, graphite and Carbon fibre composite. The resultant material was produced by pressing the components in a heated mould. The pressing procedure introduced preferential alignment of the incorporated chopped fibres in the plane of the plate. Such anisotropy of structure resulted in a differential wear rate which depended on the orientation. So that contact of glass with the edge of the plate resulted in the material having a longer life. To facilitate this in practice, much supporting equipment was redesigned to use predominantly strips of the material edge-on (Dorey and Parker, 1981). Such equipment is shown in Plate 1.4. This material was named Cerberite 1 (C1) it was first made commercially in 1977 (Anon, 1983). Other manufacturers have marketed polymeric and organic handling materials including

1. Glass fibre fabrics impregnated with PTFE (Anon, 1986). However it must be noted that the use of this material at temperatures above 250°C represents a health risk (Shugar et al, 1981).

2. Silicone composites reinforced with both glass and graphite fibres (Stewart and Spear, 1984).

3. Steel plates coated with 0.1mm of silicon which requires recoating by the manufacturers approximately every two months (Stewart and Spear, 1984).

The reported problem with all of these materials is their limited life as they all operate at or near the limit of their temperature resistance. This also results in health and safety problems for PTFE composites. The group at United Glass (Anon, 1983) found their C1 polyimide material was unsuitable for use at the lehr stacker bar and in some take out tong positions where the high ambient temperatures and high loads respectively resulted in very short lives. They introduced a Carbon/Carbon fibre composite (C10) into the lehr stacker bar position which is shown in Plate 1.3. Another Carbon/Carbon fibre composite of higher strength was recommended for the take-out tong inserts, to be known as C12 particularly for use when a thin cross section was required (Anon, 1983). Although these materials exhibit greater strength and temperature resistance they have a disadvantage in that the materials are porous in nature and so exhibit a susceptibility to oil contamination. Areas of the material contaminated are thought to cause checking, that is a crack on the surface of the container large enough to result in it being rejected during inspection. Clean practice on the production line minimises any chance of such contamination.

Budd's group at United Glass (Budd, 1980) started to record the failure strength of a 0.25 litre non-returnable soft drinks bottles in 1973, over the following years the mean strengths recorded were in the range 25-30 MPa. During

Plate 1.3 This plate shows the lehr stacker bar which pushes the hot bottles in to the lehr, where any residual stresses resulting from the forming process are annealed out.

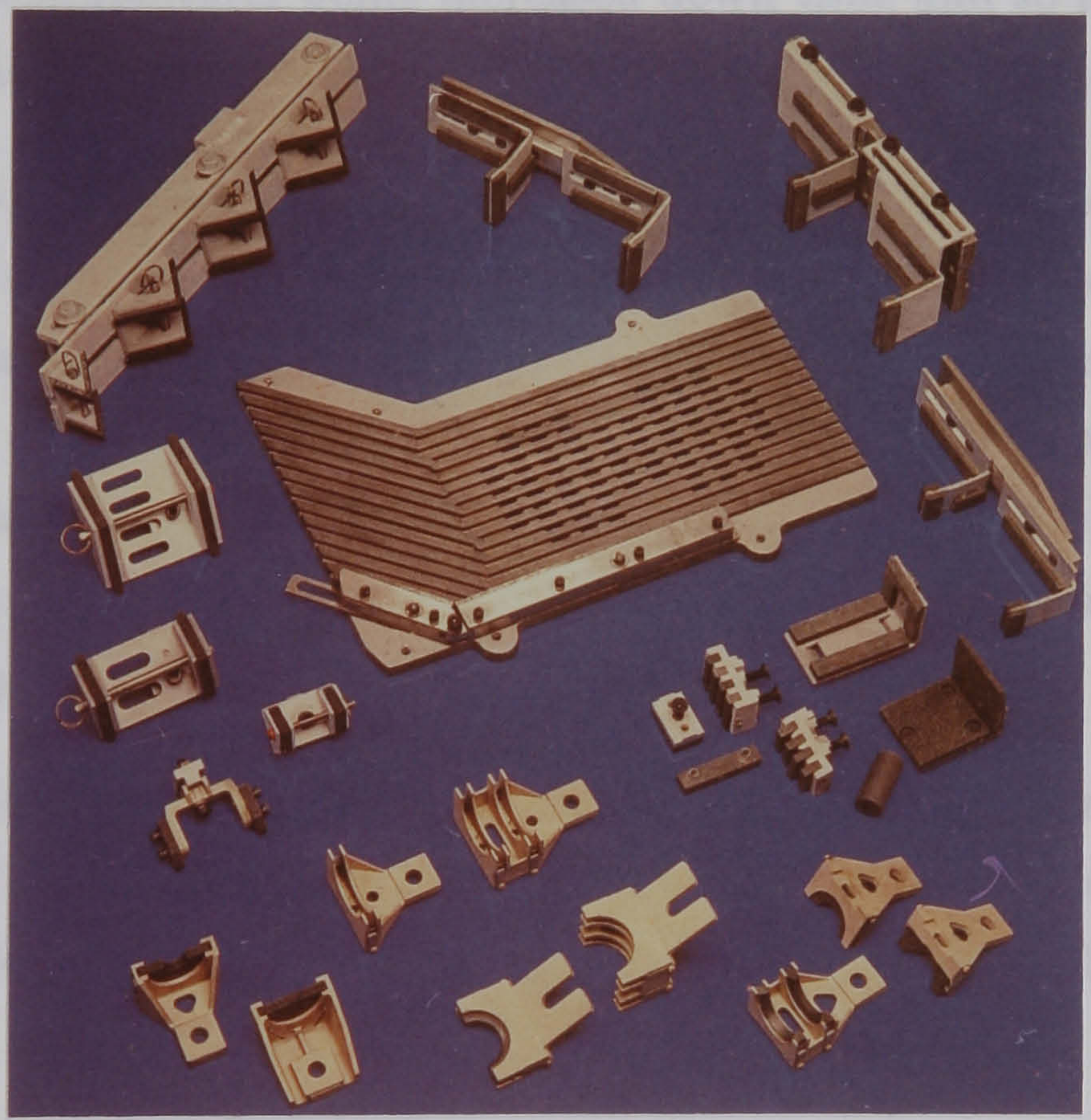

Plate 1.4 A selection of hot glass handling equipment. The specialist handling material inserts can be seen fixed to the metallic machine attachments.

1978/79 continued testing revealed a mean strength of 40 MPa for the same type of container. The only major change in production was that the line on which they were produced had been equipped with a thoughtful choice of hot glass handling equipment. Plate 1.4 shows some of the range of materials marketed by Johnson Radley mounted in their supports.

1.3.2 Durability

Although there is no doubt that new specialist hot glass handling materials have resulted in an increase in the final strength of mass produced containers, their introduction has not been without problems. In the list of desired properties set out by Budd *et al*, (1979) 'sufficient thermal stability' and 'adequate wear resistance' were detailed. Alas any new materials introduced were unlikely to match this aspect of performance of the old materials, which were chosen to optimise only these two criteria. Realistically, compromises had to be made in the development of these materials. Upon the introduction of polymer based materials the predominant reaction of the users was to applaud results but complain about their limited 'life' (McDermote, 1987). The problem arises from operating at the limit of the materials thermal stability, resulting in excessive wear rates. The outcome of this for the glass manufacturer being increased down time and so reduced profitability. This point was made clear to me on visits to glass manufacturers.

The Carbon/Carbon fibre composites (C12 and C10) introduced for their additional temperature resistance and strength, turned out to have very unpredictable lives, for instance one piece of composite may have lasted several weeks but the replacements only lasted days (McDermote, 1987). The reasons for such unpredictability were unclear, oxidation was thought to be the cause, although why rates should vary so dramatically was not understood. This will be discussed in more detail in Chapter 4.

An aim for future development of handling material was a predictable life expectancy. To be at least equal to the length of particular bottle run so that handling material inserts need only to be changed when moulds are changed.

1.4 The Future

Glass containers must be reduced, still further, in weight if sales are to be increased. The use of polymer containers has increased rapidly since their introduction in 1977 (Dourads, 1990) so that they now account for 95% of large soft drinks containers in the US. The present awareness of environmental issues has increased pressures on industry to use glass containers in preference to the plastic (polyethylene terephthalate) disposable soft drinks bottle, which is not recyclable at the moment. If glass bottles can be further reduced in weight the chance of growth being achieved could not be better than at the present time. Such environmental pressures along with competitive pressures within the glass industry spur further efforts to manufacture lighter weight glass bottles.

As a result of such pressures Johnson Radley wished to continue their development of hot glass handling materials. Thus this project was conceived. It was decided that the best way to improve hot glass handling materials was to gain a greater understanding of how the damage to containers occurs. Through such understanding it was hoped to develop existing materials and design new ones.

Three main aims were agreed upon

1. To achieve a deeper understanding of how contact between hot glass and handling materials causes damage.

2. To investigate the existing materials and develop them further.

3. To design and produce new more effective hot glass handling materials.

1.5 Thesis structure

The rest of this document is a report of the work completed to try to achieve these aims. Chapter 2 details the experimental procedures undertaken. Chapter 3 examines the effects of contact between glass and handling material. Details of mathematical models constructed to gain an insight into the interaction between thermal and mechanical damage are presented, as are the conclusions drawn from them. These are compared with experimental results of the retained strength of glass after contact with handling materials. In Chapter 4 the problems of durability of such materials are examined. Experimental investigations of the oxidation resistance of the existing materials are discussed along with details of oxidation protection systems. Both those found in current handling materials and some attempts at developing new ones are discussed. Chapter 5 is devoted to the design of new hot glass handling materials, using the findings of chapters 3 and 4 to provide the objectives for their development. Chapter 6 draws together the findings of the previous chapters, and an attempt is made to find a physical property which correlates with a material's effectiveness to handle hot glass. In Chapter 7 suggestions for further work are made. Chapter 8 concludes the document with a summing up of the conclusions drawn. The references used in preparing this document are listed alphabetically at the end.

Chapter 2

EXPERIMENTAL PROCEDURES

In this chapter the experimental procedures used in this work are detailed. They are presented under general headings giving brief explanations of why they were required.

2.1 Bench mark properties

It was thought valuable to determine the bench mark properties of existing hot glass handling materials. Of interest, for reasons set out below, were their thermal conductivity, density, and specific heat capacity.

2.1.1 Thermal conductivity

The thermal conductivity of hot glass handling materials was determined using the split column technique, similar to the comparison technique used by Griffiths and Kaye (1923) and McIvor *et al* (1990) although they used much larger diameter samples. A column was constructed from three discs, two of a standard material in this case brass, and a sample as show in figure 2.1.

Each disc had two radial holes drilled parallel to, and as near the surfaces as possible. Each hole reached the centre point of the disc. Placed into each hole was a Chromel/Alumel thermocouple, good thermal contact was encouraged by a grease paste containing colloidal graphite. It was important to measure the thermal conductivity in the appropriate direction, as some materials were very anisotropic. In one case thin strips of material had to used to construct a sample as the material was only available in 6mm thick sheets and it was the thermal conductivity in the direction parallel to the plane of the sheet which was of interest.

The top of the column was heated using an electrical heating element. The bottom of the column was constantly cooled by a water chamber, fed from a constant head source. The whole apparatus was lagged with alumina wool and

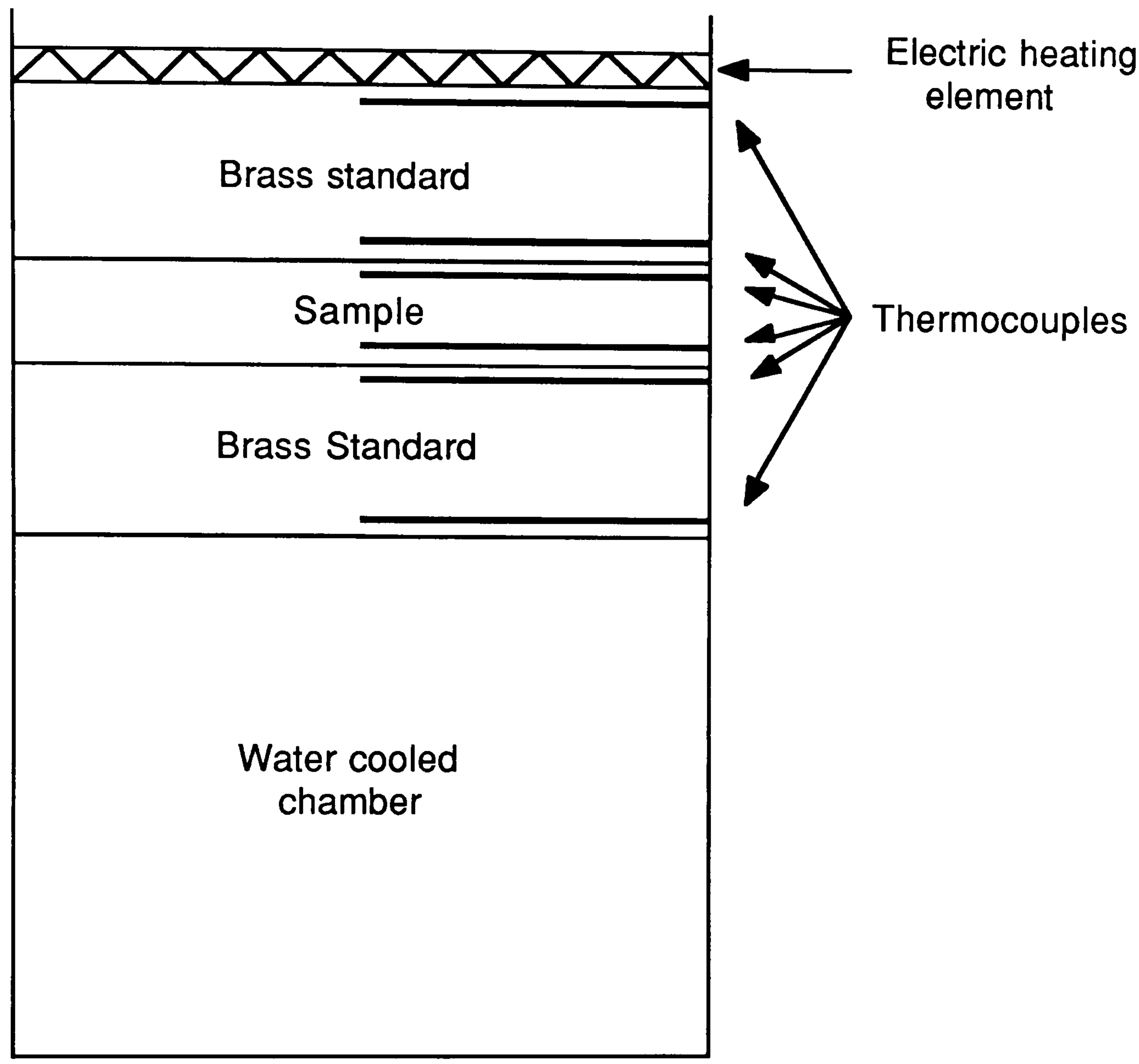

Figure 2.1 The split column arrangement used in thermal conductivity determinations.

loaded in a guard ring, which heats the surroundings to the mean temperature of the column. The system is left to reach a steady state, i.e. when all the thermocouples have steady readings.

The rate of flow of heat across each disc is

$$Q = k_{mat} A \frac{\Delta\theta_{mat}}{x_{mat}} \tag{2.1}$$

were $\Delta\theta_{mat}$ is the temperature difference recorded from thermocouples set in a material, separated by x_{mat}, A is the cross sectional area and $k_{mat}$is the thermal conductivity of a material. Because of the lagged surroundings each disc can be assumed to have the same flow of heat across it. So

$$\frac{\Delta\theta_{brass}}{x_{brass}} k_{brass} = \frac{\Delta\theta_s}{x_s} k_s \tag{2.2}$$

where the subscripts, *brass* and *s* represent the brass standards and the sample discs respectively. The thermal conductivity of the sample is therefore given by

$$k_s = \frac{\Delta\theta_{brass} x_s}{\Delta\theta_s x_{brass}} k_{brass} \tag{2.3}$$

This apparatus appears to give satisfactory results as long as great care is taken in setting up contact between the samples, standard discs, heater, and water chamber. This is ensured with a thin layer of graphite loaded grease. The results obtained for samples of soda-lime-silica glass, alumina and graphite were checked against reported values (TPRC Data Series, volume 2, 1970).

2.1.2 Density

The bulk density of the sample was determined using a Mercury displacement balance shown in figure 2.2 (e.g.Ashworth, 1969). The apparatus was first adjusted so that the brass pointers were just in contact with the Mercury surface. The sample was then immersed below the surface of the Mercury by the balance float, and weights were added until the pointers were again in contact with the surface of the Mercury. This weight (W_I) plus the weight of the sample (W_S) is a measure of the upthrust of the Mercury on the specimen, and since the volume of the sample

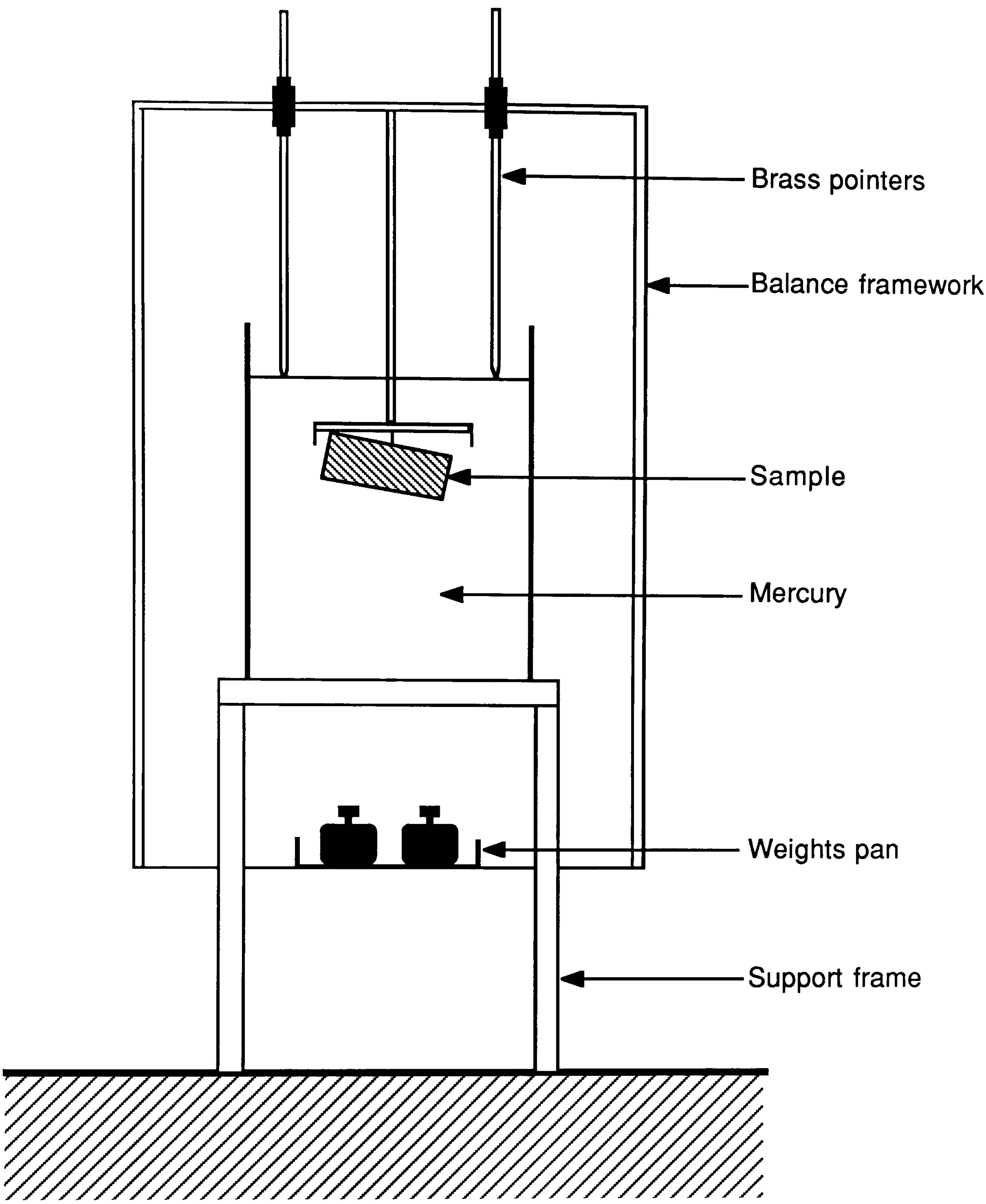

Figure 2.2 Schematic of the mercury balance.

is equal to the volume of the Mercury displaced, the bulk density was found from the following relationships.

$$\frac{\text{Weight of sample } (W_S)}{\text{Bulk density of sample}} = \frac{\text{Upthrust of Mercury } (W_I + W_S)}{\text{Density of Mercury}} \tag{2.4}$$

therefore

$$\text{Bulk density } (\text{Kgm}^{-3}) = \frac{W_S \times 135.6}{W_I + W_S} \tag{2.5}$$

2.1.3 Specific heat capacity

The specific heat capacity was determined experimentally using a simple water calorimetry. A vacuum flask embedded in an expanded polystyrene surround was used as the vessel of the calorimeter. The well fitting lid was also made of polystyrene. A Mercury thermometer with 0.1°C divisions was inserted through a small hole in the lid. This apparatus was used so as to minimise heat losses.

A known quantity of distilled water was placed in to the calorimeter vessel, after thorough mixing its temperature, T_1, was recorded. The sample was heated to approximately 80°C, its temperature, T_s, was measured by a thermocouple placed in the sample. The sample was then placed into the calorimeter, the maximum temperature, T_2, of the system was recorded.

As the heat given out by the sample was equal to the heat gained by the vessel and the water

$$m_s C_s (T_s - T_2) = m_w C_w (T_2 - T_1) + m_c C_c (T_2 - T_1) \tag{2.6}$$

where, m, represents the mass and, C, the specific heat capacity, the subscripts s, w and c representing the sample, water and calorimeter respectively. In this case the calorimeter consisted of the thin glass wall of the vacuum flask, its small heat capacity was ignored in these experiments. So that the heat capacity of the sample C_s could be calculated from expression 2.7.

$$C_s = \frac{(M_w C_w)(T_2 - T_1)}{m_s (T_s - T_2)} \tag{2.7}$$

2.2 Chemical polishing of soda-lime-silica glass rods

To mimic the damage to just-formed glass, the first requirement was high strength soda-lime-silica glass rod. To produce high strength glass rod it was necessary to remove the surface layer of material to leave as perfect a surface as possible.

This was done by polishing the as-received soda-lime-silica glass rods in a solution of hydrofluoric acid. The rods used for reasons associated with testing were 8mm in diameter and 80mm in length. The rods have to be loaded into a specially designed holder to enable them to be placed and removed from the polishing solution without contacting each other. The holder shown in figure 2.3 allows this, as each rod is free standing in its own hole. The holder had to be made of a material that would not be affected by hydrofluoric acid, and would not scratch the glass. High density polythene was chosen.

The first attempts to produce high strength glass rod tried to repeat Budd's, (1987) experiments. This involved repeatedly placing the rods into a 10% solution of HF at room temperature for 30-40 seconds. On removal from the solution the rods were washed with water to remove any CaF_2 deposits, this was repeated 4 times in all. No sufficiently high strength rods were produced, increasing the time of submersion in the polishing solution resulted in white deposites (probably CaF_2) forming on the rods.

Proctor, (1962), and Eschenbacher, (1987), both reported the successful use of HF based polishing solutions which additionally contained H_2SO_4, concentrations varying between 15-60%. Eschenbacher claimed the H_2SO_4 acted to help release the corroded particles from the surface, prevent deposits forming and to increase the sheen of the resulting glass surface. Incorporating H_2SO_4 into the polishing solution detailed above did not increase the strength of the rods produced or stop the formation of the white deposites on the rods.

It was decided to try progressively reducing the concentration of the HF in the polishing solution and correspondingly increase the time for which the rods were submerged. This adaptation of the process proved successful. A solution of 20cc of 40% HF and 600cc of water in which rods were placed for 48 hours consistently

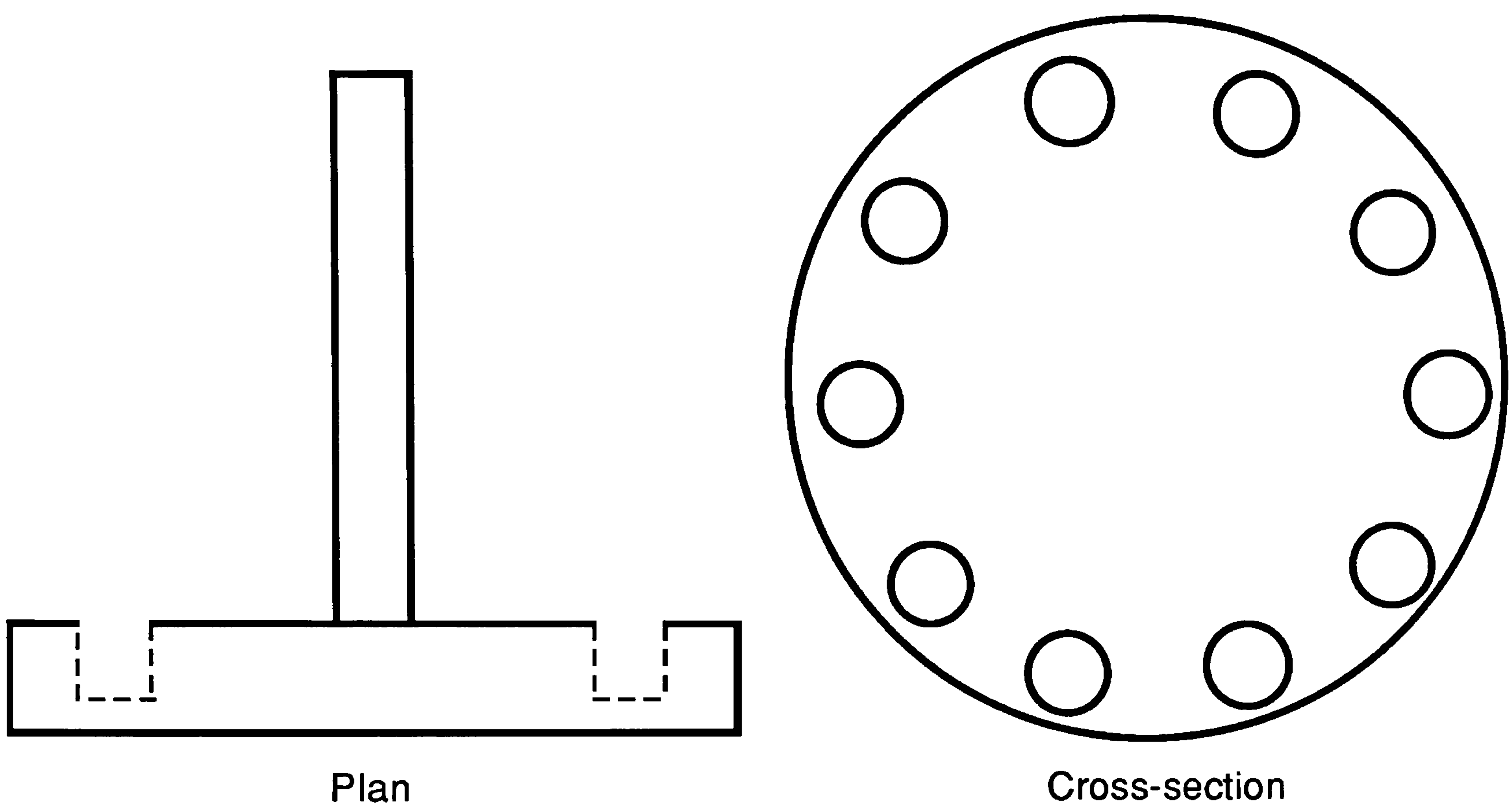

Figure 2.3 The holder in which the glass rods where placed during polishing

produced batches of high strength glass rod. This method was adopted for specimen production and continued successfully for approximately 2 months. Then on one batch of rods the deposits returned and the strength dropped dramatically. After this repeated attempts all failed to produce batches of strong rods. The problem was thought be the result of an increase in the ambient temperature of the laboratory, which increased the rate of the chemical reaction. The polishing procedure had to be reassessed.

The first step was to produce constant, controlled surroundings. This was achieved by placing the beakers containing the polishing solution into a constant temperature water bath. The bath only operated at temperatures above ambient, so it was decided to set the temperature to 30°C. The increase in temperature was compensated for by a reduction in the concentration of the solution. Various concentrations of solution were tried, to 600cc of water additions of between 1 and 10cc of 40% HF were made. Although some improvement was achieved, the strengths of the glass rods never exceeded 50% of the previous maximum.

It was decided to try and suppress the deposits chemically, with the use of sequestering or chelating agents. They act by forming soluble organic complexes in which the metal ions, which otherwise precipitate and form deposits, are captured and rendered unreactive (e.g.Gilchrist, 1980). The most widely applicable sequestering agent is (Ethylenedinitrilo)tetraacetic acid (EDTA). The addition of EDTA to the polishing solution successfully suppresses the formation of the deposits and batches of strong glass rods were produced. No further difficulties were experienced.

The optimised polishing procedure used for the production of the high strength glass rods was:-

- a polishing solution containing,

  1g of EDTA (the disodium salt),

  10cc of 40% hydrofluoric acid,

  600cc of tap water,

- at 30°C,

- in which the rods were submerged for 48 hours.

On removal the rods are washed in running water and then dried using acetone.

2.3 Testing the strength of soda-lime-silica glass rods

It was decided to determine the strength of glass rods using a four point bend test. This was chosen so as to maximise the area under maximum stress. So that the effects of contact with glass handling materials upon the strength of the rod can be determined most effectively. Figure 2.4 shows a diagram of the loading arrangement.

The expression used to determine the maximum stress under which the rod failed was derived from simple bend theory, detailed by, for example, Stephens, (1975). The stress, σ, at a distance x from the neutral axis is

$$\sigma = \frac{M}{I}x \qquad (2.8))$$

where M is the bending moment and I is the moment of inertia for a circular cross section

$$I = \frac{\pi}{64}d^4 \qquad (2.9)$$

where d is the diameter of the rod, therefore

$$\sigma = \frac{64M}{\pi d^4}x \qquad (2.10)$$

The maximum stress, σ_{max}, on the rod is at the surface, a distance of $d/2$ from the neutral axis therefore

$$\sigma_{max} = \frac{32M}{\pi d^3} \qquad (2.11)$$

where

$$M = \frac{1}{2}PL \qquad (2.12)$$

when L is the distance between the loading points,shown in Figure 2.4 and P is the applied load.

It should be noted that as the glass rod increased in strength during optimisation of the polishing, the contact at loading points caused damage to the rods.

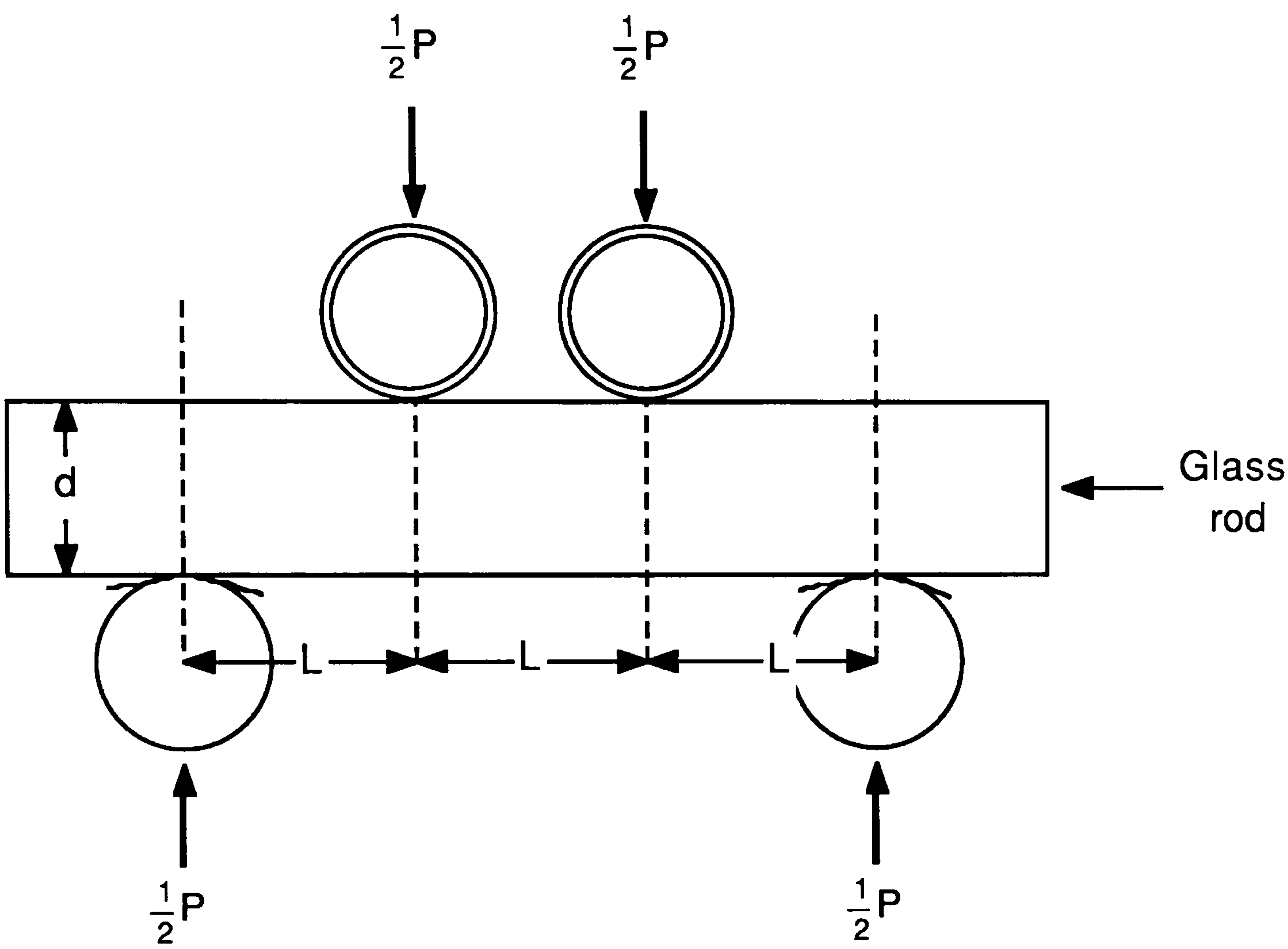

Figure 2.4 The loading arrangment for the testing of the glass rods.

This resulted in the failure occurring at the loading points rather than in the central section which is under the greatest stress. To over come this the top rollers were coated in a replaceable polythene tube and the locating grooves on the lower rollers were protected by placing small pieces of soft cloth between the steel roller and the glass rod. These measures proved successful. It was possible to have confidence that the problem had been solved by examining the debris of the failure. Instead of there being two or three pieces of rod, it disintegrated into several hundred very small pieces and a considerable amount of glass dust. An alternative approach to this problem is to lacquer the rods as soon as they are removed from the polishing solution (Proctor, 1962). This was not of use in this work as the effects of controlled surface damage were to be investigated.

The loading apparatus is mounted in a compression cage on a RDP Howden 20kN universal testing machine. The cross head speed was constant for all tests at 10mm/min.

For all tests a cylindrical perspex shield enclosed the test pieces and grips. This was most important for safety reasons as the glass debris on failure have high energy and are travelling at considerable speed. This was such that the perspex shield became damaged after each test and had to be replaced after about 100 tests.

2.4 Controlled damage of high strength glass rod

To investigate the effects of contact on the glass rod an apparatus was required to damage glass rod in a controlled way so that an attempt could be made to determine the effectiveness of hot glass handling materials. It was important that the apparatus could be used at temperatures up to 300°C and that different handling materials could easily be inserted.

Figure 2.5 shows the apparatus which was designed for this job. The rod is loaded onto the supports which locate the central section of the rod below the handling material insert. The inserts were made of graphite to minimise any damage to the ends of the rods. The rest of the apparatus was constructed from stainless steel. An insert of handling material was machined to the standard size shown in figure 2.6. The notch rested over the rod during contact. A machined

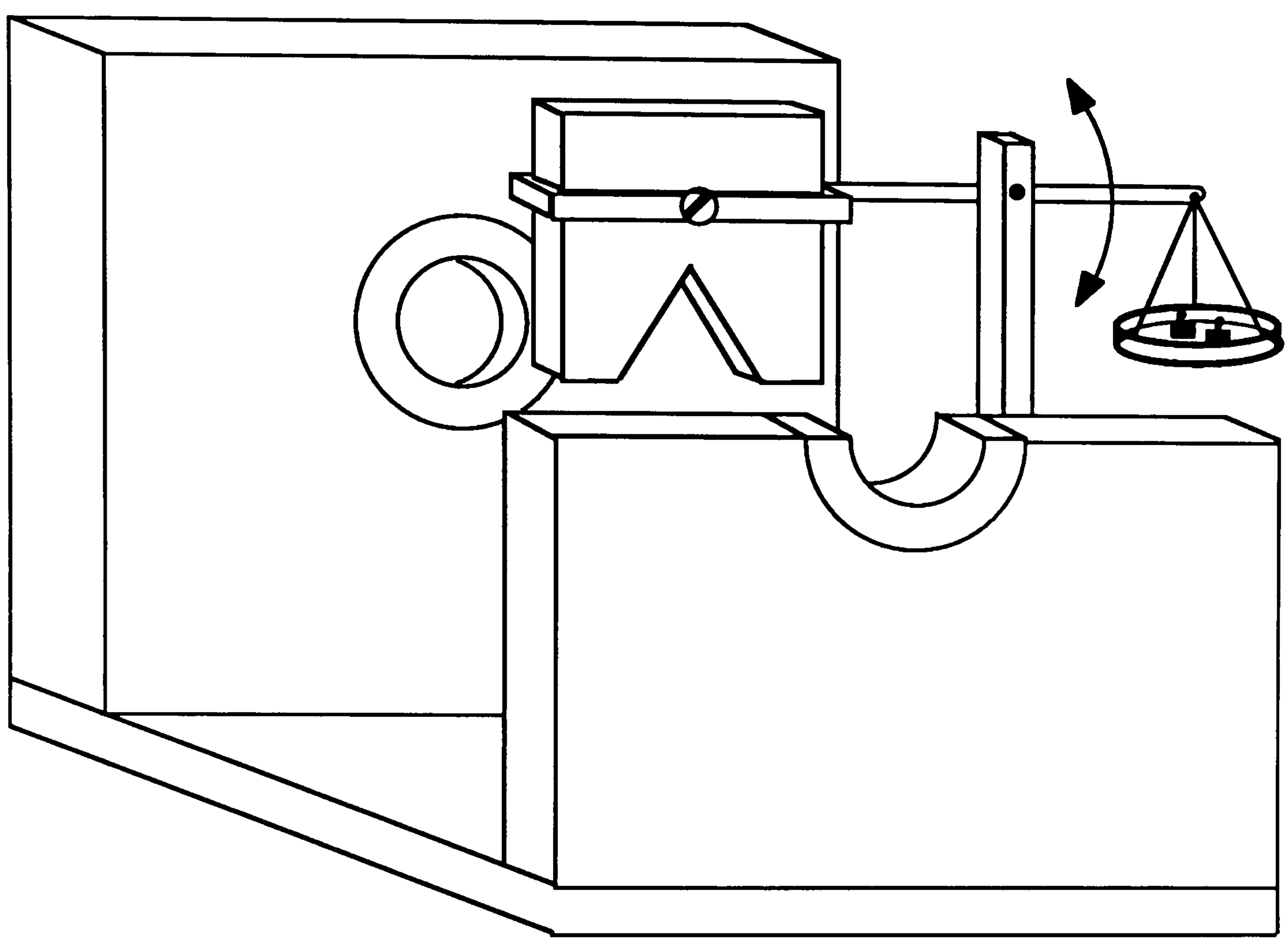

Figure 2.5 The apparatus for the controlled abrasion of high strength glass rods.

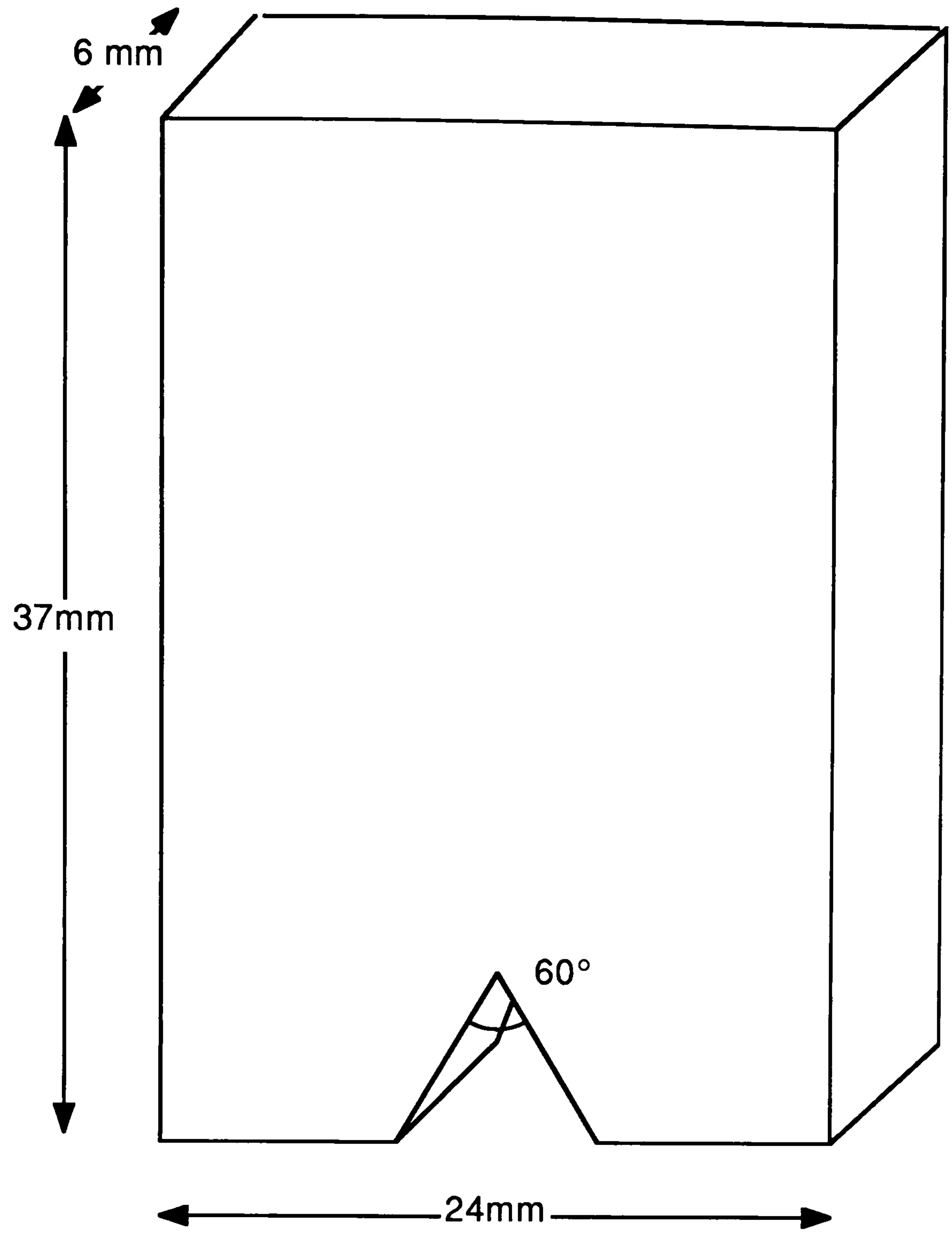

Figure 2.6 The material insert used in the contolled contact of the glass rods.

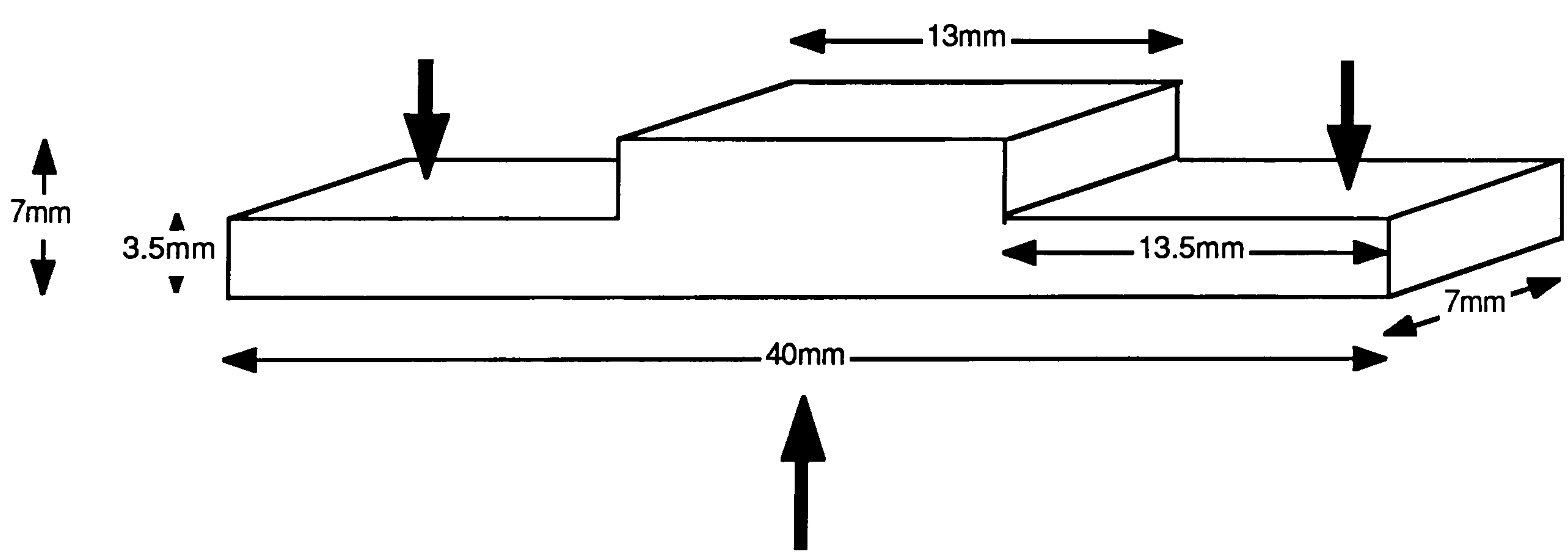

Figure 2.7 The stepped sample which was tested in three point bending.

surface finish was used in all cases as this is what is used in practice. The insert was placed into the pivoted arm and secured with a grub screw. The arm was then balanced for each material used, and a known load applied to the system.

When a component is in use the glass container it handles is at an elevated temperature and contact with the handling material can cause damage by thermal shock, as well as mechanical means. To assess handling materials fully it was important to try and investigate both. The glass rods used for this assessment were contacted in three different ways. The aim being to attempt to separate the damage caused by the two mechanisms to a degree.

2.4.1 Isothermal contact

This was undertaken with both the glass rod and the handling material at room temperature, the rod was rotated three times whilst in contact with the handling material. The rod was then removed, taking great care not to touch any part of the rod on the support system. The rod was then tested in four point bending as detailed in section 2.3

2.4.2 Thermal shock

The rod was loaded into the support apparatus with the loading arm detached, the base was then placed into a muffle furnace and heated to 300°C. It was important that the rods were heated in a muffle furnace, to minimise the damage to the rods during heating. Preliminary experiments in which the rods were heated in a fan assisted furnace resulted in the strength of the rods dropping to a level, < 500MPa, at which they could no longer be labelled as high strength glass rods. Damage by contact with the handling materials would have been masked by the damage incurred during re-heating. Once the rod had reached 300°C, as quickly as possible the assembled apparatus was removed to the mouth of the furnace and the arm attached.

In the first experiments of this type, the handling material simply touched the glass rod and was then removed. The rod was then allowed to cool, before being tested in four point bending as in section 2.3. In a second set of experiments the rod was loaded and rotated as in the isothermal test, before being allowed to cool.

2.5 Assessment of the delamination of composite materials

A two dimensional Carbon/Carbon composite revealed a susceptiblity to failure by delamination when used as an insert in the take-out tong. It was decided that it was important to be able to assess the material in a way which reflected the environment to which it is exposed. This is discussed further in section 4.3.4. A test was designed to evaluate the existing materials and attempts to improve them.

A stepped sample was designed to mimic the profiled edge of the take out tong insert, shown in figure 2.7, to be tested in three point bending. Samples were loaded to failure in a Hounsfield tensometer (load range 0-62.5 lbf.) the maximum load reached was recorded as some measure of the interlaminar bond strength of the material. Also recorded was the way in which the sample failed.

To investigate the effect of oxidation on these composites, stepped samples were placed in an air furnace for up to 96 hours at 300°C or 400°C. They were then tested to failure as above.

2.6 Coatings

In an attempt to limit the weakening of porous handling materials due to internal oxidation, a coating was applied to the surfaces of such materials.

- A pure pitch coating was applied in an attempt not to change the the surface properties of the handling material.

A pure synthetic pitch was ground in a ball mill. The mill body was a cylindrical rubber mill 100mm long with an internal diameter of 124mm. Zirconia milling media was used in the form of 17mm diameter cylinders. 100cc of propan-2-ol was used to aid the milling process. The charge was rotated at 36rpm for 24 hours.

On removal from the mill the powder was pan dried under a heat lamp, great care had to be taken, if over heating occurs the pitch will soften, bubble and refuse. The best results were achieved if the final stage of drying was carried out at room temperature. The dried mass in the bottom of the drying pan was then forced through a 710μm sieve before use.

To produce the coating medium six grams of ground pitch were dissolved in 50cc of chloroform. Two coating techniques were used,

1. The sample to be coated was dipped in to the pitch solution. Once saturated it was then removed and the solvent allowed to evaporate. The sample was then redipped. This procedure was repeated three times.

2. The coating solution was used to paint the samples. Three coats were applied.

Once a coating had been applied the samples were left to dry over night. They were then loaded into a vacuum furnace and were heated at a rate of 4°C per minute up to 700°C. The samples were held at this temperature for four hours and then cooled at a rate of 1°C per minute.

2.7 Youngs modulus and the coefficient of friction

The contact tests described in section 2.4 give an assessment of the effectiveness of a glass handling material, but to prepare enough glass specimens and complete the contact tests is very time consuming. It was thought that the modulus of a material, and the coefficient of friction between it and glass, could be associated with a materials contact properties. Consequently they were evaluated to facilitate attempts to correlate them to a materials handling efficiency

2.7.1 Measurement of Youngs modulus

To measure the modulus of handling materials an apparatus was used which utilised a four point bend loading system. The deflection of the centre of the beam with respect to an inner loading point could be measured using a transducer and compensator system. The specimen used was a rectangular bar of material, $3\times$ 3mm square and 50mm long. The specimen was loaded via 5:1 lever arm.

Figure 2.8 and 2.9 show the loading system and the geometry of the bar under load respectively.

If, W, and ,w are respectively the weights of the pan load and loading strut plus saddle assembly, the bending moment between the inner loading points, M is

A.

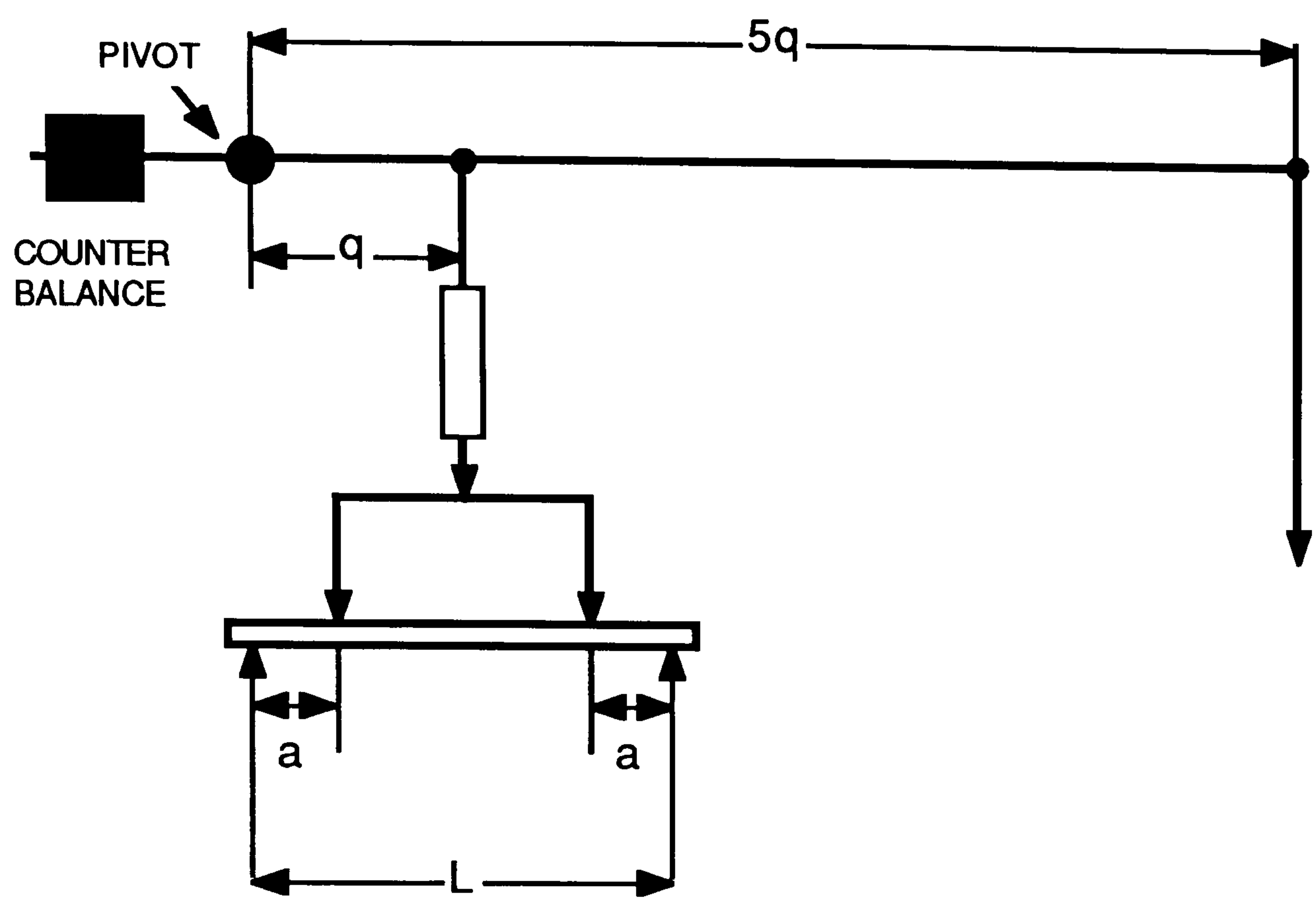

B.

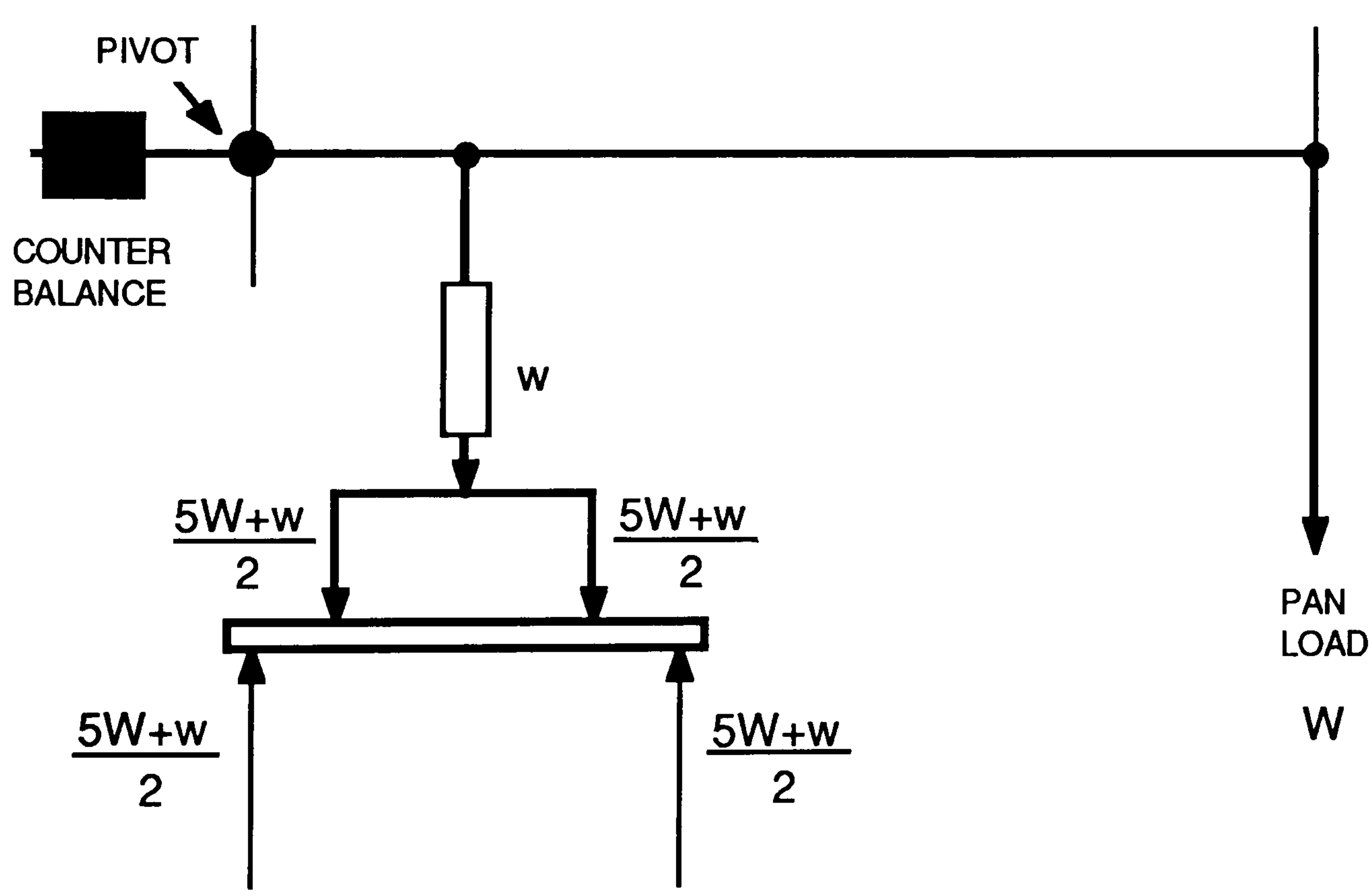

Figure 2.8 A. The dimensions of the specimen and separation of the loading points.
B. The loading arrangement of the apparatus used to determine the modulus of elasticity.

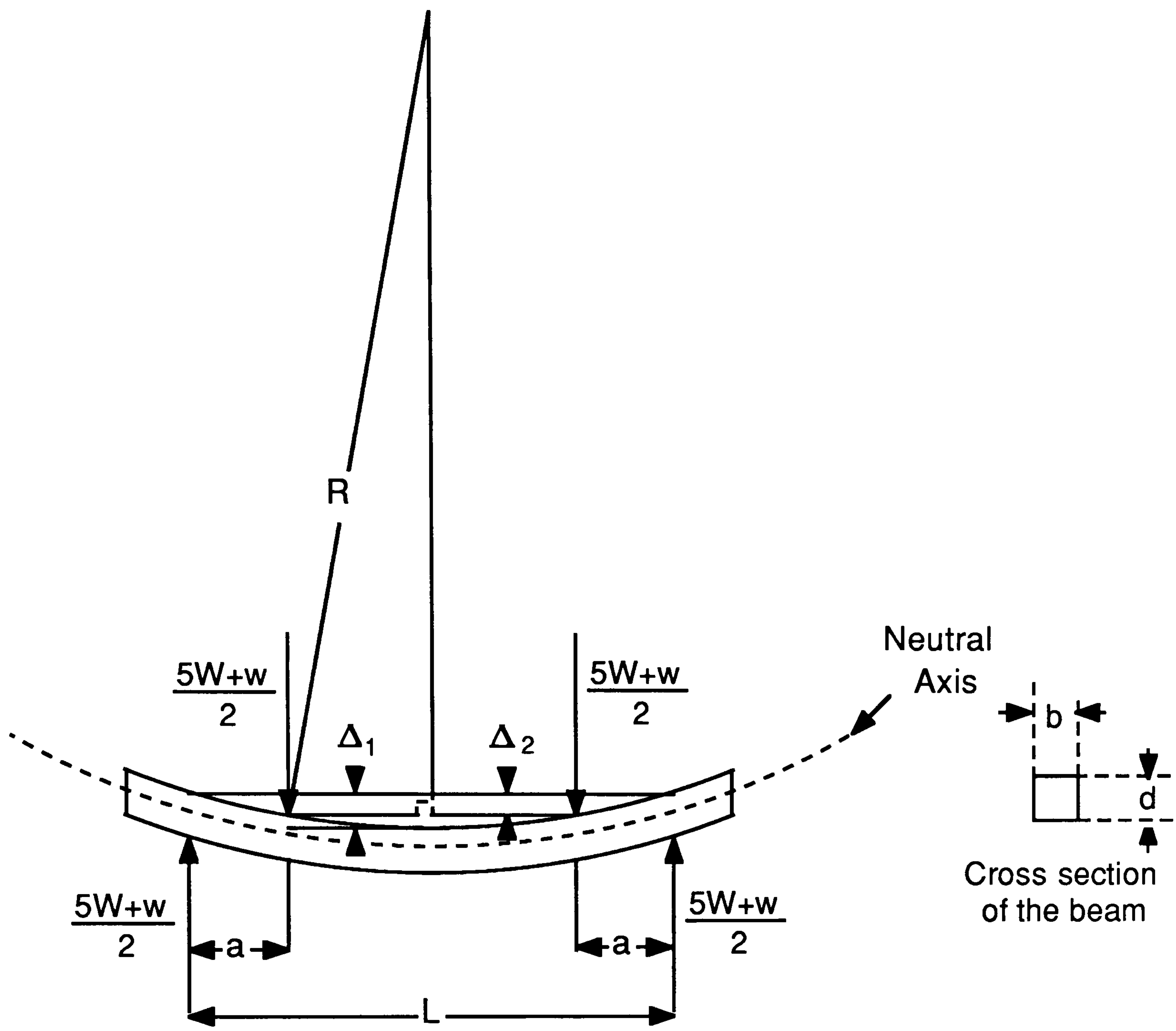

Figure 2.9 Elastic bending of a rectangular bar in four point loading.

given by

$$M = \frac{(5W + w)a}{2} \tag{2.13}$$

were a is one quarter of the outer span length L. Classic bend theory states that for an elastic beam in four point loading,the deflection Δ_1 and Δ_2 in figure 2.9 are given by

$$\Delta_1 = \frac{\left(\frac{5W+w}{2}\right)}{24EI} a(3L^2 - 4a^2) \tag{2.14}$$

$$\Delta_2 = \frac{\left(\frac{5W+w}{2}\right)}{6EI} a^2(3L - 4a) \tag{2.15}$$

Where E is the modulus of the material and I is the moment of inertia of a rectangular beam, which is

$$I = \frac{bd^3}{12} \tag{2.16}$$

where b is the breadth, and d the depth of the beam. Thus the differences in deflections $\Delta = \Delta_2 - \Delta_1$ is given by equation 2.17

$$\Delta = \frac{\left(\frac{5W+w}{2}\right)}{8EI} a(L - 2a)^2 \tag{2.17}$$

Δ, which is independent of any deformation directly under the loading points, was determined from the change in the transducer voltage, ΔV, and the calibration constant of the transducer, C, thus

$$\Delta = C\Delta V \tag{2.18}$$

C was determined with the use of a micrometer calibration jig. The Young's modulus can now be written in terms of measured parameters.

$$E = \frac{3a(5W + w)(L - 2a)^2}{4C\Delta V bd^3} \tag{2.19}$$

The specimen was loaded into the apparatus. Very carefully the load was applied and then removed several times. The change in the transducer reading was noted. For each material several different loads were used.

2.7.2 Coefficient of friction

To determine the coefficient of friction, μ, between a glass rod and a handling material a simple apparatus was developed which enabled the determination of the force needed to overcome the frictional force between the two materials under a known load. Lengths of polished rod was loaded into the apparatus shown in figure 2.10.

The apparatus was developed from that used to produce controlled damage to the surface of glass rods. Instead of the rod being supported at its ends in graphite sleeves which gave unknown torsional resistance, the rod was rested in two 'v' shaped grooves in inserts of the handling material under test. These were similar to those used in the arm on the damage apparatus. The same arm was used in the friction measuring system to apply a known load. To complete the apparatus a light balanced arm was attached to one end of the the glass rod being tested. Weight was added to the small pan on the arm as pellets of approximately 0.1g. When the frictional force between the rod and the handling material was overcome the rod rotated. The exact weight of the added pellets was then measured on an electronic balance.

The forces acting on the rod are considered in figure 2.11. Where: N is the load applied to the system; m is the mass of the glass rod and arm; S is the total frictional force between the rod and the handling material; R is the distance between the loading pan and the centre of the rod; M is the load added to the pan just sufficient to over come the total frictional force; and r is the radius of the glass rod.

To calculate μ consider the total frictional force to be overcome before the rod can rotate, it is the sum of the forces acting at the points of contact. The force resulting from contact with the top insert of handling material, $S_1 = \mu N$, and the equal forces at the two bottom contacts, S_2 and $S_3 = \mu((N + mg)/2)$,
so that

$$S = 2\mu N + \mu mg$$

when the frictional force is overcome

$$RMg = Sr \tag{2.20}$$

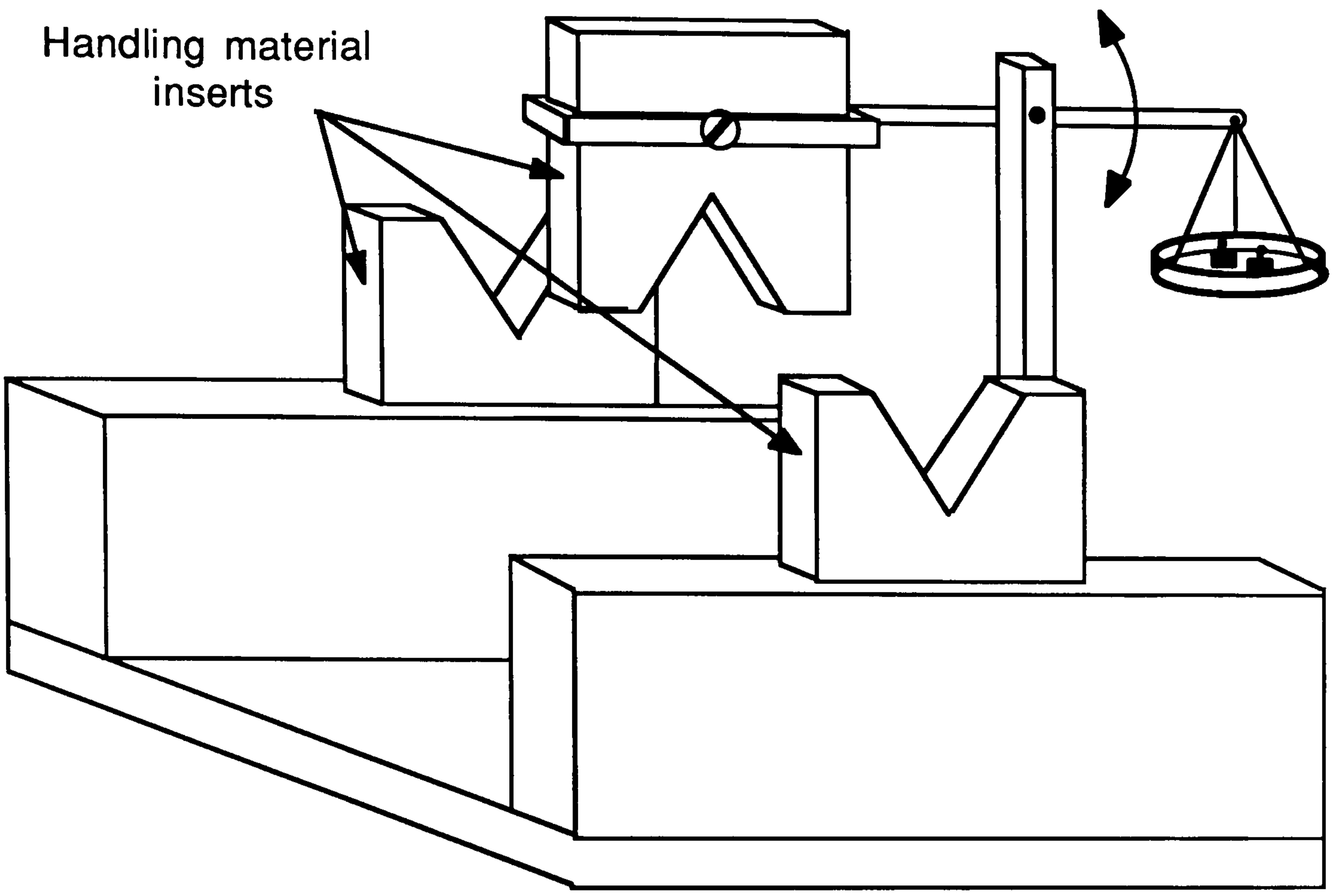

Base of apparatus

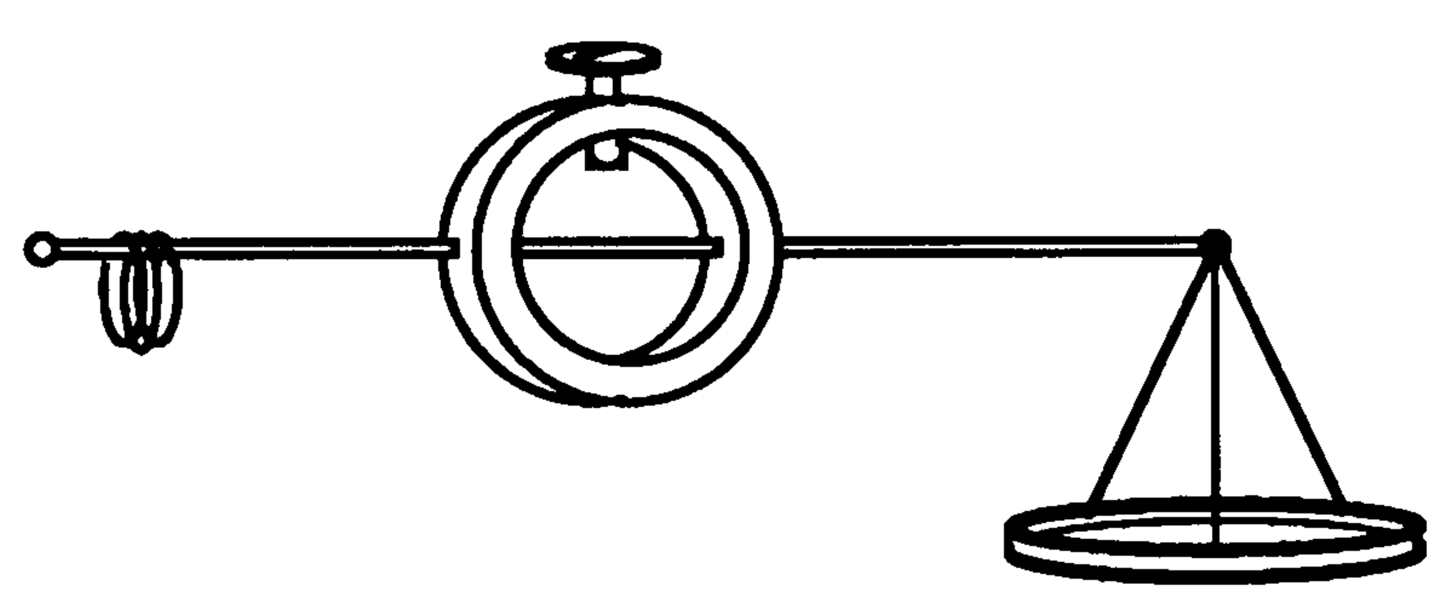

Balanced arm attached to the polished rod

Figure 2.10 A schematic representation of the apparatus for measuring the coefficient of friction between polished soda-lime glass rod and hot glass handling materials.

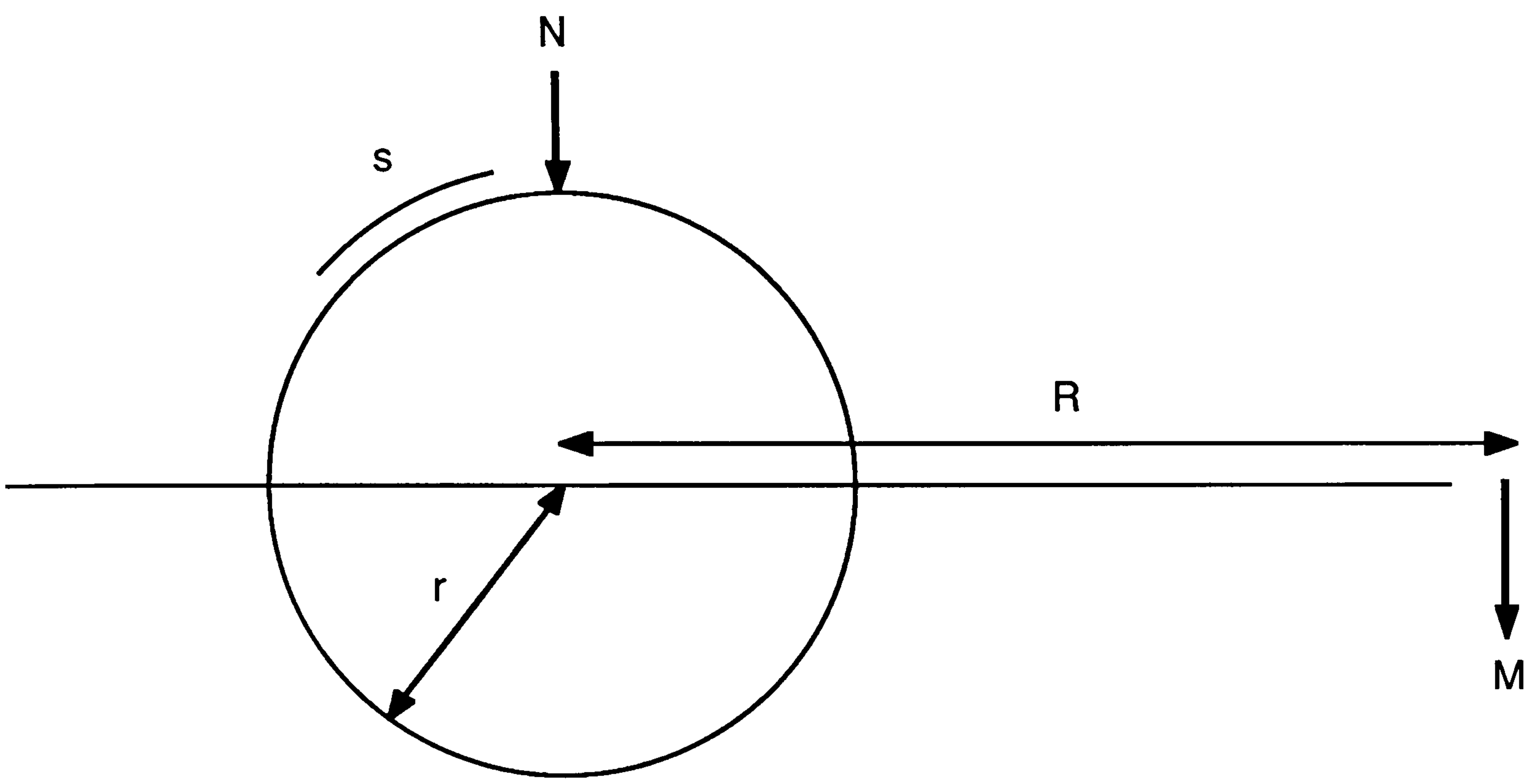

Figure 2.11 Forces acting on the glass rod during the evaluation of the coefficient of friction.

therefore

$$S = \frac{RMg}{r} \tag{2.21}$$

so by substitution with the expression for the total frictional force

$$\mu = \frac{RMg}{(2N + mg)r} \tag{2.22}$$

The test was repeated four times for each material, a different freshly polished rod was used for each test, so as to eliminate any possible effects due to surface contamination.

2.8 Scanning electron microscopy

Scanning electron microscopy (SEM) was used throughout the project to examine the surfaces of handling materials. The large depth of focus of the SEM was required for examining fracture surfaces, especially of fibre reinforced materials. Both a Jeol T20 and a Camscan S4 were used.

Secondary and back scattered electrons were imaged. The back scattered images giving useful atomic number contrast in some composite materials. On the Camscan S4 the Energy Dispersive X-ray technique (EDX) was used to identify impurities and antioxidant additives in materials.

The disadvantage of this technique is that electrically insulating materials charge up under the electron beam, distorting the image. To minimise any such problems insulating materials were coated with a thin layer (few nm) of gold, thus providing an escape route for the electrons.

2.9 Thermal gravimetric analysis

As part of the assessment of a handling materials resistance to oxidation, samples were analysed in a thermo-balance manufactured by Stanton Redcroft. The sample was located on the balance over which the furnace is lowered. The sample was in an air atmosphere. The temperature of the furnace was linearly increased at a rate of approximately 10°C per min. The weight of the sample and the temperature of the sample were constantly recorded. This enabled a calculation of the % weight loss with respect to temperature.

2.10 Compression tests

Samples were cut to the specifications shown in figure 2.12. The samples were then tested in compression on a RDP Howden 20kN testing machine with a cross head speed of 1mm/min. Laminated samples were orientated so that the laminates were perpendicular to the faces of the compression blocks of the apparatus. The sample size used was the same as Johnson Radley use in their quality control test for incoming material. This facilitated direct comparison with their present and past recorded data. The odd dimension of 6.3mm was used to minimise cutting as most incoming sheets of material are 6.3mm thick.

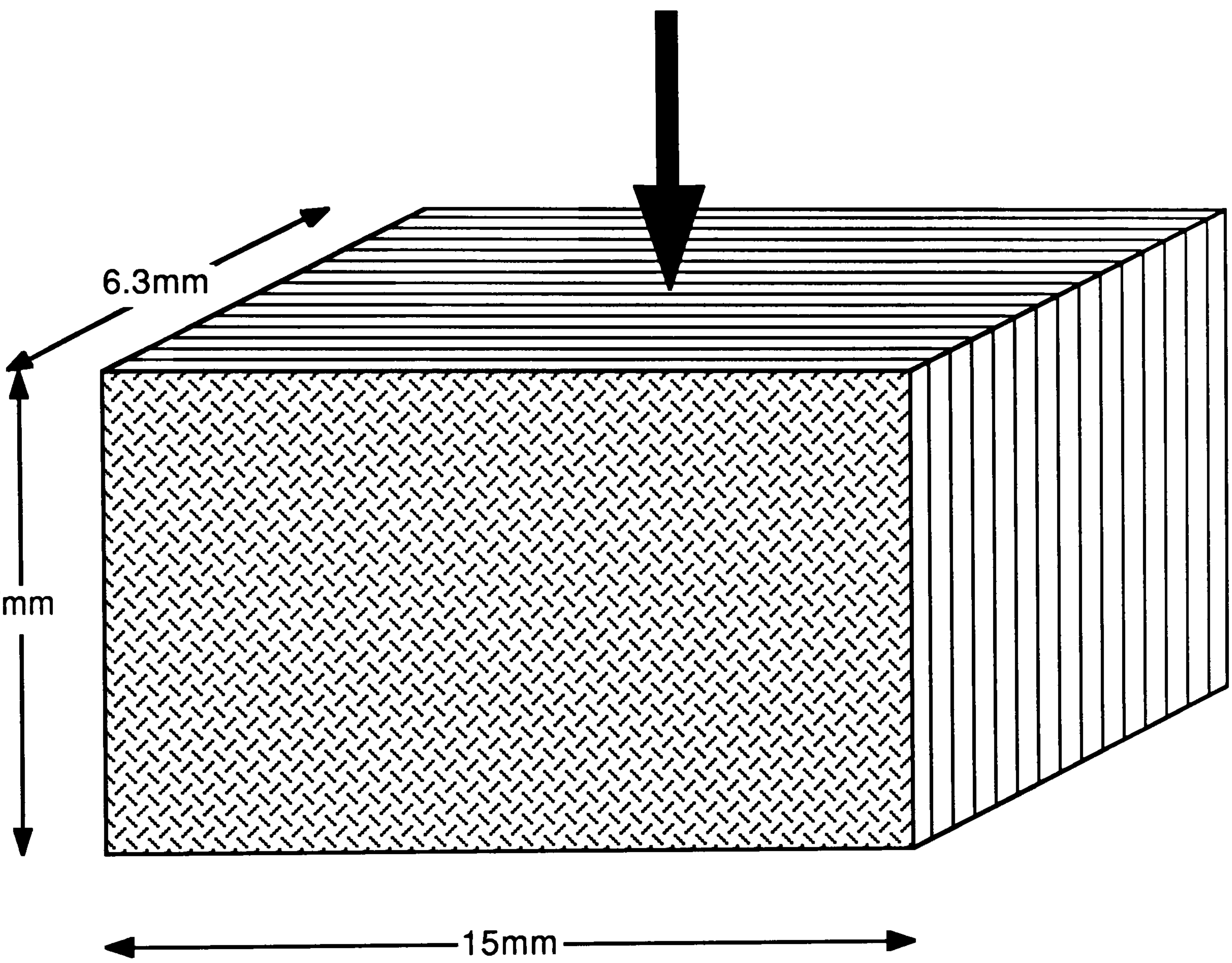

Figure 2.12 Sample cut from 2-D Carbon/Carbon composite which was tested in compression .

Chapter 3

CONTACT

3.1 Introduction

This chapter is the first of three which will present the results of the experimental work completed. It is an investigation of contact between a glass container and handling material, looking at the problems of both mechanical and thermal damage. The properties of handling materials which may affect contact are examined, and this leads to the construction of a computer model of contact. To help assess the model, contact was carried out in a controlled way on soda-lime-silica glass rods, which were then tested to failure in an attempt to determine the effect of contact on the strength of the glass.

It is known that contact between glass and a material causes damage which results in a reduction in the strength of the glass, this was discussed in chapter one. It is also known that hot glass containers are damaged by being handled during production both mechanically and by thermal shock, resulting from the temperature difference between the container and the handling material. What was not known was the way in which these two mechanisms interacted, if one mechanism dominated or if the total damage was a cumulative effect.

3.2 The theory of damage

To understand these mechanisms and how they interact it is important to understand how damage affects the strength of the glass.

The theoretical strength of glass is estimated to be about 10GPa, where-as commonly determined strengths of glass articles are in the region of 48MPa. Glass containers tested by Budd (1980) regularly had strengths of only 30MPa after passing quality control tests. Griffith (1920) in his classic work postulated that the discrepancy between the observed and the theoretical strength of glass was due to the presence of cracks on the surface of the material. Such cracks or fissures at the surface or in the interior of a solid were acting as stress concentrators so causing the stress at the end of the flaw to be many times greater than the applied load. Thus failure occurred on the growth of such pre-existing cracks under the effect of a stress many times less than the theoretical strength of the material.

To investigate this, Griffith (1920) looked at the energy balance of the total system, that is a loaded crack in a thin infinite plate, see figure 3.1

If the crack was to extend by a small amount δa there would be a consequent change in the energy of the system. This can be described by

$$\delta E_{surf} + \delta E_{el} + \delta E_{pot} = 0 \tag{3.1}$$

were $E_{surf}$is the energy needed to create the new free surfaces of the crack, E_{el} is the elastic energy of the plate, and E_{pot} is the potential energy of a loading weight.

It is possible to consider the change in the potential energy (δE_{pot}), as the crack growes by δa, in terms of the change in the elastic energy (δE_{el}) (Eshelby, 1968). If they are considered in terms of the areas under the curves in the force displacement plot in figure 3.2, which assumes linear elastic conditions. Then

$$E_{el}(a) = OAB \tag{3.2}$$

$$E_{el}(a + \delta a) = OA'B' \tag{3.3}$$

Hence

$$\delta E_{el} = \frac{1}{2}OA' \times A'B' - \frac{1}{2}OA \times AB \tag{3.4}$$

As

$$AB = A'B' \tag{3.5}$$

for dead load as we have imagined then

$$\delta E_{el} = \frac{1}{2}AB(OA - OA') \tag{3.6}$$

which can be written

$$\delta E_{el} = \frac{1}{2}AA'B'B \tag{3.7}$$

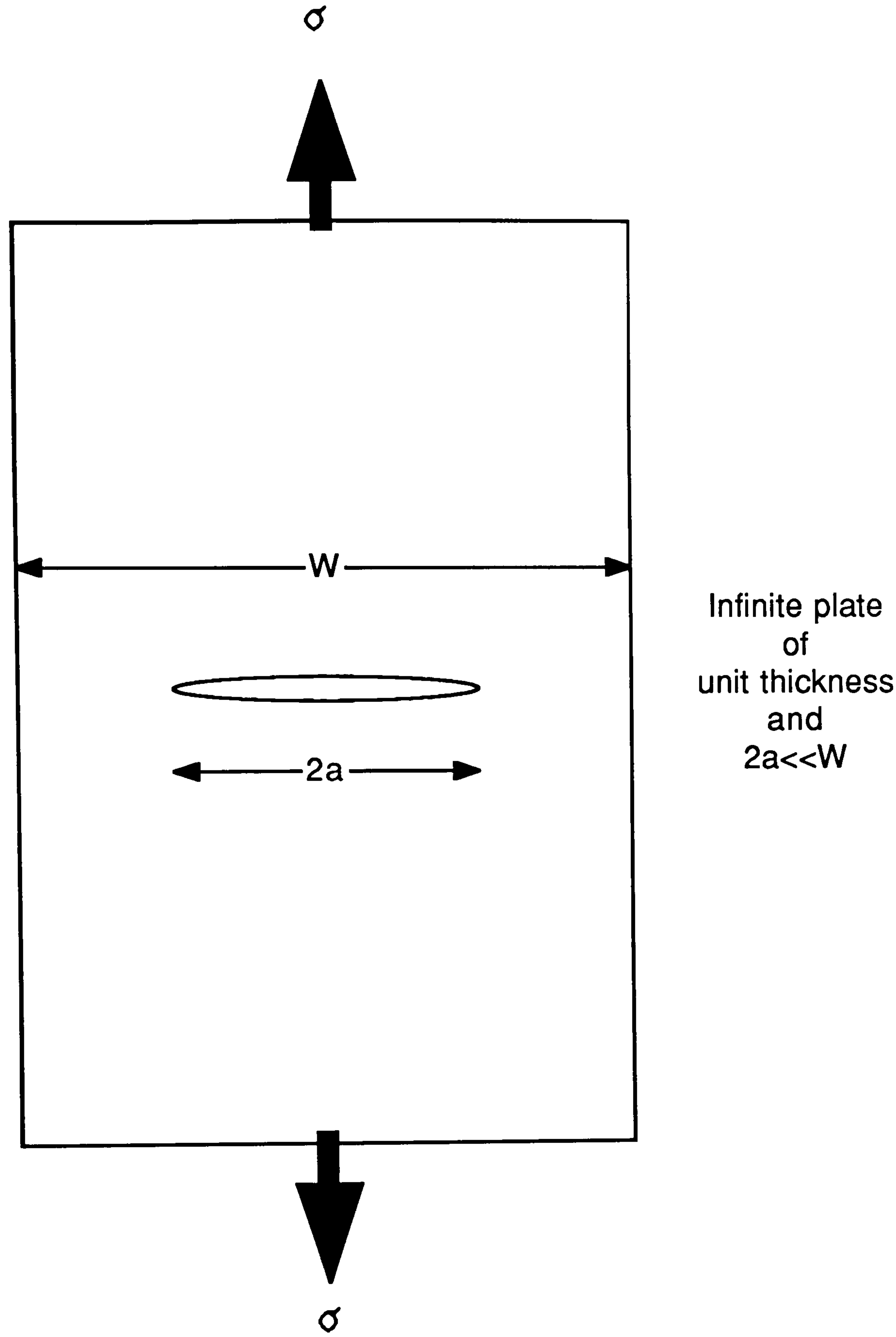

Figure 3.1 A through-cracked plate (Ewalds and Wanhill, 1985).

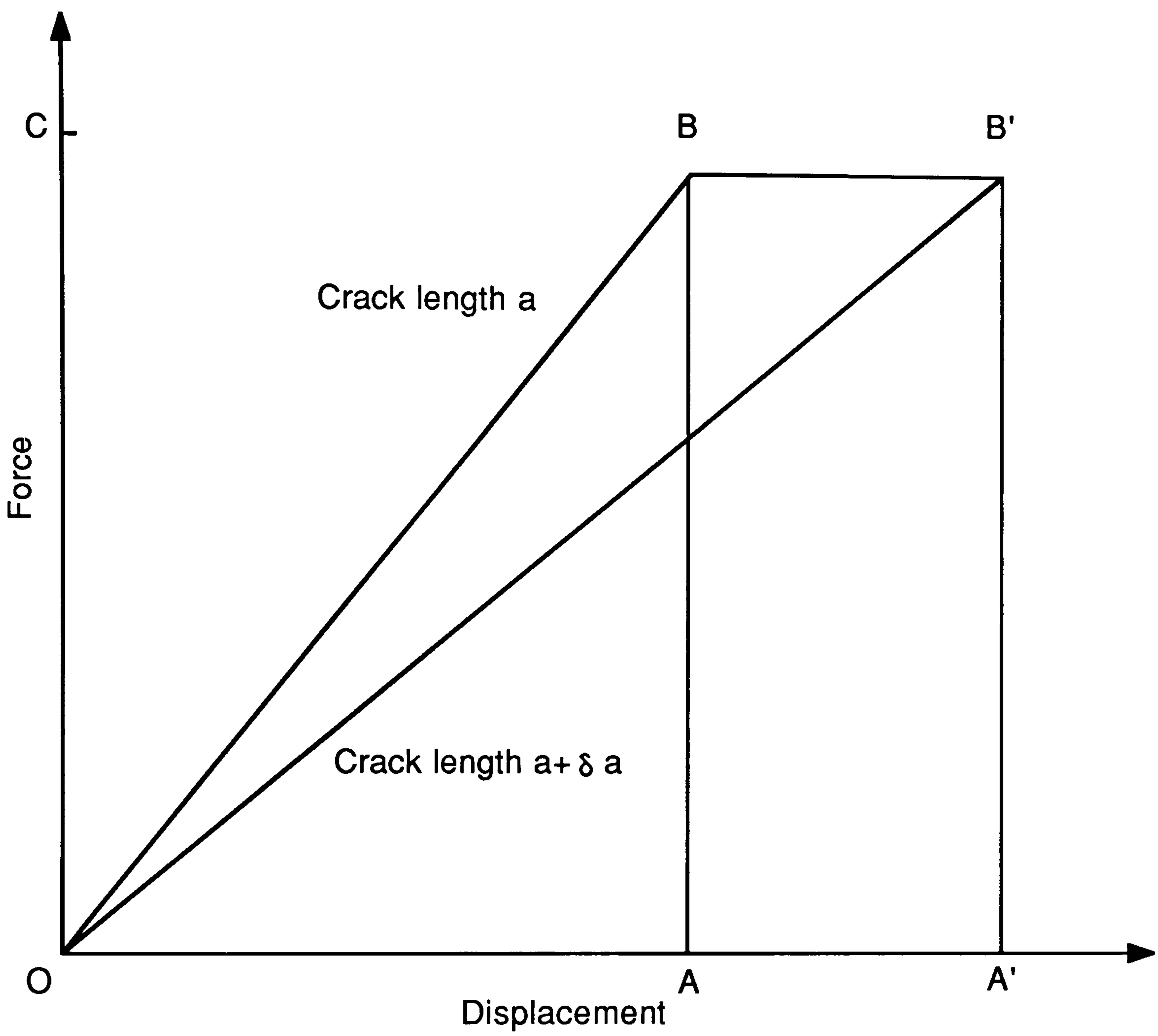

Figure 3.2 A graphical representation of the energy considerations in The Griffith Energy Balance approach to fracture.

The change in the potential energy produced by the weight dropping is

$$\delta E_{pot} = -AA'B'B \tag{3.8}$$

Thus the magnitude of the change in the elastic energy is half that of the change in the potential energy

$$\delta E_{el} = -\frac{1}{2}\delta E_{pot} \tag{3.9}$$

Substituting in to 3.1 and rearranging

$$\delta E_{surf} = -\delta E_{el} - (-2\delta E_{el}) \tag{3.10}$$

$$\delta E_{surf} = \delta E_{el} \tag{3.11}$$

The change in the energy of the free surface is simply a function of the surface energy per unit area γ. Thus

$$\delta E_{surf} = 4\gamma\delta a \tag{3.12}$$

Using the stress analysis developed by Inglis (1913), the elastic energy associated with a crack of length $2a$ can be shown to be

$$E_{el} = \frac{\pi\sigma^2 a^2}{E} \tag{3.13}$$

where E is the Youngs modulus. By writing $\delta E_{el} = \frac{\mathrm{d}E_{el}}{\mathrm{d}a}\delta a$ it is possible (Using equations 3.11, 3.12 and 3.13) to write the condition for fracture to occur as

$$\frac{\pi\sigma^2 a}{E} > 2\gamma \tag{3.14}$$

Thus saying that for the crack to grow the energy available must be greater than the energy needed to create the new free surfaces. The two sides of the inequality are known as G and R respectively. R is a property of the material and is known as the crack resistance force. G is known as the energy release rate and is a function of the specimen geometry and applied loads. For a crack to propagate G must exceed R.

Rearranging 3.16 it is clear that the tensile stress which must act perpendicular to a flaw to cause it to propagate is

$$\sigma = \sqrt{\frac{2E\gamma}{\pi a}} \tag{3.15}$$

Figure 3.3 illustrates the relationship for soda-lime-silica glass between crack size and strength. It can be seen that even very small cracks cause considerable reduction in the strength of the glass.

There are practical mathematical difficulties in using the energy balance for non ideal situations, Irwin (1957) developed an alternative approach. He showed that the stresses at the crack tip have the form

$$\sigma_{ij} = \frac{K}{\sqrt{2\pi r}} f_{ij}(\theta) \tag{3.16}$$

where r and θ are the cylindrical coordinates of a point ahead of the crack tip, and K is the stress intensity factor, a constant which determines the magnitude of the elastic stress field ahead of the crack. It is solely dependent on the loading configuration and the specimen geometry. In this approach it is assumed that a critical stress at a small distance ahead of the crack tip must be reached before fracture can occur. This critical stress is proportional to K_{1c} the critical stress intensity factor, where the subscript 1 denotes the mode of loading. There are three modes which are shown in figure 3.4, mode 1 is the most commonly used and so is the most often quoted. For fracture to occur K must be greater than K_{1c}, thus the criterion for fracture is

$$K > K_{1c} \tag{3.17}$$

The stress intensity factor for the idealised situation in figure 3.1 is

$$K = \sigma\sqrt{\pi a} \tag{3.18}$$

This expression for K only holds for the idealised situation. In most cases a geometrical factor must be introduced which takes account of such things as the proximity of boundary surfaces or other cracks, the orientation of the cracks, and

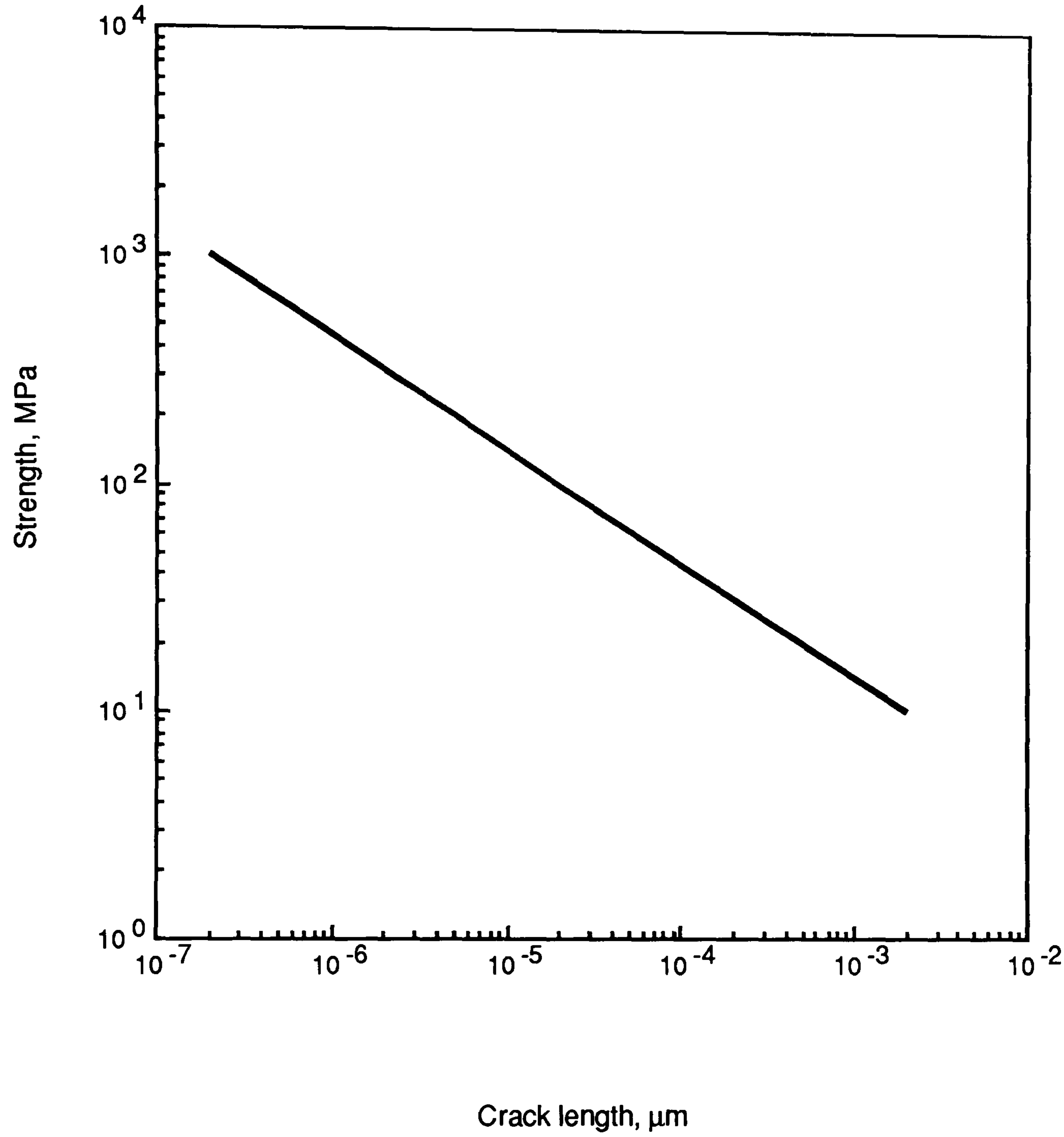

Figure 3.3 The relationship betweeen glass strength and flaw size for soda-lime-silica glass.

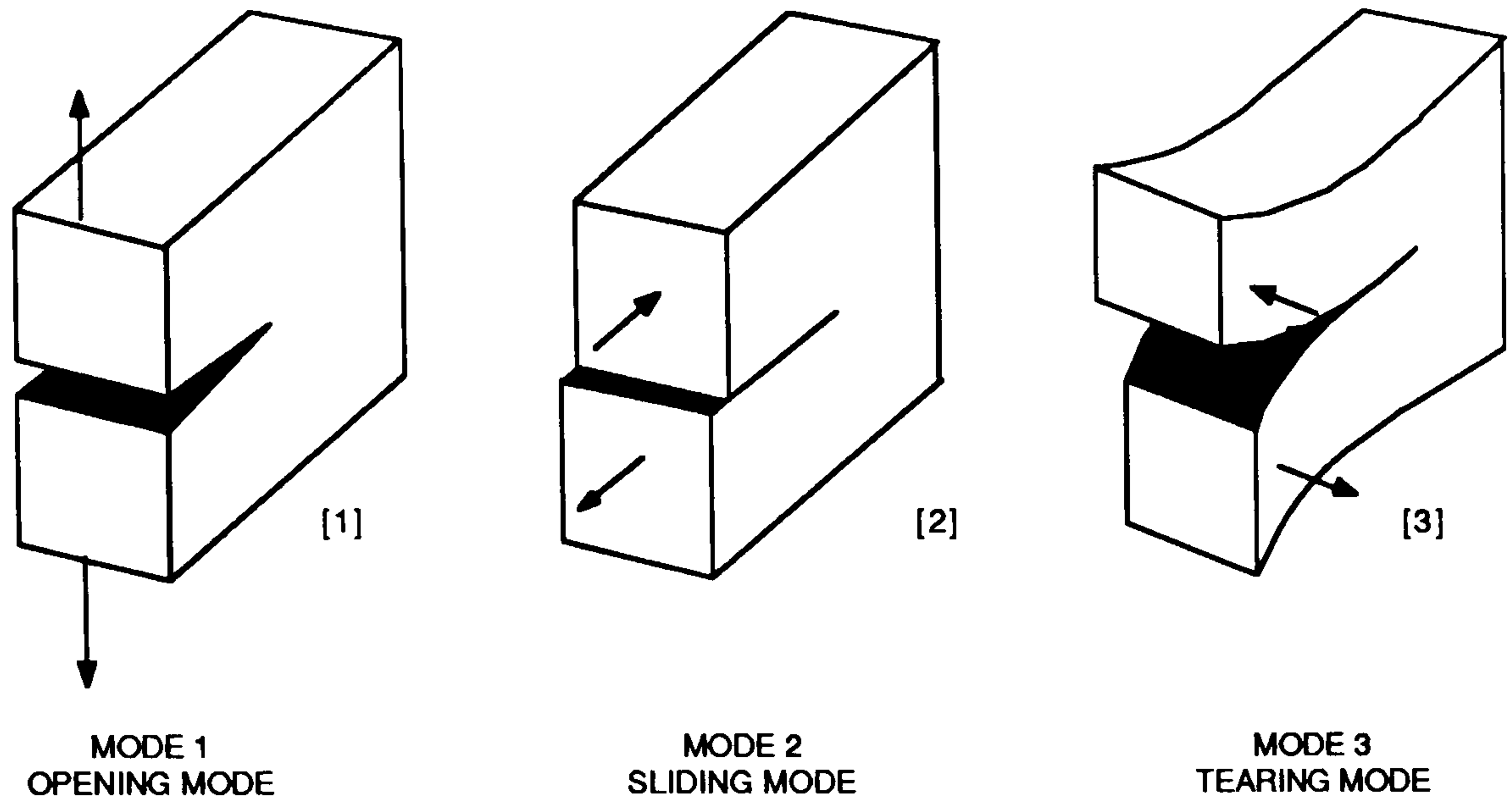

Figure 3.4 The three modes of loading (Ewalds and Wanhill, 1985)

the shape of the crack. These can be calculated analytically for simple geometries (for example Paris and Shi, 1965. Dugdale and Ritz, 1971). More complex geometries may be found in reviews by Cartwright and Rooke (1976,1978).

These two approaches can be related. Irwin (1957) showed that for plane stress conditions

$$G = \frac{K^2}{E} \tag{3.19}$$

The next step is to consider the theory, as it relates to the damage caused by handling hot glass.

3.3 Hypothesis of damage mechanism

The hypothesis is that; the total contact damage is caused by the action of thermally induced stresses, propagating mechanically produced flaws.

This is postulated after consideration of the results of Budd, Chown and Bourne (1980) who tested the effect of contact on the high strength internal surface of containers at 20°C and 300°C. They concluded that although significant damage occurred at 20°C a greater loss of strength resulted after contact at 300°C.

It was decided to investigate the mechanism further with the help of a mathematical model. This modelling was completed on a Research Machine Nimbus microcomputer.

3.4 The temperature distribution

The first step in the investigation was to establish the temperature distribution in the glass container and the handling material upon contact. This was impossible to determine experimentally as the contact is so short, less than one second (LeGood, 1987). It would be impossible to attach a temperature measuring device to such high speed machinery, any temperature sensitive paint would affect the contact. It was decided to model the situation mathematically.

To do this it was essential to examine the flow of heat across the interface from one material to another.

3.4.1 The analytical solution

The flow of heat is controlled by the differential equation,

$$\frac{\partial^2 T}{\partial x^2} - \frac{\rho c}{k}\frac{\partial T}{\partial t} = 0 \tag{3.20}$$

the equation of linear heat flow, where T=temperature, x=distance, ρ=density, c=specific heat capacity, t=time, and k=thermal conductivity.

The problem must be further defined by the specification of initial and boundary conditions. The simplest approximation used here is to assume perfect thermal contact between the glass and the contacting material. It is also assumed that the depth of the material effected is small compared with the dimensions of the contact zone. These assumptions allow the use of an existing analytical solution (Carslaw and Jaeger, 1959) for two semi-infinite materials (see Figure 3.5) coming together at time $t = 0$. The initial conditions of the problem can be expressed as

1. The temperature of the glass, T_g, has a constant value T_0

$$\text{when} \quad t = 0 \tag{3.21}$$

2. The temperature of the contact material, T_m, is constant and equal to zero

$$\text{when} \quad t = 0 \tag{3.22}$$

The conditions at the contact face, namely the boundary conditions are that there is perfect thermal contact so that

$$T_g = T_m \quad \text{at} \quad x = 0 \quad \text{when} \quad t > 0 \tag{3.23}$$

and that all the heat leaving the glass enters the contact material.

$$k_g \frac{\partial T_g}{\partial x} = k_m \frac{\partial T_m}{\partial x} \tag{3.24}$$

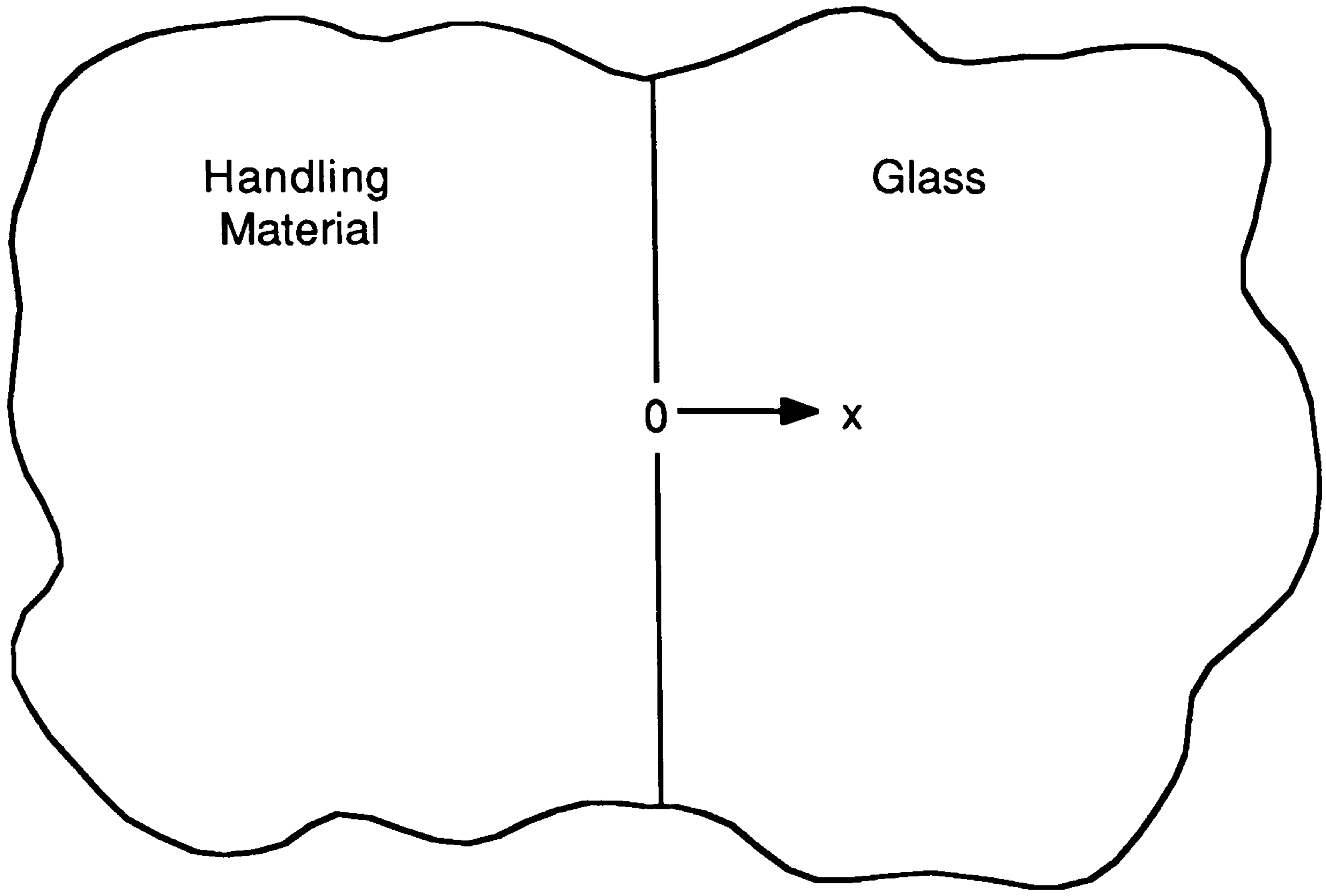

Figure 3.5 Representation of a semi-infinite composite solid.

$$\text{at} \quad x = 0 \quad \text{when} \quad t > 0$$

where the subscript g or m indicates that the symbol represents a property of either glass or handling material respectively.

For two semi-infinite materials the analytical solution was found in the literature (Carslaw and Jaeger, 1959) and is of the form

$$T_g = A_g + B_g \mathrm{erf} \frac{x}{2\sqrt{\frac{k_g t}{\rho_g c_g}}}, \quad x > 0 \tag{3.25}$$

$$T_m = A_m + B_m \mathrm{erf} \frac{|x|}{2\sqrt{\frac{k_m t}{\rho_m c_m}}}, \quad x < 0 \tag{3.26}$$

The constraints A_g, B_g, A_m, B_m, are chosen to satisfy the initial and boundary conditions, by applying the initial conditions 3.21 and 3.22

$$A_g + B_g = T_0 \tag{3.27}$$

$$A_m + B_m = 0 \tag{3.28}$$

the boundary conditions 3.23 and 3.24 give,

$$A_g = A_m \tag{3.29}$$

and

$$B_g k_g \left(\frac{k_g}{\rho_g C_g} \right)^{-\frac{1}{2}} = -B_m k_m \left(\frac{k_m}{\rho_m C_m} \right)^{-\frac{1}{2}} \tag{3.30}$$

Solving these equations and substituting into 3.25 and 3.26 the solution can be written as

$$T_g = \frac{k_g \kappa_g^{-\frac{1}{2}} T_0}{k_g \kappa_g^{-\frac{1}{2}} + k_m \kappa_m^{-\frac{1}{2}}} \left\{ 1 + \frac{k_m \kappa_m^{-\frac{1}{2}}}{k_g \kappa_g^{-\frac{1}{2}}} erf \frac{x}{2\sqrt{\kappa_g t}} \right\} \tag{3.31}$$

when $x > 0$ and

$$T_m = \frac{k_g \kappa_g^{-\frac{1}{2}} T_0}{k_g \kappa_g^{-\frac{1}{2}} + k_m \kappa_m^{-\frac{1}{2}}} erfc \frac{|x|}{2\sqrt{\kappa_m t}} \tag{3.32}$$

when $x < 0$ where κ_1 is the thermal diffusivity which is $k_i/c_i\rho_i$,where i can be g or m.

3.4.2 A dimensionless constant

The above solutions hold for the whole system, of particular interest was the interface at $x = 0$. A property of the solution is that as time proceeds the temperature at the interface remains constant.

$$T_g = T_m = \frac{k_g \kappa_g^{-\frac{1}{2}} T_0}{k_g \kappa_g^{-\frac{1}{2}} + k_m \kappa_m^{-\frac{1}{2}}} \tag{3.33}$$

By dividing this expression by $k_g \kappa_g^{-\frac{1}{2}}$ it was possible to express the constants as a dimensionless group (H)

$$T_g = T_m = \frac{T_0}{1 + \frac{k_m \kappa_m^{-\frac{1}{2}}}{k_g \kappa_g^{-\frac{1}{2}}}} = \frac{T_0}{1 + H}$$

where

$$H = \frac{k_m \kappa_m}{k_g \kappa_g} = \frac{\sqrt{\rho_m C_m k_m}}{\sqrt{\rho_g C_g k_g}} \tag{3.34}$$

The dimensionless group $H_m = \sqrt{\rho_m C_m \kappa_m}/\sqrt{\rho_g C_g \kappa_g}$ was isolated as it's value determines the temperature of contact which in turn influences the amount of thermal damage occurring. Table 3.1 shows the value of this grouping for some materials of interest.

Material	Density $\frac{kg}{m^3}$	Specific heat capacity $\frac{kJ}{kgK}$	Thermal conductivity $\frac{W}{mK}$	Dimensionless ratio H
Cu	8920	384	394	26.2
Ag	10500	235	427	23.2
Au	19310	129	315	19.9
Al	2702	202	237	17.1
Be	1850	1674	176	16.6
Ni	8900	442	92	13.6
SiC	2500	1422	84	12
Fe	7874	444	80	11.9
Pt	21450	133	7104	10.2
Cu10Al	7550	1375	51	8.6
P1	1880	648	112	8.3
Mn	1740	476	153	8.1
Al_2O_3	3900	795	25.6	6.2
Stainless steel	8020	461	17	5.6
Zn	7140	388	23	5.6
Ti	4500	519	22	5.1
Pb	11344	129	35	5.1
Zr	6500	233	23	4.2
C10/C12	1446	627	30	3.7
Ti5Al	4460	523	8	3.1
Ti7Al3Mo	4480	515	6	2.6
C1	1525	737	5	1.7

Table 3.1 Value of the grouping arranged in order of magnitude.

The first figures calculated were for the existing handling materials who's problem was durability, this is discussed in chapter 4. These acted as a bench-mark. Data was obtained from the T.P.R.C. data series, (1970), volumes 1, 2, 4 and 5. Data were not reported in the literature for C1, C10, C12† or P1†† and so was experimentally determined as described in chapter 2. The materials tabulated fall into three categories,

- Those historically used for glass handling.
- Those presently used for glass handling.
- Those possibly possessing properties that could be exploited for hot glass handling.

The aim was to identify materials worth further investigation. From the list several materials were identified as having similar thermal properties to existing hot glass handling materials. Alumina, silicon carbide and other industrial ceramics were not pursued because of their high hardness. Of interest were the metals found to possess a likely set of properties, in earlier work (United Glass Research Group, 1979) metals were ruled out in general terms because of the historical use of steel and brass both with dimensionless constants indicating an inappropriate set of properties. Lead, Zirconium, Titanium and stainless steel were identified as candidate materials. Lead was abandoned on health grounds and it was interesting to discover that stainless steel mosquito netting is a common glass handling material in some parts of the world (Vickers, 1987).

It was decided to look further at the possibility of both Titanium and Zirconium as hot glass handling materials.

3.4.3 Model of single contact temperature distribution

Equation 3.31 was used to calculate the temperature distribution in a glass container in contact with a certain handling material. The temperature was calculated for $1\mu m$ intervals from 0 to $1500\mu m$ at time t. The calculated data was then transferred to a data file.

† The materials prefixed with the letter C are all Johnson Radley materials, marketed as Cerberites.

†† The material labelled here as P1 is marketed under the name Poco glassmate.

The program was checked by calculating on paper, with the aid of a pocket calculator and an error function table, the result for a particular situation and comparing the answer with that produced by the program. The answers arrived at by the two different routes, for three such situations, are compared in Table 3.2.

Values of			The answer determined using calculator and tables (°C)	The answer determined by the computer program (°C)
T_0 (°C)	t (seconds)	x (μm)		
600	0.01	10	251	250
300	0.1	50	132	132
300	0.001	30	219	220

Table 3.2 Comparison of calculation made to check the computer program.

The computer program was assumed to be correct.

Figures 3.6-3.10 show the results of computations for some existing materials and Titanium, at t=0.001, 0.01 and 0.1 second. The contact temperature is constant for each material, but as time progresses, the temperature distribution changes. The time of contact affects the depth from which heat is drawn from the glass although the depth from which heat is drawn is hardly changed by which material contacts the glass. C1, C10 and Titanium give approximately the same effect and for P1 and iron there is only an 8% increase in the penetration. The difference between these materials is the temperature at the interface upon contact. They range from 23°C for iron to as high as 112°C for the polymer based C1. These variations will drastically affect the thermal stresses at the surface of the glass.They are examined in section 3.5.

3.4.4 Finite difference solution

The analytical solution enabled the evaluation of the temperature distribution at any time after the handling material and the container have come into contact, but it did not allow for the consideration of any cumulative effects on the second, third or fourth etc. bottle to contact the handling material. To enable

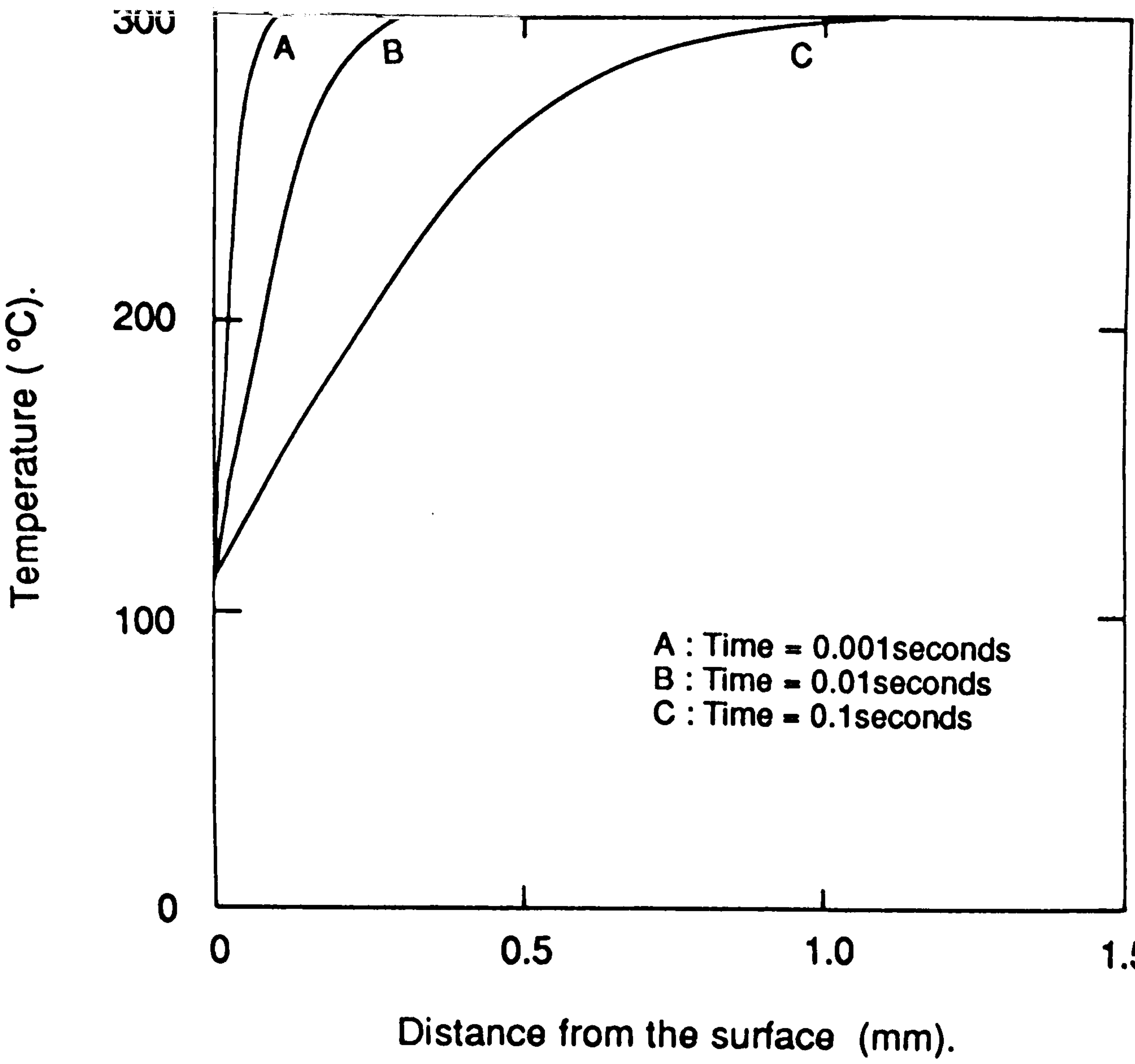

Figure 3.6 The temperature distribution in the glass after contact with C1, as calculated by the computer model

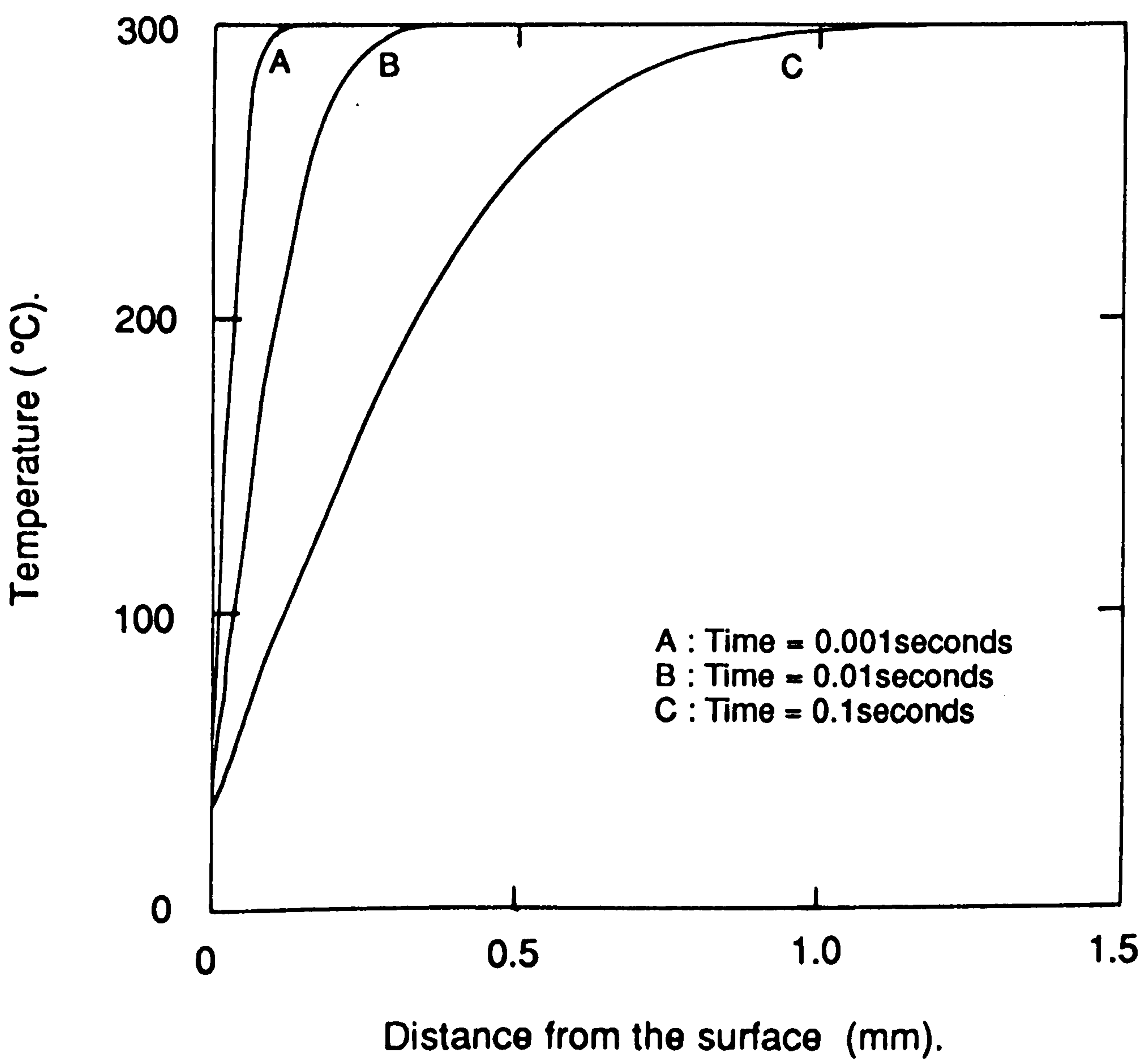

Figure 3.7 The temperature distribution in the glass after contact with P1, as calculated by the computer model

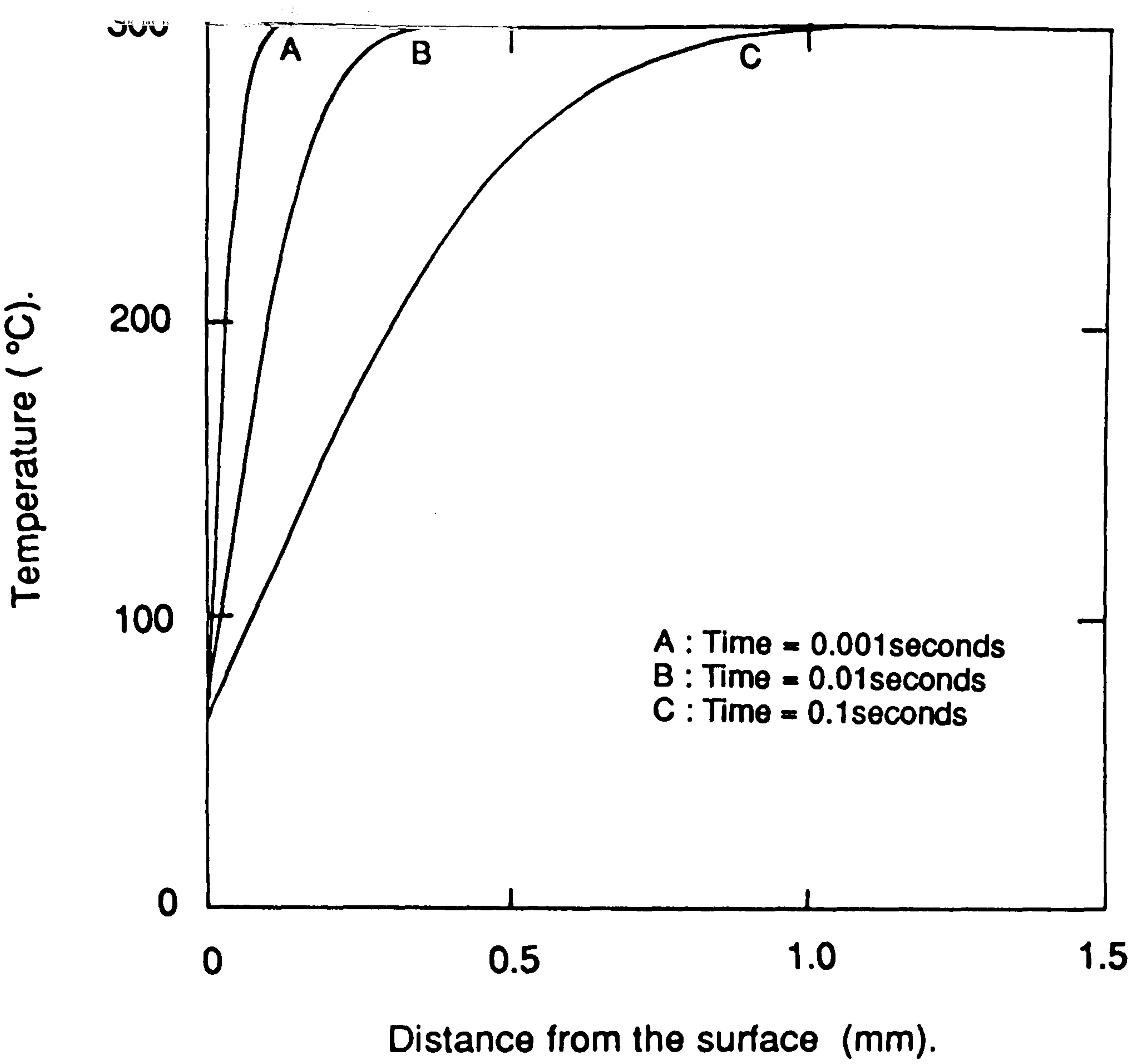

Figure 3.8 The temperature distribution in the glass after contact with C10, as calculated by the computer model

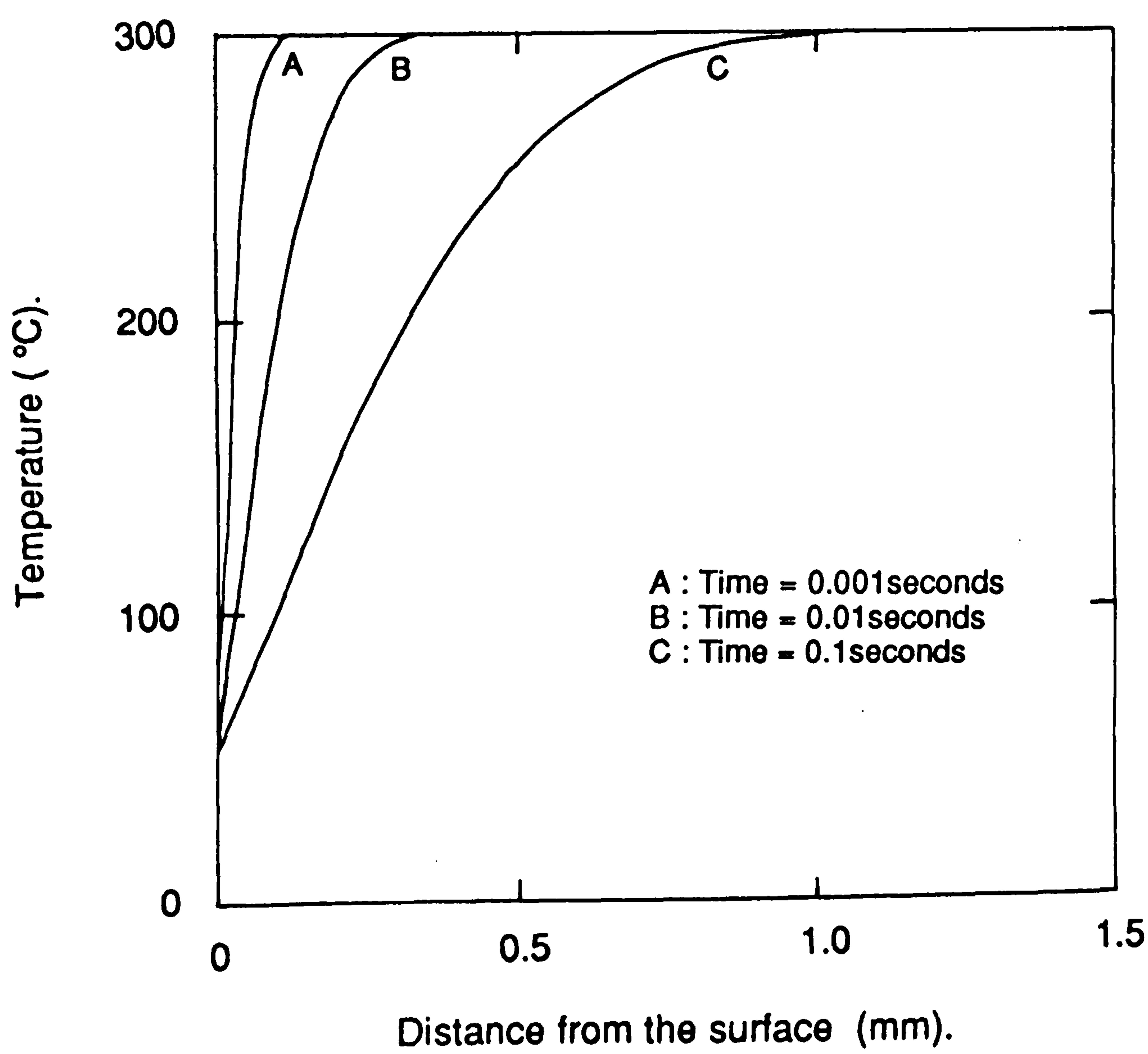

Figure 3.9 The temperature distribution in the glass after contact with Ti, as calculated by the computer model

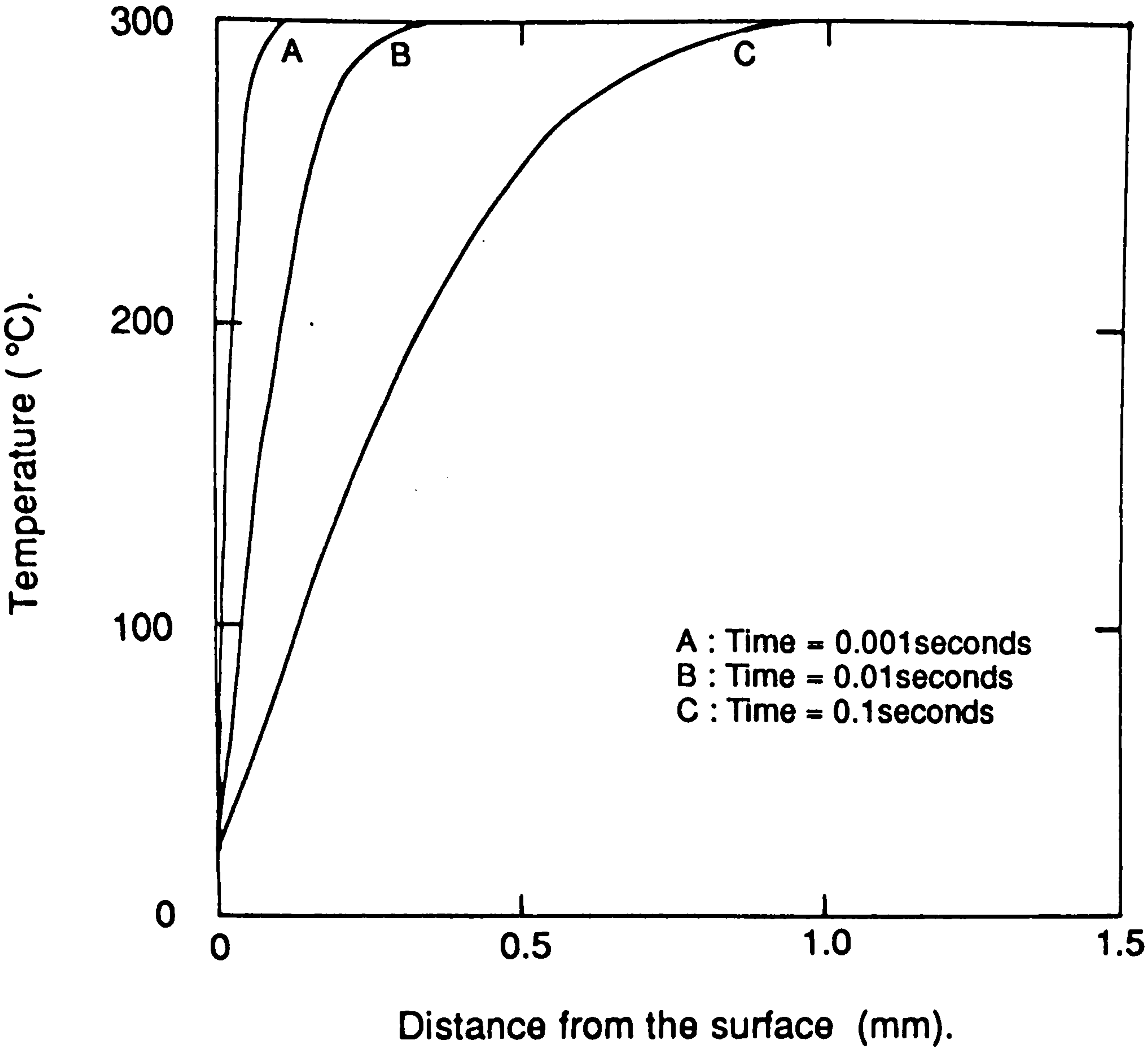

Figure 3.10 The temperature distribution in the glass after contact with Fe, as calculated by the computer model.

the evaluation of the effects of multiple contacts a second method of solution was considered. The second method of solution uses finite difference techniques, from which an approximate computational solution is obtained. This method does not require the assumption to be made that the materials are semi-infinite solids. So calculations can be made of the temperature distribution in finite materials. It is important to realise that the term approximate is used, in that the derivatives at a point are approximated by difference quotients over a small interval i.e.$\partial\phi/\partial x$ is replaced by $\delta\phi/\delta x$ where δx is small.

The finite difference estimate of a derivative at a point is made in terms of the values of the function $f(x)$ at several neighbouring points. If a function $f(x)$ is considered, see figure 3.11, $\mathrm{d}f(x)/\mathrm{d}x$ at $x = 0$ can be estimated from expressions for $f(x)$ at x_{-1}, x_0 and x_1. As the depth of the material being considered is small compared with it's other dimensions, the problem can be considered in one dimension. An estimate of $\mathrm{d}f(x)/\mathrm{d}x$ at $x_{\frac{1}{2}}$ is

$$\frac{\mathrm{d}f(x_{\frac{1}{2}})}{\mathrm{d}x} = \frac{f(x_1) - f(x_0)}{\Delta x} \tag{3.35}$$

and at $x = -\frac{1}{2}$

$$\frac{\mathrm{d}f(x_{-\frac{1}{2}})}{\mathrm{d}x} = \frac{f(x_0) - f(x_{-1})}{\Delta x} \tag{3.36}$$

If either of these were used as an estimate of $\mathrm{d}f(x)/\mathrm{d}x$ at $x = 1$ it would be termed a forward or backward difference estimate respectively. Clearly these are one sided, a better estimate would be made using points on either side as in equation 3.37

$$\frac{\mathrm{d}f(x_0)}{\mathrm{d}x} = \frac{f(x_1) - f(x_{-1})}{2\Delta x} \tag{3.37}$$

known as the central difference estimate. It is equal to the average of the two other estimates. The same method can be used to estimate the second derivative, by using the estimates of $\frac{\mathrm{d}f(x)}{\mathrm{d}x}$ made at $x_{\frac{1}{2}}$ and $x_{-\frac{1}{2}}$.

$$\frac{\mathrm{d}^2 f(x_0)}{\mathrm{d}x^2} = \frac{\left(\frac{f(x_1)-f(x_0)}{\Delta x}\right) - \left(\frac{f(x_0)-f(x_{-1})}{\Delta x}\right)}{\Delta x} \tag{3.38}$$

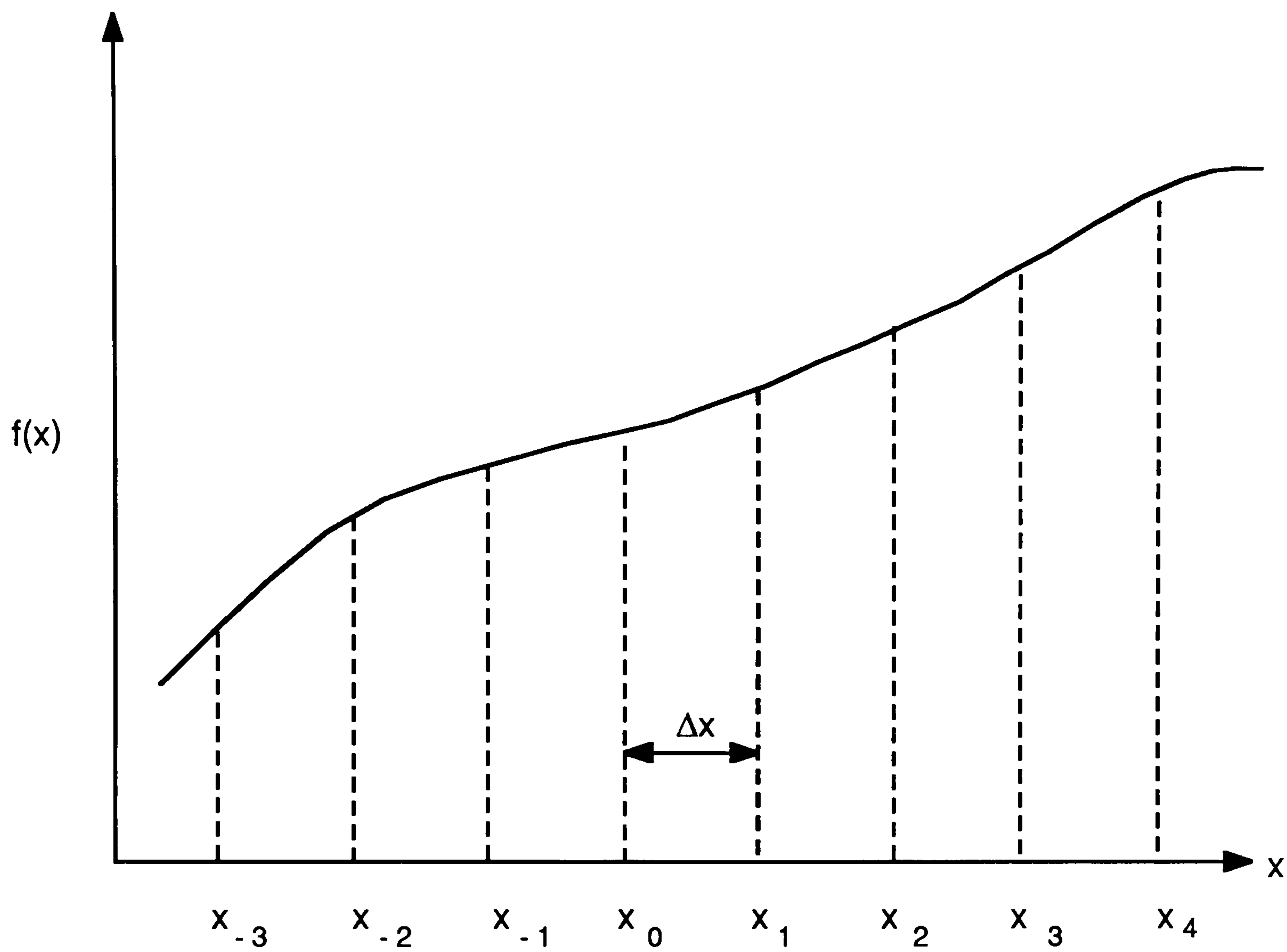

Figure 3.11 Schematic representation of a function.

$$= \frac{f(x_1) - 2f(x_0) + f(x_{-1})}{\Delta x^2} \quad (3.39)$$

this is again a central difference estimate.

Returning to the problem, the heat equation

$$\frac{\partial^2 T}{\partial x^2} = \frac{\rho c}{k}\frac{\partial T}{\partial t} \quad (3.40)$$

the left hand side of the equation can be expressed as

$$\frac{T_1 - 2T_0 + T_{-1}}{\Delta x^2} \quad (3.41)$$

where T is the temperature at equidistant sites spaced Δx apart at time t.The derivative in the right hand side of the equation can be expressed as

$$\frac{T_0' - T_0}{\Delta t} \quad (3.42)$$

where T_0 is the temperature at x_0 at time t and T_0' is the temperature at the same point at time $t + \delta t$. This is the forward difference quotient.

Thus equation 3.40 can be expressed in finite difference terms as

$$\frac{T_1 - 2T_0 + T_{-1}}{\Delta x^2} = \frac{\rho c}{k}\left(\frac{T_0' - T_0}{\Delta t}\right) \quad (3.43)$$

If we rearrange this expression and isolate the dimensionless group known as the Fourier number(Fo) $= \frac{k\Delta t}{\rho c \Delta x^2}$ then

$$T_1 - 2T_0 + T_{-1} = \frac{1}{\mathrm{Fo}}T_0' - \frac{1}{\mathrm{Fo}}T_0 \quad (3.44)$$

thus

$$T_0' = \mathrm{Fo}\left[T_1 + T_{-1} + \left(\frac{1}{\mathrm{Fo}} - 2\right)T_0\right] \quad (3.45)$$

The Fourier number (Fo) is defined to assist in the representation of transient heat flow calculations and is an indication of the speed at which a body will react to a temperature change.

Equation 3.45 enables the calculation of the temperature at points or nodes within the body of the container or the handling material. However, to complete a computation of the temperature distribution expressions were also required for the back faces and the contacting faces. In the model the back face of the handling material and the internal face of the container were set at a fixed temperature thus introducing further boundary conditions. This was believed to be a reasonable simplification, as the handling material is attached to the large bulk of the handling machinery and so likely to be kept at ambient temperature. The glass container was believed to lose heat from a surface layer only, so the internal surface would be relatively unaffected. The interface upon contact presented a more complex situation. It was intended that the modelled handling material would contact a hot container, and then before meeting the next container the free surface of the material would undergo cooling by convection.

Consequently two further finite difference equations were needed. Firstly an expression for a node representing the interface during contact. Equation 3.46 (Croft and Lilly, 1977) does this taking account of the fact that neighbouring nodes are in different materials

$$T_0' = \bar{\mathrm{Fo}}\left[\left(\frac{k_g T_1 + k_m T_{-1}}{k_g + k_m}\right) + T_0\left(\frac{1}{\bar{\mathrm{Fo}}} - 1\right)\right]$$

where

$$\bar{\mathrm{Fo}} = \frac{2\Delta t}{\Delta x^2}\frac{k_g + k_m}{\rho_g c_g + \rho_m c_m} \tag{3.46}$$

A second expression is used during noncontact, heat is lost from the free surface by convection. The rate at which heat is lost from the handling material is a further boundary condition. It is controlled by the differential equation 3.47

$$\frac{\partial T}{\partial n} = -\frac{h}{k}(T - T_A) \tag{3.47}$$

where T is the surface temperature, T_A is the ambient temperature, n is the direction normal to the surface and h is the heat transfer coefficient. Equation 3.48 is the finite difference expression used for this boundary node (Croft and Lilly, 1977)

$$T_0' = 2\mathrm{Fo}\left[T_1 + \mathrm{Bi}T_A + T_0\left(\frac{1}{2\mathrm{Fo}} - 1 - \mathrm{Bi}\right)\right]$$

where

$$\text{Fo} = \frac{k\Delta t}{\rho c \Delta x^2} \quad \text{and} \quad \text{Bi} = \frac{h\Delta x}{k} \tag{3.48}$$

A further dimensionless group has been extracted in this expression known as the Biot number (Bi) it is the ratio of the surface conduction to the internal conduction. Its value gives an assessment of whether surface heat transfer or internal conductance will be controlling the temperature of the body. The higher the Biot number is, the more likely internal conduction will be the controlling factor.

3.4.5 Constructing a model of repeated contact

The finite difference expressions 3.45, 3.46 and 3.48 were used to construct a program which models the way the temperature distribution changed through multiple contacts. Writing the program consisted mainly of producing a procedure which calculated the new temperature at a particular node after considering the position of that node in the system and thus which expression was appropriate to it. A flow diagram of the program is shown in figure 3.12.

The ambient temperature in the model was set at 0°C and the temperature of each new glass container at 300°C, identical conditions to those used in the analytical model. The heat transfer coefficient used was $15\text{Wm}^{-2}\text{K}^{-1}$, typical for natural convection (Coulson and Richardson, 1985). The times of contact and cooling were varied but the time step was kept constant for all runs at 0.0001sec. Such a small time step was needed to retain stability in the finite difference equations. The reasoning behind this can best be explained by examining a finite difference equation such as 3.45

$$T_0' = \text{Fo}\left[T_1 + T_{-1} + \left(\frac{1}{\text{Fo}} - 2\right)T_0\right]$$

If the coefficient of T_0 is negative the equation dictates that the lower T_0 was the higher T_0' would be but this would violate the principles of thermodynamics and it thus follows that a condition for stability is that for a given Δx, Δt must be chosen so that $(\frac{1}{\text{Fo}} - 2)$ is not negative. This simple rule is sufficient for explicit expressions such as those used here. In the calculations undertaken the limiting equation was 3.46 calculating the temperature at the interface.

Figure 3.12 Flow chart representation of the computer program for calculating the temperature distribution.

The node spacing was 0.0001m, (0.1mm), with 60 nodes calculated for each material the program was modelling. Each material was 6mm thick.

3.4.6 Initial estimates

Table 3.3 shows the temperatures after contact of 0.1sec at the interface between the glass and the various handling materials, predicted by the finite difference model. Alongside are those evaluated by the analytical solution. The two models calculate the complete distribution but for comparison the contact temperatures are sufficient.

	Temperature at contact interface	
Handling Material	Finite difference solution	Analytical solution
C1	112	112
C10	64	64
Titanium	50	50
Poco glassmate	31	32
Iron	23	23

Table 3.3 Temperatures at the contact surface calculated by the analytical and finite difference models.

It is clear that the two models agree. The advantage of this second finite difference model is that it is possible to adapt this model to investigate different plant conditions. Of interest is the effects of multiple contacts on the handling material, particularly that of varying times of contact and the ratio of contact to cooling.

3.4.7 Effects of varying contact times

C1 was used to investigate the effects of changing system parameters. The program was executed with equal contact and cooling times and then with different ratios of contact to cooling. The times chosen were not exact line conditions as non were available, but they were reasonable.

With all the combinations tried the system reached a pseudo steady state where the heat lost during cooling was equal to the heat gained through contact with the next hot bottle. At any stage in the cycle the temperature distribution was constant. The program reached this state after a particular number of cycles, the number depending on the conditions. In table 3.4 the contact temperature at the pseudo steady state is shown along with the number of cycles to reach it.

Contact time (seconds)	Cooling time (seconds)	Number of cycles to reach pseudo steady state	Contact temperature °C
0.1	0.1	30	238
0.3	0.3	17	210
0.5	0.5	12	195
0.1	0.2	30	214
0.2	0.4	16	194
0.3	0.6	11	182
0.1	0.05	41	257
0.2	0.1	25	243
0.3	0.15	17	233

Table 3.4 Variations in the pseudo steady state due to different contact and cooling times.

Generally it is seen that the temperature of the interface rises as the rate at which the bottles are presented to the material increases. This is as would be expected as more heat is being supplied in a set time interval. This also correlates with observed experiences (McDermot, 1987) that as line speeds have increased more oxidation resistant materials have been demanded by customers. Increases in the temperature of the handling material resulted in increased oxidation rates. The greatest variations in the contact temperature are between executions with different ratios of cooling and contact.

3.4.8 Temperatures at the pseudo steady state

For set conditions of contact t = 0.1 sec and cooling t = 0.2 sec and ambient temperature = 30°C the pseudo steady state was calculated for the five materials previously examined. The temperature distribution at the end of a contact cycle is shown in figure 3.13.

The temperature gradient established in the handling material is approximately linear for all materials whilst the temperature profiles in the glass are of similar shape to those for after a single contact although the temperatures at the interfaces are higher. Such data could be used to estimate the temperatures likely to be experienced by handling materials when line speeds or ambient temperatures are changed and so assist in the decision of which material is best suited to a particular position on the line.

3.4.9 Time to reach the pseudo steady state

Also examined was the way the different materials reached their pseudo steady state. Figure 3.14 shows the way the interfacial temperature increased with time. The same system conditions were used as in the previous section. The different materials reach the plateau at different rates, the higher their placing in the list of dimensionless ratio the slower they are to enter the steady state. All have reached it after 30 cycles which represents 1min 40secs. It is interesting to note that some of the profiles cross before reaching the plateau.

3.5 Effects of temperature distribution

3.5.1 Introduction

In section 3.4 the temperature distribution in a hot glass container, during contact, was determined. The next step was to investigate the way in which the effects of the distribution affect the strength of the glass containers. Many temperature distributions were calculated for each material in the last section, their values depending on the conditions set in the model. As the values varied so much depending on time of contact, cooling or ambient temperature it was decided to use

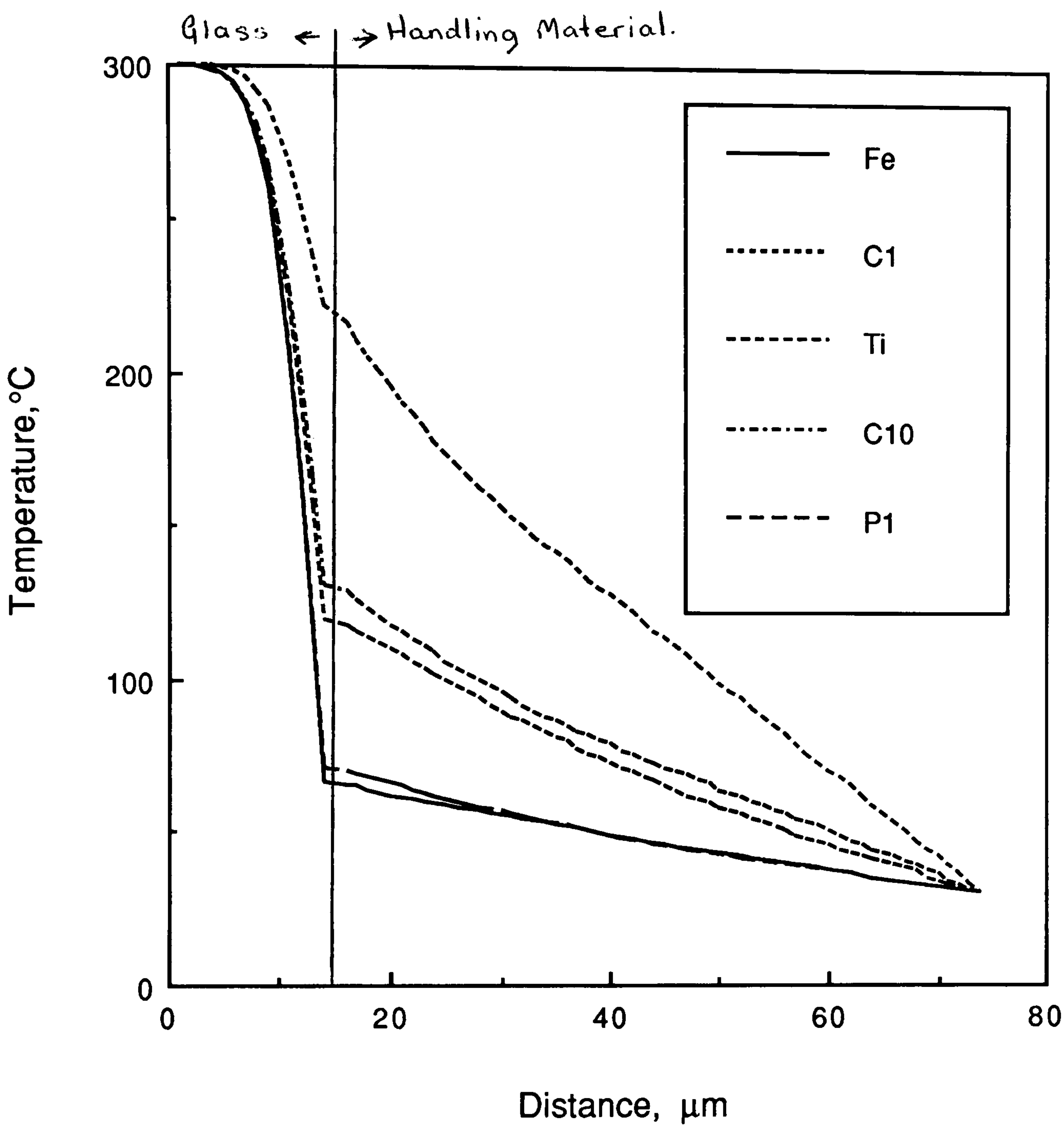

Figure 3.13 The pseudo steady state temperature distributions from the finite difference model.

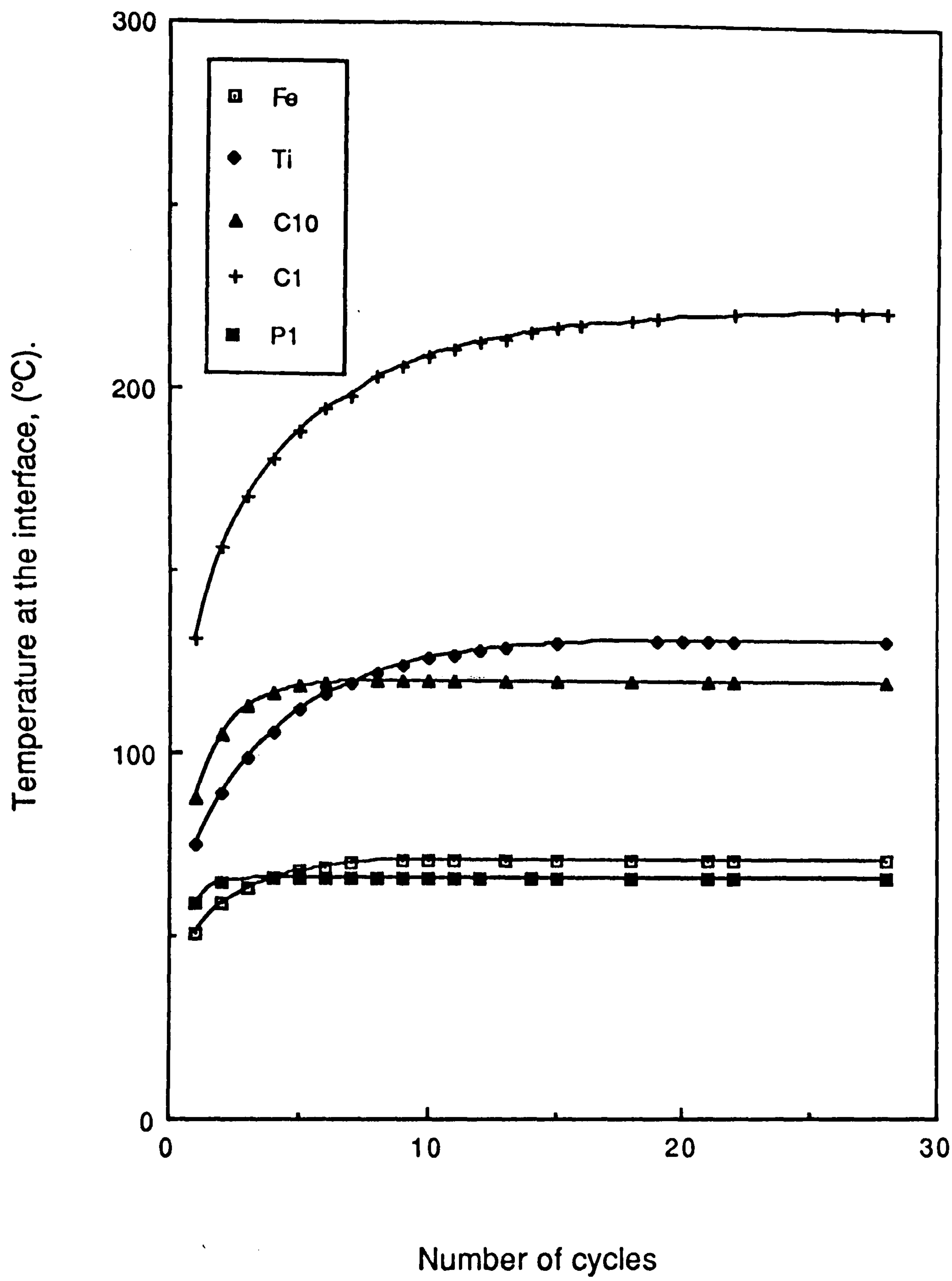

Figure 3.14 The way the temperature at the interface between the glass and the handling material increases with each cycle.

the initial distribution after one contact of 0.1sec where the ambient temperature was 0°C as a standard to use in further calculations.

3.5.2 Thermally induced stresses

Thermal stresses result from the temperature gradient in a material producing differential expansion. In a material with Young's modulus E, and coefficient of thermal expansion α (for soda lime glass $=9 \times 10^{-6}\mathrm{mK}^{-1}$)the stress field exerted can be calculated from equation 3.49.

$$\sigma = \alpha E(T_0 - T) \tag{3.49}$$

were T_0 is the bulk temperature and T is the temperature at the point of interest. The temperature distribution produces a stress distribution in the glass. The problem was to investigate the effect of these stresses on the glass surface.

The probability of the glass surface being completely free from flaws, even before contact, is so low that the actual problem is that of the effect of the thermal stresses on a flawed glass surface.

It was decided to investigate the interactions of the stresses and the flaws by the evaluation of stress intensity factors. Previous investigations (Emery and Kobayashi, 1980) of the thermal stresses resulting from quenching had used a similar approach. Their work centred on the effects of different configurations of cracks on a single material. Whereas the aim of this project was to assess different materials. For this reason a single configuration was considered. That of the idealised flat edge crack shown in figure 3.15 where $a/b \Rightarrow 0$.

It was believed that contact by handling materials produced further mechanical damage to the already flawed glass surface. To enable the effects of varying amounts of mechanical damage to be considered the stress intensity factors for cracks varying in length were to be evaluated.

3.5.3 Determining the stress intensity factor

In section 3.3 the concept of the stress intensity factor K was introduced. Equation 3.18 is the simplest expression for K, which holds only for a uniform

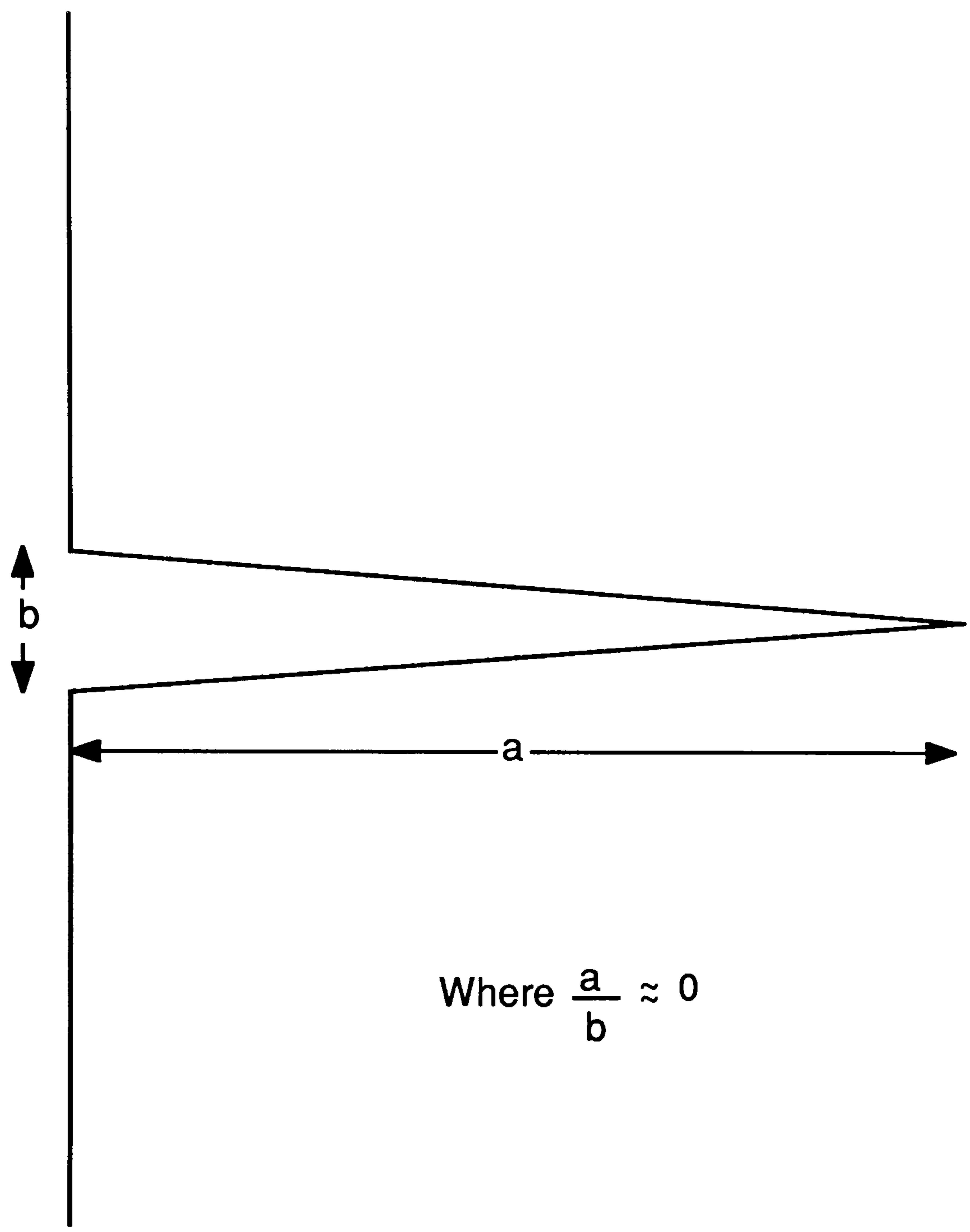

Figure 3.15 Idealised representation of an edge crack.

stress field in a semi-infinite solid. In this problem where the thermal stresses change over the length of a crack there is an inhomogeneous stress field and a more complex expression is needed. K in such a stress field can be evaluated from equation 3.50 (e.g.Lawn and Wilshaw, 1975)

$$K = 2\left(\frac{a}{\pi}\right)^{\frac{1}{2}} \int_0^a \left[\frac{\sigma_x}{(\sigma^2 - x^2)^{\frac{1}{2}}}\right] dx \tag{3.50}$$

where the integral sums the varying stresses over the length of the crack. Combining 3.49 and 3.50 in 3.51, K can be determined directly from the previously calculated temperature distributions.

$$K = 2\alpha E\left(\frac{a}{\pi}\right)^{\frac{1}{2}} \int_0^a \left[\frac{(T_0 - T_x)}{(a^2 - x^2)^{\frac{1}{2}}}\right] dx \tag{3.51}$$

It has been assumed that the flaws are far enough apart not to interact.

3.5.4 Computer program to calculate K

A program was written utilising equation 3.51 to evaluate K at a given time of contact t, for cracks varying in size from $0 - 1500\mu$m. A flow diagram is shown in figure 3.16 . This model uses the temperature distributions calculated by the program detailed in section 3.5.2, which were stored in data files.

A procedure was written to evaluate the integral. As the function in 3.50 has a singularity at $x = a$ this involved splitting the function into two parts to enable evaluation.

$$\int_0^a \frac{\Delta T_x}{(a^2 - x^2)^{\frac{1}{2}}} \mathrm{dx} = \int_0^a \left\{\frac{\Delta T_x - \Delta T_a}{(a^2 - x^2)^{\frac{1}{2}}} + \frac{\Delta T_a}{(a^2 - x^2)^{\frac{1}{2}}}\right\} \mathrm{dx} \tag{3.52}$$

This is shown graphically in figure 3.17.

By splitting the expression in this way the first fraction (Region A in figure 3.17) can be calculated through numerical integration, in this case the trapezium rule was used. The second half of the integral was evaluated using it's analytical solution, shown in equation 3.53.

$$\int_0^a \frac{\mathrm{dx}}{(a^2 - x^2)^{\frac{1}{2}}} = \arcsin\frac{x}{a} \tag{3.53}$$

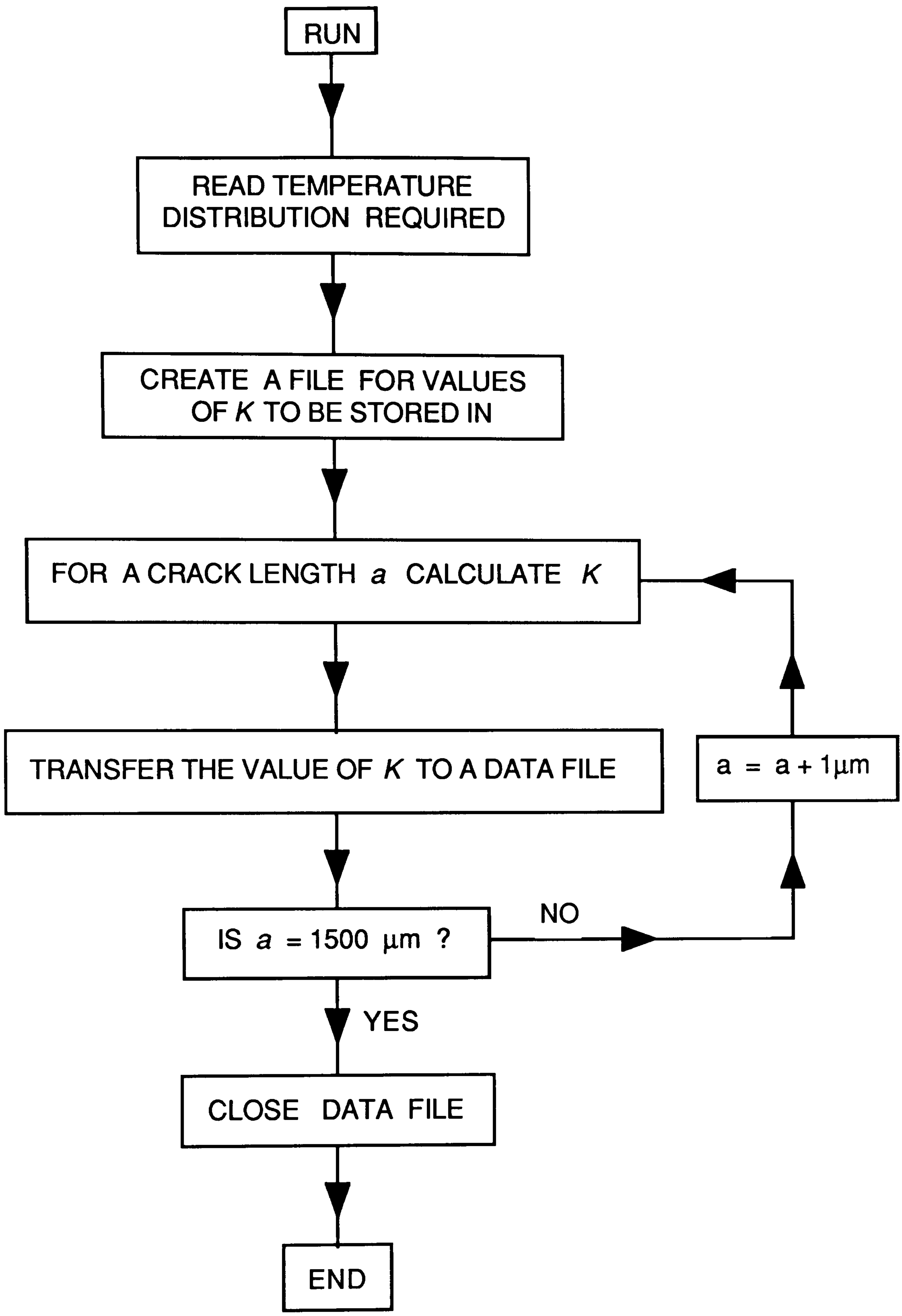

Figure 3.16 Flow chart representation of the computer program for calculating the stress intensity factor.

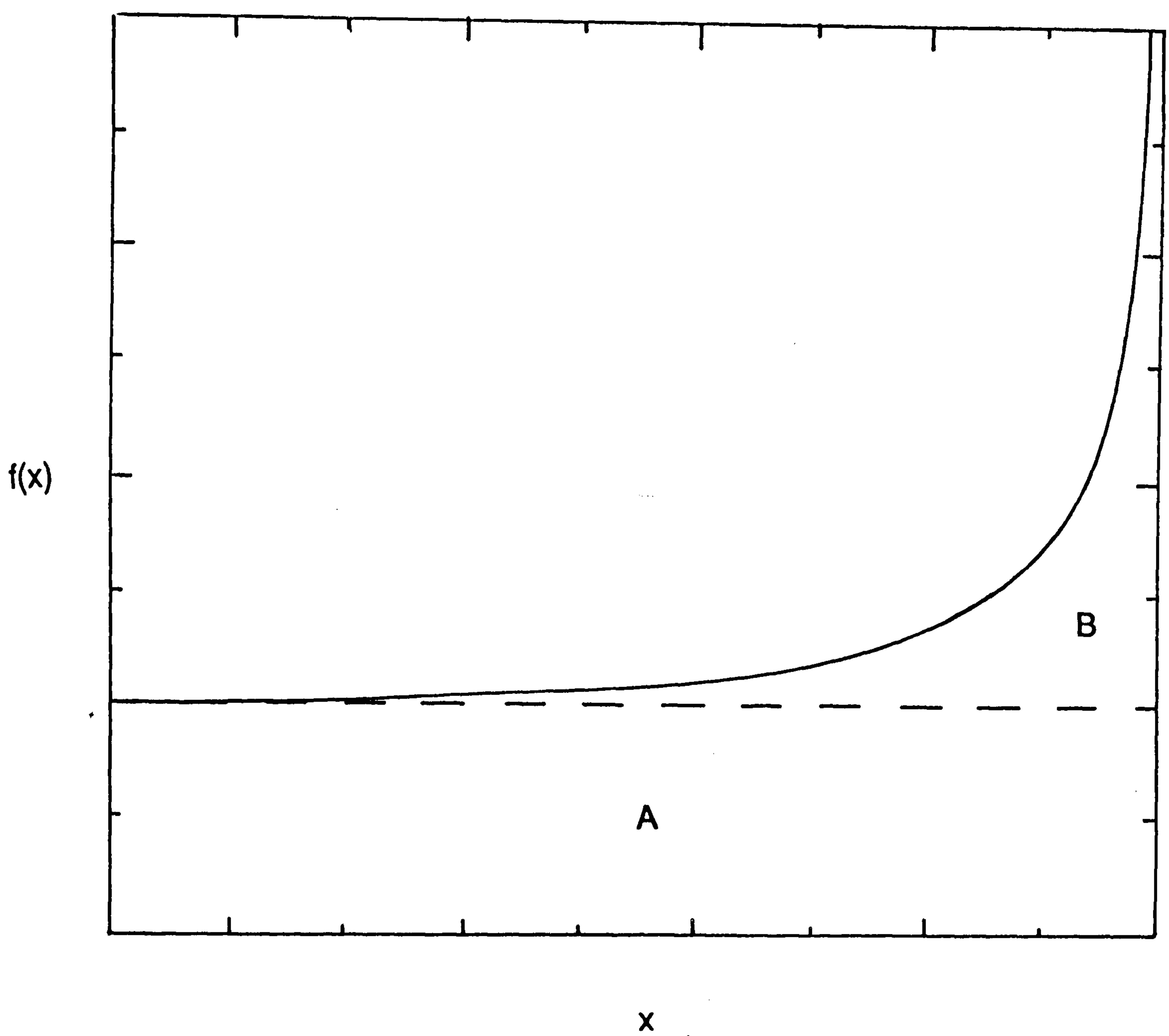

Figure 3.17 Representation of how the function is split up to enable the calculation of the integral of the function. The area, A is calculated numerically and B from a known analytical expression.

The integrals of the two parts were then summed to evaluate the total integral. The program's integration procedure was checked by using it to evaluate the integral of a function with a known analytical solution.

The values of the stress intensity factors were evaluated from the temperature distributions representing contact, with the materials already considered. Once determined they were also stored in data files, they are plotted in figures 3.18-3.22. Each curve shows how K changes for increasingly large cracks, in a single temperature distribution at time t. The horizontal line on each plot shows the critical value of the stress intensity factor K_{1c} for soda lime glass which is $0.8\text{MNm}^{-\frac{3}{2}}$. The form of all the families of curves is the same, the value of K increases to a maximum and then falls off. This characteristic form is very important and its interpretation enables a greater understanding of damage mechanisms.

3.5.5 Interpretation of the calculated stress intensity factors

As a consequence of the glass being subjected to an inhomogeneous thermal stress field, once a crack propagates it does not always lead to catastrophic failure. Looking closely at a single curve as in figure 3.23 it can be seen that K rises as the crack size increases but it has a value less than the critical K_{1c} until $a \approx 64.5\mu\text{m}$. For any crack below this size there is insufficient force on the leading atomic bonds for the crack to grow, it is stable. Any crack with length $\geq 64.5\mu\text{m}$ will propagate, and become, initially, unstable. But this will not result in the failure of the container as when the crack has grown to the length of $258.6\mu\text{m}$ the value of the stress intensity factor again falls below the critical value and the crack ceases to grow. In figure 3.24 the curves generated for each material after contact of 0.01 of a second are plotted to enable comparisons to be made.

It is clear that all the curves are very similar in shape each appearing to be simply shifted up or down from its neighbour, but these small differences change the amount of damage likely to occur. To enable the differences to be seen clearly the two extremes will be considered.

- In a glass container handled for 0.01 of a second by C1, no crack propagation takes place if the flaws present are less than $64.5\mu\text{m}$. If a crack is greater than $64.5\mu\text{m}$, a crack of $258.6\mu\text{m}$ will be produced.

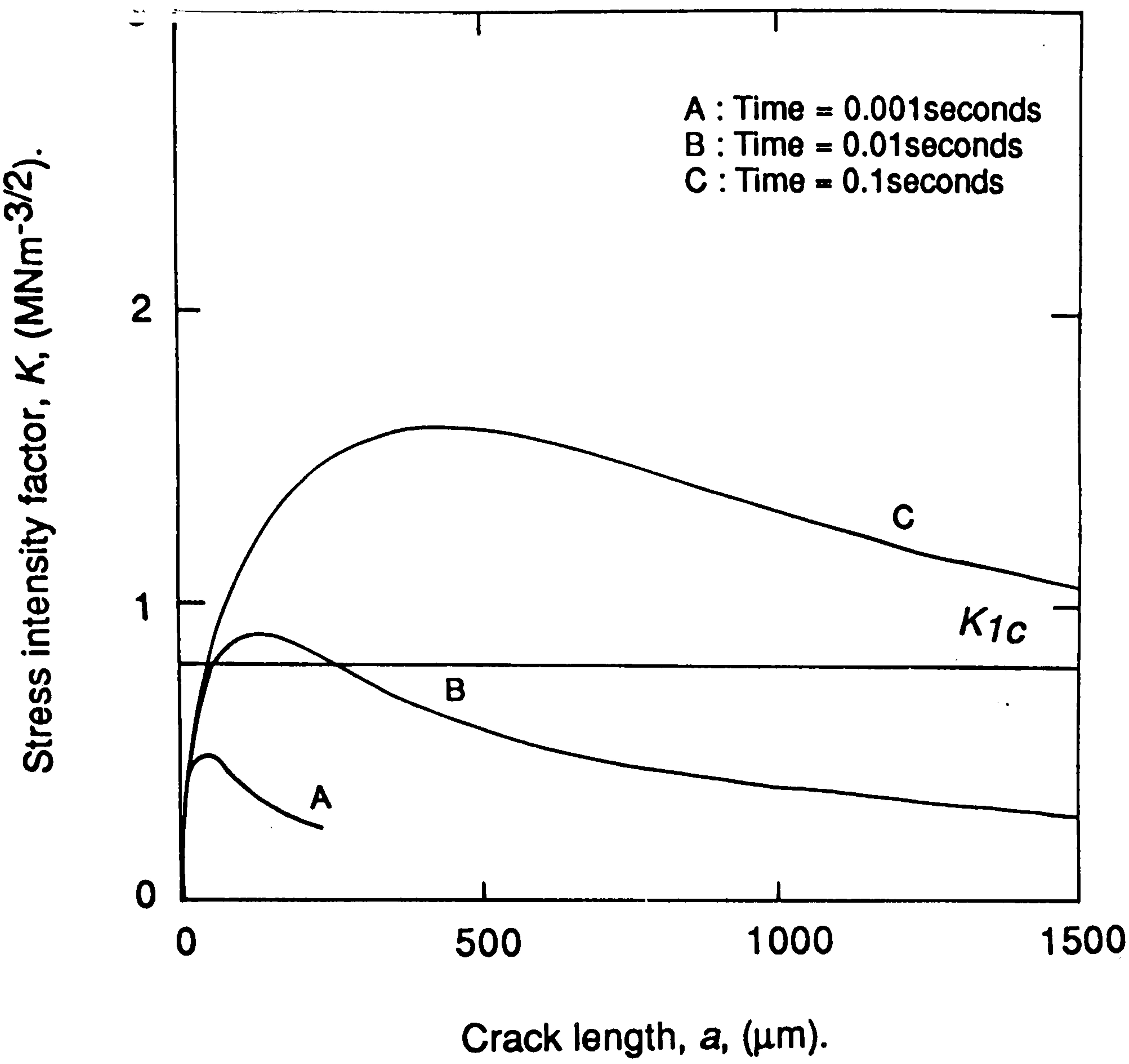

Figure 3.18 Stress intensity factors calculated by the computer model, for cracks in the thermal stress fields resulting from contact between C1 and hot glass.

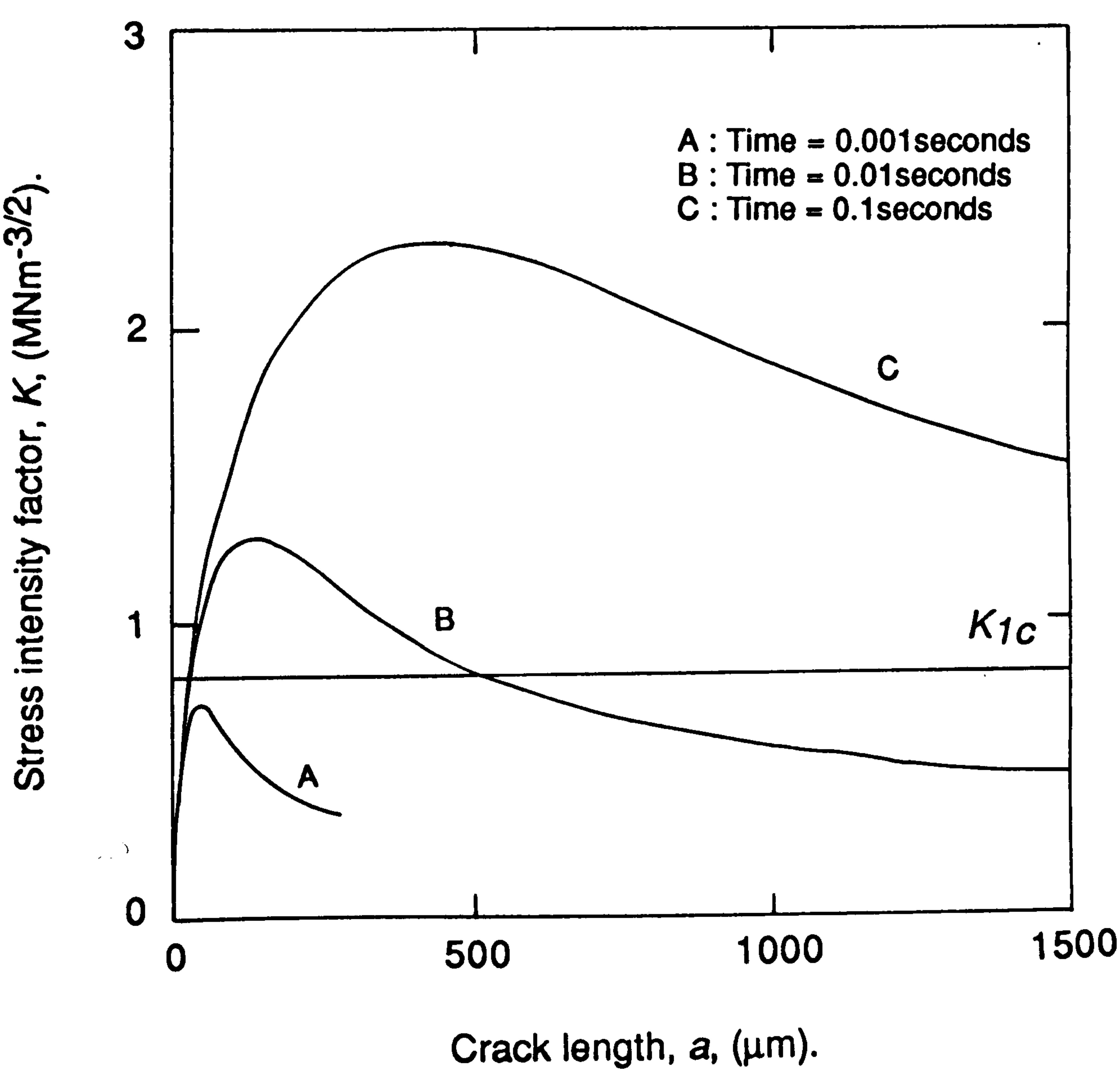

Figure 3.19 Stress intensity factors calculated by the computer model, for cracks in the thermal stress fields resulting from contact between P1 and hot glass.

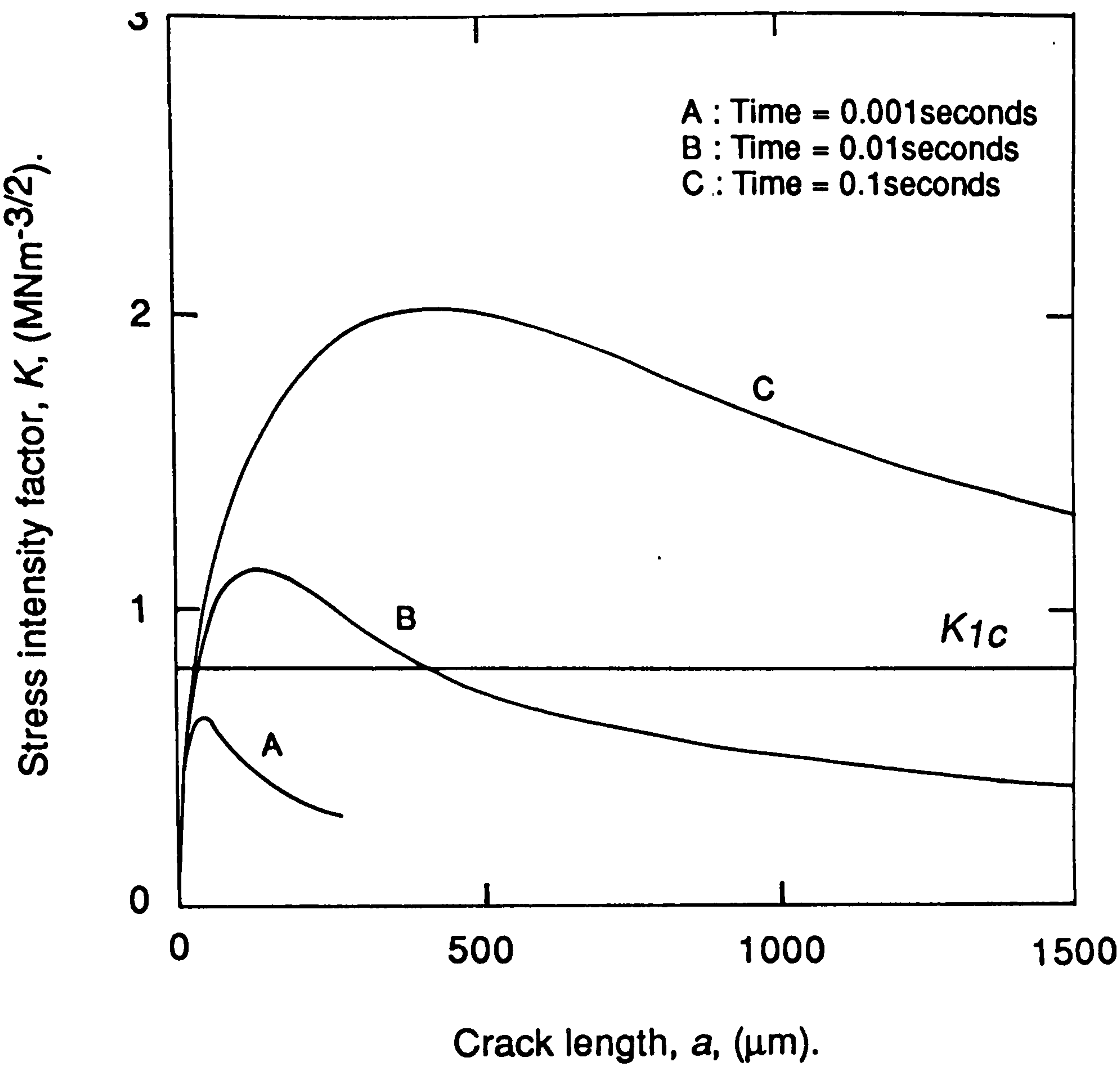

Figure 3.20 Stress intensity factors calculated by the computer model, for cracks in the thermal stress fields resulting from contact between C10 and hot glass.

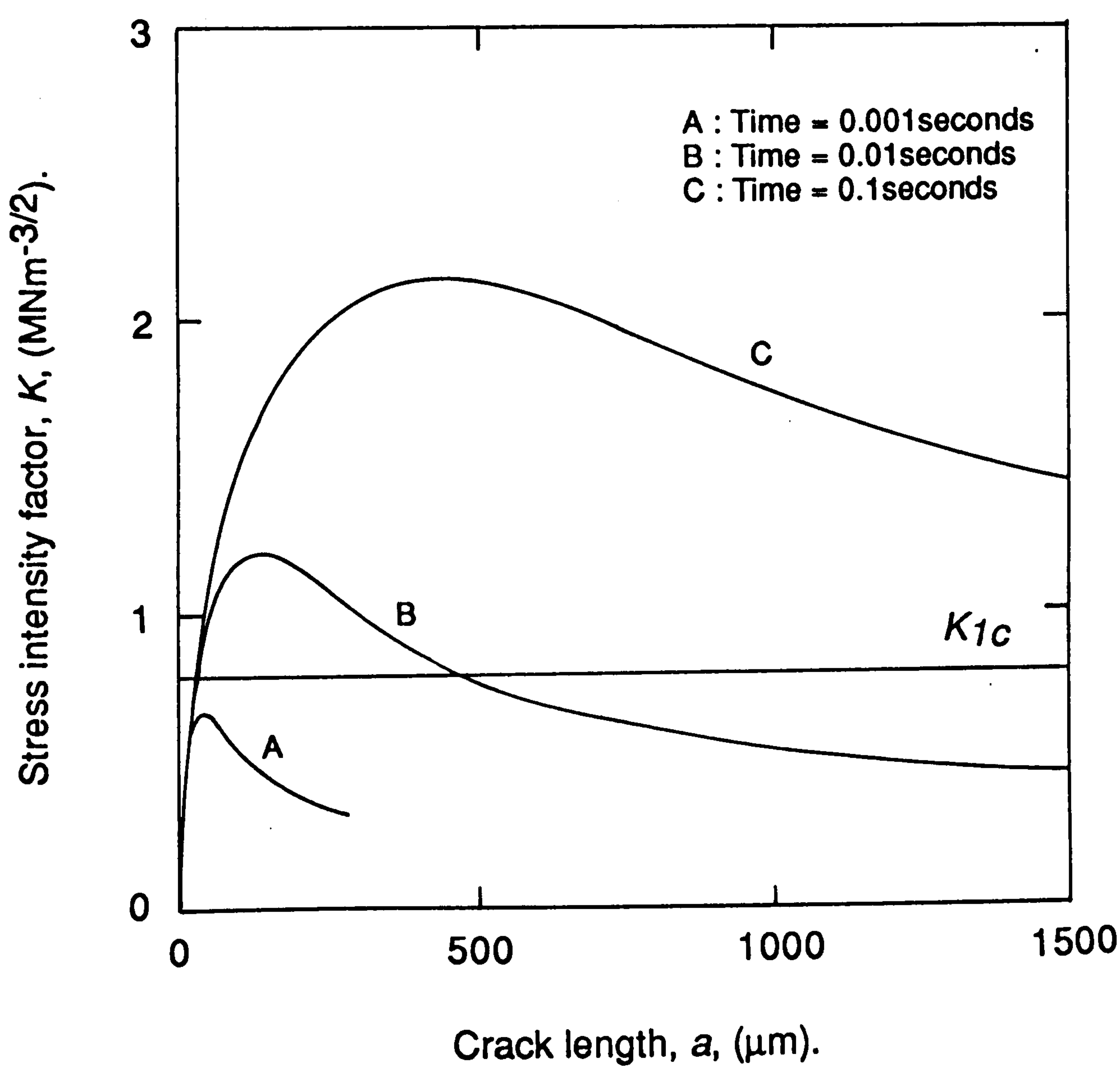

Figure 3.21 Stress intensity factors calculated by the computer model, for cracks in the thermal stress fields resulting from contact between Ti and hot glass.

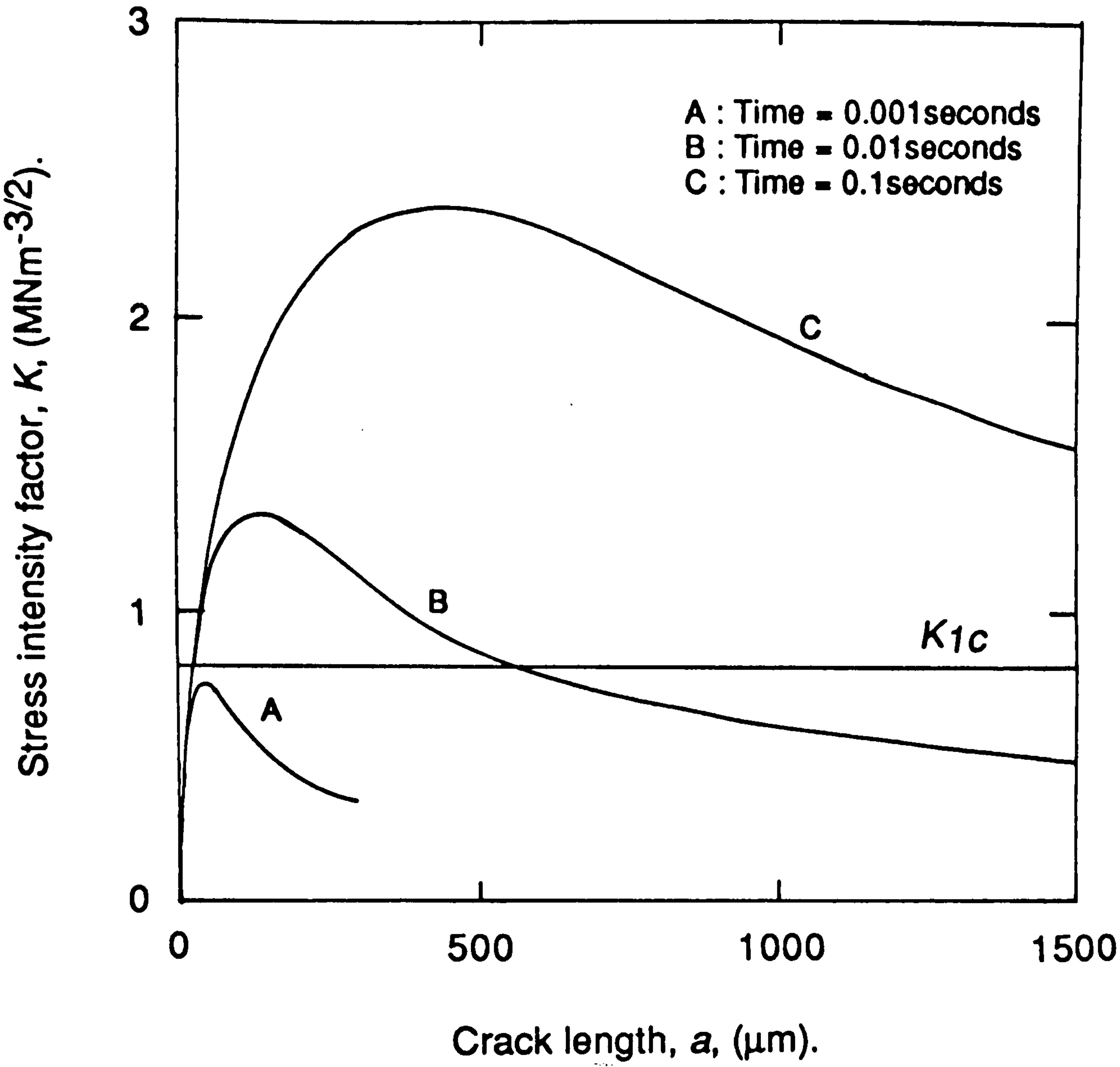

Figure 3.22 Stress intensity factors calculated by the computer model, for cracks in the thermal stress fields resulting from contact between Fe and hot glass.

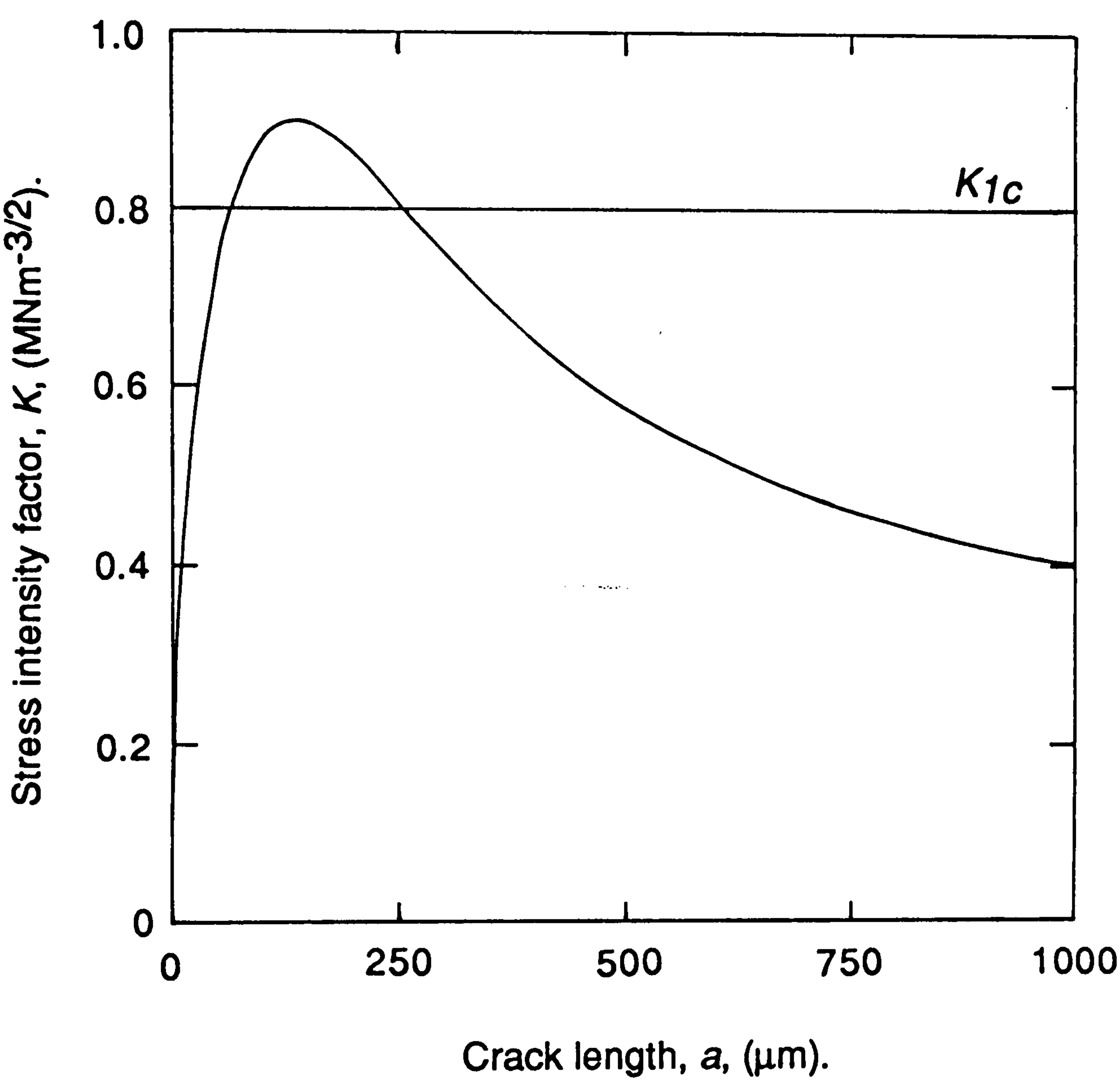

Figure 3.23 The stress intensity factors calculated for cracks in glass which has been contacted by C1, for 0.01 of a second.

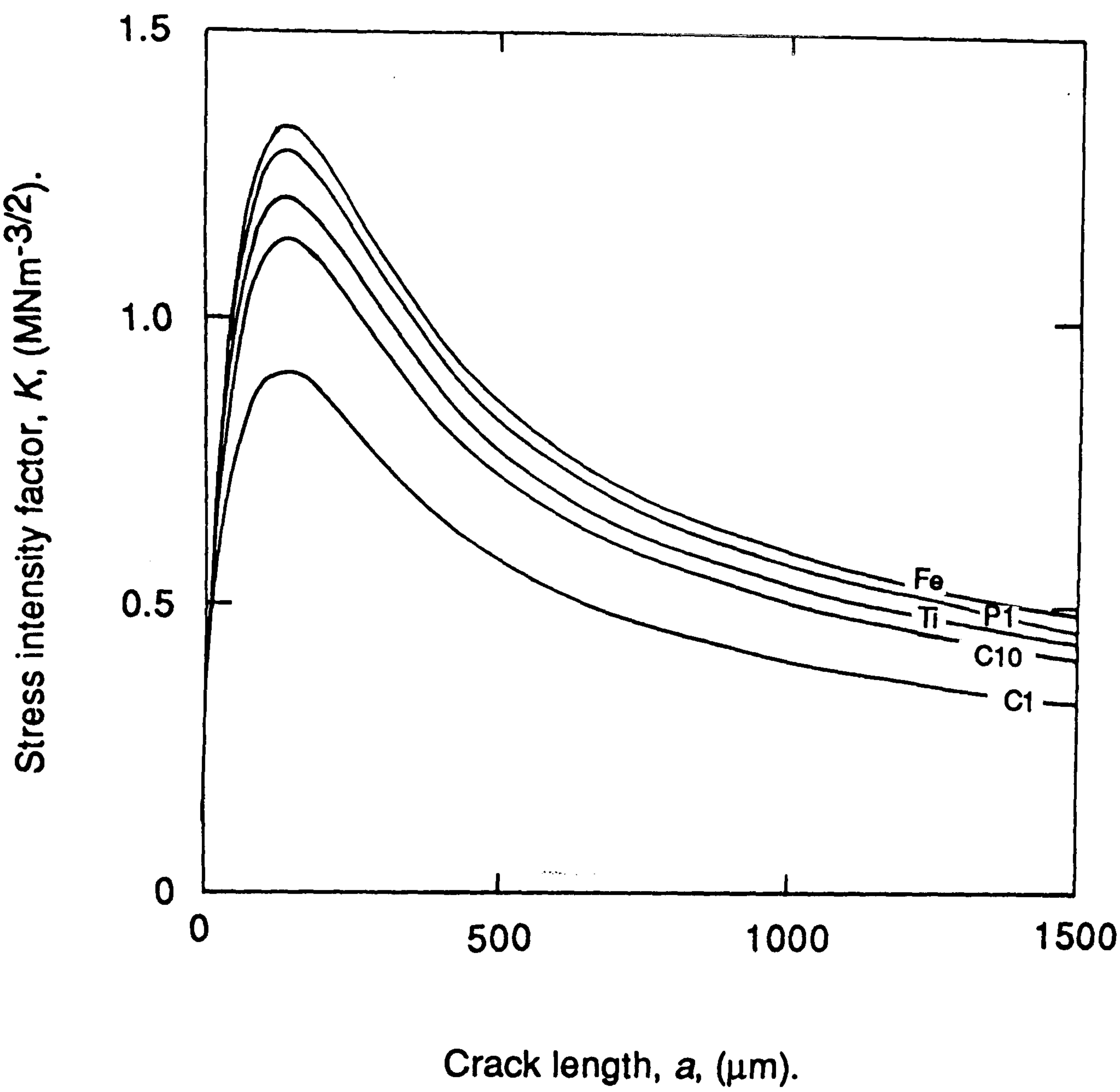

Figure 3.24 In this figure the curves generated by the computer model, which represent contact for 0.01 of a second by each of the materials are plotted to allow comparisons to be made.

- In a glass container handled for 0.01 of a second by Iron, no crack propagation takes place if the flaws present are less than 22.9μm. If a crack is greater than 22.9μm, a crack of 562.5μm will be produced.

Cracks up to the size where propagation begins in either of these cases would not result in the container being rejected, but both the propagated flaws would be detected by light beam quality control apparatus and the container scrapped.

It is worth noting at this stage the effects of the P1 material.

- In a glass container handled for 0.01 of a second by P1, no crack propagation takes place if the flaws present are less than 24.8μm. If a crack is greater than 24.8μm, a crack of 528.7μm will be produced.

This Graphite based material produces thermal stresses very similar to the Iron.

What do these crack sizes mean in terms of the resulting container strength ?

A glass sample containing a flaw of size, a, when exposed to a uniform stress, will have a corresponding strength. The strength of the sample can be calculated from equation 3.18, which rearranged gives

$$\sigma = \frac{K}{\sqrt{\pi a}}$$

The strength of the glass in a container in which there is a crack which was just too small to have propagated under the action of the thermal stresses, was calculated for glass contacted by the five materials considered here. The strengths range from 56 to 94MPa these figures correspond with reported strengths of glass containers of between 30 to 48MPa (Budd, 1980).

What do these results add to our understanding of how contact damage occurs ?

It is fair to say that although the ideal hot glass handling material would have no thermal conductivity and cause no mechanical damage, this is of course unlikely if not impossible. Considering the data produced from the computer model, it can be concluded that if the mechanical damage a material produces is limited to such a size that the thermal stresses produced by the material do not cause the cracks to propagate, then the material will be approaching the ideal as nearly as can be expected. In terms of the materials considered here this amounts to the fact that the mechanical damage a piece of C1 causes can be approximately three times that an Iron handling component could cause before the large thermally propagated cracks occurred.

In an attempt to verify these conclusions and gain further knowledge of handling materials, experimental investigations of the effects of contact on glass both at ambient and elevated temperatures were proposed. If the conclusions drawn from the model are realistic then it would be expected that the amount of mechanical damage a material produces is the critical factor as this will determine whether large cracks will form or not. Consequently it is expected that experimental investigations will reveal that current handling materials will be similarly ranked in efficiency whether there is an element of thermal shock damage or not.

3.6 Experimental investigation

The model highlighted the importance of mechanical damage, as initiation sites for thermal damage. Any test utilised had to be completed both with the glass at room temperature and at elevated temperatures. The aim was to try and separate to some degree the effects of the two components of damage.

3.6.1 Previous investigations

Budd *et al* (1980) had similar aims, they completed tests using four materials in the hope that each would perform in a different way, glass, steel, asbestos and a Carbon fibre composite were examined. Their preliminary investigations involved contact with the external surface of glass containers collected from production lines. Although such experiments highlighted the differentials in thermal shock damage by the different materials, differences in isothermal contact damage were masked by damage which had already occurred as the bottles were manufactured. As with the present investigation their aim was to understand how materials affect pristine high strength glass. They overcame this by testing the internal surface of containers, which have not been contacted in the production, other than by the atmosphere. A levered arm was used to maintain constant loading on the internal surface of the container as the sample material was moved up and down the side wall region. The containers were then tested in compression, with the bottles loaded on their sides in a cradle, shown in figure 3.25 (Budd and Cornelius, 1979) a ball contact above the abraded region was used to apply the load.

3.6.2 Choice of specimen

It would have been logistically difficult to use large numbers of containers to test as Budd and Cornelius (1979, Budd *et al* 1980) did. It was decided to test lengths of soda lime glass rod as Proctor (1962). This would enable a relatively small specimen size but eliminate edge effects which would dominate the results if glass slides were used.

The samples were chemically polished to produce a high strength material similar to that of the just-blown glass bottle. 8mm diameter rods were purchased from Gallenkamp in 1.5m lengths. The rods were then cut in to 80mm lengths. The chemical polish used hydrofluoric acid. The experimental method is detailed in section 2.2.

3.6.3 Analysis of experimental results

The rods were tested to failure in four point bending to assess their strength. The testing procedure is explained in section 2.3. After the optimisation, detailed in section 2.2, of the polishing technique the mean strength of the rods tested was 1447MPa the frequency distribution of the results is shown in figure 3.26. The large spread of the results is typical of brittle material failures. It is a direct result of the range of flaw sizes still present on the surface of the glass after polishing. Similar distributions were reported by Proctor (1962) also after chemical polishing. When considering a statistical distribution such results may be fitted to it is important it includes parameters quantifying such effects.

Weibull's theory of failure is a statistical representation of failure, which takes into account the damage condition of the material. It has been used in statistical studies of factors influencing the strength of glass (Kroenke, 1966) as well as in the analysis of many other situations (Weibull, 1951).

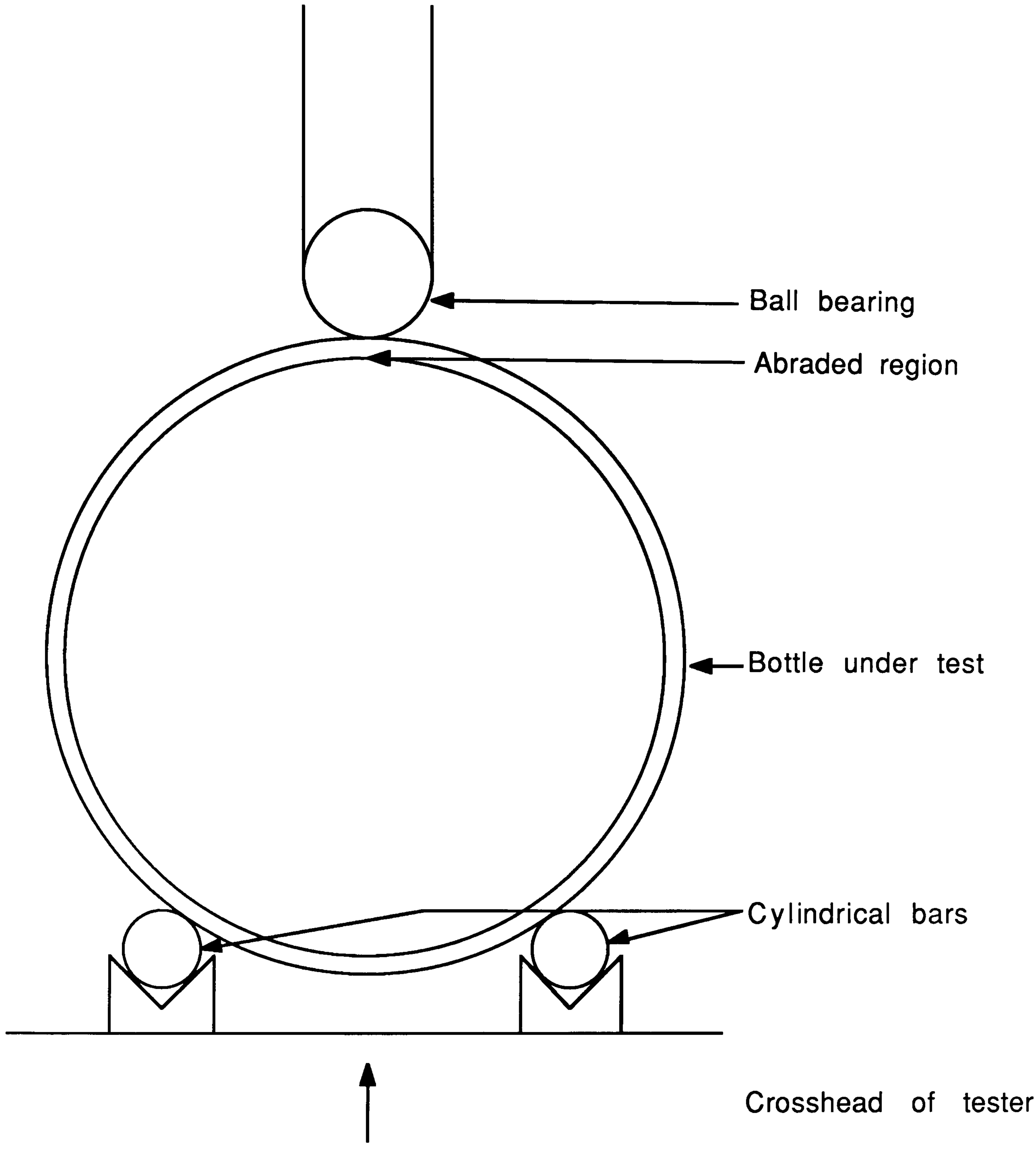

Figure 3.25 Schematic of the container testing apparatus used by Budd *et al* , (1980).

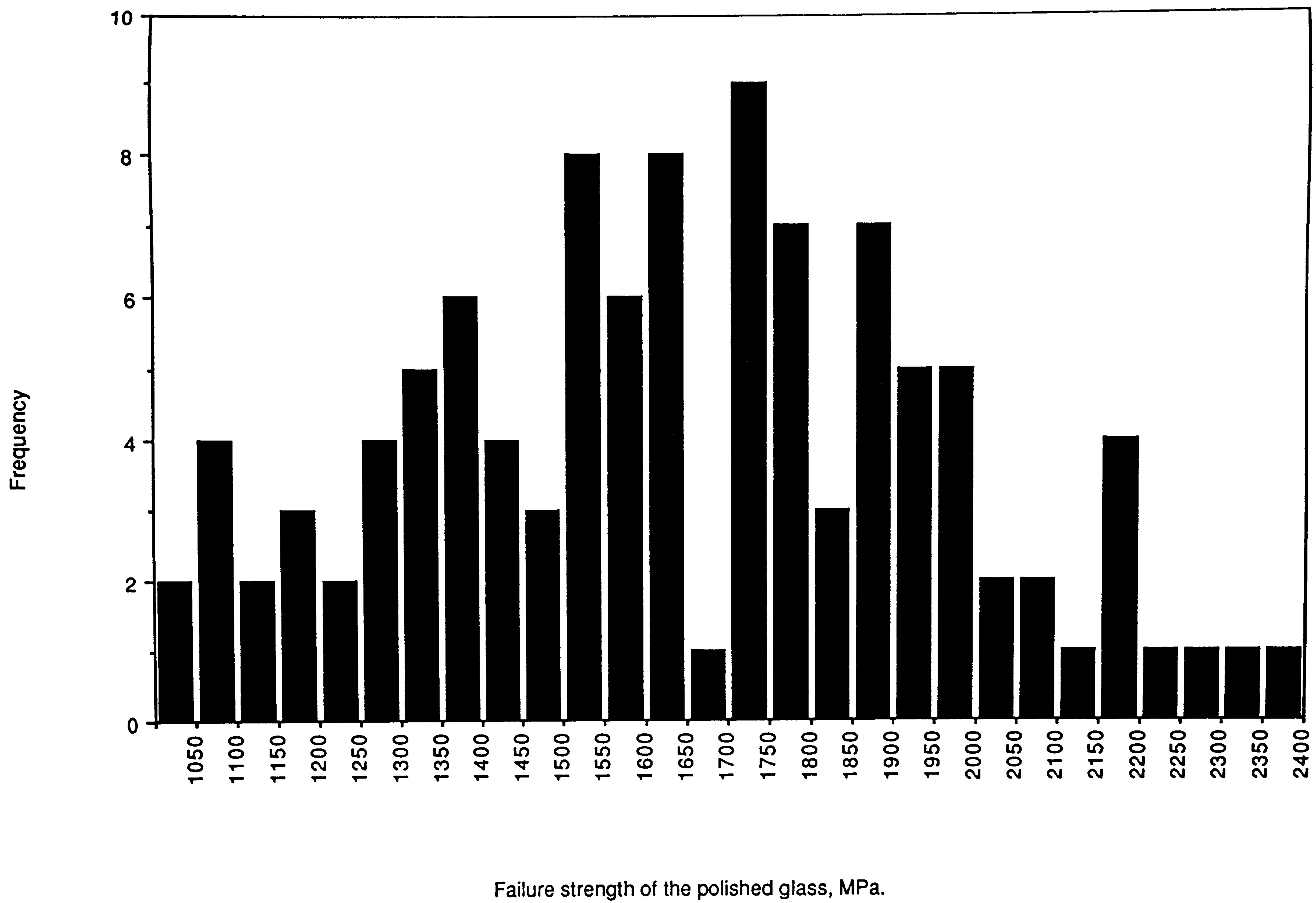

Figure 3.26 Frequency distribution of the failure strengths of the virgin glass rods.

3.6.4 Weibull's theory

A piece of material being tested is considered to be divided up into many small elements, figure 3.27. The probability that one element will survive is P_s^i but the probability that the whole sample will survive is P_s

$$P_s = \prod_{i=1,n} P_s^i \tag{3.54}$$

if the probability of an element failing is P_f^i then it is true that

$$P_s = \prod_{i=1,n} (1 - P_f^i) \tag{3.55}$$

taking natural logarithms of both sides

$$\ln P_s = \sum_{i=1,n} \ln(1 - P_f^i) \tag{3.56}$$

as $\ln(1 - x) \approx -x$

$$\ln P_s \approx \sum_{i=1,n} -P_f^i \tag{3.57}$$

or by reducing to infinitesimal size

$$\ln P_s \approx -\int P_f \mathrm{dv} \tag{3.58}$$

thus

$$P_s \approx \exp\left\{-\int P_f \mathrm{dv}\right\} \tag{3.59}$$

Weibull suggested the requirements for (P_f) a simple function which would fulfil the observed requirements of a probability function listed below.

1. To be a function of stress.

2. With $P_f(0) = 0$.

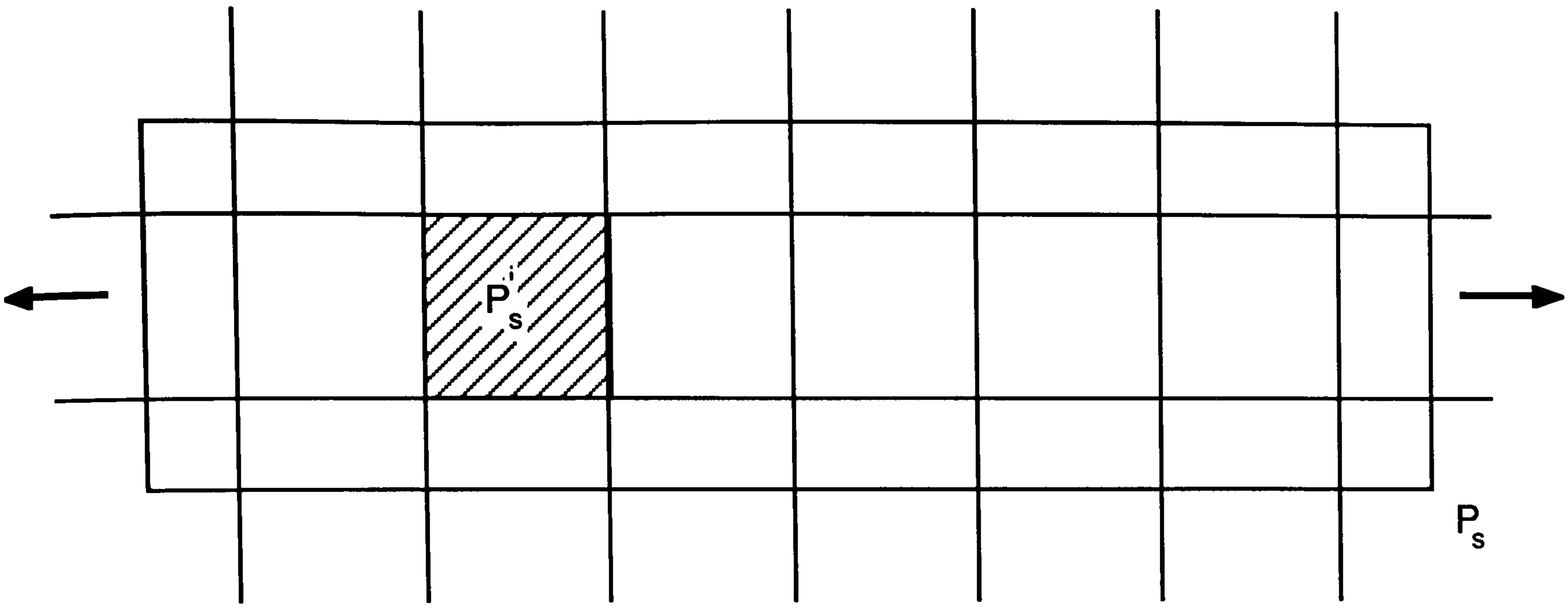

Figure 3.27 Schematic representation of a sample divided into small elements. The probability of the survival of an individual element being P_s^i.

3. To be monatomically increasing.

Such a function is

$$P_f = \left(\frac{\sigma_i - \sigma_0}{\sigma_s}\right)^\beta \tag{3.60}$$

and using it gives

$$P_S = \exp\left[-\left(\frac{\sigma_i - \sigma_0}{\sigma_s}\right)^\beta\right] \tag{3.61}$$

where σ_i, is the failure stress of the sample. σ_0, is the stress below which no failure will occur, it is often assumed to be zero. σ_s, is the characteristic strength of the distribution. β, is the Weibull modulus.

In considering the failure of the glass rods, a good fit to the distribution of the experimental results was achieved when σ_0 was assumed to be zero thus

$$P_s = \exp\left[-\left(\frac{\sigma_i}{\sigma_s}\right)^\beta\right] \tag{3.62}$$

The function is shown graphically in figure 3.28, when the applied stress is zero all the samples will survive and $P_s = 1$, as it increases more and more specimens will fail and P_s will decrease. Large applied stresses will result in virtually all the samples failing so as

$$P_s \to 0 \quad , \quad \sigma \to \infty$$

β the Weibull modulus reflects the degree of variability in the strength of a material. The higher β is the less variable is the strength, see figure 3.29. For pottery, brick and cement β typically has a value $\approx$ 5, for engineering ceramics it has a value of $\approx$ 10 and steel which shows little variation in strength has a modulus of $\approx$ 100 (Ashby and Jones, 1986). When $\sigma_i = \sigma_s$ then $P_s = 1/e$ therefore σ_s the characteristic strength is the tensile stress which results in 37% of the samples surviving.

Although it is straightforward to determine σ_s from a plot of the type shown in figure 3.29 β would have to be found by curve fitting. A different way which allows β to be determined more easily result from taking natural logarithms of equation 3.62 so

$$\ln P_s = -\left(\frac{\sigma_i}{\sigma_s}\right)^\beta \qquad 3.63$$

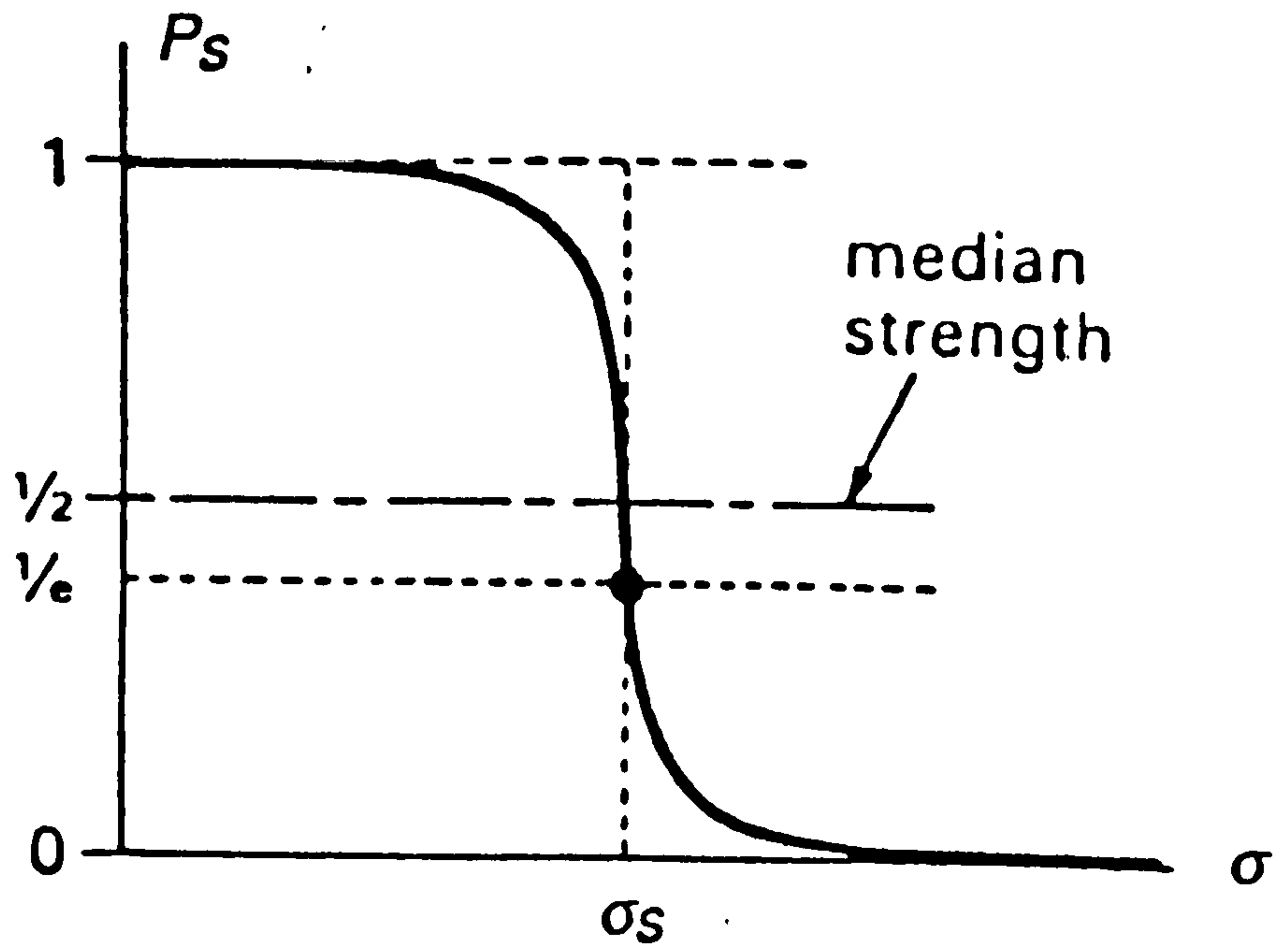

Figure 3.28 The standard form of the Weibull distribution, (Ashby and Jones, 1986).

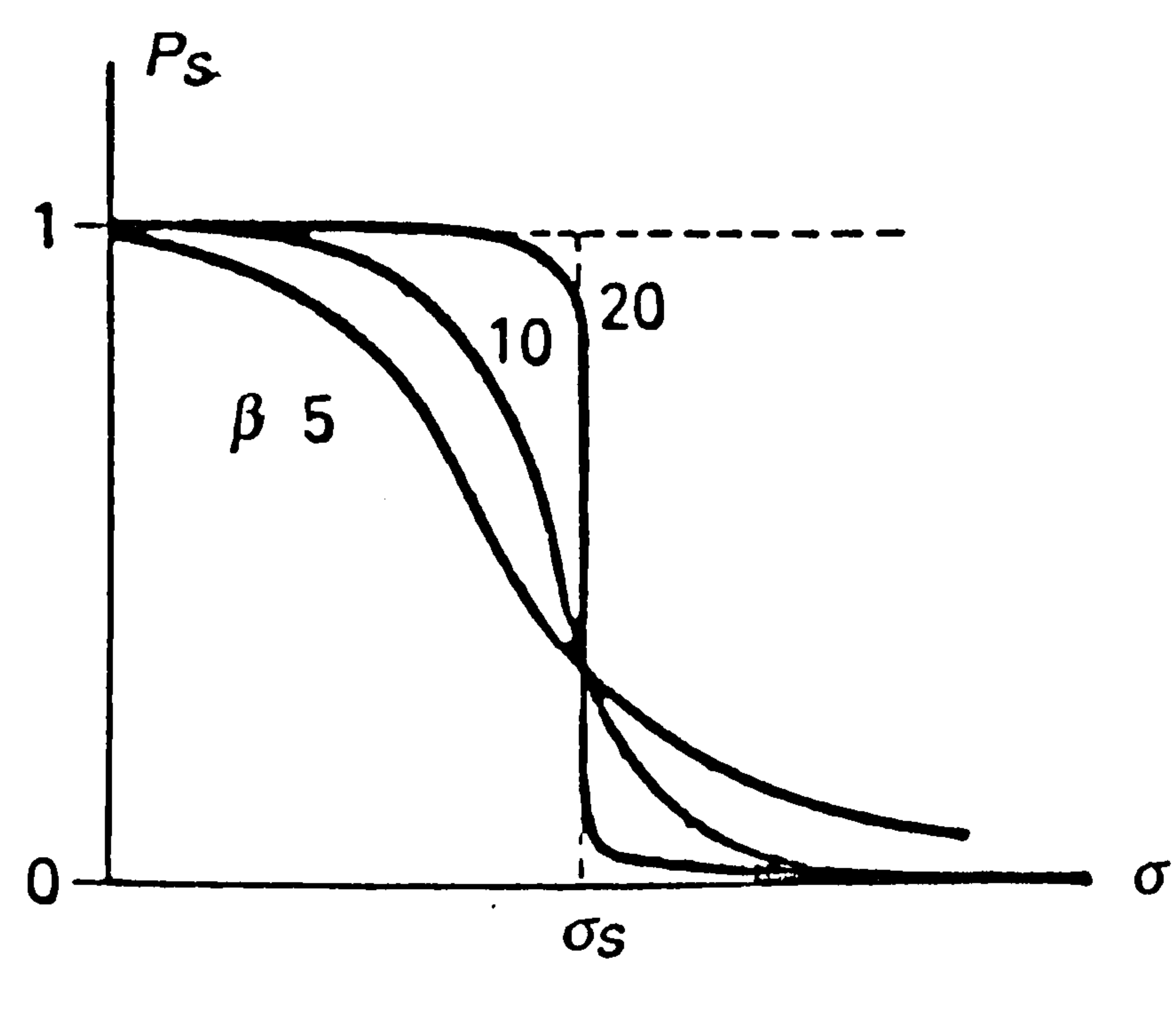

Figure 3.29 Representation of the way the Weibull distribution changes with the Weibull modules, (Ashby and Jones, 1986).

therefore

$$\ln\left(\frac{1}{P_s}\right) = \left(\frac{\sigma_i}{\sigma_s}\right)^{\beta} \qquad 3.64$$

taking logarithms again

$$\ln\left[\ln\left(\frac{1}{P_s}\right)\right] = \beta\ln\sigma_i - \beta\ln\sigma_s \qquad 3.65$$

P_s can be calculated for each σ_i from a ranked list of n data points, for σ_i $P_s = \frac{i}{n+1}$. Equation 3.65 is now of the form $y = mx + c$ where

- $y = \ln\left[\ln\left(\frac{1}{\left[1-\frac{i}{n+1}\right]}\right)\right]$.
- $m = \beta$.
- $c = \beta\ln\sigma_s$.

So a plot of $\ln[\ln(\frac{1}{P_s})]$ against $\ln\sigma_i$ will enable evaluation of the distribution parameters.

Such plots were used to obtain the modulus and characteristic strength of data sets obtained from contact tests. Figure 3.30 shows such a plot for the virgin polished rods. From this the characteristic strength of the virgin rods was estimated to be 1736MPa with a Weibull modulus of 6.1.

3.6.5 Controlled contact damage of the glass rods

The high strength glass had been produced to enable the evaluation of the effects of contact. To do this the rods needed to be contacted in a controlled and reproducible way.

Any apparatus constructed was intended to contact glass rods at 300°C, so it was important that it could withstand such temperatures. The apparatus which was designed enabled a rod to be rotated in contact with a sample of handling material whilst under a constant, known load. The load that was chosen for all the investigations was 150g, that is the weight of a milk bottle. Each test was repeated at least 6 times, the results were processed using Weibull statistics as discussed above for the virgin rods. The details of the apparatus are discussed in section 2.4.

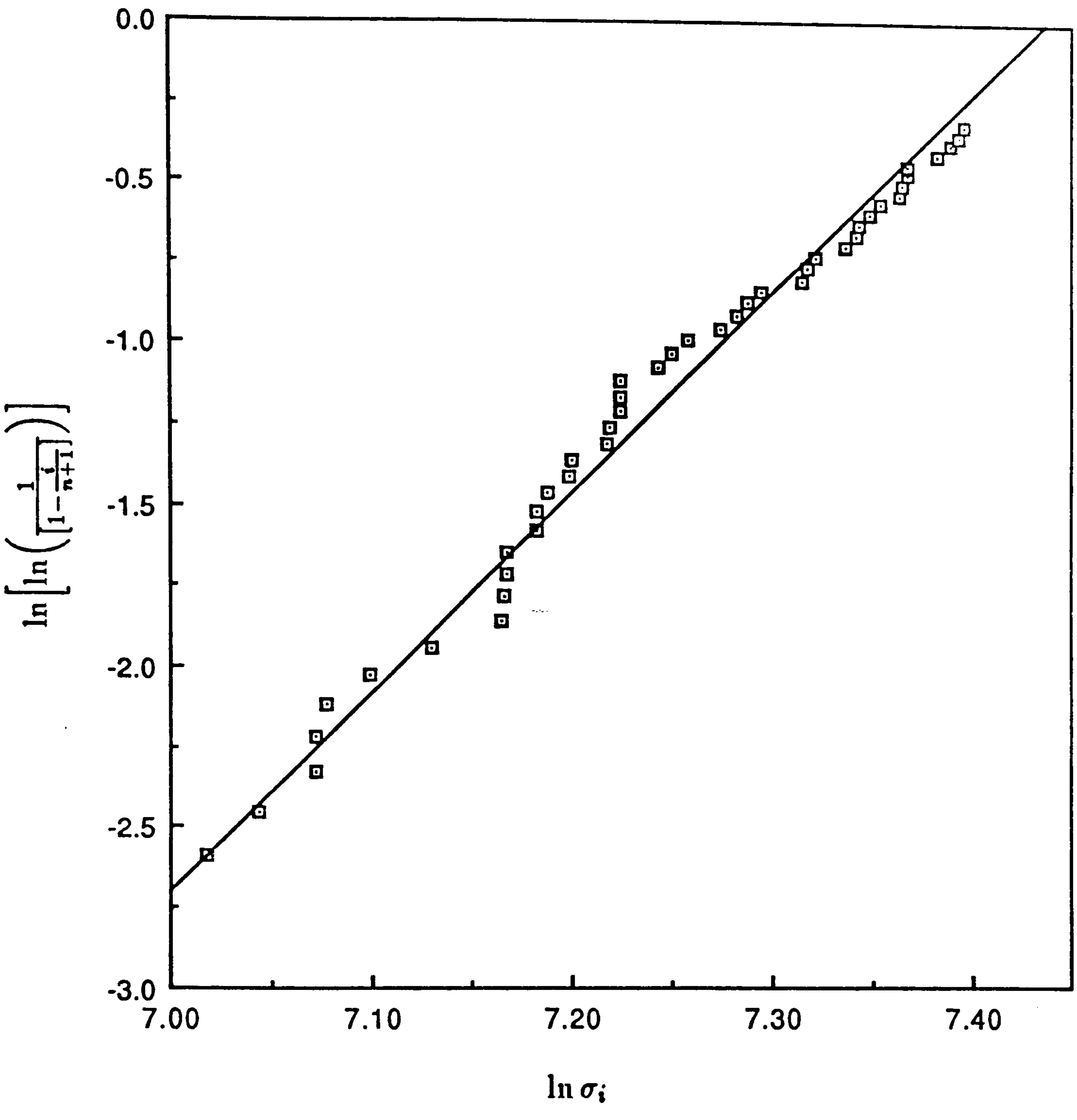

Figure 3.30 Plot from which the Weibull modulus and characteristic strength of the virgin polished rods was obtained.

3.6.6 Isothermal contact

The first set of contact experiments undertaken were with the rod and the contact material at ambient temperature so that all the damage was the result of mechanical contact. The mathematical model highlighted the significance of such damage as initiation sites.

As many handling materials were tested as samples could be obtained, along with some prospective handling materials. They fall in to three main categories,

1. **Metallic materials**, those examined in this category were Titanium, Zirconium, Damaron† (D1) and steel.

2. **Non-fibrous carbonaceous materials**, those examined were C25, C22, P1 and D2††.

3. **Material containing Carbon fibre**, those examined were C10, C30 and C1.

The results of these tests for each material are represented by three points, the central large circle represents the Weibull characteristic strength and the small circles above and below it the highest and lowest, respectively, recorded strengths of glass rods contacted by that material. The materials are plotted in descending order of their Weibull characteristic strength. This representation was thought to give the clearest indication of a materials performance. The data labelled as 'none' represents the virgin rods.

It can be seen from figure 3.31 that generally the carbonaceous materials cause the least mechanical damage, the fibre reinforced materials are grouped in the centre of the rankings and the metallic materials which cause the most damage complete the order. Why the carbon materials perform so much more efficiently is considered in chapter 6.

These results indicate that Titanium and Zirconium produce low strength glass after contact in comparison to the Carbon based materials. This is of course

† Damaron is the trade name of an aluminium bronze handling material here after it will be refered to as D1.

†† This material who's trade name is Duratemp is discussed in section 4.4.

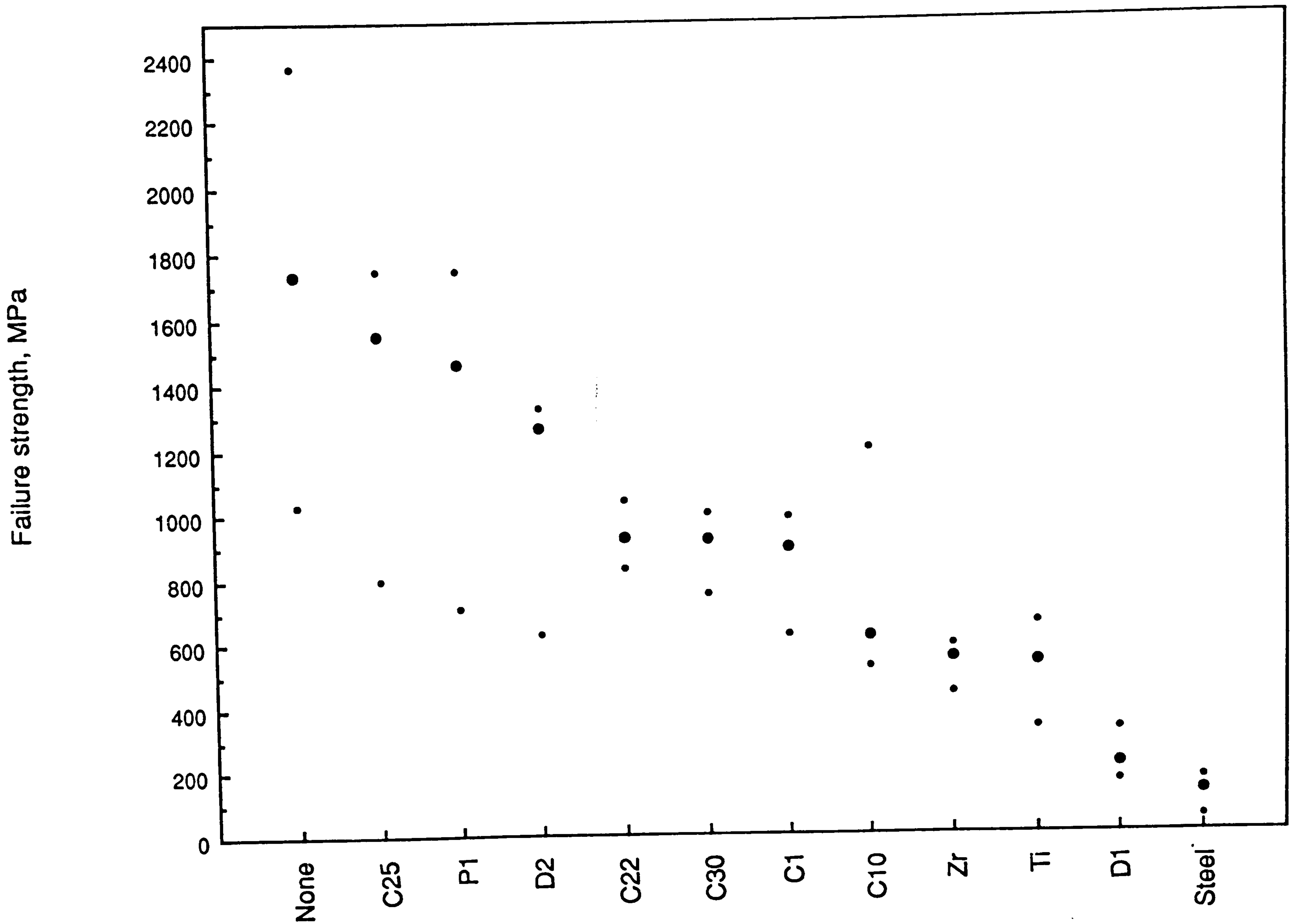

Figure 3.31 Results of the contact tests completed with the glass rod at ambient temperature and rotated under a load of 150g

true, but they should be considered in comparison to the other metallic materials tested. Titanium and Zirconium cause considerably less damage than either the steel sample or the D1 material. As these materials were chosen specifically for their thermal properties these results were considered encouraging.

3.6.7 Thermal shock

The natural progression from isothermal tests was to incorporate the potential for thermal shock damage into the experimental procedure. This was achieved by heating the glass rods to 300°C before its contact with the handling material which remained at ambient temperature. In an attempt to try and quantify the extent of the thermal damage alone, the contact was completed without rotation. Although the damage caused by mechanical mechanisms can never be eliminated it was hoped the omission would minimise such effects. The experimental details of this procedure are detailed 2.4.2.

Figure 3.32 depicts the results of these investigations, the same notation has been used as above. The data labelled as 'none' represents rods which were heated in the same way as those to be contacted, then cooled and tested, it is clear that heating the rod has reduced its strength but it is still very strong, the effects of contact can still be observed. It can be seen that the difference in performance between the carbonaceous materials with and without fibres, evident in the isothermal contact data is not observed and that generally the fibre composite materials are ranked higher. This agrees with the predicted ranking of a materials thermal efficiency from the dimensionless ratios, calculated and tabulated in table 3.1.

The Titanium and Zirconium although at the bottom end of the ranking compare very favourably with the carbonaceous materials. They straddle in the ranking the P1, a carbonaceous material which was one of the most efficient material in terms of limiting mechanical damage. The drastic drop in the ranking of this material brings it into line with that of the predicted ranking in table 3.1. The thermal damage is thought to be a consequence of the P1's high thermal conductivity, but we will see later in section 4.5 that this is not the reason for the drop in the ranking of this material.

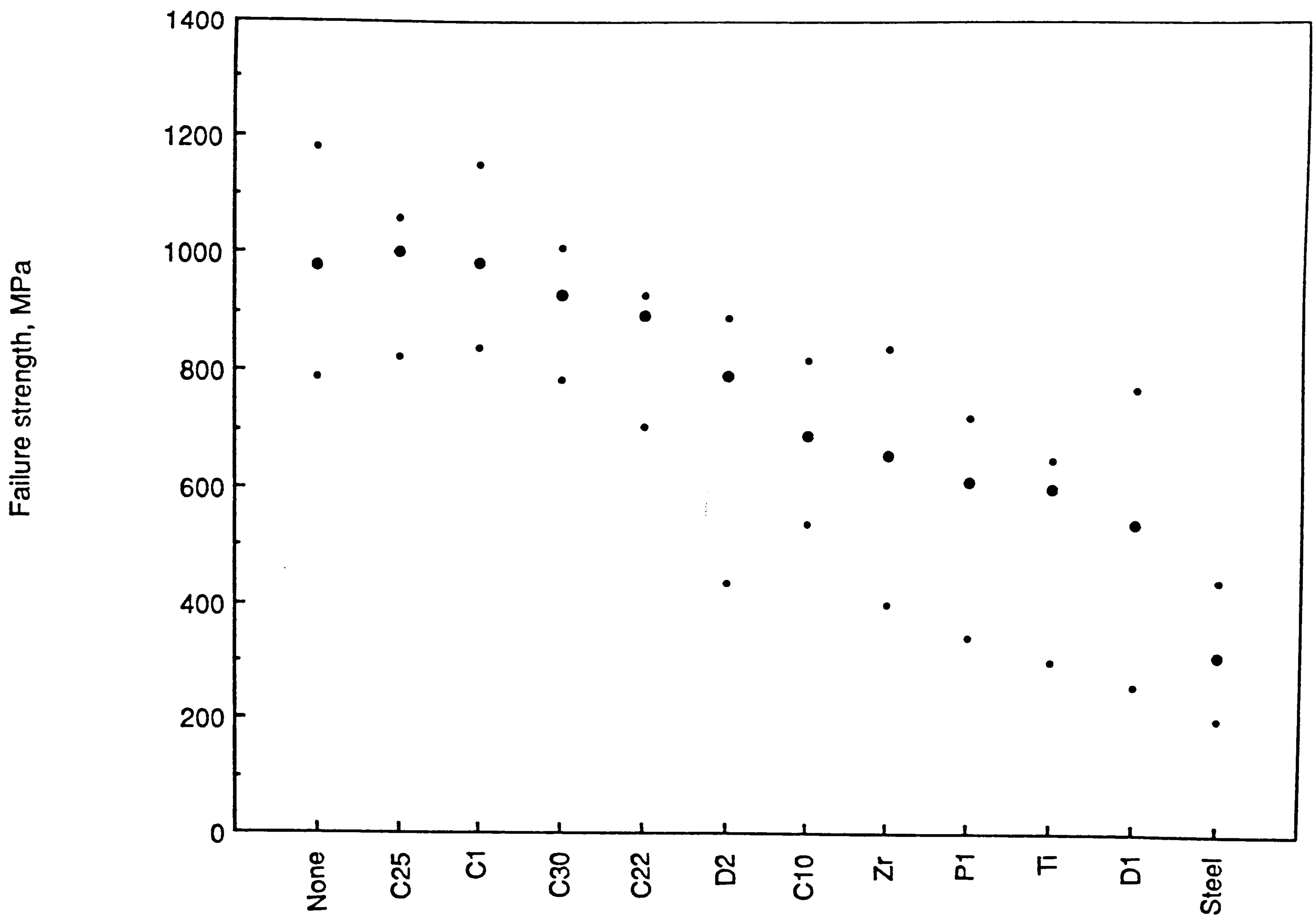

Figure 3.32 Results of the contact tests completed with no rotation and the glass rod at 300°C

To conclude the assessment of contact damage, tests were completed which included the rotation of hot glass rods contacting handling material under a constant load. This was intended to be the closest simulation to the actual plant situation.

The results of these experiments are plotted, in the same format as the previous contact data, in figure 3.33. The first thing to note, is that in every case the strengths of the rods are lower than when thermal or mechanical damage alone was the cause. This is as predicted.

As with the other tests the carbonaceous materials out performed all the other materials but clearly Titanium and Zirconium are much better glass handling materials than D1 or steel. The interaction of thermal and mechanical properties is particularly evident in the case of the P1 material, whose ranking dropped so dramatically when thermal shock was introduced.

Carbonaceous materials cause the least damage to glass but Titanium and Zirconium as predicted are much more efficient glass handlers than traditionally used metallic materials. They may have a role to play in glass handling, their high strength in thin sections could be of particular importance, but it is unlikely that they will be utilised as bulk material for commercial reasons.

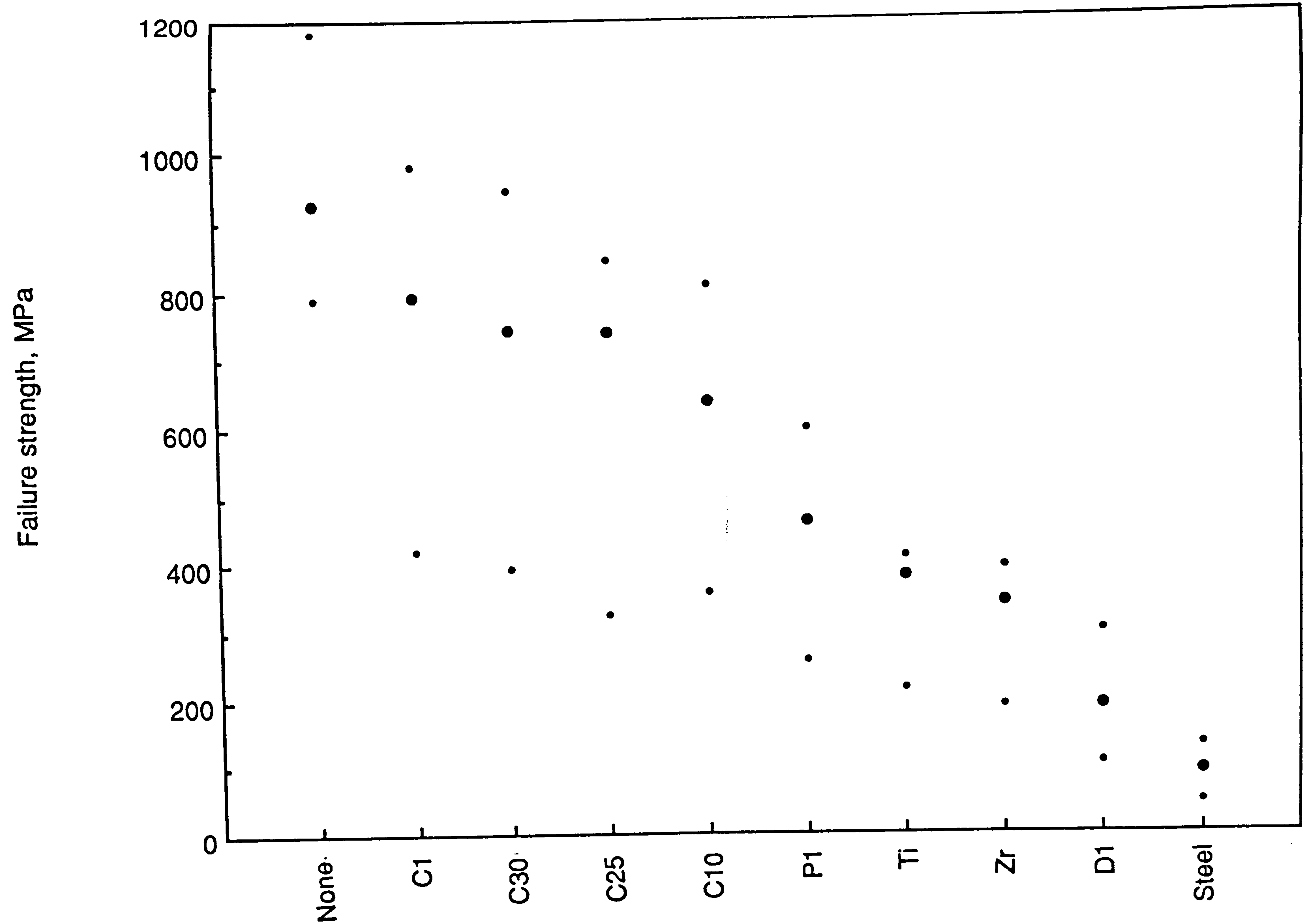

Figure 3.33 Results of the contact tests completed with the glass rods at 300°C, rotated under a load of 150g

Chapter 4

DURABILITY

4.1 Introduction

In this chapter the problems associated with the elevated temperatures handling materials must withstand are examined. It was discussed in the introduction to this document that the present specialist handling materials major flaw is their limited life, due to thermal degradation and oxidation.

Throughout the investigation of contact damage recorded in chapter 3 it became clear that although some materials not previously considered showed potential, especially Titanium and Zirconium, little was going to improve on carbonaceous materials in terms of limiting mechanical damage. Therefore even greater emphasis was placed on the aim of trying to prolong the life of present and future Carbon based materials.

The problems of degradation were addressed in two ways

- Identification of weaknesses in present materials and so suggested modifications.
- Designing new materials with improved durability.

The existing materials could be split into three main types,

1. Polymer based composites,
2. Carbon/Carbon composites,
3. Fine grained carbonaceous materials.

Each type of material was examined in turn.

4.2 Polymer based composites

These materials have an inherent weakness to use at elevated temperatures as they suffer from thermal degradation. Johnson Radley's polyimide/graphite composite known as C1 decomposes at 300°C and is not recommended for use above 250°C (Jacobs, 1987) because of such thermal instability. It was decided not to investigate these materials further as a result of this inherent instability.

4.3 Carbon/Carbon fibre composites

Two Carbon/Carbon materials are marketed by Johnson Radley as hot glass handling materials. Little was known about these materials, but they were known to be two-dimensional Carbon fibre reinforced materials with a carbonaceous matrix. The two materials are known as Cerberite 10 and Cerberite 12, denoted by C10 and C12 respectively. The C10 originates from the same process as C12 but is put through a further heat treatment. As a result it was reported (Budd, 1987) to have better oxidation resistance but a lower strength than C12. These two materials were recommended for different positions at the hot end. The C10 material was recommended for use in the stacker bar where the ambient temperature is greatest due to its close proximity to the lehr mouth. The C12 material was utilised in the take out tongs where its strength was said to be required for the profiled edge which lifts the bottle from the mould to the sweep out position.

4.3.1 Optical microscopy

Cross-sections of the materials were mounted in bakelite resin and metallographically polished. The samples were examined using parallel polars with a half wave retarder plate between the specimen and the analyser (e.g.Edwards, 1989. Forrest and Marsh, 1977) the general arrangement is shown in figure 4.1. Plates 4.1 and 4.2 show typical regions of C10 and C12 respectfully. The purple colour of the binding phase which is not changed by rotating the samples, reveals the binding phase to be isotropic probably derived from a phenolic resin. Around the fibres there are small areas of optically active material this is thought to be the result of material flow during pressing. The resin will be forced to flow around the fibres as they are pushed closer together, and so produce the alignment of the material platelets. Figure 4.2 shows a possible production route for the Carbon/Carbon

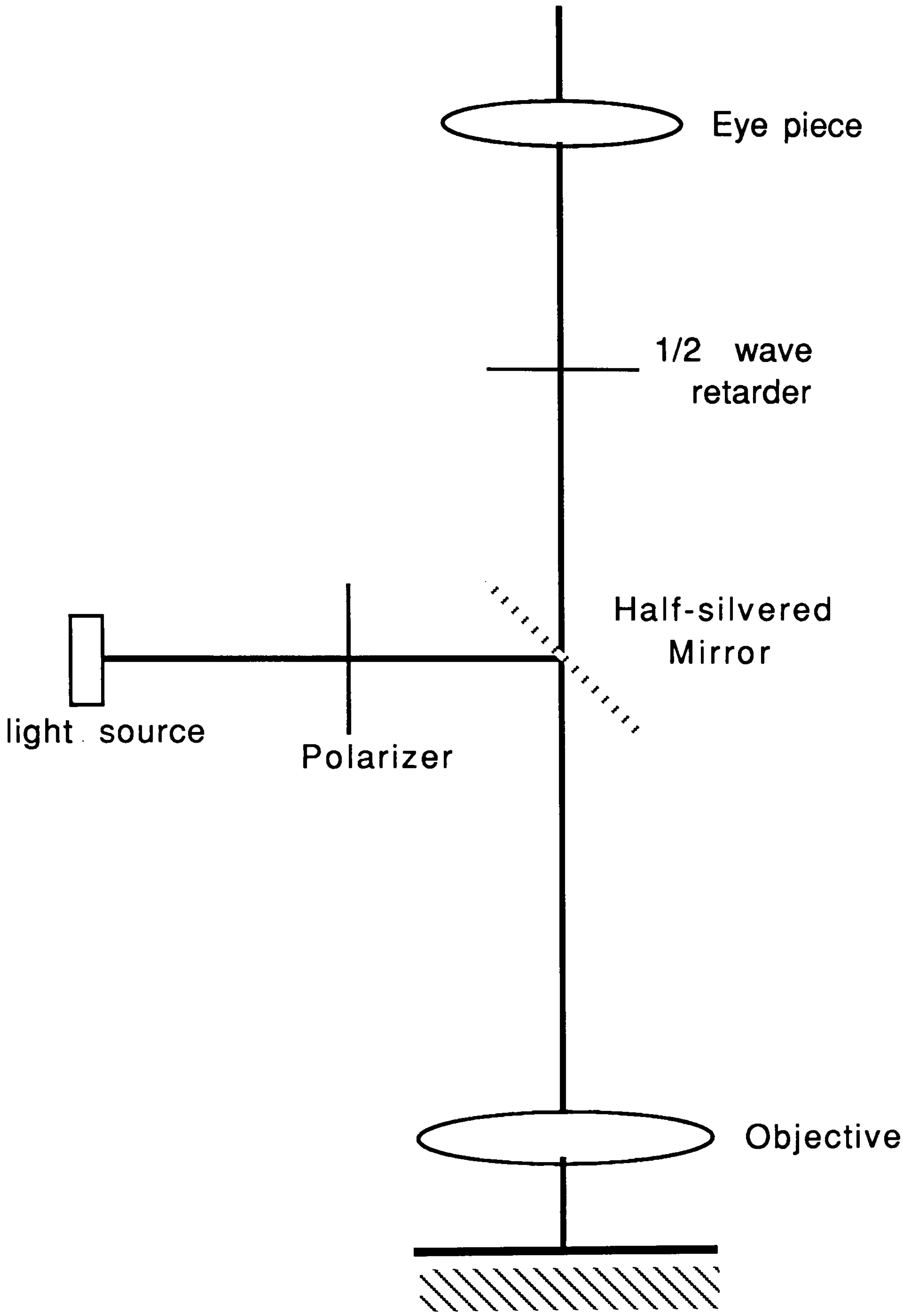

Figure 4.1 Representation of a polarized light optical microscope.

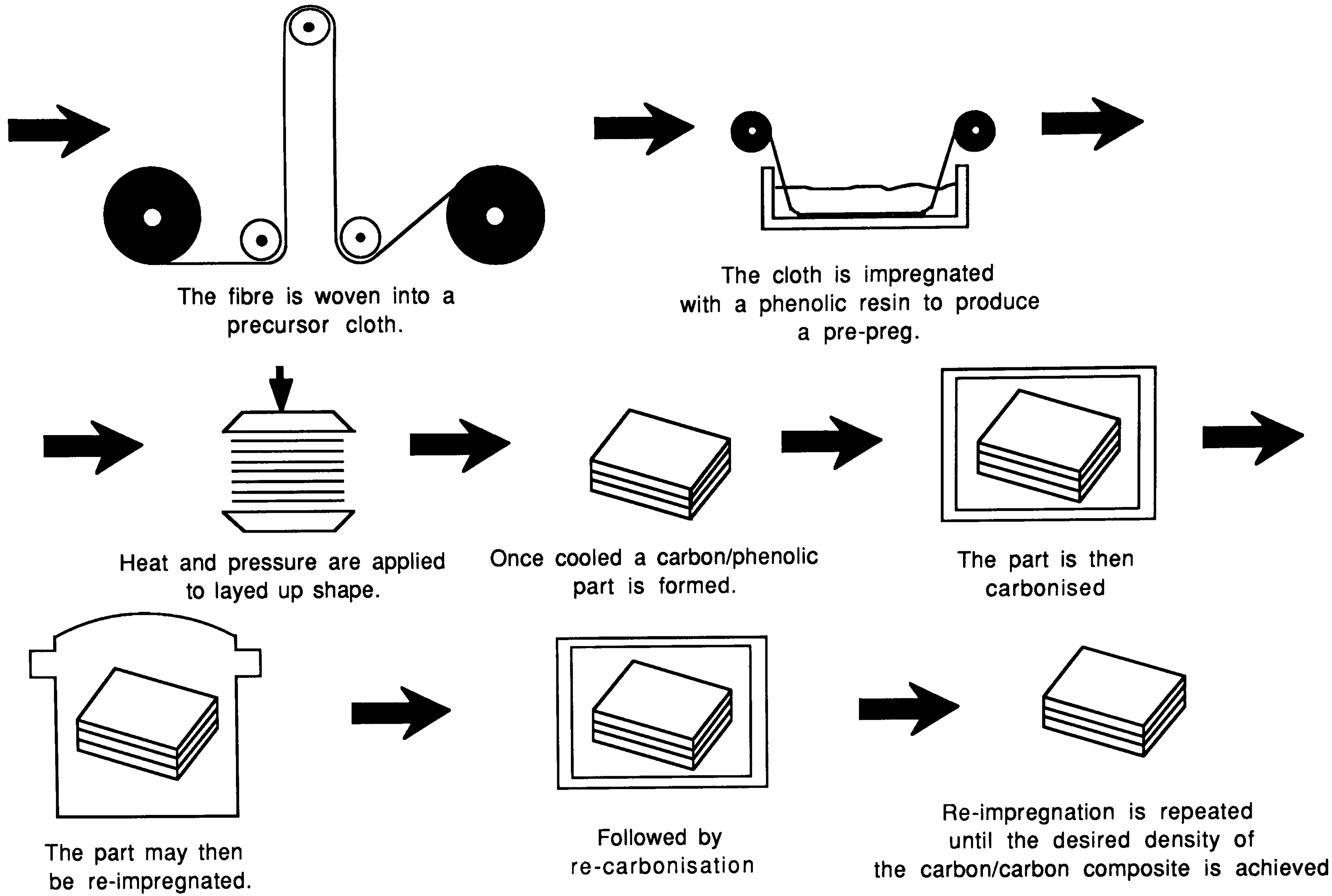

Figure 4.2 Schematic representation of the production of carbon/carbon composites.

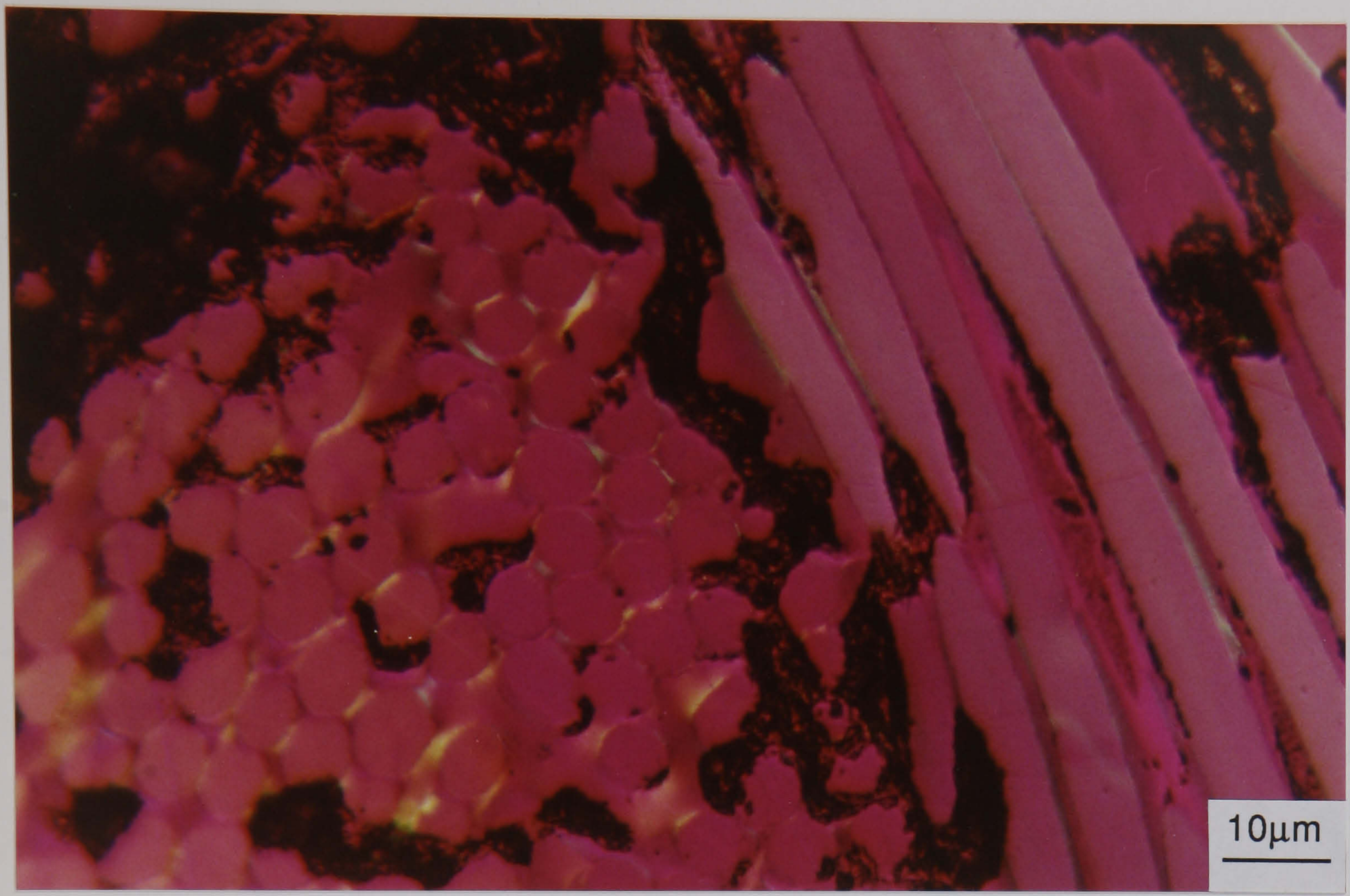

Plate 4.1 Optical micrograph of C10 material taken on a polarized light microscope with a half wave retarder plate.

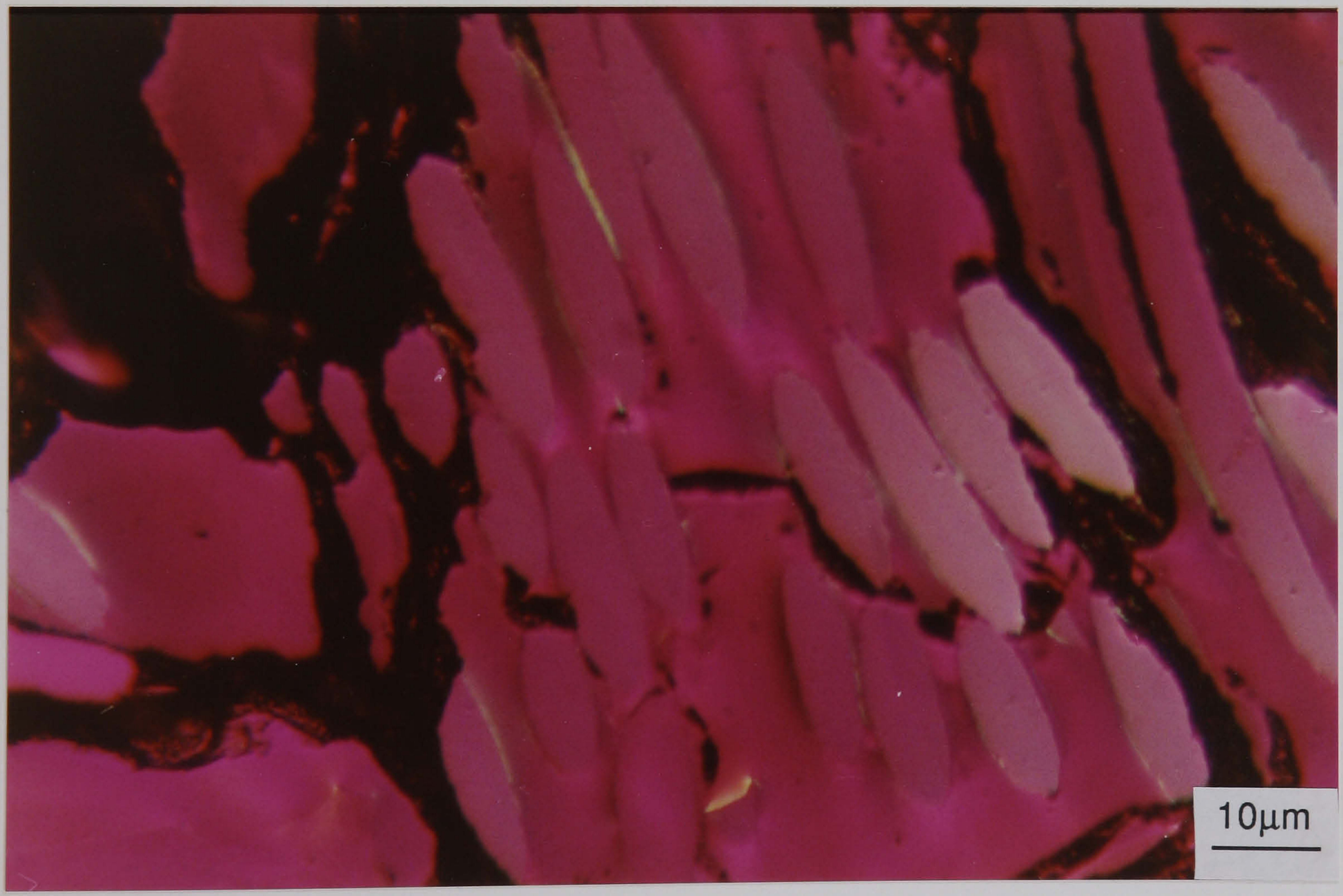

Plate 4.2 Optical micrograph of C12 material taken on a polarized light microscopy with a half wave retarder plate.

materials. Layers of woven Carbon fibres impregnated with the precurser, binding phase are 'laid up' ie stacked on top of each other until the desired thickness is achieved. The pile of fibre mats is then pressed and heated in an inert atmosphere to carburise the binder. The C10 material is then put through a further process, the details of which were unknown. Plate 4.3 is a stereo pair of the edge of a 2-D woven Carbon/Carbon composite, viewed through the coloured glasses a clear idea of the way the structure is built up in can be gained.

4.3.2 Electron microscopy

Fracture surfaces of the two materials were examined in the scanning electron microscope plates 4.4 and 4.5 show typical fibre matrix interfaces. It is clear that the peripheral crack would provide a path for preferential oxidation of the interface. The crack or fissure could be the result of poor wetting of the fibre by the binding phase during production or excessive shrinkage of the binder during carburisation resulting in such interfacial cracks after heat treatment, as reported by Edwards (1989).

4.3.3 Chemical analysis

The samples of C10 and C12 were qualitatively analysed using windowless EDX analysis. The traces are shown in figure 4.3 and 4.4. The important findings were the presence of Potassium, Calcium and Iron which are all known to catalyse the oxidation of Carbon by O_2 (McKee, 1965) The other impurities probably originating from the binding phase are of less importance. The findings were discussed with Johnson Radley, it was revealed that C12 has no minimum impurity specification but that C10 must have an Iron content below 25 parts per million. This level being obtained by a purification by Chlorine at 2000°C (Parker, 1982). This is the type of treatment which presumably turns C12 in to C10. The amount of Iron is singled out as it is the one of the most commonly found contaminants. Its presence is a good indicator of the general purity of the material.

As levels of Iron contamination were not normally monitored by Johnson Radley it was decided to assess current level in C10 and C12. Samples of the current stock were analysed by Johnson Radley using XRF analysis on 40mm diameter disc samples, C10 material gave results from 19 up to 25 ppm: below

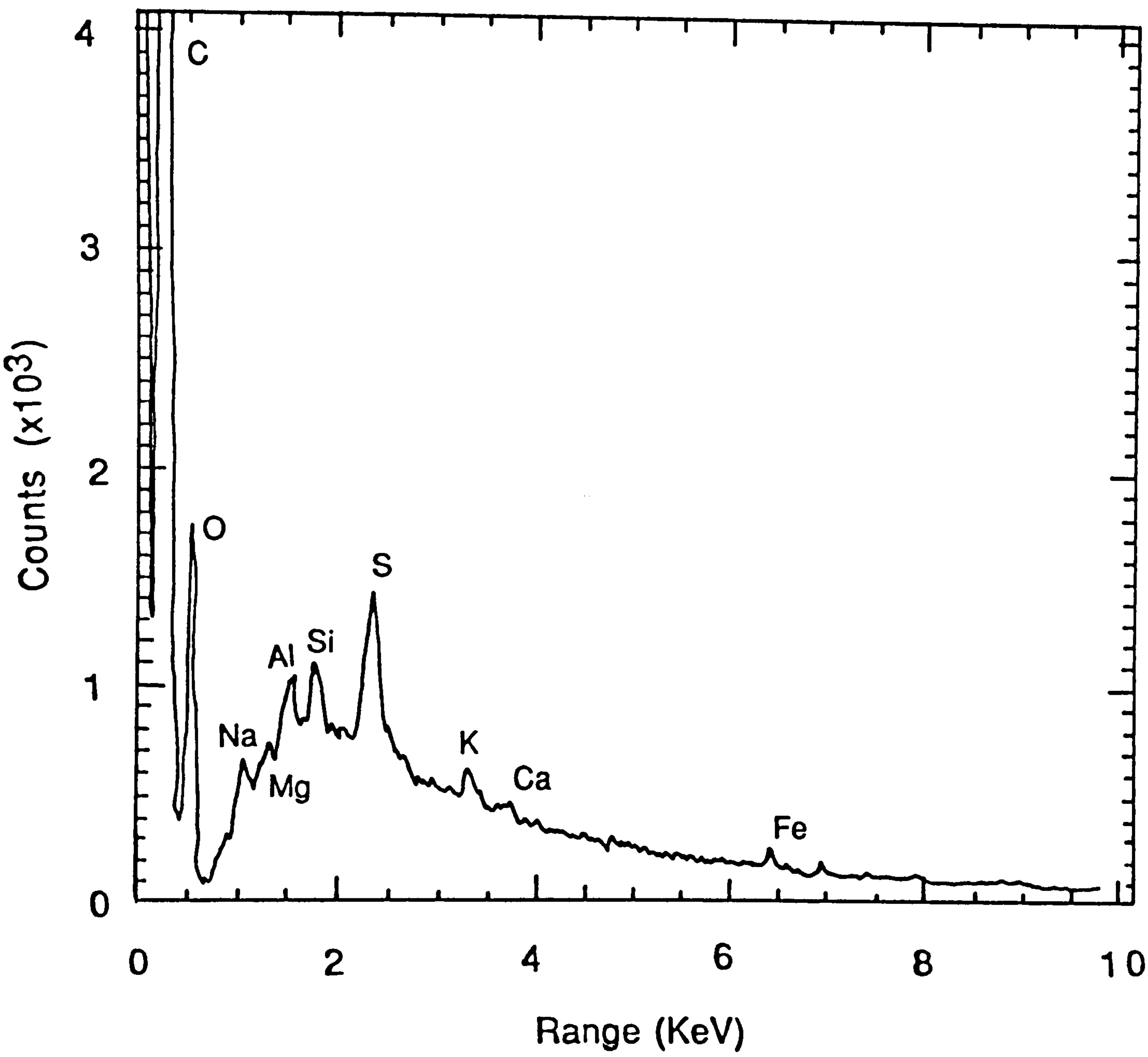

Figure 4.3 EDX trace for C10 material, taken with a windowless detector, the electron beam current was 15KeV.

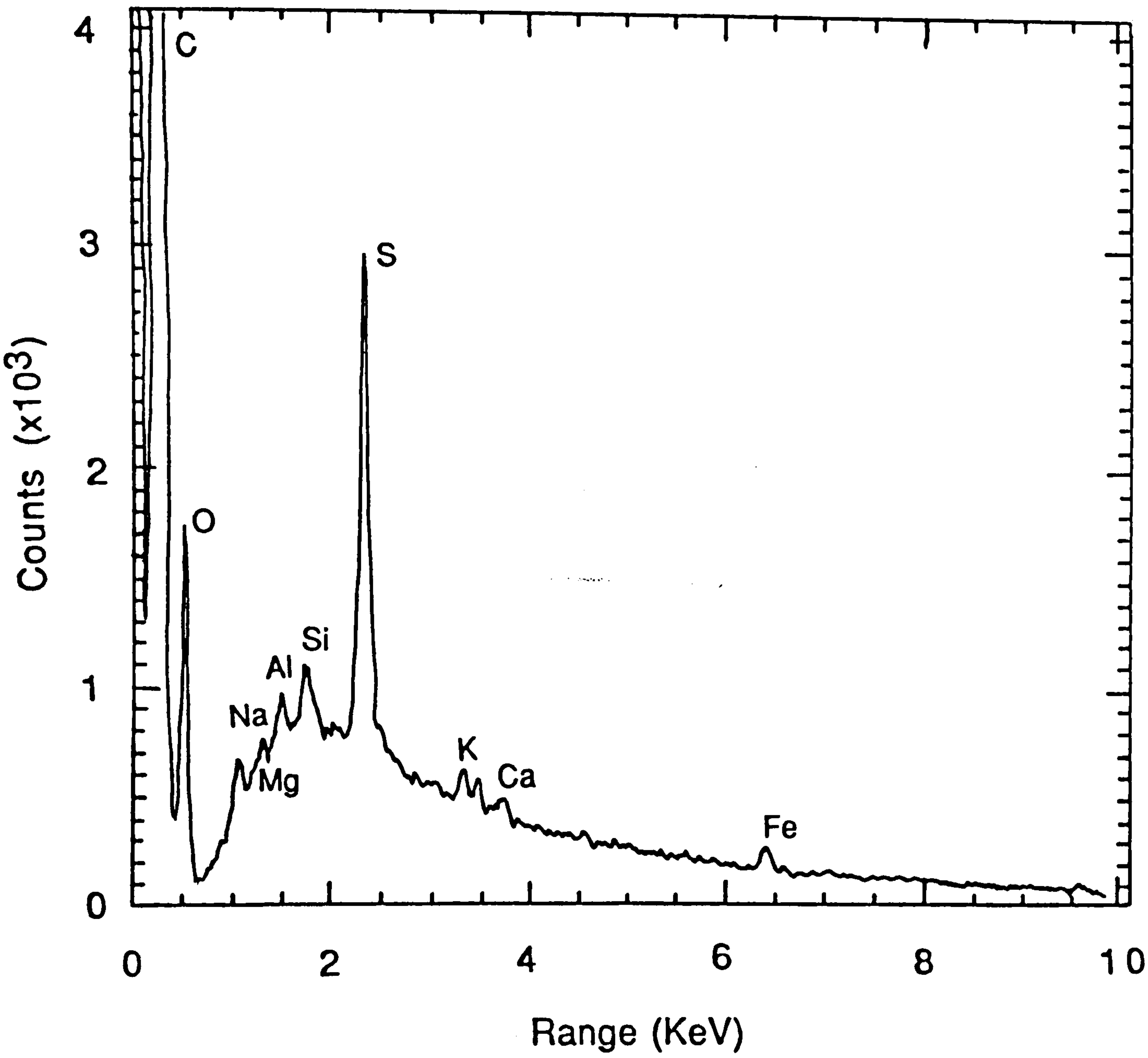

Figure 4.4 EDX trace for C12 material, taken with a windowless detector, the electron beam current was 15KeV.

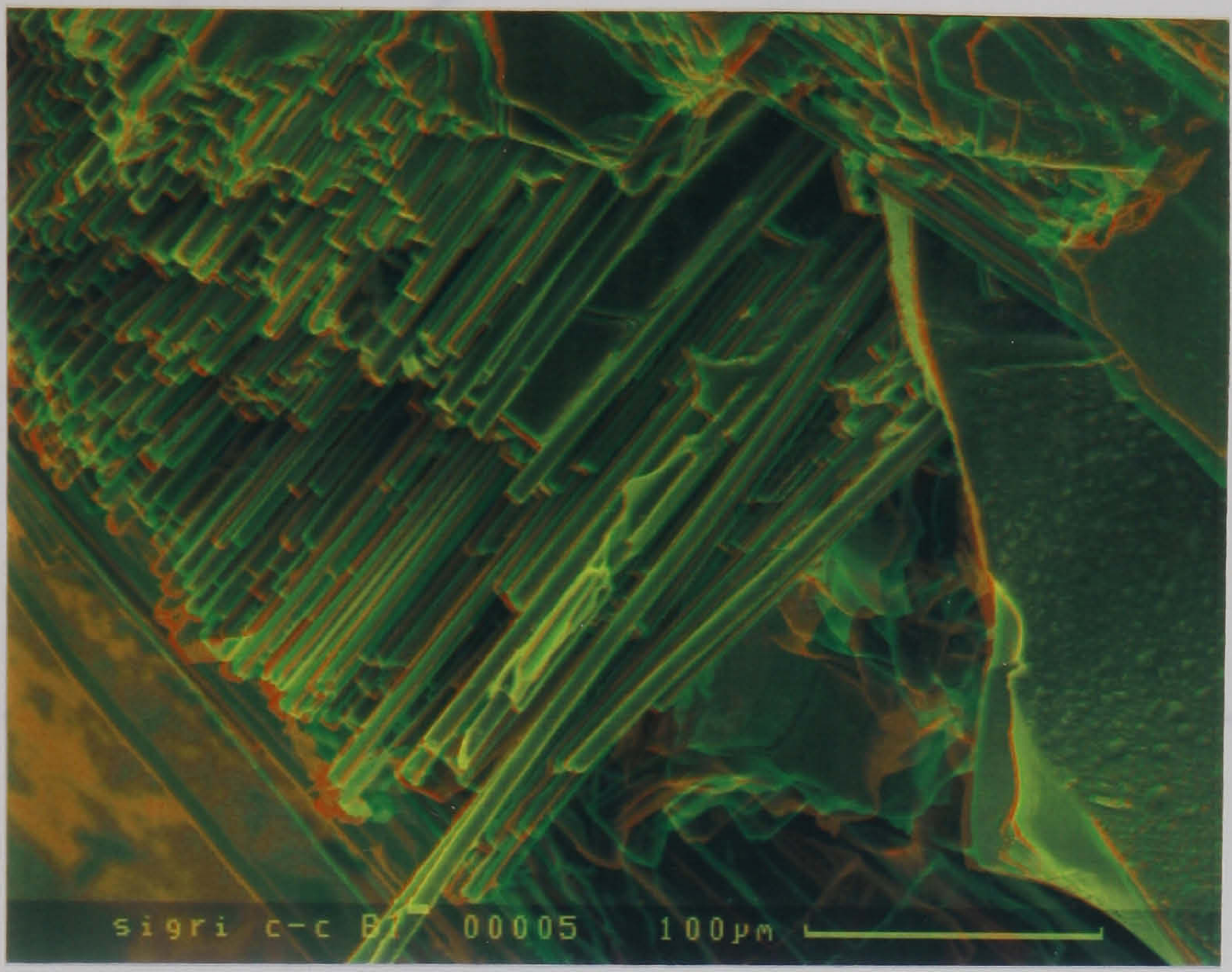

Plate 4.3 This plate combines the two secondary electron images taken on the scanning electron microscopy in the form of a stereo pair. When viewed through the green and red glasses a 3-D image can be seen. This stereo pair shows the nature of the weave in a 2-D Carbon/Carbon composite.

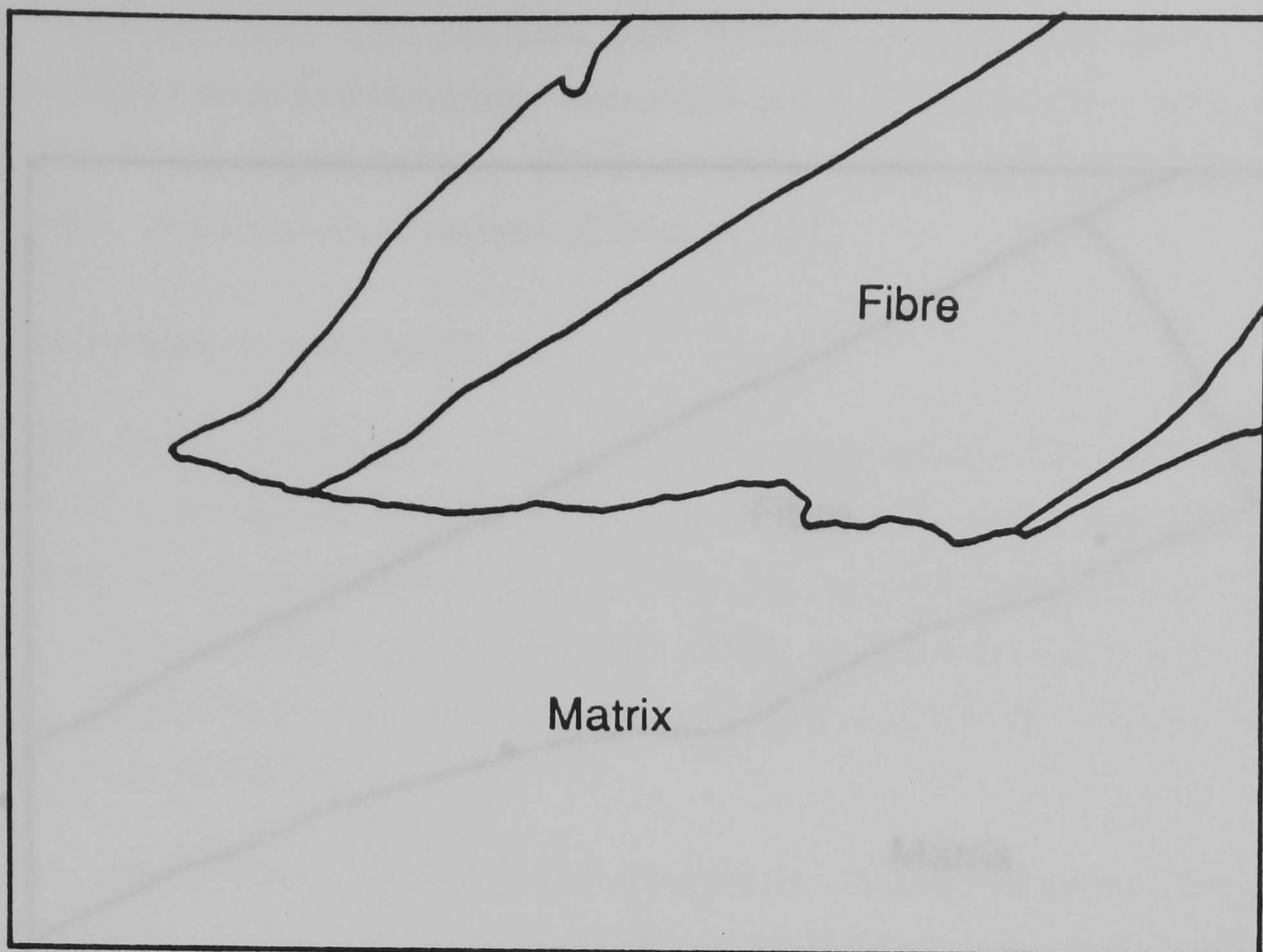

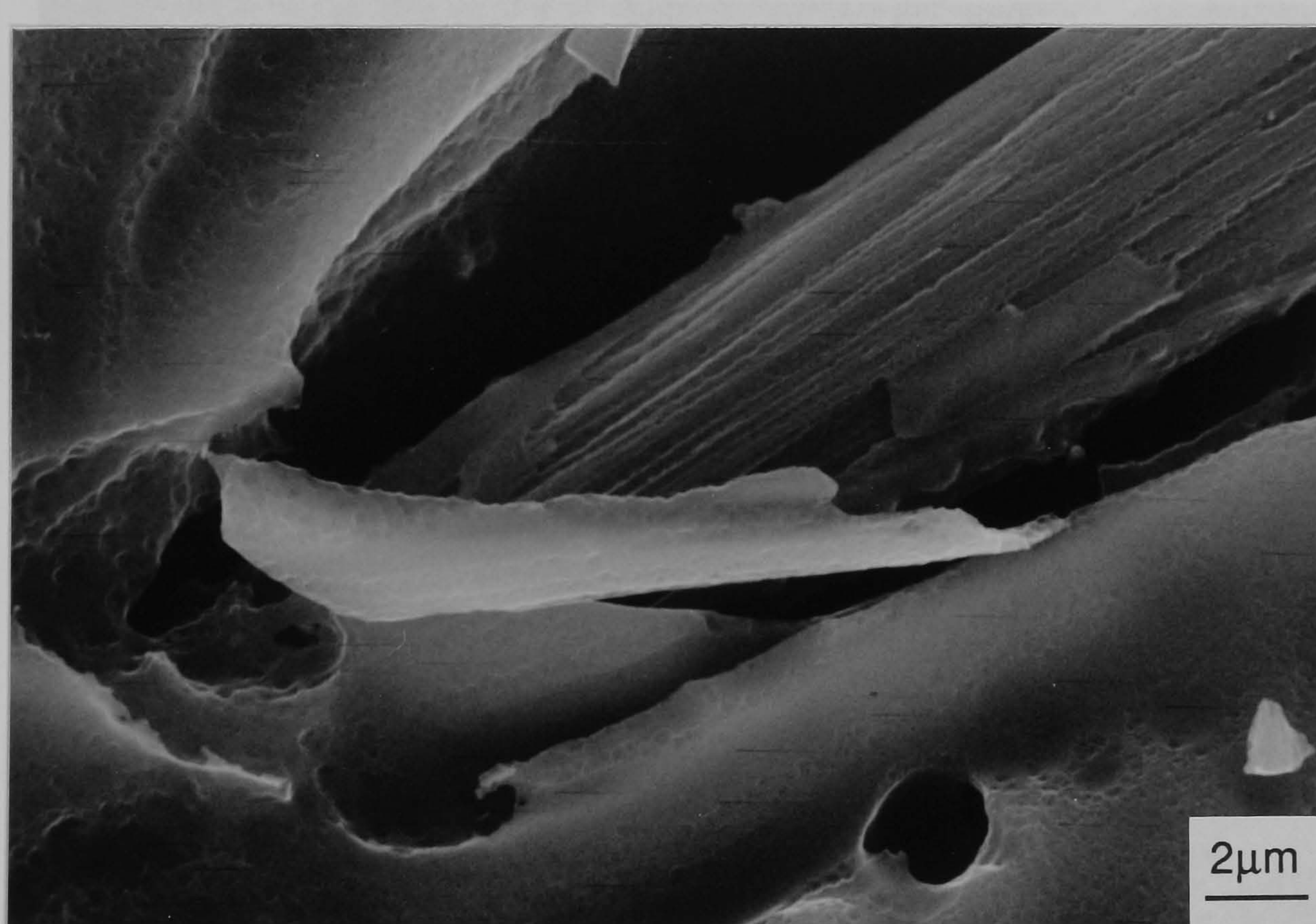

Plate 4.4 Scanning electron micrograph of the fracture surface of the Carbon/Carbon composite. The line drawing identifies the different phases in the micrograph. A peripheral crack around the fibre can be seen

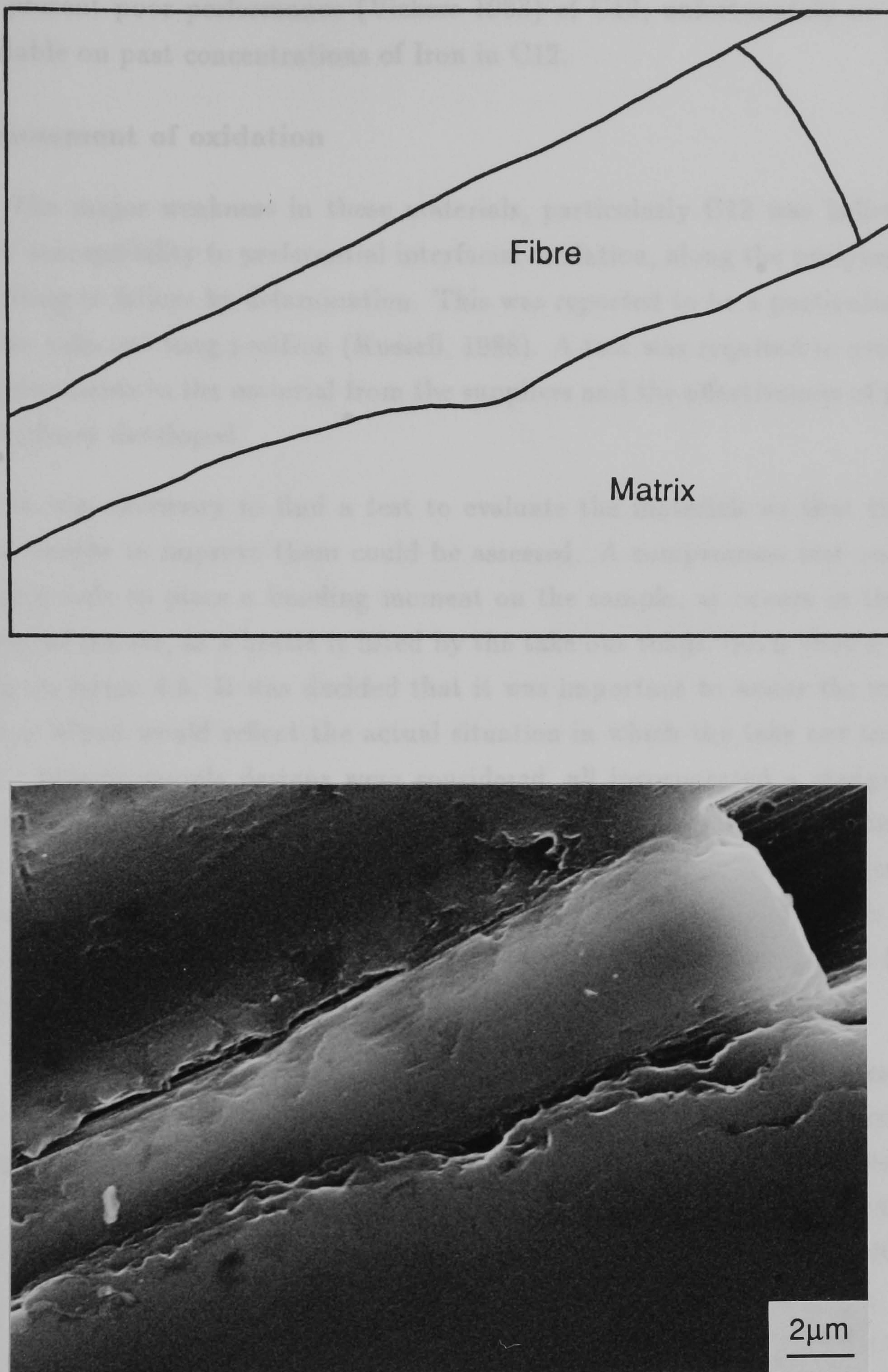

Plate 4.5 Scanning electron micrograph of a Carbon/Carbon composite. The line drawing identifies the different phases in the micrograph. The micrograph clearly shows a crack running along the fibre matrix interface

the limits specified. C12 samples gave readings ranging from 90 up to 150ppm. These high values and the range were both cause for concern but helped to explain the present poor performance (Vickers 1988) of C12, unfortunately no data were available on past concentrations of Iron in C12.

4.3.4 Assessment of oxidation

The major weakness in these materials, particularly C12 was believed to be their susceptibility to preferential interfacial oxidation, along the peripheral cracks resulting in failure by delamination. This was reported to be a particular problem in the take out tong position (Russell, 1988). A test was required to evaluate any improvements in the material from the suppliers and the effectiveness of protective procedures developed.

It was necessary to find a test to evaluate the materials so that the success of attempts to improve them could be assessed. A compression test on a cuboid sample fails to place a bending moment on the sample, as occurs in the profiled material inserts, as a bottle is lifted by the take out tongs. This is shown schematically in figure 4.5. It was decided that it was important to assess the material in a way which would reflect the actual situation in which the take out tong inserts fail. Several sample designs were considered, all incorporated a stepped profile, as the take out tong inserts had failed most often at the corner of a step. In the most severe cases sections of the top layer of the laminate had become completely delaminated and sections flaked off. The stepped test piece, designed to be tested in three point bending, chosen to fulfil these requirements is shown in figure 2.7. The details of the testing procedure are given in section 2.5.

Once testing began it quickly became clear that samples cut from different sheets of material had very variable strengths, resulting in an extremely large scatter of results. Before any treatment the breaking load of samples, ranged from 133 to 214N. Samples that had been exposed to an oxidisation treatment, comprising 12 hours at 400°C in air, had breaking loads ranging from 116 to 178N. The analysis of the effects of oxidation depended upon realising that variations between samples cut from the same plate were slight. This was possible as samples had been labeled according to their sheet of origin. Unfortunately only small sheet of material were available and it was impossible to assess different oxidation

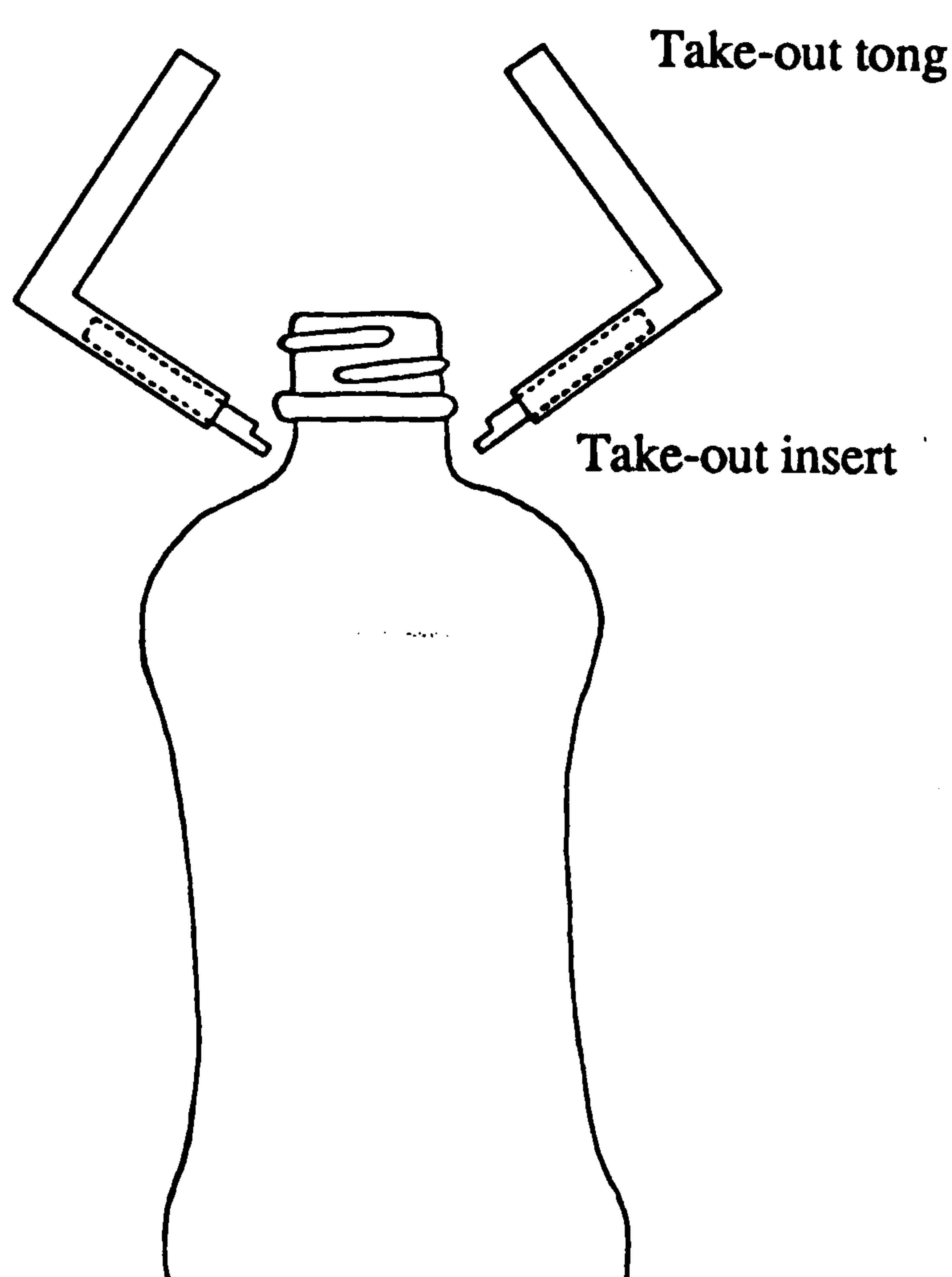

Figure 4.5 Representation of the take-out position, note the step in the take-out insert which lifts the container.

treatments with samples from the same sheet. In an attempt to allow comparison of results from samples cut from different sheets of C10/12 to be made it was necessary to normalise the data. This was achieved by dividing the breaking load recorded for a sample by the maximum breaking load of a non oxidised sample cut from the same sheet. Thus all the results are expressed as a decimal between 0 and 1.

It is interesting to note at this point the way in which the samples failed Figure 4.6 shows schematically the two different modes of failure. The complete delamination in 4.6b occurred in the oxidised C12 samples, so supporting the theory that preferential oxidation along the fibre/matrix interface results in delamination.

The small number of samples tested at each temperature was due to the limited amount of material available at the time. In figure 4.7 the loads at which samples of C10 and C12 failed after oxidation at 400°C, for varying lengths of time are compared. It can be seen that C10 is a more oxidation resistant material as was reported previously.

To enable comparisons to be made with Johnson Radley's quality control results, the failure strength of the two materials before oxidation was tested in compression as detailed in 2.10 the mean failure stress for C10 was 73MPa and for C12 it was 78.3MPa. It can be seen that the C10 material was only slightly weaker than C12. Comparing these results with Budd's (1986) who found that the mean failure stress in compression for C10 and C12 was 85MPa and 145MPa respectively, it is evident that a drop in the strength of both the supplied materials has occurred, the drastic change in the strength of the C12 material caused great concern. Dr Budd supplied samples of material supplied in 1986 when the original tests were carried out, their oxidation resistance was evaluated using the stepped specimen test. Figure 4.8 shows the results of these tests on old C12 along with those for present material.

It is clear that the old material has a much greater resistance to oxidation than the more recently produced material. These results explained the more rapid failure of C12 in service reported at the time (Vickers, 1988). A comparison of old and new C10 material shows the two have similar oxidation resistance although the strength has fallen, the results are shown in figure 4.9.

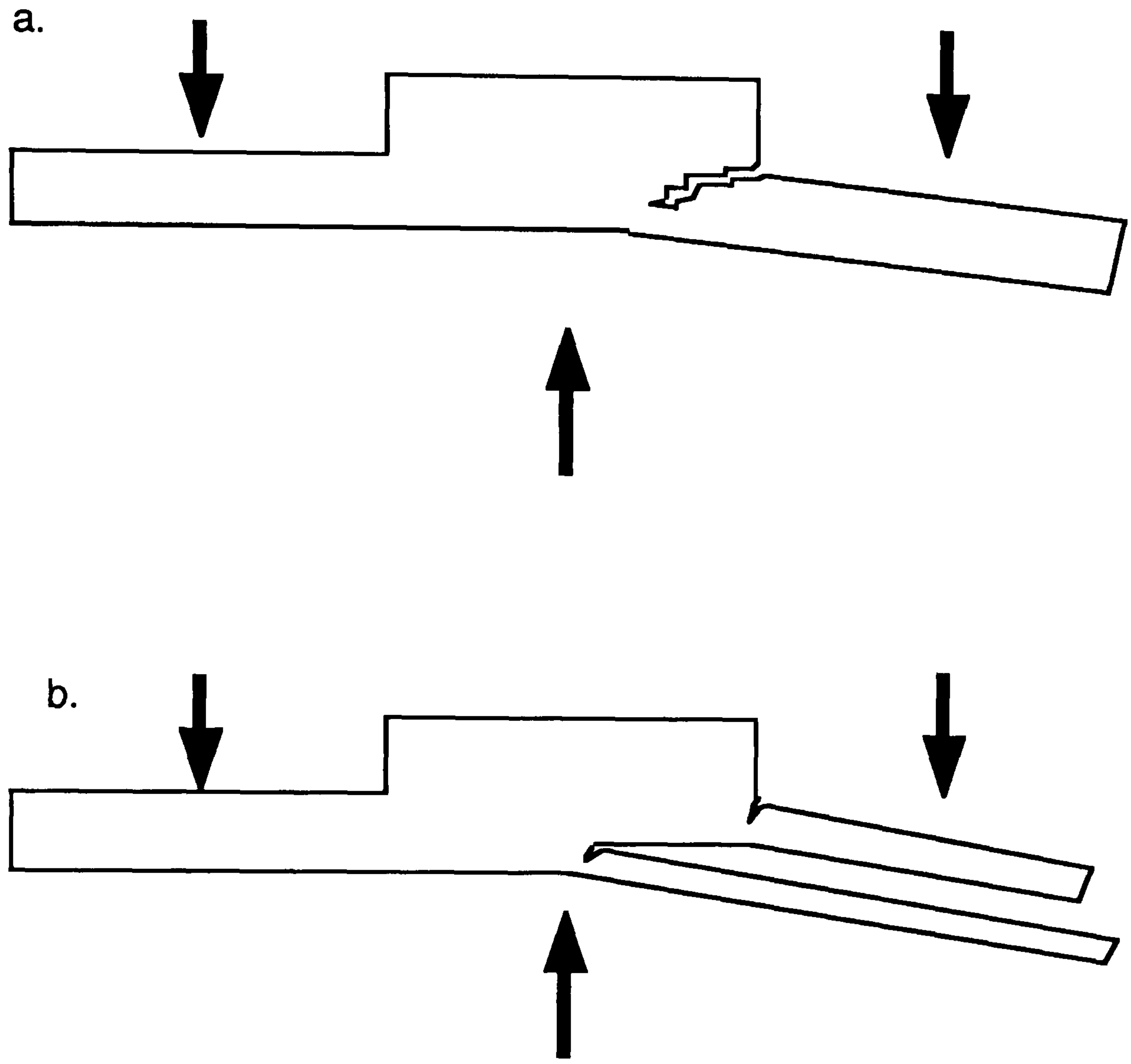

Figure 4.6 a.Schematic representaion of a typical failure in C10 material.
b.Schematic representation of a typical failure in C12 material.

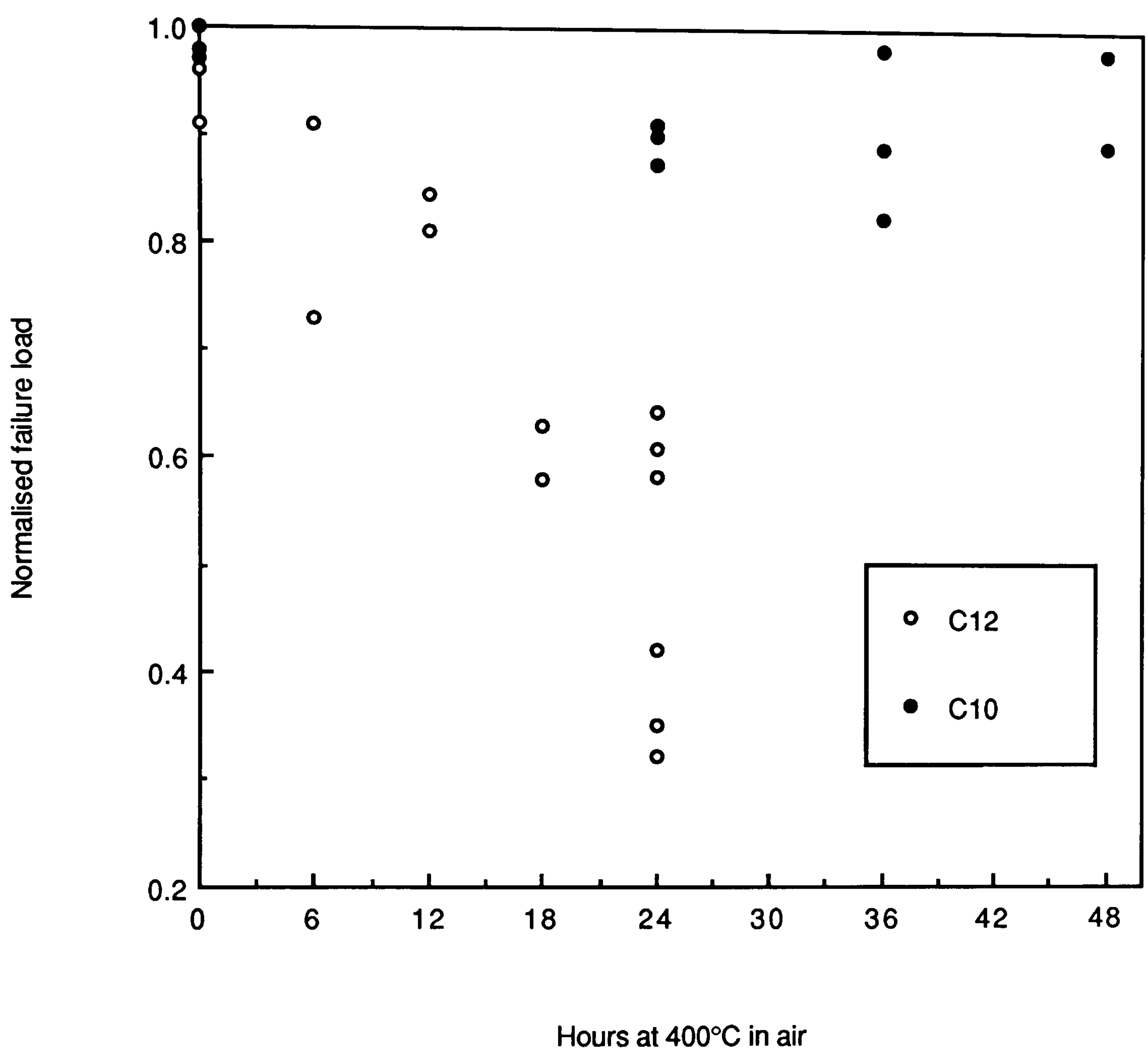

Figure 4.7 A comparison of the oxidation resistance of C10 and C12.

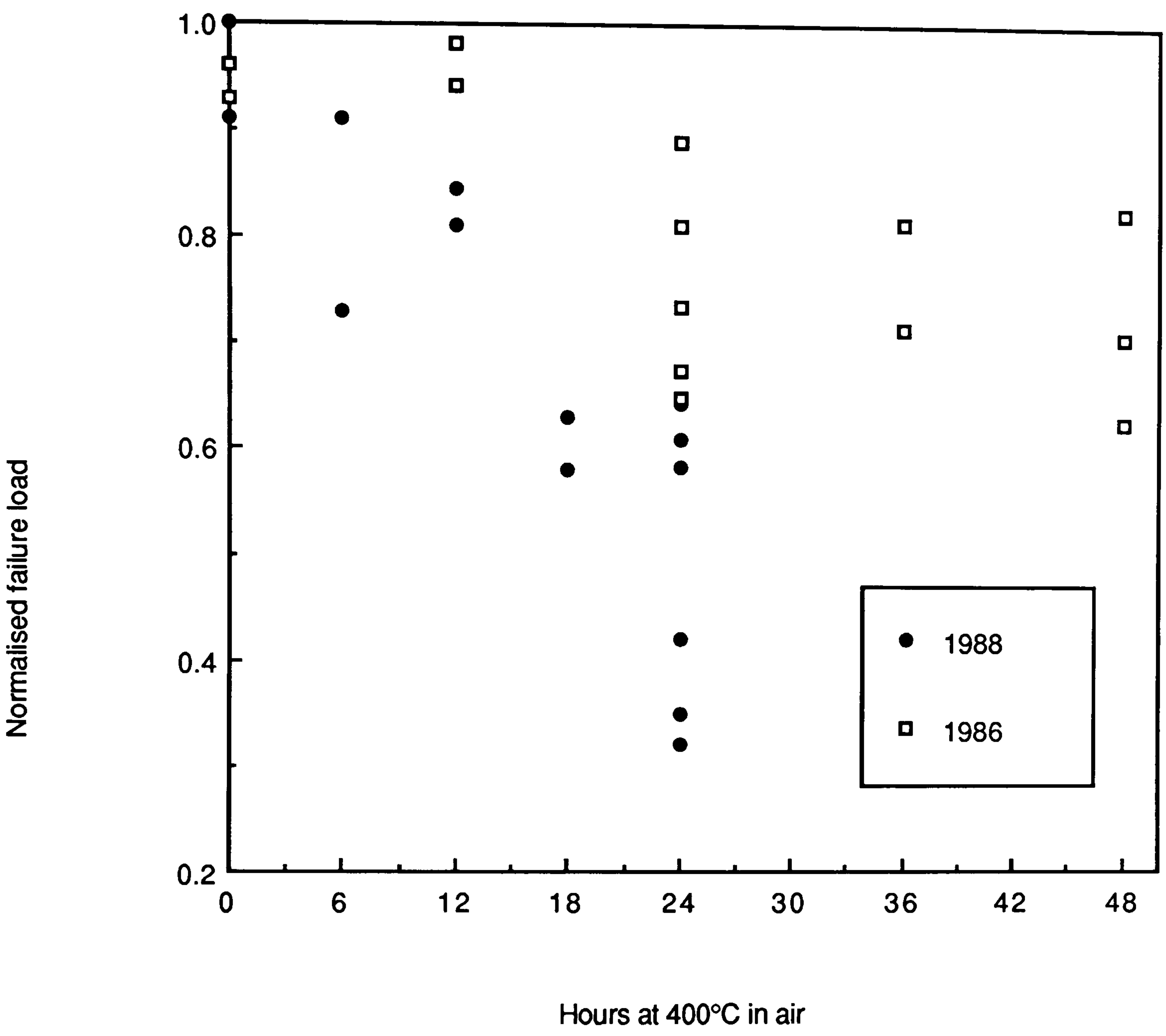

Figure 4.8 Comparison of the oxidation resistance of old and new C12 material

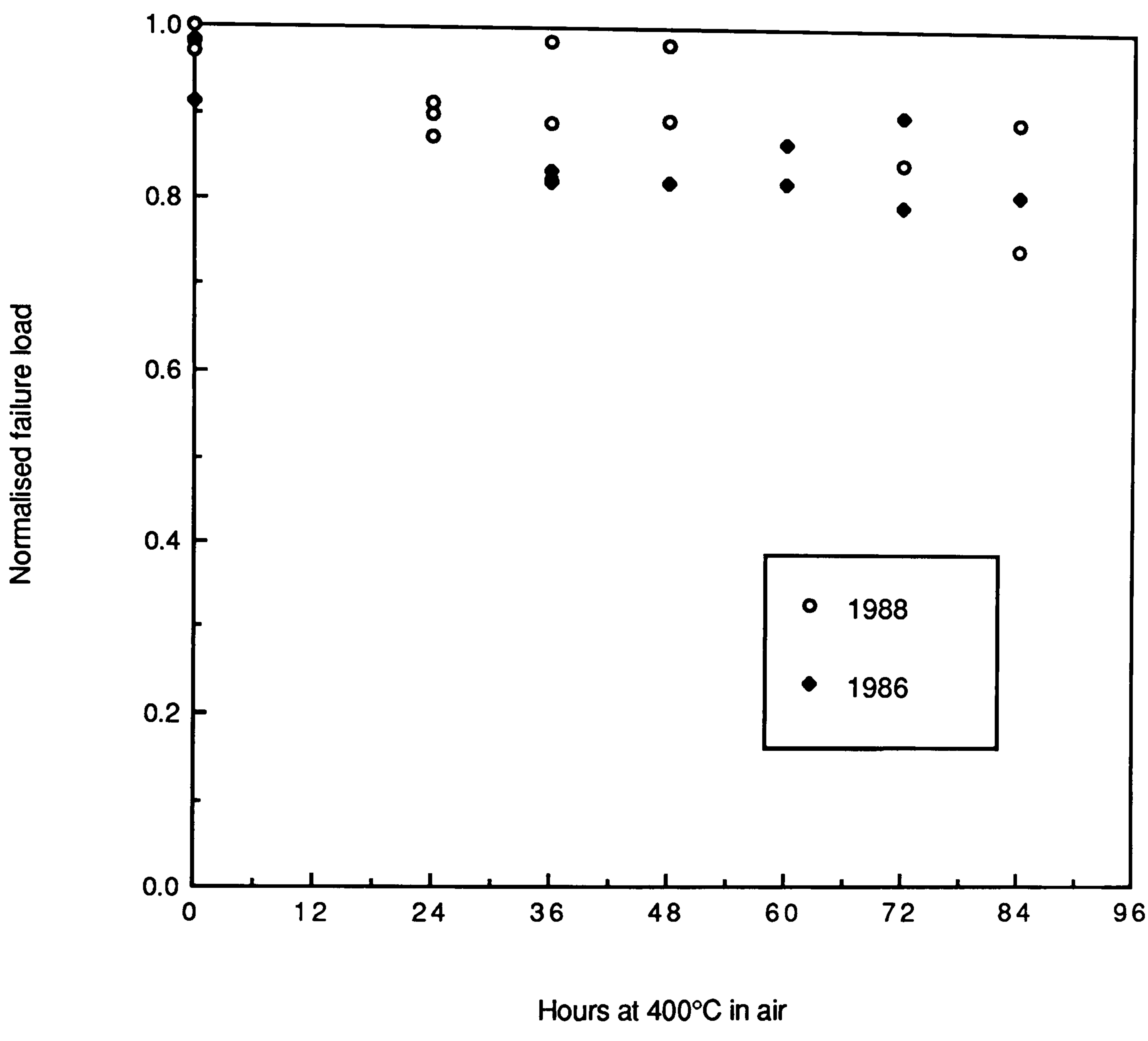

Figure 4.9 Comparison of the oxidation resistance of new and old C10 material

4.3.5 Protection of Carbon/Carbon composites

It was thought that if the surface porosity of these materials could be sealed with some form of coating, then internal oxidation would be limited and the life of the component extended. The difficulty being in doing this and retaining the handling properties of the material.

It was not surprising after considering the attractive structural properties of Carbon/Carbon composites, achievable in excess of 2000°C, when the environment is not oxidising that much work has been completed on the protection from oxidation of such materials. The threshold for which is approximately 370°C (Strife and Sheeham, 1988) and which can be rapid at temperatures as low as 500°C (McKee, 1986). The protection of carbonaceous materials from oxidation has been the aim of work for more than 50 years but the first efforts to protect Carbon/Carbon composites were in the early 1970's. The aim being the protection of heat shield materials for the shuttle orbiter vehicles. Carbon/Carbon composites were used on the leading edge of the wings and on the nose cone. They were protected from oxidation at temperatures ≈ 1650°C by a silicon carbide coating impregnated with silica. The silicon carbide coating was produced by a pack cementation process, where the fully carbonated Carbon/Carbon composite was packed in a mixture of Silicon carbide, alumina and metallic Silicon. The complete system was then subjected to a baking cycle at ≈ 1650°C in an Argon atmosphere. The outer layers of the composite are converted to Silicon carbide by the process to a depth of between 0.05-0.1cm. However the resulting Silicon carbide layer was micro-cracked, as a result of the difference in thermal expansion between the silicon carbide layer and the substrate. Further protection was provided by the silica present in the coating. The silica was added by a pressurised impregnation of tetraethyl orthosilicate followed by high temperature treatment developing silica deposits in the pores of the laminated substrate (Korb *et al*, 1981). Huettner et al (1988) also used pack processing to produce a silicon carbide coating further protected by borate or phosphate glassy sealants. The phosphates being the most effective as a result of the lower rate of diffusion of O_2 through it. These authors also produced Silicon carbide coatings by chemical vapour deposition (CVD) processing as have Fitzer *et al* (1988)where they compared Silicon carbide deposited by CVD from methyl-trichlorosilane with that formed by the impregnation of Carbon/Carbon composites by a Silicon-organic compound followed by subsequent thermolysis of the polymer to Silicon carbide. In this material the resulting Silicon carbide was not so much a surface layer as a further densification of the composite, this did not prove as effective as the CVD Silicon carbide in limiting oxidation.

Protection at temperatures greater than 1500°C was achieved by McKee (1987) utilising borates as a sealant for a Silicon carbide coating. He also used Borate based coatings containing refractory particles, including

- the borides of Zirconium, Hafnium, Silicon and Aluminium,
- the oxides of Zirconium, Hafnium, Silicon and the rare earth metals,
- Silicon carbide,
- Zirconium silicide,
- Boron nitride.

The use of these materials was also discussed by Strife and Sheeham (1988) in their comprehensive review of coatings for the protection of Carbon/Carbon composites. They also consider the development of silica coatings from additives, designed to oxidise once the material in which they are placed is exposed to an oxidising environment.

All the above coatings identified in the literature are based upon ceramic materials which would completely alter the surface properties of a handling material. Such a system is discussed in section 4.5. In this problem a different approach would be needed.

Chemical analysis had shown that the C12 material contained many catalytic impurities. It was decided to try and apply a protective surface of very pure Carbon. The Carbon would act to seal the pores in the surface so limiting the internal oxidation and also protecting against oil contamination. As the coating would be of Carbon containing only very small amounts of catalytic impurities it would oxidise at a slower rate than the matrix, hopefully extending the life of the component. Most importantly doing this with out changing the nature of the surface of the handling material.

A synthetic pitch produced from a polymer precurser was used to provide the Carbon coating the method of application is described in 2.6. Figure 4.10 shows the results of stepped sample tests carried out on coated C12 samples, along with those of non-coated material. From these few experiments the indication was that the technique would be effective in prolonging the life of the C12 material but no further work was completed once a decision was made by Johnson Radley after discussion based on the results of this work to concentrate on C10 and on improving the base material rather than protection mechanisms for a poor base material.

4.4 Fine grained Carbons

There were several hot glass handling materials available at the start of this project best described as fine grained Carbons, marketed under several trade names including, Duratemp (D2). This materials handling ability was excellent as shown in figures 3.31 – 3.33 but the fine grained materials were not tough and had a tendency to fail catastrophically during machining (McDermott, 1987). Johnson Radley did not market this type of material. In mid 1988 a product called Poco glassmate (P1) appeared in the market. In use the material showed a longer life than any other Carbon based material (Vickers 1988). Although some users of the material reported 'checking' of containers by the material, it became very widely used.

4.4.1 Chemical analysis

Samples of the D1 and P1 were analysed using EDX analysis as for the Carbon/Carbon composites, figures 4.11, 4.12, show the traces. The trace for P1, figure 4.12 shows a very smooth background indicating that the material is free from impurities. The only peaks other than Carbon are Phosphorus, Oxygen and Zinc. It is though that these are the result of specific additions in the form of Zinc Phosphate to act as a protection mechanism against oxidation.

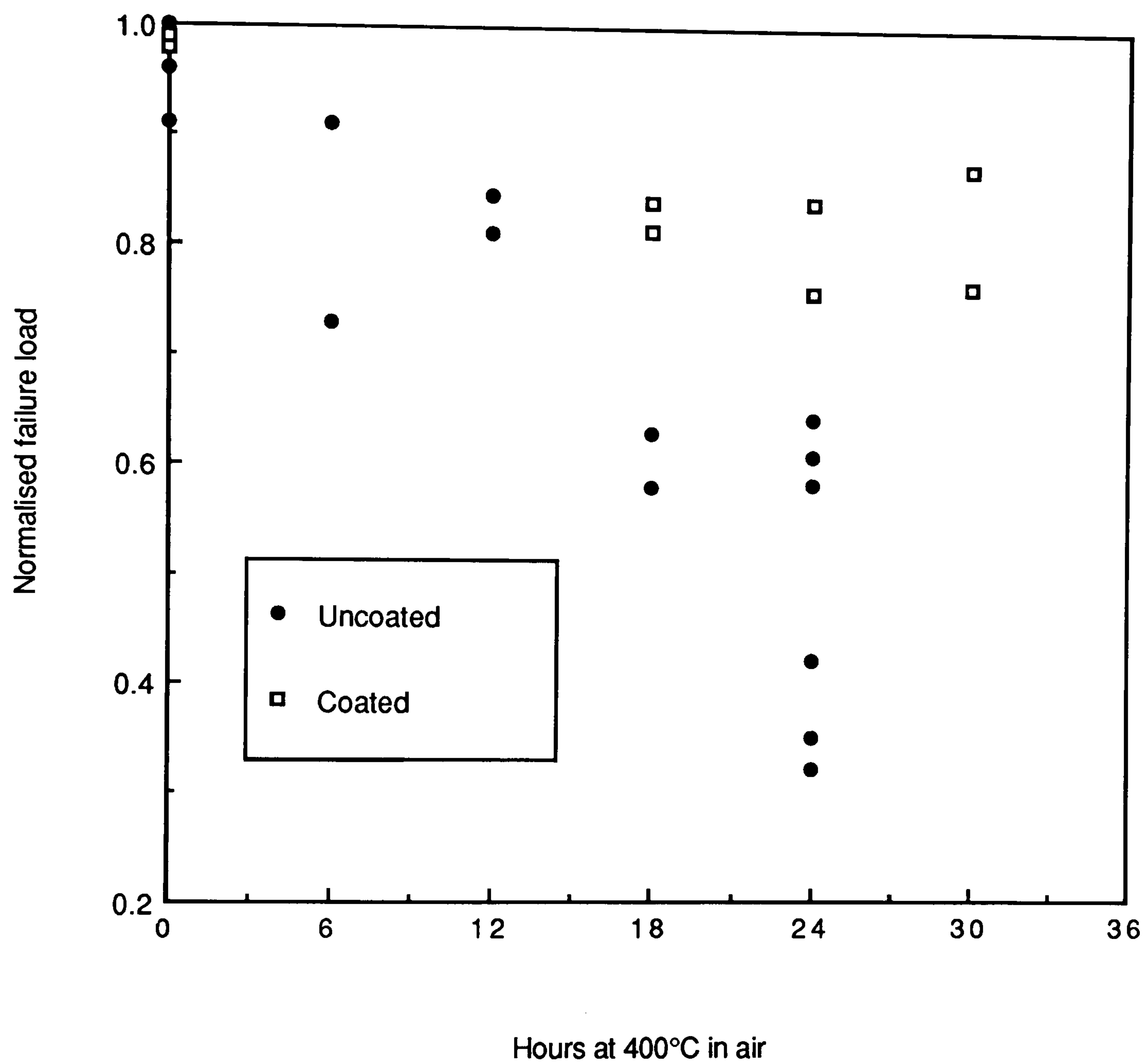

Figure 4.10 A comparison of the coated and uncoated C12 material

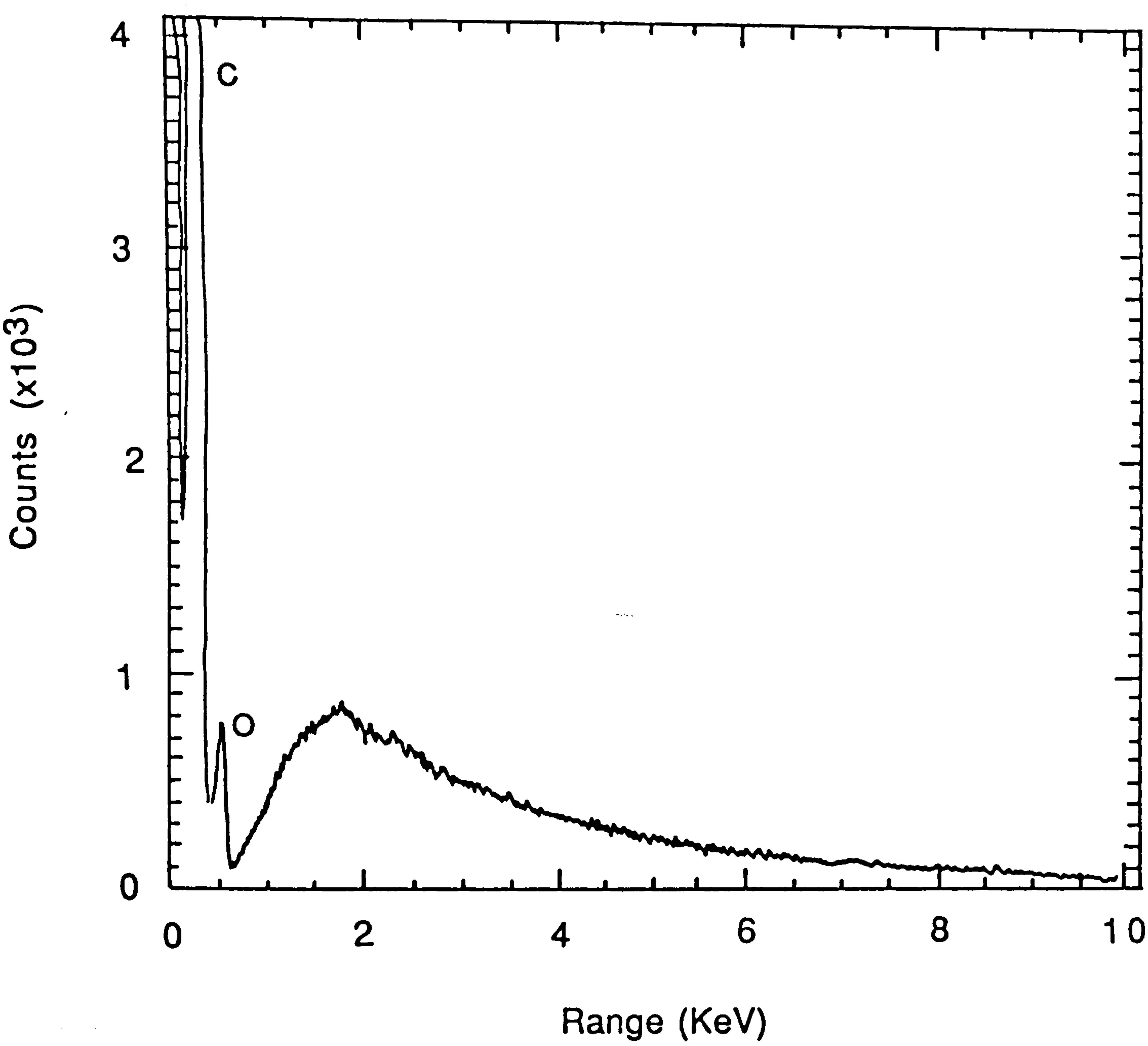

Figure 4.11 EDX trace for D2 material, taken with a windowless detector, the electron beam current was 15KeV.

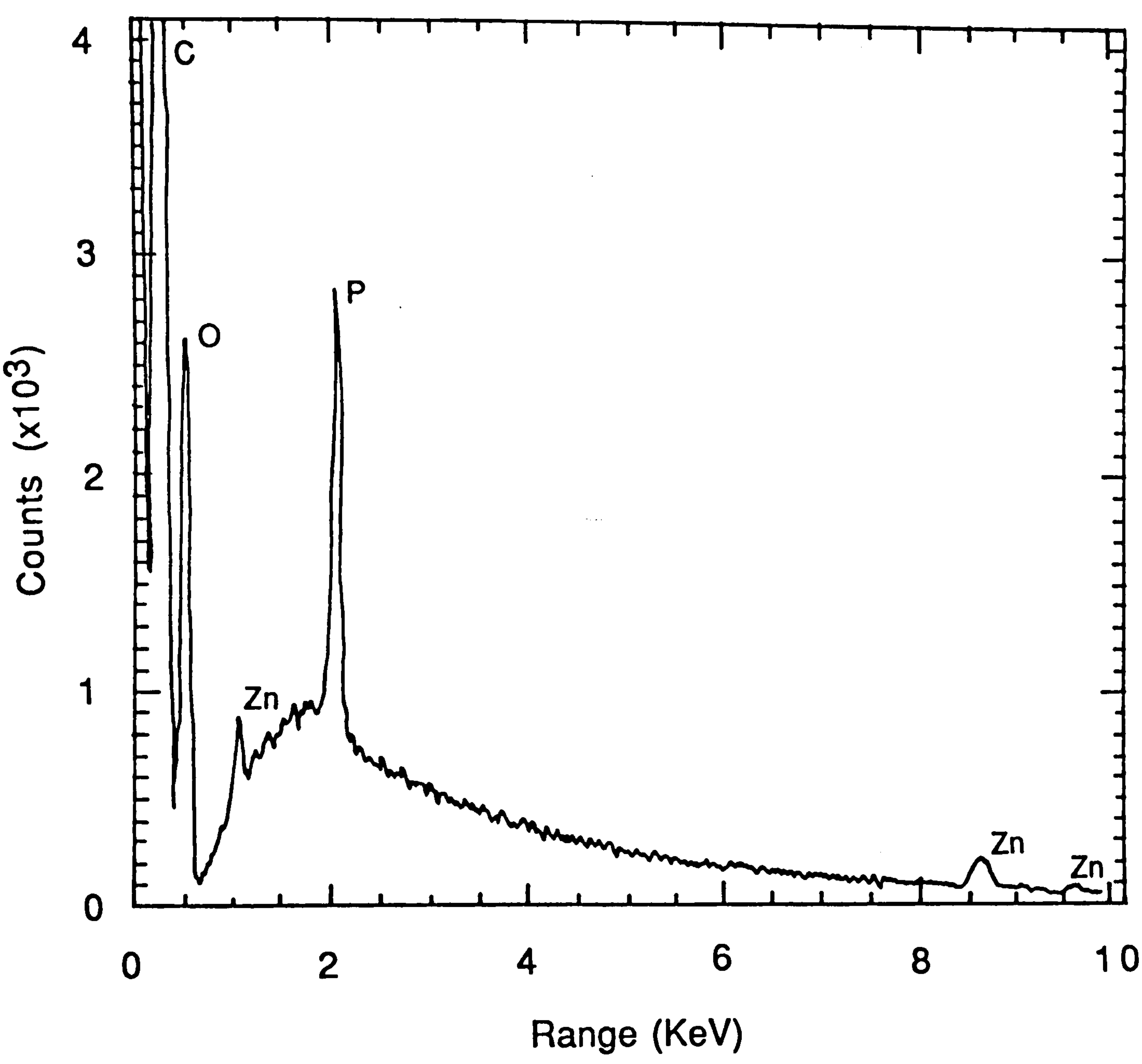

Figure 4.12 EDX trace for P1 material, taken with a windowless detector, the electron beam current was 15KeV.

The protection system could act in one of two ways.

1. By inhibiting the reaction.

2. By forming a glassy physical barrier at the surface so smothering the reaction.

Metal phosphates are one of very few compounds reported as oxidation inhibitors (Magne *et al*, 1971). Phosphates were also reported as successful inhibitors by McKee *et al* (1984) where they were added in the form of phosphate esters in alcoholic solutions. They concluded that OPO_3 groups strongly adhered to the surface at active sites. It was noted that the adsorption resulting from the treatment could amount to a complete monolayer coverage of the graphite used in the study. Although other Phosphorus based inhibitors particularly $POCl_3$ are known to markedly reduce the rate of oxidation at concentrations very much less than that necessary to cover the complete surface (McKee, 1981). Optical studies by McKee (1972) on single crystal graphite showed that the additive strongly adsorbs at dislocation cores and on the edges of pre-formed etch pits in the basal plane. McKee (1981) doubts that metal phosphates act as inhibitors so much as smothering oxidation by the production of a glassy phase at the surface. This view is also supported by Strife and Sheehan (1988).

Oxidation of P1 at 800°C resulted in a glassy residue in the crucible of 7.4 weight percent. The added percentage of phosphate was reported by Vickers (1988) to be 7%. It was thought that in the P1 the Zinc phosphate produced a glassy phase at the surface so protecting it from oxidation.

4.4.2 Assessment of oxidation

These materials are utilised in many different sites at the hot end of a glass production line. They are not specifically take out tong materials. This fact, plus the isotropic nature of the materials meant that the stepped sample tested in three point bending was inappropriate to assess the effects of oxidation on these materials.

The materials were evaluated by thermal gravimetric analysis. Both the D2 and P1 materials were analysed as in section 2.9 as was C10 so that comparisons could be made. In figure 4.13 the results of these analyses are plotted as percentage weight loss against temperature. It is clear that the P1 material is protected from oxidation up to 700°C. The other materials all show varying amounts of oxidation resistance. The material exhibiting the least resistance to oxidation is the C10, this was expected as the material is porous and so exposes the largest surface area to the oxidising environment. The D2 material, a fine grained carbon without a protection system lies between the other two.

The effectiveness of the P1 material's protection system resulted in the material becoming widely used in the take out tong position by many manufacturers. As a result of the popularity of the material Johnson Radley introduced two fine grained carbon based materials. The first with out an oxidation protection system known as C22. The second was the same basic material protected by aluminium phosphate impregnation to be known as C25. They also decided to market a similarly protected Carbon/Carbon composite, the impregnated C10 was to be known as C30.

These new materials were analysed in the same way. The results are also shown in figure 4.13. It is evident the addition of the phosphate protection system has been successful in limiting the oxidation of the C10 material (called C30 in it's protected form). The C25 begins to show a small weight loss just above 500°C considerably lower than the P1 material.

4.5 The handling efficiency of impregnated materials

C22, C25 and C30 were each used to complete the standard contact test to assess the retained strength of polished glass rods after contact with them. The details of the tests are given in section 2.4, the results of this test completed for existing handling materials were presented in section 3.6.

It was noted in section 3.6.7 that P1 rated as one of the most efficient handling materials when tested isothermally dropped in rank dramatically when thermal shock was introduced to the test. The P1 material then ranked below the fibre composites in effectiveness (see figures 3.31 and 3.33). A first reaction was that this was due exclusively to the high thermal conductivity of the material which was noted during calculations in section 3.4.3. This would have meant that the thermal

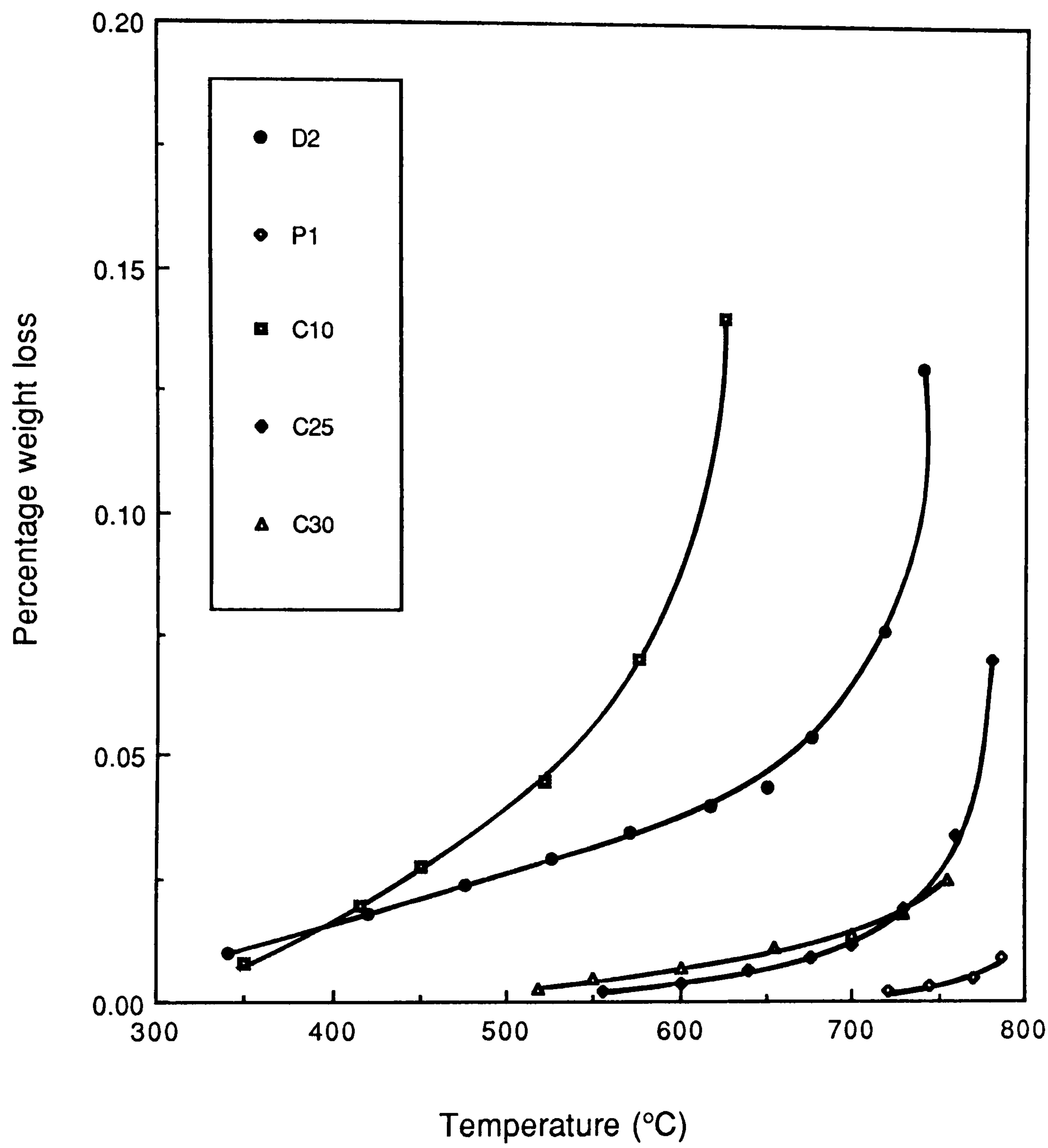

Figure 4.13 Results of thermal gravimetric analysis of handling materials

stresses upon contact caused the propagation of the minimal mechanical damage caused by the P1 material (this is discussed in section 3.5.5). But calculations showed this was unlikely to occur.

After examining the oxidation protection system and identifying the likely presence of a glassy phase, it was postulated that this may be affecting the contact. It is known that glass on glass is one of the most damaging contacts (e.g.United glass research group, 1979. Budd *et al*, 1980). It was thought that an effect of the insert repeatedly contacting hot glass rods could well have been the activation of the protection system. If a glassy surface layer resulted from the activation of the oxidation protection system, this could easily have resulted in glass on glass contact occurring. This would be a more likely explanation of why the contact with a hot glass rod ranked P1 so much lower than isothermal contact.

To investigate this possible phenomenom further a contact insert of P1 was 'sweated', that is exposed to an oxidising atmosphere at 600°C for 24 hours. The aim of this treatment being to fully activate the oxidation protection system and so any surface changes.

The insert on removal from the furnace was allowed to cool before being used to preform the standard isothermal contact test at room temperature. The results are shown along with those for non 'sweated' P1 in figure 4.14. The drop in retained strength of the glass rod after contact shows that the oxidation protection once activated does drastically reduce the efficiency of the handling material. Although it should be remembered that in operating conditions the glassy phase may be softer than at room temperature, its presence is still likely to affect contact.

These results correlate with reports from users (Vickers, 1989) of P1 handling material, that several days after installation the material starts to check bottles. This was particularly pronounced on the lehr stacker bar where the ambient temperature is greatest.

The discovery that the glassy phase although limiting oxidation, has a deleterious effect upon the amount of contact damage raised questions about the wisdom of impregnating C22 and C10 with Aluminium phosphate. Inserts of these impregnated materials C25 and C30 were 'sweated' and then tested in the same way as

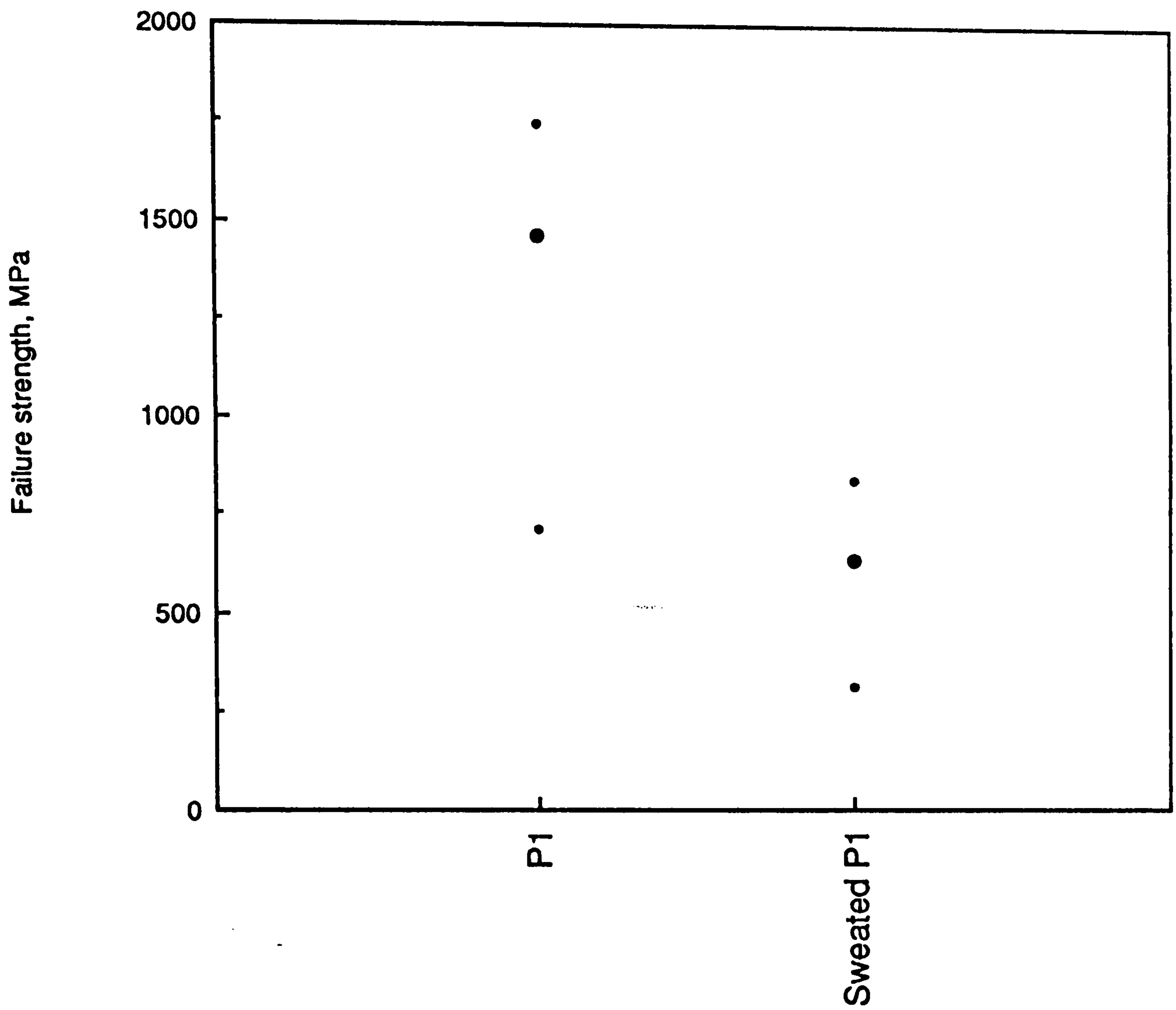

Figure 4.14 The effect of the glassy phase on handling ability

the P1 had been. The results of the contact tests are shown in figure 4.15, these show a small drop in the retained strength but not the dramatic fall P1 did. The probable explanation for this is the smaller percentage of phosphate incorporated in to the C25 and C30 materials. Both are manufactured under the specification of a concentration of between 2-4 weight percent with a mean not greater than 2.8 percent. While P1 has a phosphate concentration of 7 weight percent.

Johnson Radley still market their C25 and C30 materials along with their non impregnated counterparts.

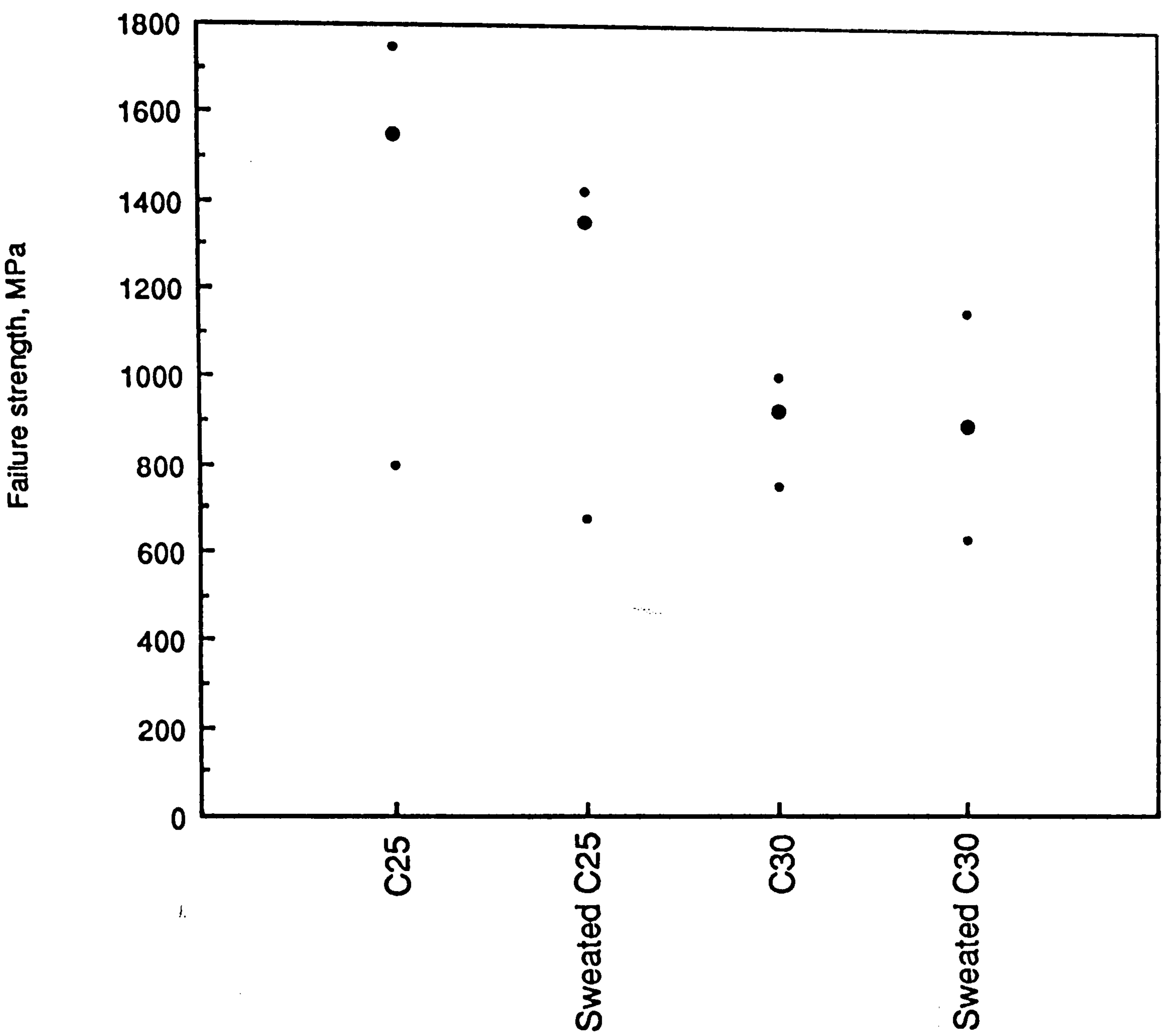

Figure 4.15 Effects of oxidation protection systems on materials handling abillity

Chapter 5

NEW MATERIALS

5.1 Introduction

The work presented so far has been an evaluation of the existing hot glass handling materials, and an investigation of damage mechanisms. However, part of the aim of this project was to develop new materials.

The assessment of existing materials has revealed the requirements of an ideal handling material. In this chapter the attempts to produce such a new material are examined. Through the computer model Titanium and Zirconium were identified as possible new materials. Although the residual strength after contact indicated comparable handling properties to C10 these materials were not pursued. This was because in the form of bulk metals, any user could produce their own components, after analysis of samples.

The work completed revealed that the two main requirements for a new handling material were that

1. It should present a non abrading, probably carbonaceous surface to contact with the glass.
2. It should retain a high proportion of its strength throughout its predicted life.

In an attempt to achieve these aims it was decided to design a composite material. Where the different constituent materials should satisfy the two requirements. A load bearing skeleton resistant to oxidation would support a carbonaceous phase which contacted the glass.

Two different ways of achieving this were pursued. They will be examined independently in the rest of this chapter.

5.2 Ceramic/Carbon composite

It was thought that a load bearing skeleton could be provided by a porous ceramic and the carbonaceous phase provided by infiltrating the skeleton with pure pitch. The resulting composite would give the surface properties required, and because of the purity of the Carbon phase it would have a minimal oxidation rate.

The mineral Meerschaum, hydrated magnesium silicate, chemical formula $Mg_4Si_6O_{15}(OH)_2.6H_2O$, was chosen as the skeleton, it is known to be stable up to 700°C (Singer, 1989); is extremely porous approximately 66% and so would be ideal to infiltrate; is easy to shape, it can be carved with a sharp knife when wet; is readily available at reasonable cost; and does not possess the extreme hardness of other possible ceramic skeletons, see table 5.1. A strict comparison can not be drawn between the value of hardness recorded for the magnesium silicate and the other ceramics as the other values represent dense materials, but it is clear that the silicate is very different from the other materials.

Possible skeletons	True hardness number (MNm^{-2})
Al_2O_3	15,000
TiC	12,000
ZrO_2	12,000
WC	18,000
SiC	30,000
$Mg_4Si_6O_{15}(OH)_2.6H_2O$	3.85

Table 5.1 Vickers hardness of possible skeleton materials.

Samples of the composite were prepared by soaking sections of the skeleton in a solution of synthetic pitch, prepared as for the coating used on C/C composites detailed in section 2.6. Once the skeleton was saturated, it was removed from the solution and placed in a fume cupboard until the solvent had evaporated. This procedure was then repeated twice more. The pitch impregnated skeleton was then heated to 700°C at a rate of 4°C per minute under vacuum. The temperature was held for 6 hours before cooling at 1°C per minute This treatment increases the weight of samples by 7% on average.

One of the resulting samples of composite was halved to determine whether or not the impregnation penetrated throughout the cross section of the sample. Such examination confirmed that impregnation was complete. Plate 5.1 shows a typical fracture surface of the composite, the fibrous nature of the ceramic skeleton is clearly seen.

The samples of the composite were used to evaluate the materials ability to handle glass without damaging it. The standard test on high strength glass rod was used. The results are shown in figure 5.1 along with results for the existing materials shown here to allow easy comparisons. These data represent the efficiency of the as impregnated surface as the shape of the standard contact test piece was cut from the skeleton before it was impregnated. These results suggest that the composite is suitable to handle glass. The retained strength of the glass it has contacted is not significantly different to those handled by C10. Before proceeding to investigate the material's useful life expectancy, the effect of machining on the surface needed to be examined. As the composite is not moulded it would need to be machined to produce a profiled component. If the skeleton is machined before impregnation the tolerances required at the neck ring would be very difficult to achieve. The standard contact test piece shown in figure 2.6 was cut from a sample of prepared composite. The material's effectiveness was then reassessed; figure 5.2 shows the resulting data along with that for the skeleton alone. It can be seen that the strength of a glass rod contacted by the machined surface lies between that of rods contacted by an as impregnated surface and the skeleton alone. It was concluded that the optimum properties of this material could not be obtained in machined inserts and so this composite would not be ideal for a future handling material. Further densification by multiple impregnation was unlikely to change the properties of the machined surface. As it was believed that the additional damage to the glass was caused by filaments of the ceramic skeleton exposed by the cutting tool. No further investigation of this system was undertaken

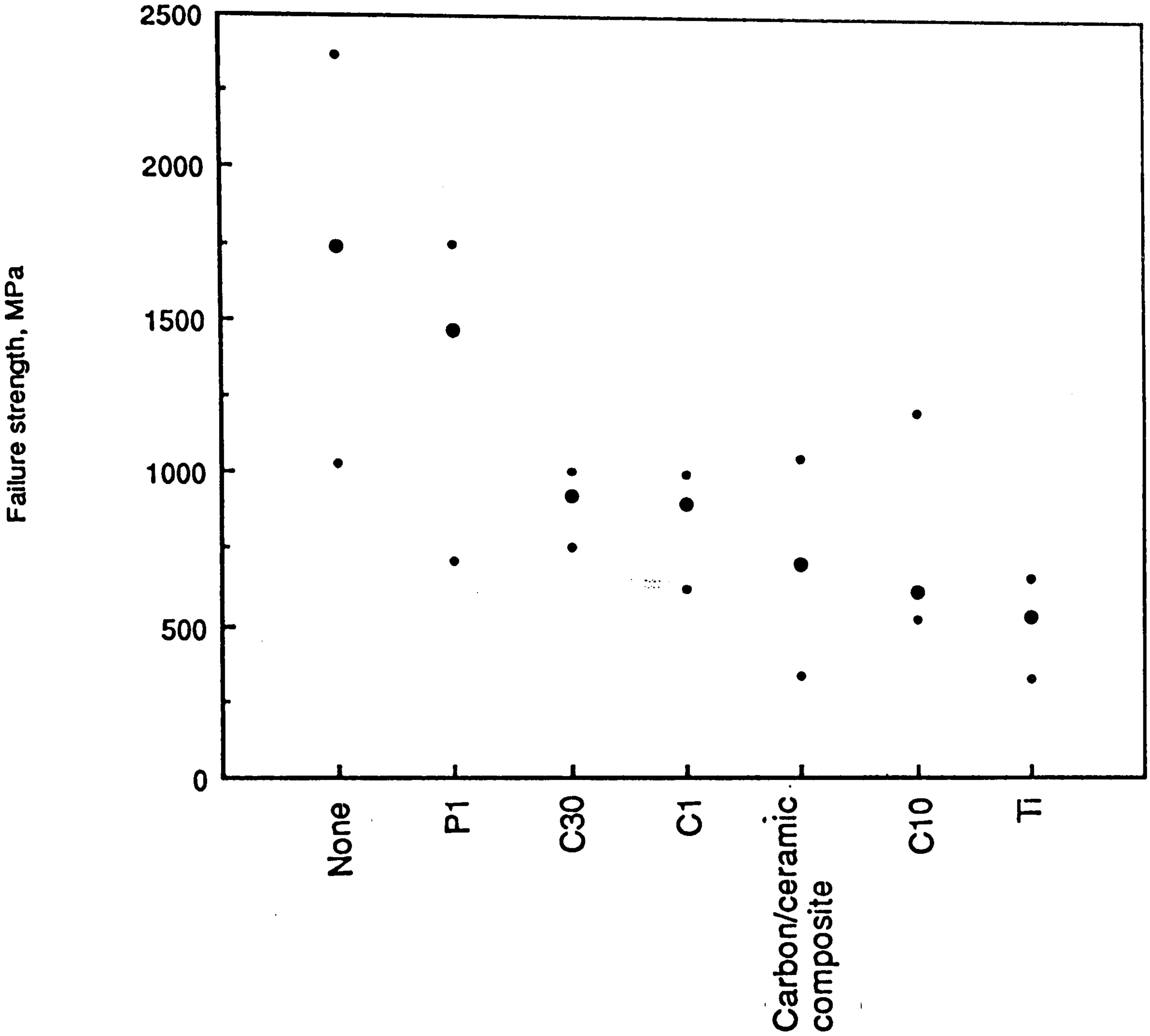

Figure 5.1 The Weibull characteristic strength of glass rods contacted by the ceramic/carbon composite compared with other handling materials.

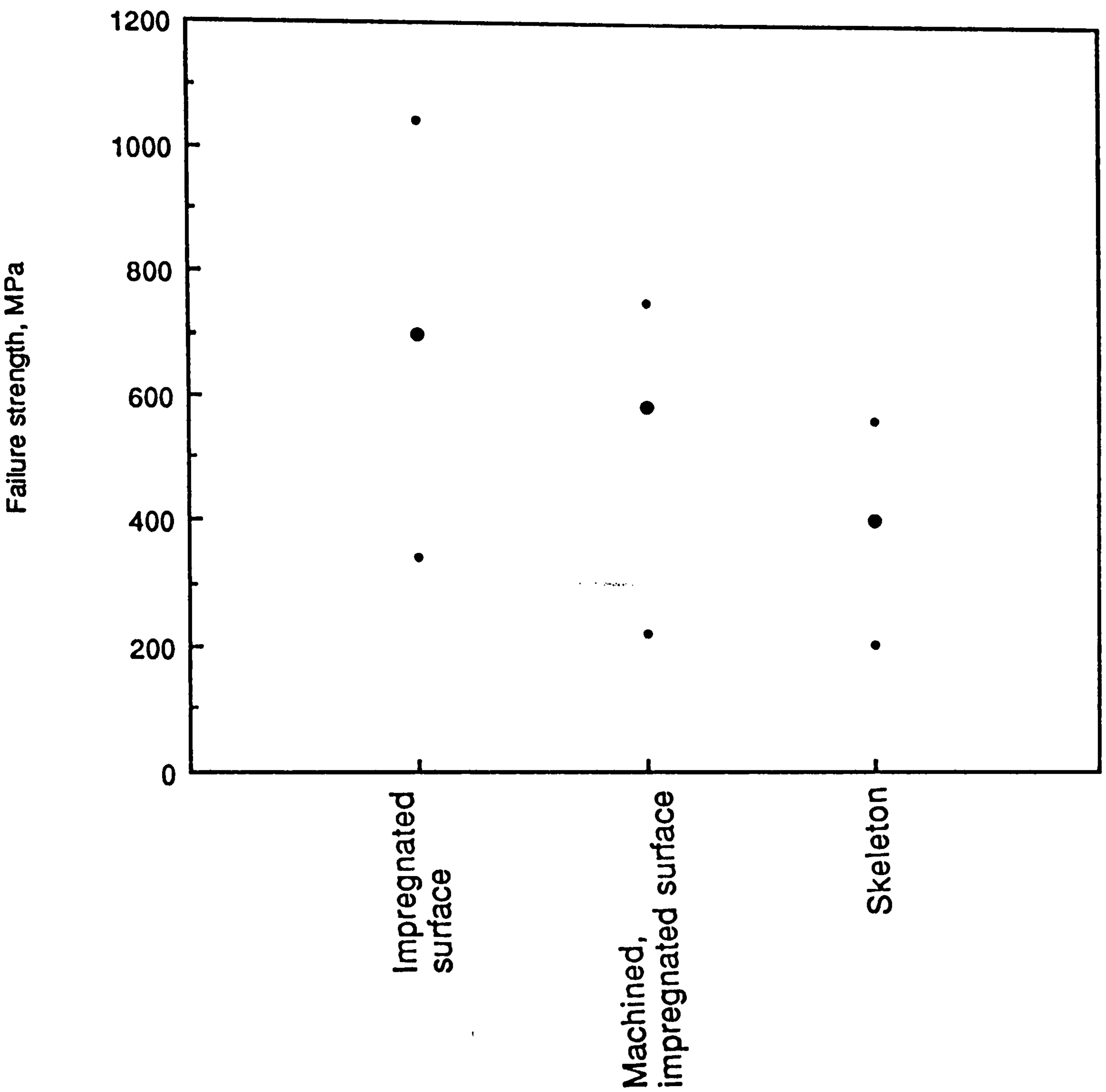

Figure 5.2 The results of contact tests which compare the ceramic skeleton and the carbon/ ceramic composite with an as impregnated and machined surface.

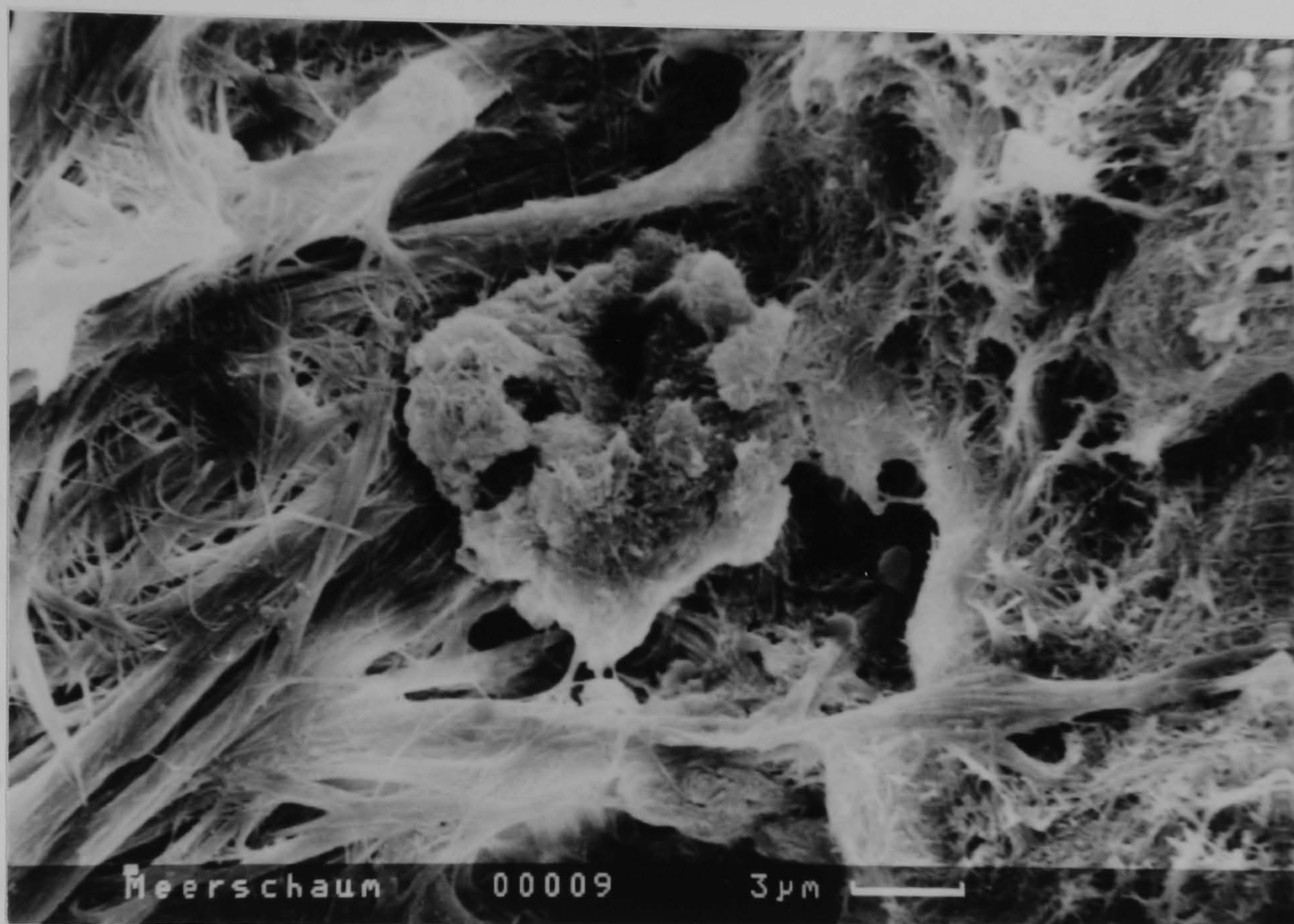

Plate 5.1 Scanning electron micrograph of the Carbon/ceramic composite.

5.3 Titanium/graphite composite

A way was sought to utilise Titanium as a skeleton in a composite handling material. Efforts were focussed on the use of powders, that when compacted and possibly sintered would produce a porous strong body into which a carbonaceous phase could be incorporated. In this instance rather than trying to impregnate the Titanium skeleton with pitch as in the case of the ceramic skeleton, the idea was to incorporate powdered graphite in to the starting, or feed mix. Then during compaction the graphite would be encapsulated in a Titanium matrix. If additional strength was required the compact could then be sintered in an inert atmosphere.

5.3.1 Titanium compacts

The first stage in the development of such a material was to try and produce a compact of pure Titanium, if this was successful then the inclusion of the graphite particles could then be considered.

The feed material was Titanium sponge powder $< 250\mu m$ in diameter supplied by Deeside Titanium †. The size distribution of the powder is presented in table 5.2.

ISO sieve aperture size (μm)	% mass retained
250	Nil
150	0.3
106	54.4
75	16.5
53	20.9
Base	7.9

Table 5.2 Percentage size distribution of Titanium powder used in compact production.

† Deeside Titanium, Weighbridge Road, Sealand, Deeside, Clwyd, CH5 2LL. Tel. (0244) 821121

Six grams of Titanium powder were compacted in a closed cylindrical mould to a pressure of $20.7kNm^{-2}$ the resulting compacts were easily ejected. They had a compressive strength of 59 MPa. The particles at the surface of the compact were tightly bonded. Such compacts were considered of a standard satisfactory to proceed with the investigation of the incorporation of graphite.

5.3.2 Titanium/graphite compact type A

30% by volume of the graphite powder was to be added to the feed mix.

$$\text{Density of graphite} = 2.2gcm^{-3}$$

$$\text{Apparent density of Titanium} = 4.5gcm^{-3}$$

Thus used

5g titanium to 1g of graphite

The graphite powder added to the starting mix was of mixed sizes. The distribution is detailed in table 5.3.

ISO sieve aperture size (μm)	% mass retained
710	8.0
300	33.0
106	53.5
75	2.7
45	2.0
Base	0.8

Table 5.3 Percentage size distribution of graphite powder used in compact production.

The two powders were mixed and then moulded in the same way as the Titanium only compacts. The resulting pellets of material although easily ejected had a very loose surface, rubbing a finger across the surface of the compact resulted in the loss of both Titanium and graphite. The strength of the compact in compression was 31MPa.

The changes in the compact on the introduction of the graphite were thought to be due to the graphite particles stopping the Titanium particles contacting each other and so cold welding under pressure. It is well known that graphite acts as a lubricant. The idea was conceived that if shear loading could be used to compact the powders rather than axial compression, the Titanium particles would be forced over each other and so push the graphite out from between them resulting in Titanium/Titanium contact were bonding may occur. This is shown schematically in figure 5.3.

5.3.3 Shear compaction of Titanium/graphite composite

The first process used to try and achieve this was extrusion. The aim was to extrude a die compacted pellet of material. Attempts to do this were abandoned as galling of the sides resulted in the friction forces between the compact and the side walls of the die being too great. This problem is overcome by encapsulating the Titanium in a Copper sheath (Congleton, 1989).

It was not possible to coat a compact while maintaining the dimensions needed to fit into the extrusion die. An alternative method was tried, by using Copper piping as a sheath/mould it was possible to produce a Copper coated titanium/graphite rod to be compacted. One end of an annealed length of Copper pipe, external diameter 12mm, was clamped and then sealed by brazing. The tube was then filled with mixed Titanium and graphite powder as used to produce the compacts. After ramming the powder home the open end was sealed. The rod was then compacted by swaging, a form of forging where the cylindrical rod is forged by passing it through a rotary machine in which it is hammered by converging dies.

The rod was reduced in section by passing it through successively smaller diameter dies. The dies used were 9.27, 7.87, 6.35, 5.59 and 5.48mm in diameter resulting in a reduction from 12 to 5mm in the cross-section of the rod. The length of the swaged rod had increased from 292 to 775mm, this amounts to a reduction

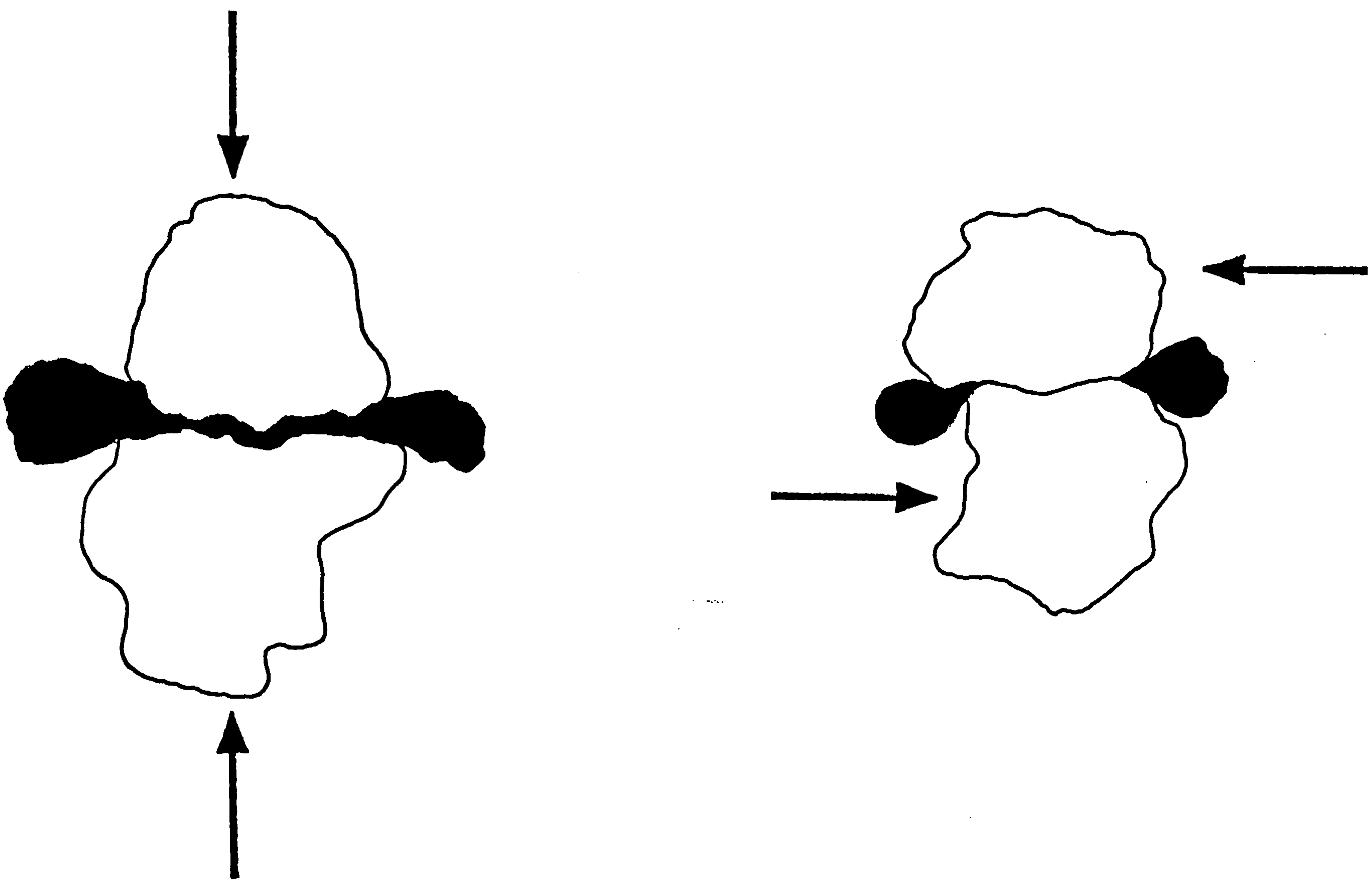

Figure 5.3 Representation of how shear loading acts to maximise Ti/Ti contact during compaction of a Ti/carbon composite.

in the volume of 54%. To retrieve the composite material from its Copper sheath required a two stage process. Firstly the majority of the Copper was machined off, then the remaining was removed chemically by nitric acid

$$Cu + H_2NO_3 \rightarrow Cu(NO_3)_2 + H_2$$

The resulting material was well consolidated and could be cut with a hack saw. This prototype production route appeared successful. Unfortunately the size of the resulting material limited analysis of its properties and would be of no use in producing bulk material suitable for use in present handling apparatus.

The question was posed 'How can larger sections be manufactured ?' Swaging was inappropriate for a larger diameter rod, but larger pieces of material could be handled by a forging press. It was decided to try forging a larger section. The same feed mix was constrained with-in a 300mm length of 52mm diameter pipe, wall thickness 2mm. The ends of the pipe were clamped and then sealed by brazing. The material was then forged to a pressure of 27.6MN/m^2 the maximum available in the department. A section of the composite was cut from the centre of the forged material shown diagrammatically in figure 5.4 The Copper sheath was then removed as before. It is of interest to note that although the pipe has been flattened the wall thickness remained unchanged.

The unsheathed composite was easily handled with no loose particles at the surface. The composite had a compressive strength of 140MPa. This high strength was believed to be a result of the high pressures, along with the shear loading. A preliminary test of the efficiency of this composite as a hot glass handling material was undertaken by measuring the strength of a glass rod after contact with it, in a similar way to that described in section 2.3. A standard contact test piece was cut, the unsheathed surface was contacted onto the glass under the standard load (150g). The result are compared with those for C10 and other handling materials in figure 5.5. It is clear that this surface is satisfactory as a glass handling material.

It appeared that in this material a prototype new hot glass handling material has been found, achieved by combining Titanium and graphite. The strength of the composite maintained by the Titanium whilst retaining the contact properties associated with the graphite. Examination of the fracture surface of the material

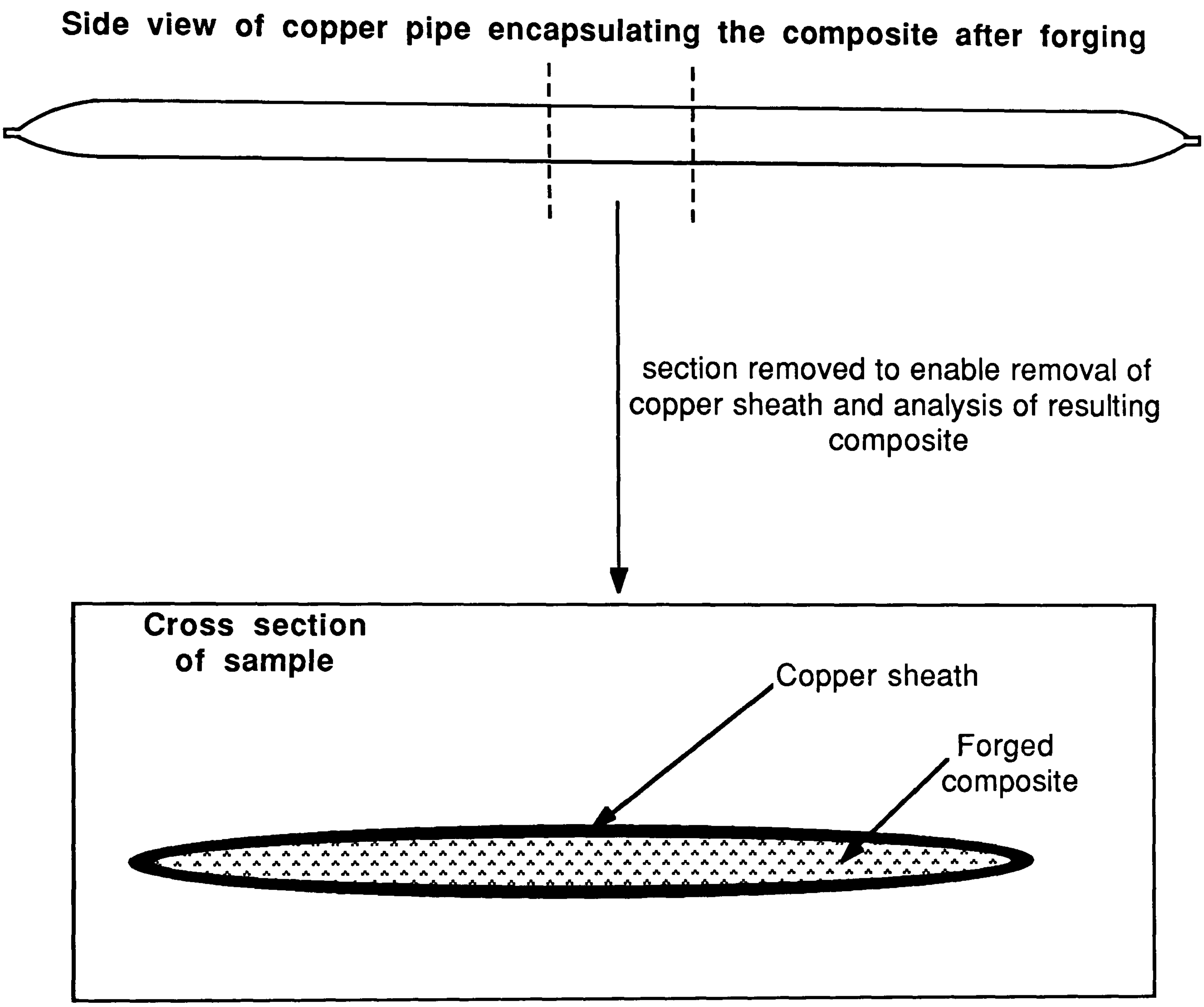

Figure 5.4 Schematic representation of forged Titanium/graphite composite.

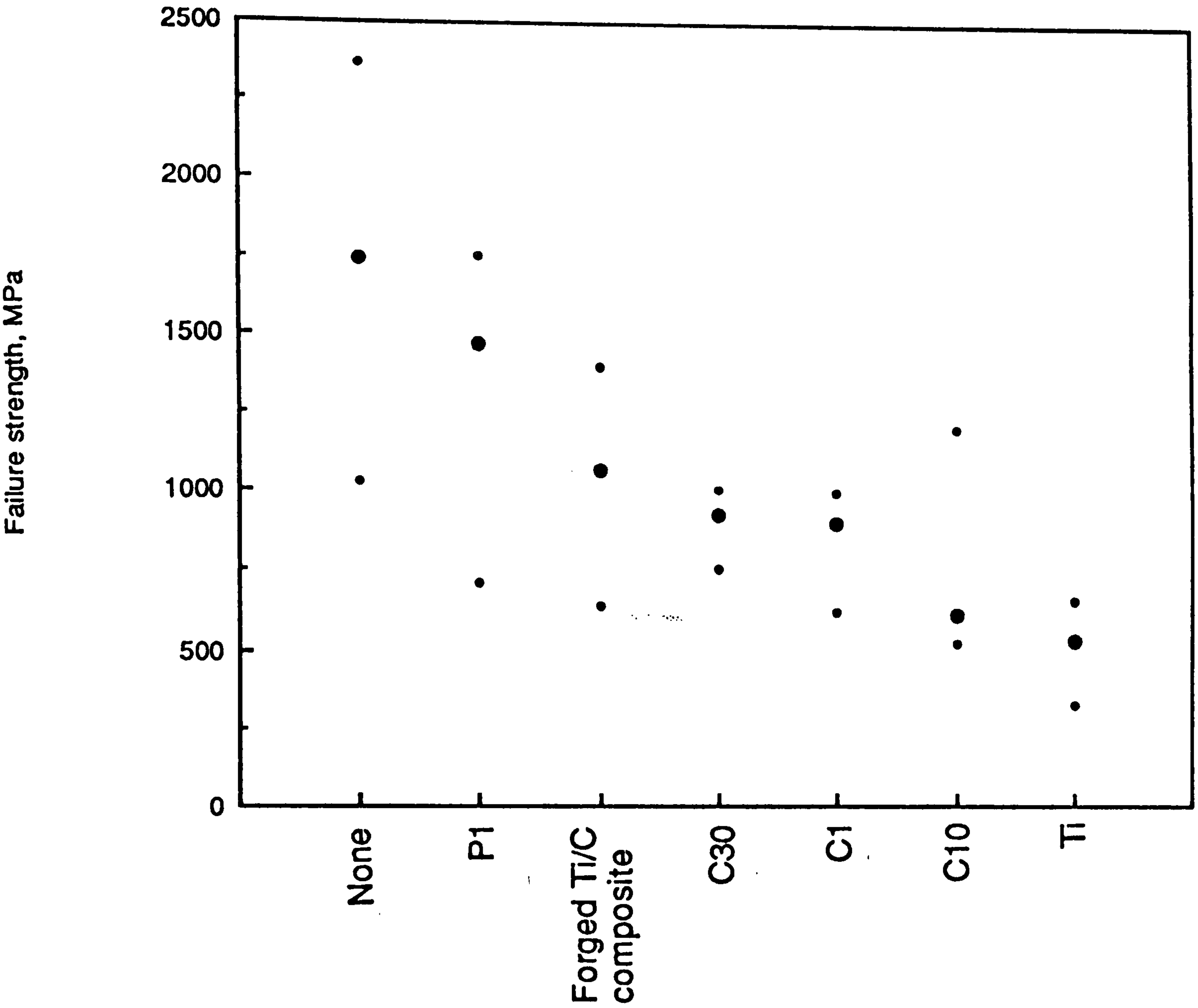

Figure 5.5 The Weibull characteristic strength of glass rods contacted by the Titanium/carbon composite compared with other handling materials.

was undertaken in the SEM. In plate 5.2, a secondary electron image, it is difficult to distinguished between the two phases present. By utilising back scattered imaging techniques, as in the images of the same field of view shown in plates 5.3 and 5.4, the two phases are easily identified. The contrast achieved in these images are a result of the difference in the atomic numbers of the two materials, so that the graphite appears dark and the Titanium light. A point of contact between Titanium particles is shown in plate 5.5.

It appears that a Titanium skeleton has formed as it was expected to, so that the composite is unlikely to be weakened drastically by oxidation, although this needs to be investigated by the assessment of the materials strength and handling properties after oxidation treatments. Such evaluations were not completed in the time available on this project, but they are a priority for future work.

One disadvantage of the forging procedure is the time taken up by the removal of the Copper sheath. A further production adaptation was investigated. It was decided to look again at die pressing. A second attempt centred on producing a component free from the Copper coating to enable direct moulding of components.

5.3.4 Titanium/graphite compact type B

In the evaluation of type A compacts the reduced compressive strength and the loose material at the surface were attributed to the presence of the graphite particles between the Titanium ones preventing bonding. It was likely that the graphite causing these problems was in the form of fines, the very smallest particles in the distribution. In this second attempt at cold pressing such small particles were removed. In fact the only particles incorporated were greater than 1mm in diameter. To facilitate an even mix of these large particles within the Titanium powder and as an aid to pressing, a binder of sugar solution was used. The graphite particles alone were first mixed with the binder until all the particles were well coated. The Titanium powder was then added and thoroughly mixed. Each particle of graphite becoming coated by the smaller Titanium particles. This is schematically represented in figure 5.6.

This carefully prepared feed mix 30% by volume graphite was then pressed in a closed cylindrical steel die to a pressure of 150 MPa. The compact was then

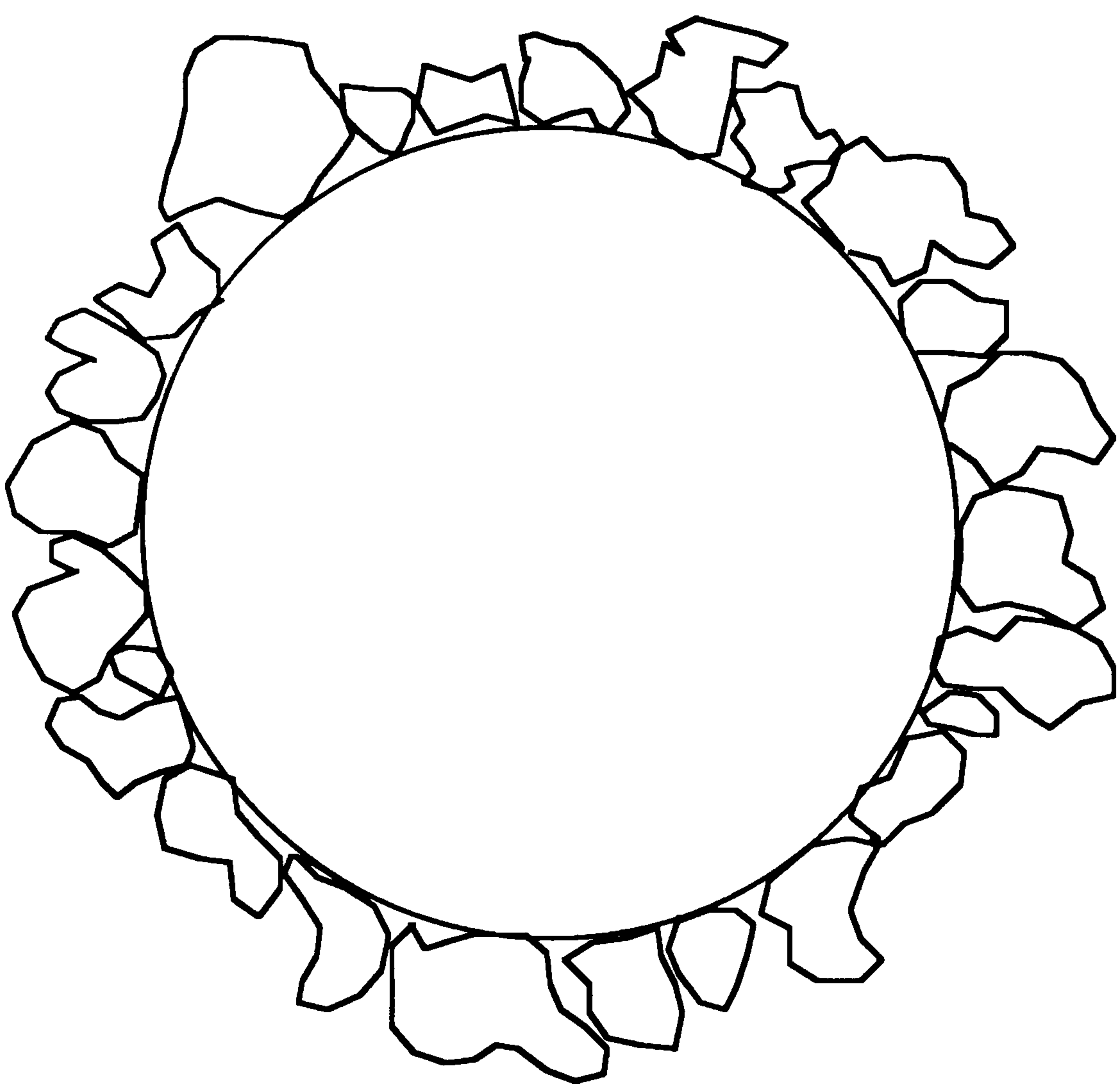

Figure 5.6 Representation of a Carbon particle encapsulated by Titanium before pressing

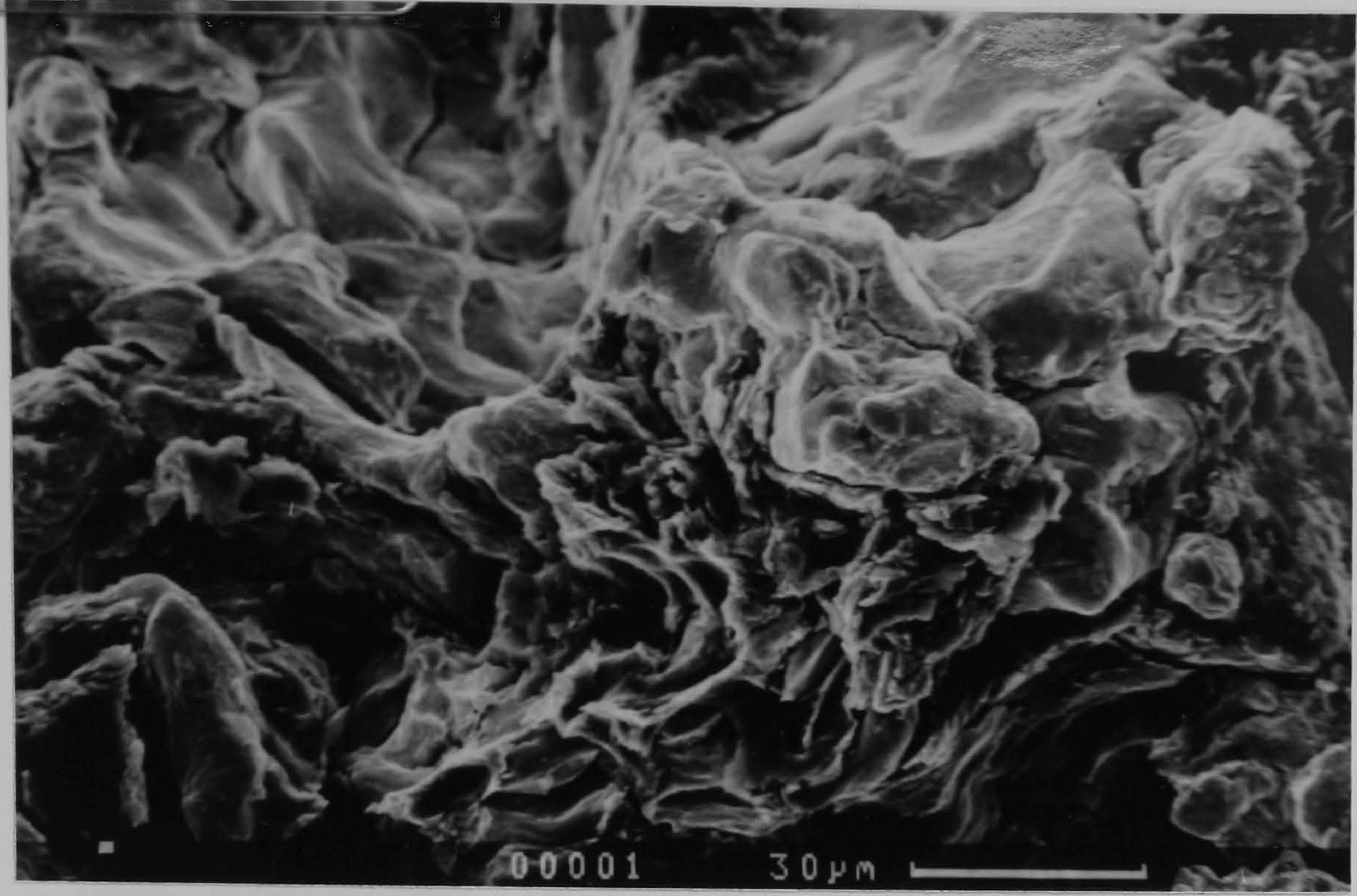

Plate 5.2 Secondary electron image of the Titanium/Carbon composite

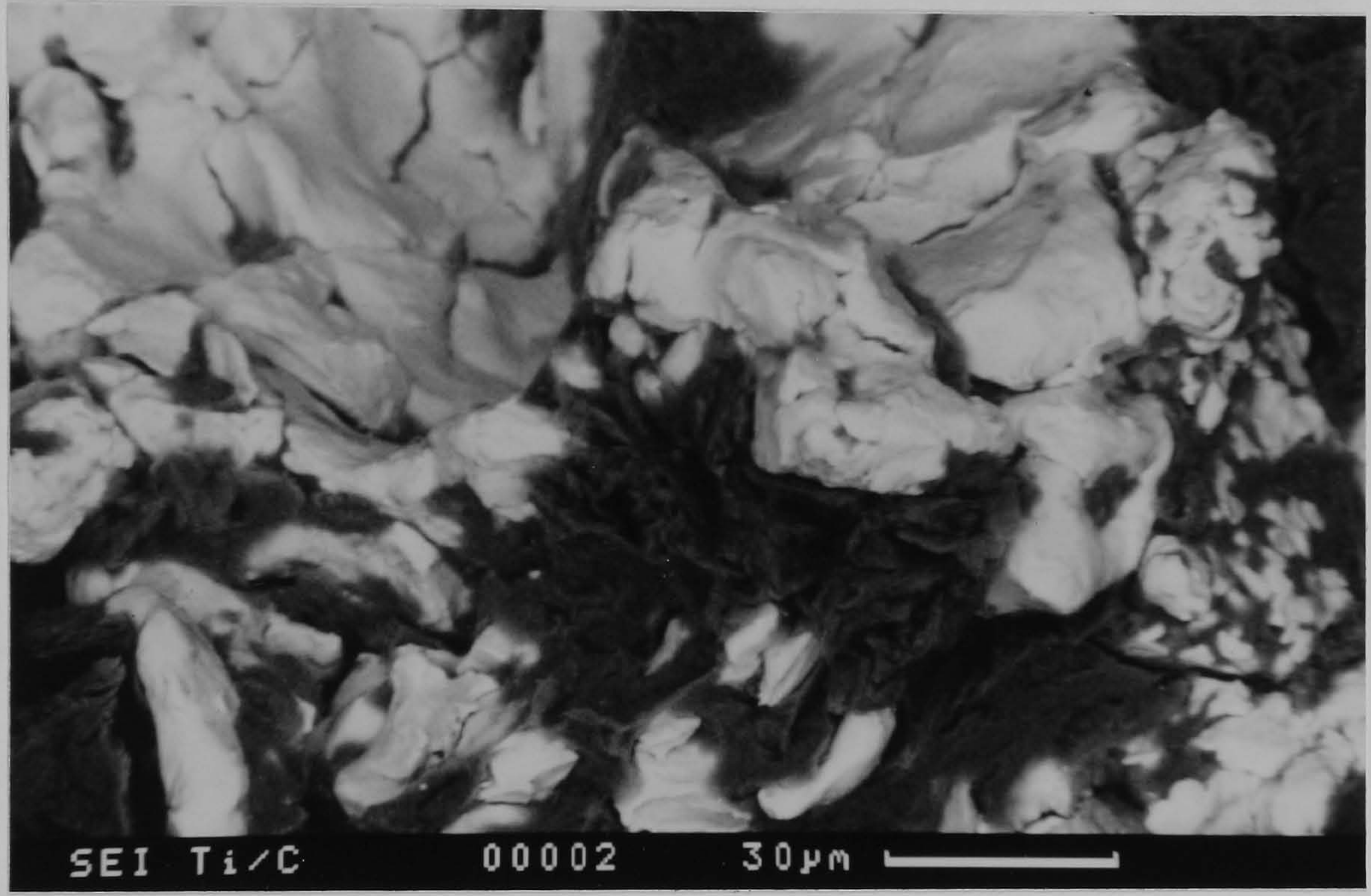

Plate 5.3 Back scattered electron image of the Titanium/Carbon composite.

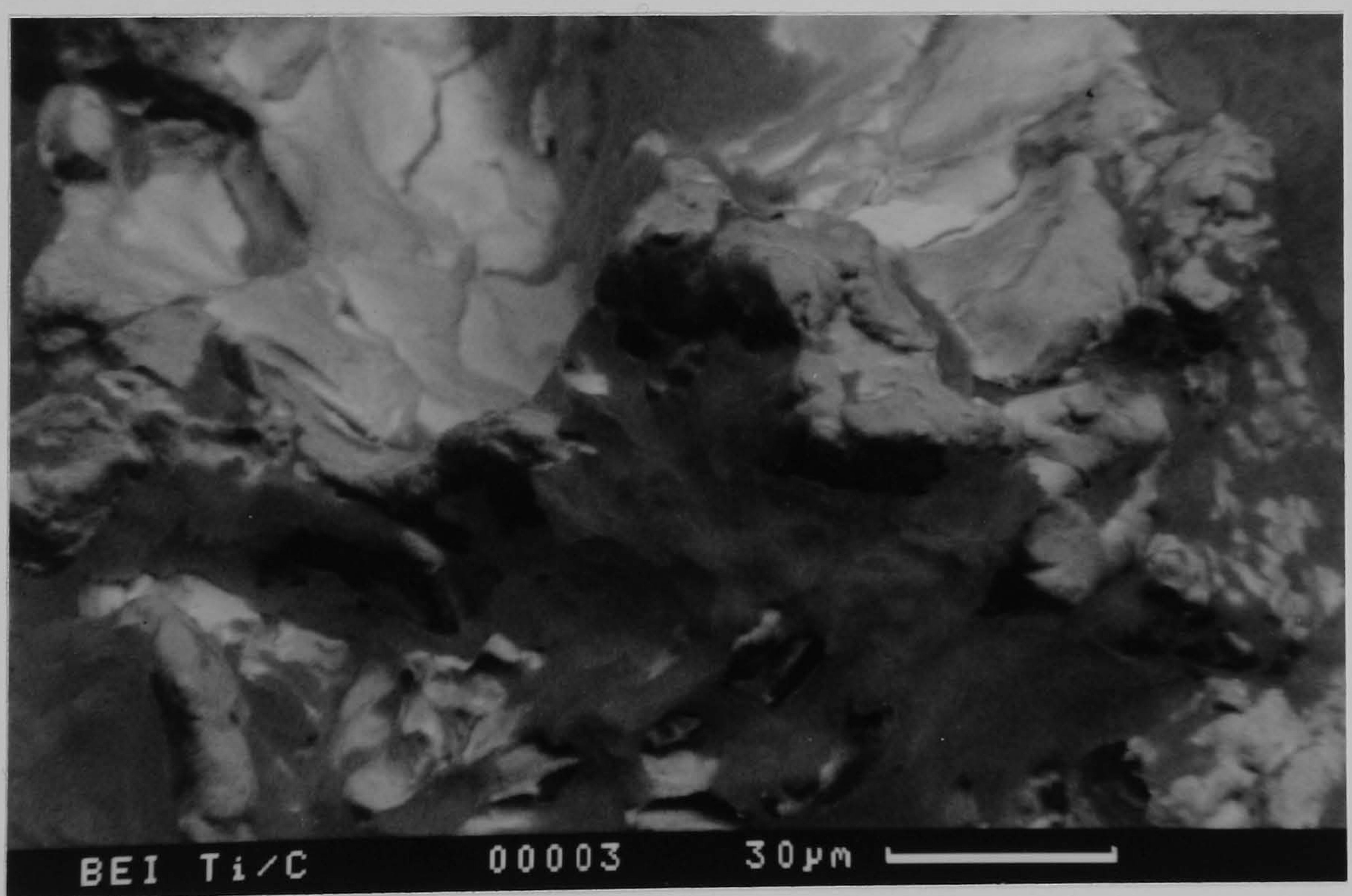

Plate 5.4 Back scattered electron image, with topographic contrast of the Titanium/Carbon composite.

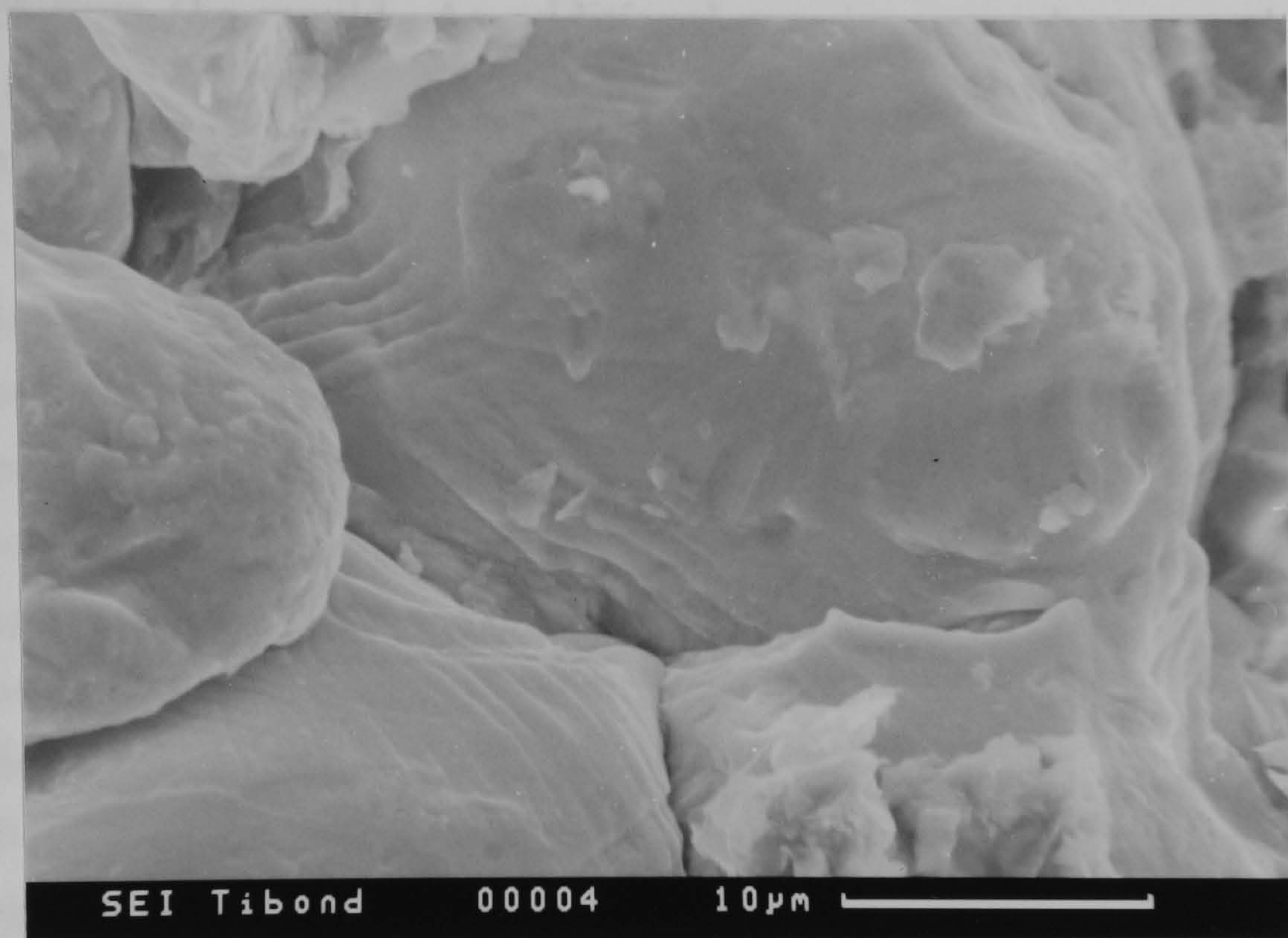

Plate 5.5 Scanning electron micrograph of two Titanium particles contacting in the forged Titanium/Carbon composite

removed from the mould. An additional pressing procedure was then introduced to the process, the compact was isostatically pressed to a pressure of 173.4 MPa. This process acted in two ways. Firstly the whole compact is further consolidated and as the pressure is applied isostatically any anisotropy resulting from the first pressing is minimised. Secondly as the particles of the Titanium sponge powder are compressible individually and the graphite is not, the surface topography is changed. The isostatic pressing has the effect of leaving the graphite particles proud of the Titanium. This is shown here in an SEM micrograph, plate 5.6, taken by imaging the back scattered electrons in topographic mode. Further analysis of the topography of the surface would have been useful in quantifying and optimising this affect but as this was the final work to be completed time did not allow for this. It would be a topic for further investigation. Plate 5.6 also illustrates the effective encapsulation of the graphite by the Titanium particles.

The effect of this stippled surface is considerable when it is used to handle glass. As a result the part of the composite which will come into contact with the glass will be predominantly the proud graphite particles which have excellent handling properties. The effectiveness of such a surface is seen clearly by examining the strength of glass after contact shown in figure 5.7 where it is compared with C10 and C25.

The figures shown are for the pristine surface and although very optimistic about the materials ability it is important as for the forged materials to investigate how the material will be affected by exposure to an oxidising environment. It is hoped that the surface will last sufficiently to make it a viable hot glass handling material. If should be remembered that an infinitely lasting material is not desired for commercial reasons. An investigation of the materials strength retention and its handling efficiency after periods of oxidation are the priorities for future work, as is the optimisation of the feed mixture and the process route, particularly the relative pressures applied axially and isostatically.

Although this material is still in need of much development it shows great promise probably its biggest advantage over the other materials considered is the fact that it can be moulded.

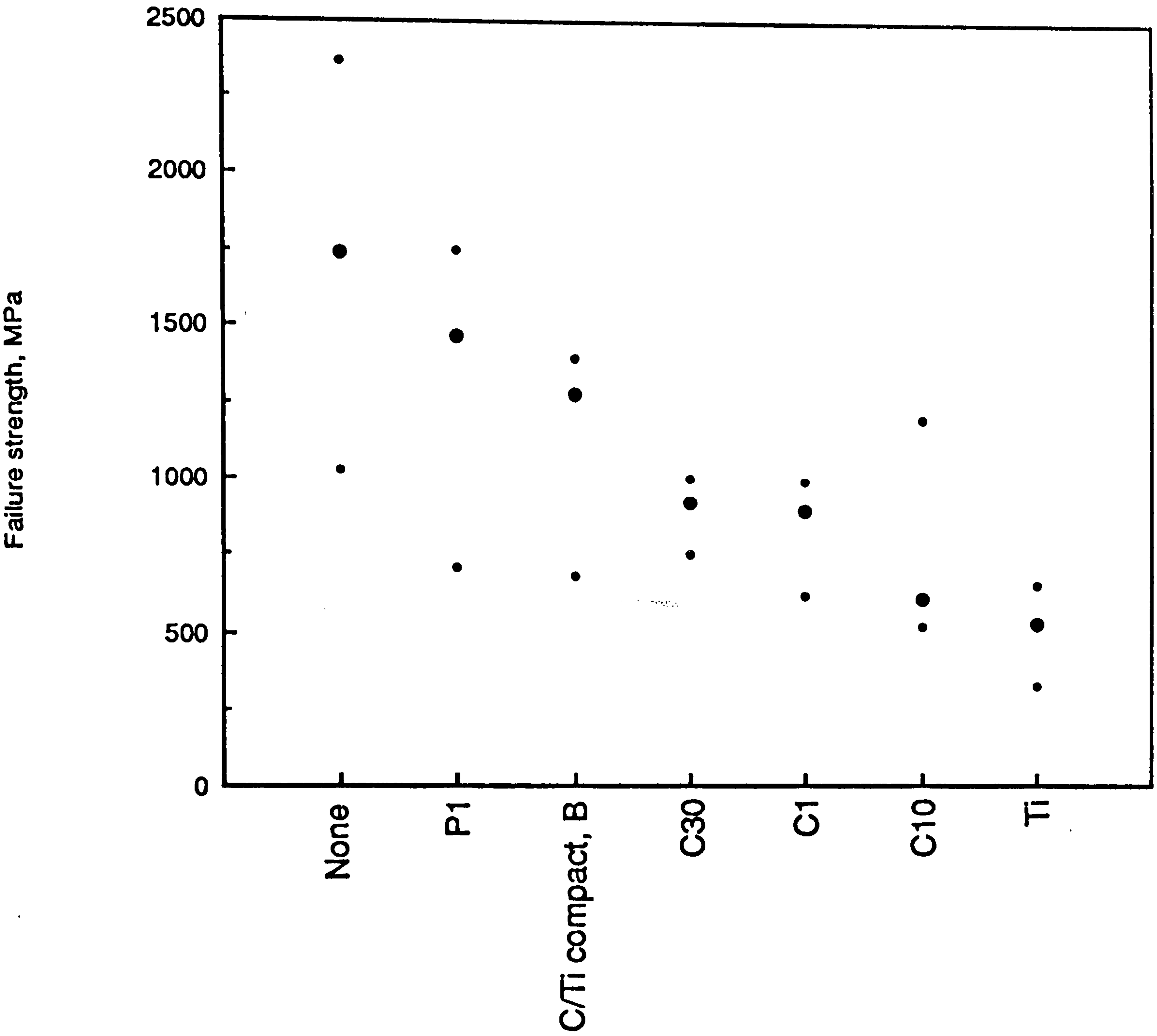

Figure 5.7 The Weibull characteristic strength of glass rods contacted by the Titanium/carbon composite which has been isostatically pressed compared with other handling materials.

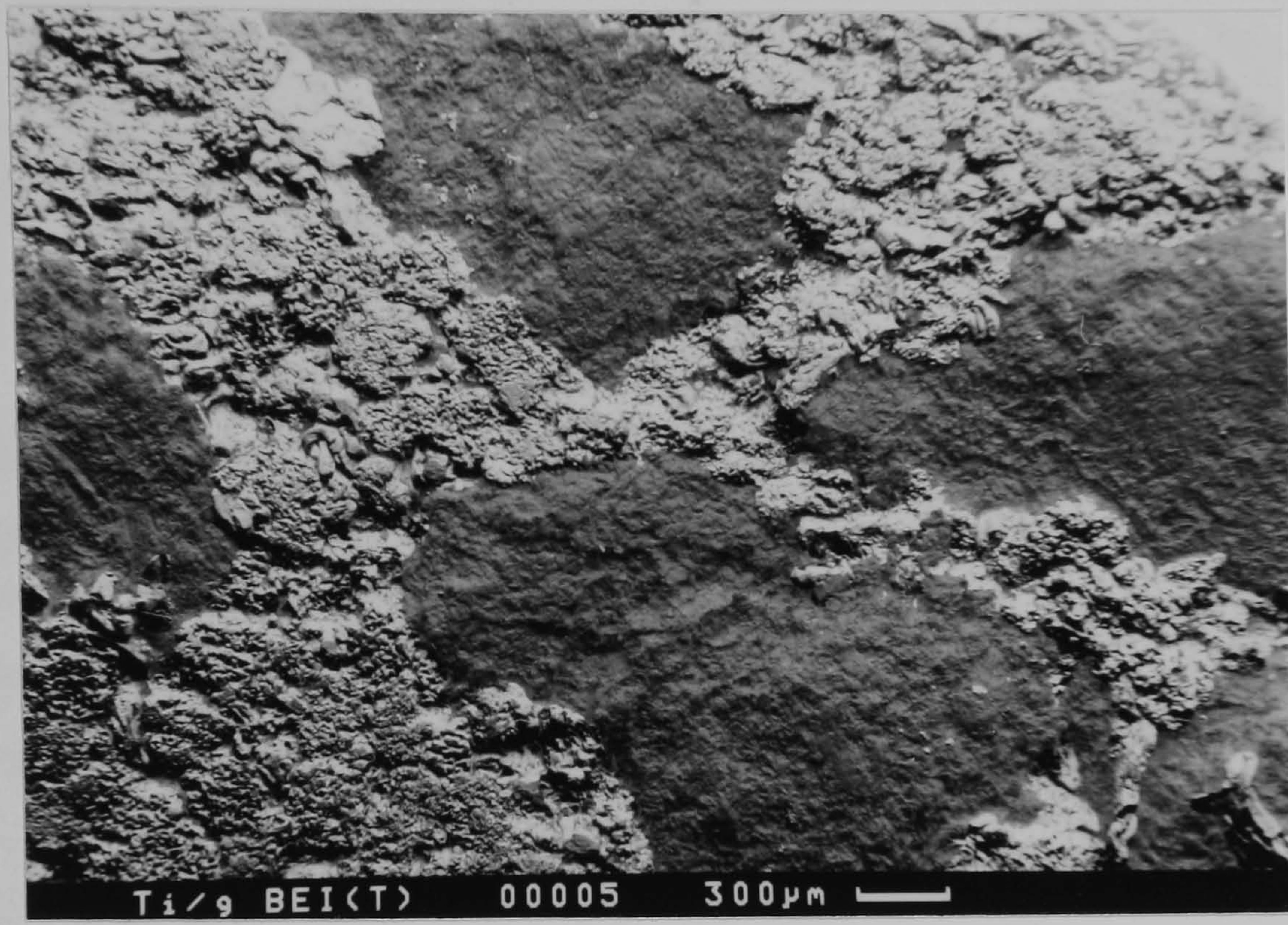

Plate 5.6 Back scattered electron image of the type B compacted, Titanium/Carbon composite.

Chapter 6

MORE ABOUT CONTACT

One of the aims of this investigation was to achieve a deeper understanding of how contact with handling materials, causes damage to hot glass. In chapter 3 a likely mechanism for damage was established. That is that damage is caused by thermally induced stresses acting upon mechanically produced flaws causing them to propagate. The mechanism resulting in the two processes interacting to produce much greater damage than either could alone. Through this greater understanding of the correlation between the thermal properties and contact damage Titanium was realised to possess suitable thermal properties for hot glass handling.

In the mathematical models the interaction between mechanical flaws and thermal stress was the main consideration from which a great insight into the damage process was gained. As yet the causes of the mechanical damage have not been examined. The experimental investigations so far undertaken have concentrated on the effects of material contact on the strength of glass. A great many tests have been completed to assess different materials fitness for purpose and it has been concluded from such tests that Carbon in one of many forms provides the best handling material, as it causes little mechanical damage. Much of this project has been an attempt to optimise the life of carbonaceous materials in an oxidising environment.

What has not been addressed is why carbonaceous materials cause so little mechanical damage. It was hoped that if an insight could be gained into this by investigating the materials properties which may render them so suitable for hot glass handling. Then, other materials may be identified for further investigation without the need for extensive testing.

Bourne *et al* (1984) correlated mechanical damage caused by metals to their hardness, this was discussed in chapter 1. As many of the materials now of interest are porous composites the Vickers hardness of the material was meaningless, the materials crushed under the indenter and no measurable indent was formed. A different approach was needed. The origins of mechanical damage were considered. For damage to occur two materials must come into contact so the interaction at the surface of the materials is the basis of any investigation.

6.1 Mechanical interfacial interactions

When the surface of one body moves or tries to move over that of another, as will happen during the handling of containers, each body experiences a frictional force. Historically, Da Vinci in 1500AD was the first person to formally propose laws of friction. He concluded from experimental investigations that the force, F, required to move a block of one material across the surface of another was proportional to the normal load, L, acting on that block ie $F \propto L$ so

$$F = \mu L \tag{6.1}$$

where μ is the constant of proportionality known as the coefficient of friction. Da Vinci also observed that the frictional force was independent of the apparent contact area between two surfaces. These laws of friction, at least approximately, still hold today.

Amonton and Coulomb in the seventeenth and eighteenth centuries respectively also postulated similar theories, additionally they realised that surface roughness played a part in the way surfaces interact. The significance of surface roughness was not confirmed until the 1950's by Bowden and Tabor (1954) when they proposed the true contact area between two surfaces is where asperities on the two surfaces meet. Overcoming the adhesion by cold welding at such point of contact is one of the sources of the frictional force along with the ploughing of softer surfaces by harder asperities. During this process cracks may also be produced. An example of this which may be familiar to some readers are the cracks in the bottom of a ploughed furrow.

6.1.1 The coefficient of friction

To try and establish whether frictional forces are a significant factor in determining the amount of mechanical damage caused by a handling material. It was decided to evaluate the coefficient of friction between various handling materials and soda-lime-silica glass.

The coefficient of friction was evaluated for those handling materials for which samples were available. Values were calculated by determining the force required to rotate a glass rod in contact with a handling material and so overcome the frictional force between the two. The experimental detail is described in section 2.2. The principles of this test are the same as for the test used to evaluate μ for flat surfaces in contact, where the force required to pull a block of one material across the other is recorded (e.g.Muncaster, 1981).

Figure 6.1 enables the consideration of any correlation between μ and the mechanical suitability of a handling material.It displays the mean values of μ plotted versus the Weibull, characteristic retained strength of glass after isothermal contact.

It can be seen there is little correlation between the coefficient of friction and the retained strength. But some conclusions may be drawn when the nature of the materials is considered. It appears that the presence of fibres within a material account for some of the lack of correlation, but it can not be said that the fibres have a consistent quantifiable effect. C1 and C30 which both contain Carbon fibres appear to cause more damage than their frictional interaction would suggest. This could be expected, fibres can be perceived to cause more damage than the 'flat' surface of bulk material. In the case of magnesium silicate, which has a fibrous morphology, Plate 5.1, it causes less damage than its frictional interaction would suggest. Clearly it would be difficult to use the coefficient of friction as a means of assessing a materials potential for hot glass handling.

6.1.2 The Young's modulus of a handling material

The evaluation of the contact interface between the two materials was approached in a different way. The mechanics of contact were examined by Hertz (1896), when he considered a blunt contact between two materials shown, in figure 6.2. He concluded that the radius, a, of the mutual contact circle could be

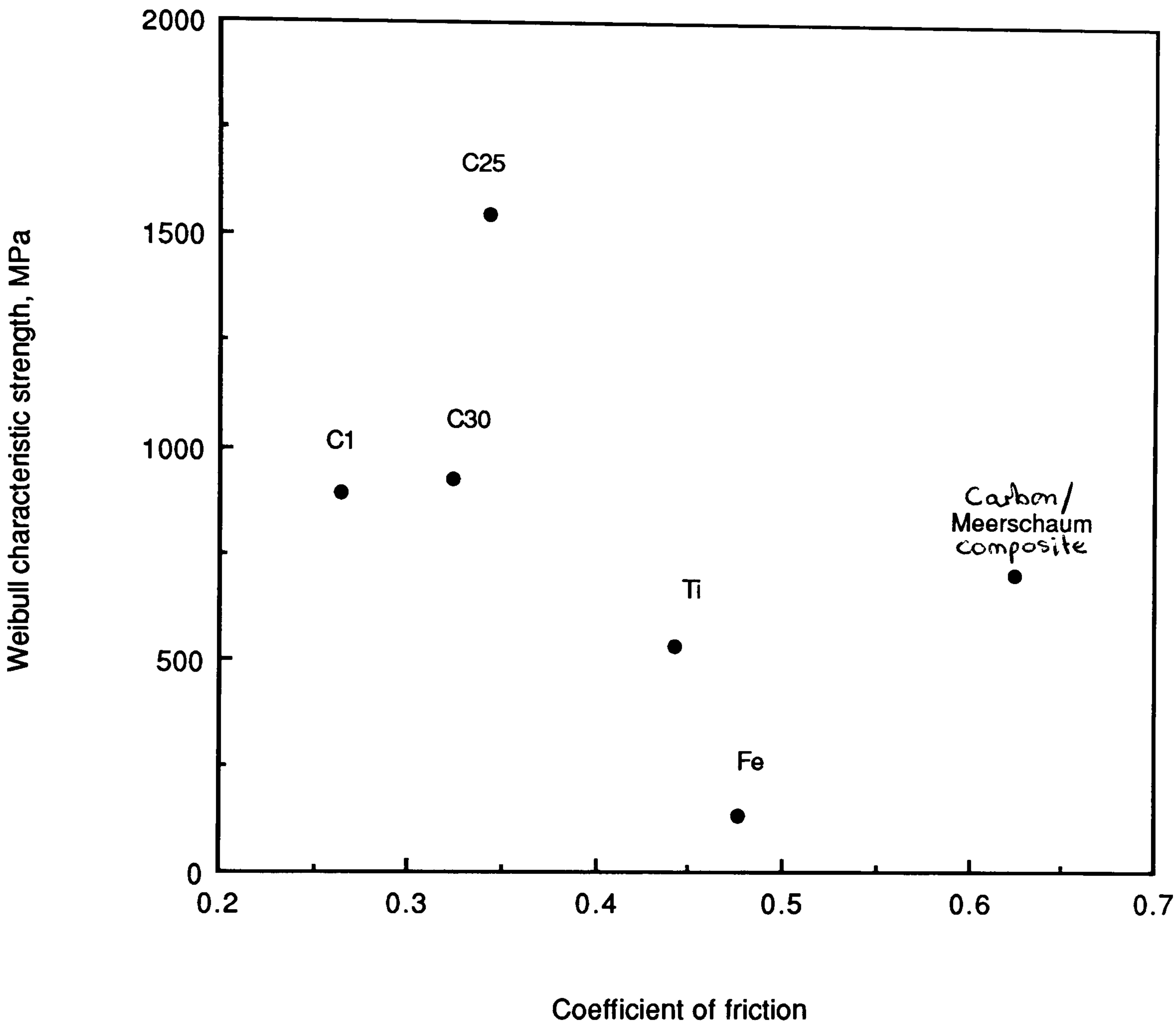

Figure 6.1 The coefficient of friction between polished soda-lime-silica glass and various handling materialsplotted against the Weibull characteristic strength of glass rod contacted by the material

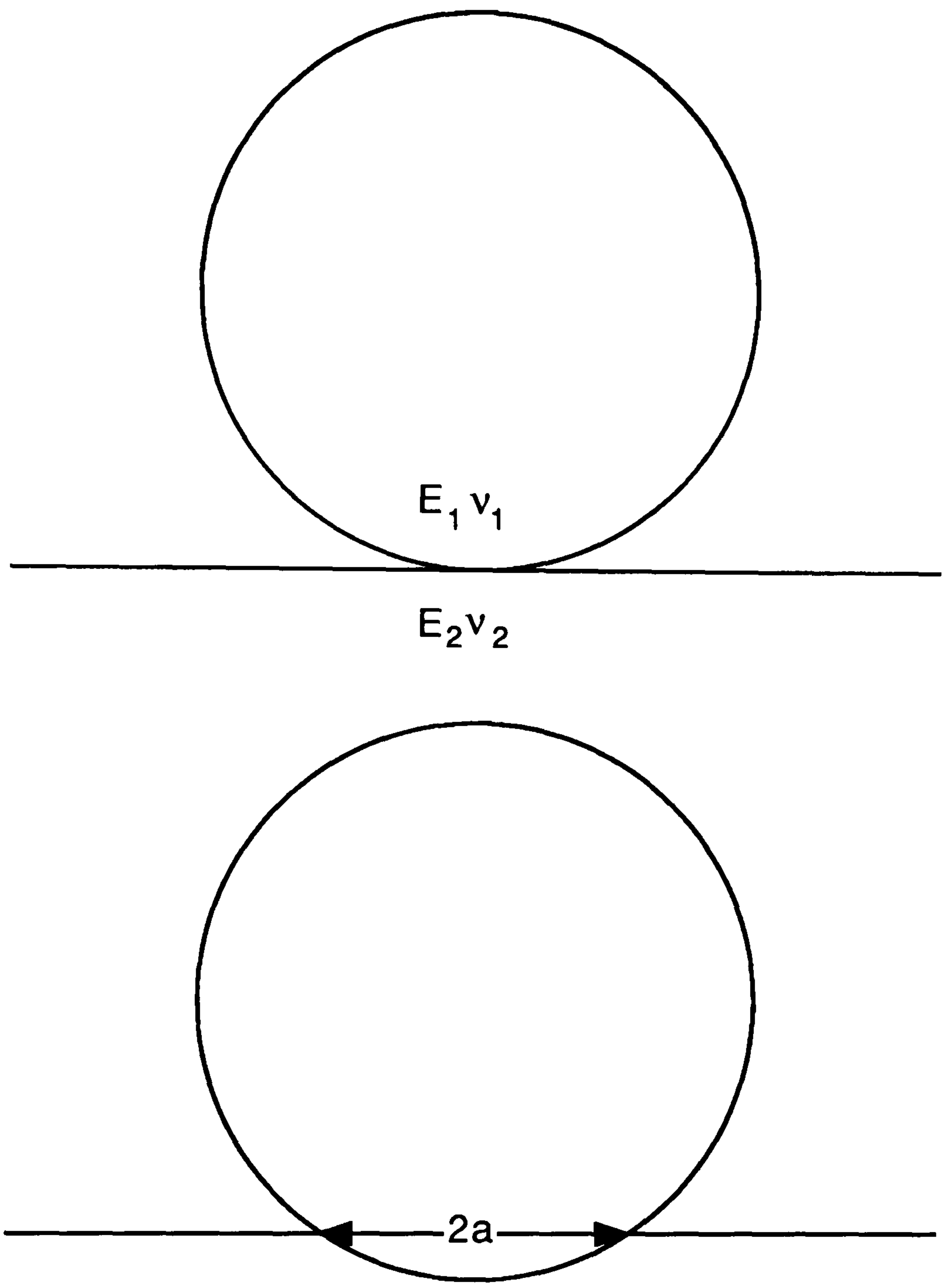

Figure 6.2 Schematic repesentation of Hertzian contact.

calculated from the expression

$$a = \left\{ \frac{3}{4} LR \left[\left(\frac{1-\nu_1^2}{E_1} \right) + \left(\frac{1-\nu_2^2}{E_2} \right) \right] \right\}^{\frac{1}{3}} \tag{6.2}$$

Where L is the applied load, R is the radius of curvature of the asperity, ν is the Poissons ratio and E is the Young's modulus of the material, the subscript 1 denoting the material of the spherical asperity and 2 the surface it is contacting.

As Poissons ratio is about a $\frac{1}{3}$ for most materials it is fair to say that the Young's moduli of the materials will control the real contact area between them, so that the higher the value of E a handling material has the smaller the real area of contact between it and the glass would be. It would therefore be expected that the higher the modulus of a material the less mechanical damage it will cause.

Alas the contact area is not the only consideration. The modulus of a material basically defines the rigidity of a material. The higher the modulus the stiffer the material. In terms of the mechanical contact between two materials, a material with a low modulus could be imagined to bow away from the glass on contact, where as a material with a high modulus will tend to act like a hardness indenter. These arguments suggest a material with a low modulus would be a more efficient handling material

The Young's modulus of available handling materials were determined. Beams of the materials were loaded in four point bending and a transducer system measured the true deflection of the beam under various loading conditions. The details of the experimental procedure are given in section 2.7.1.

In figure 6.3 the modulus of various handling materials are plotted against the characteristic retained strength of glass rods after contact with material. The results suggested that generally the lower the modulus of a material then the better it will be as a handling material. But one of the least efficient materials examined, hydrated magnesium silicate has a very low modulus. This is thought to be a result of the fibrous nature of the magnesium silicate, this was clearly shown in the electron micrograph of plate 5.1.

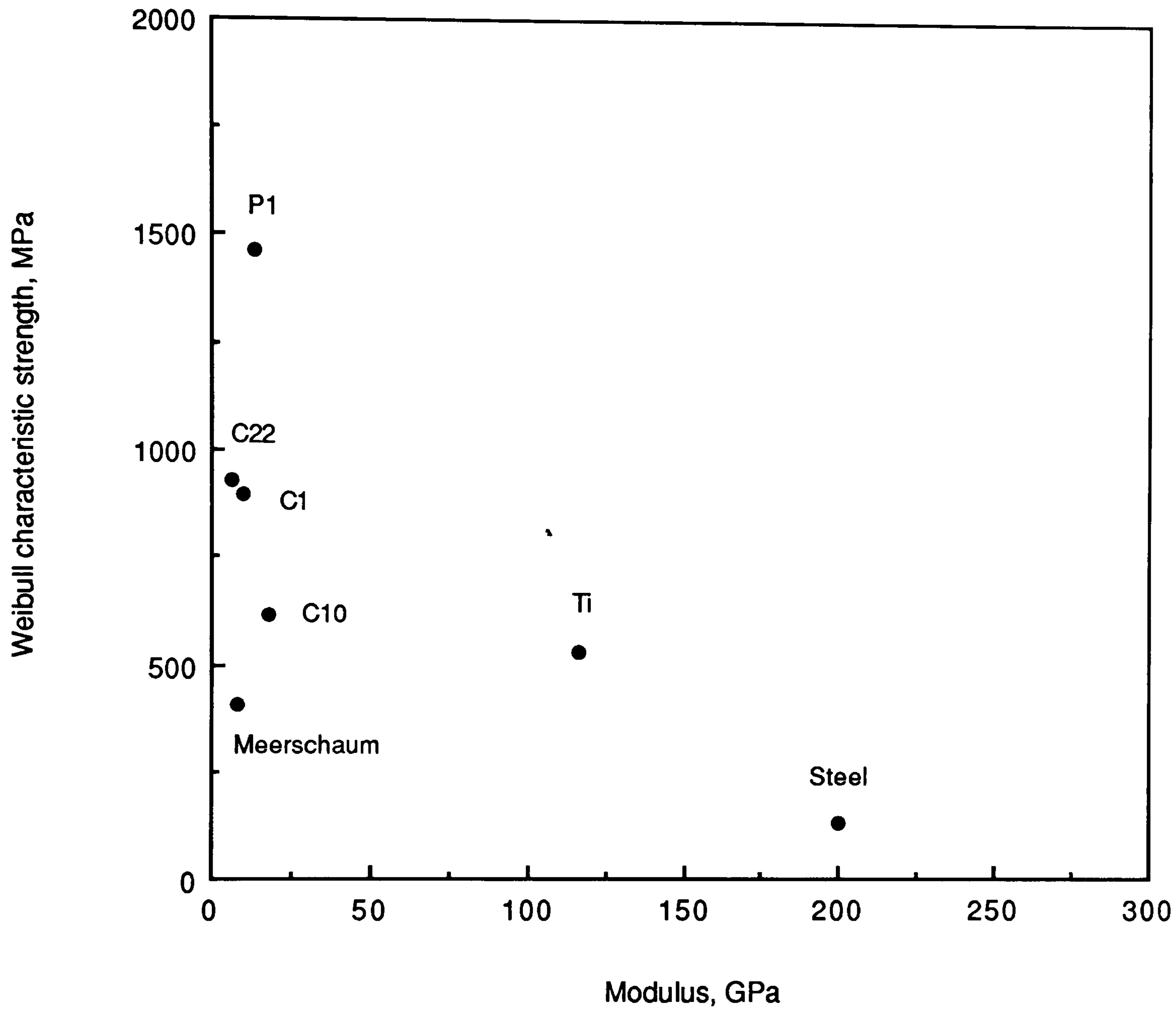

Figure 6.3 The modulus of handling material plotted against the Weibull characteristic strength of glass rod contacted by each material

It is evident that the amount of mechanical damage caused as a result of contact is dependent on a combination of parameters. From those considered here it can be seen that the greater the frictional force between the contacting materials, then with other things equal, the greater the amount of damage to the glass. The presence of fibres in a material can overshadow this correlation although not in a predictable way. Materials which present a small real area of contact cause more damage, this is likely to be the result of indentation type effects. So a material with a low Young's modulus is to be recommended, but again the nature of the material may mask such phenomena. The abrasive nature of fibres resulting in the amount of damage being directly proportional to the real contact area.

It is concluded that although a material with a high Young's modulus would be unsuitable as a hot glass handling material the fact that a material has a low modulus does not guarantee that the material will be ideal further qualification would be required. It should also be remembered that a materials thermal properties must also be considered when making an assessment of possible hot glass handling materials. The mathematical models enabled the comparison of possible handling materials with existing ones. So that in future investigations other materials can be assessed by the same criteria, it was decided to represent the many calculations undertaken by the computer models (sections 3.4 and 3.5) in a single figure.

6.2 Single representation of the results of the computer models

The computer models evaluated (section 3.2.5) the maximum crack size, mechanical contact could produce without such a crack being propogated by the thermal stresses resulting from contact between hot glass and cooler handling material. That is in figures 3.18 to 3.22 the crack size corresponding to the first point of intersection between the line representing K_{1c} and the plot of the computed values of K for cracks in the thermal stress distribution which resulted from contact. Any crack greater than this critical size would propogate, but catastrophic failure does not always result from such crack growth as the cracks are not in a constant stress field. The calculations predicted that the crack would grow until it reached a new stable state, represented in figures 3.18 to 3.22 by the second intersection between the two curves. So the points of intersection identify the two critical crack sizes.

A glass sample containing flaws of these critical sizes would, when exposed to a uniform stress, have a corresponding strength which can be calculated from equation 3.18.

$$K = \sigma\sqrt{\pi a}$$

So for each handling material considered by the computer models, the critical sizes of mechanical damage correspond to certain glass strengths. To plot these strengths in dimensionless form they were divided by the Weibull characteristic strength of the polished rods (section 3.6.4). The materials in this investigation were considered as samples, with a certain group of thermal properties, represented by the dimensionless group H (section 3.4.2). In figure 6.4 the two critical strengths for the five materials considered by the computer model in this investigation are plotted against their value of the dimensionless parameter H.

The upper curve represents the first transition between stability and instability, that is where mechanically produced cracks start to propagate in the thermal stress field resulting from contact. The lower curve represents the conditions where crack growth is arrested and a crack returns to a stable state.

The plot can be used to help assess future possible handling materials without the need for thermal shock testing. If the amount of mechanical damage produced by a material with a certain value of H is determined, it can be seen from the plot if such damage is stable or if it will propagate to form checks.

The analysis of the materials undertaken here have not provided an explanation of why carbonaceous materials are such successful glass handling materials. It is thought that other factors play a significant role, the chemical inactivity of the Carbon materials with the glass may be a vital factor. This would be a fascinating study for future investigations.

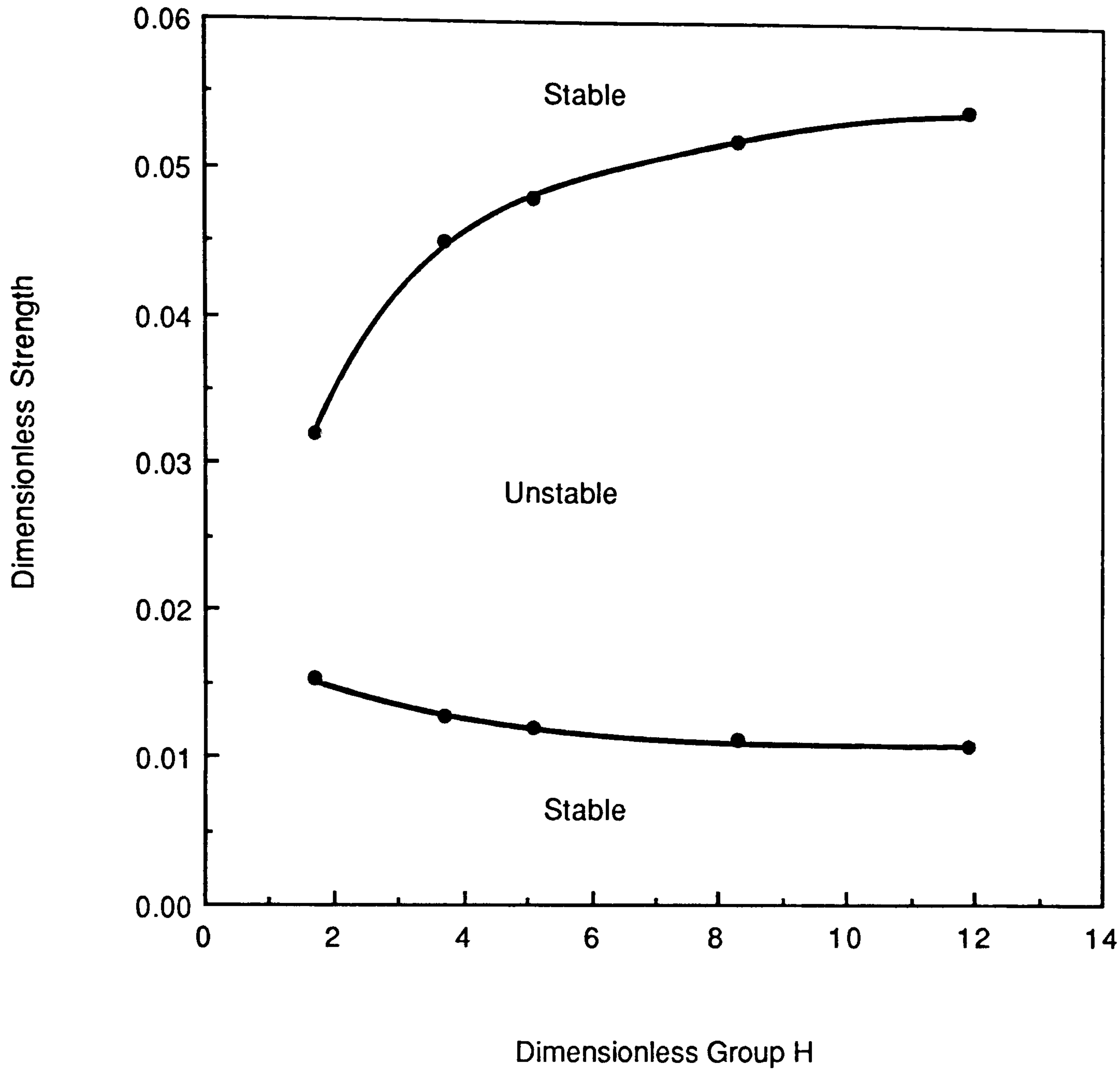

Figure 6.4 The relationship between dimensionless strength and the dimensionless group H.

Chapter 7

SUGGESTIONS FOR FURTHER WORK

1. An investigation of the effect of oxidation on the strength of Titanium/graphite composites, manufactured by the forging process and by the die compaction route.

2. An assessment of the way the handling properties of the Titanium/graphite composites change after exposure to an oxidising environment.

3. Optimisation of the process route for the production of Titanium/graphite composite by die pressing. Including: the composition of the feed mix; the size distribution of the feed mix; and the relative pressures applied axially and isostatically.

4. Continued investigation of why it is that carbonaceous materials are the best handling materials, particular the roll of carbons chemical inactivity towards glass.

Chapter 8

CONCLUSIONS

It was concluded that:

1. Mechanical damage on the surface of a container, produced during contact with a handling material, act as initiating flaws. These flaws are propagated by thermally induced stresses, so greater damage results from the combined action of the two mechanisms than either could alone.

2. If the mechanical damage a hot glass handling material produces is limited to such a size that the thermal stresses produced by the material do not cause the cracks to propagate it will be approaching the ideal as nearly as possible.

3. Titanium is an effective metallic hot glass handling material. It was identified as a possible hot glass handling material after considering its thermal properties. This was confirmed during experimental investigations of the effects of contact.

4. Of all the materials considered in this investigation carbonaceous materials were the best hot glass handling materials.

5. The presence of catalytic impurities, including Fe, in the Carbon/Carbon composite C12 in addition to inadequate bonding between the binding phase and the fibres contributed to it's poor oxidation resistance.

6. The coating of a Carbon/Carbon composite with a very pure Carbon coating successfully limits oxidation of the material.

7. P1 material is an ineffective glass handling material due to its, phosphate based, oxidation protection system. this is because A phosphate glass develops on the surface of the material once it has been exposed to an oxidising environment.

8. A Titanium/graphite composite, designed specifically for handling hot glass, is an effective hot glass handling material, especially when the production route develops raised graphite particles on the surface of the material.

9. There is little correlation between the coefficient of friction, between a handling material and soda-lime-glass, and the amount of damage a material causes. Consequently determining the appropriate value of μ for a material is not an effective method of assessing a materials glass handling ability.

10. Generally the lower the Young's modulus of a material then the better it will be as a handling material, but the presence of fibres in a material can over shadow this effect. So a material with a high Young's modulus would not be a suitable glass handling material and could be eliminated from further investigations. A material with a low Young's modulus may be an effective glass handling material but experimental investigation of the materials ability would still be required.

11. A hot glass handling material with a very low value of the dimensionless number H, will reduce thermal damage but still produce mechanical damage. Total damage can therefore be reduced by either

    a. producing little mechanical damage, like the carbonaeous materials, irrespective of their thermal properties or

    b. producing little thermal damage, like the Titanium, the mechanical damage may be moderate but it will not be exacerbated by thermal shock.

Chapter 9

REFERENCES

Anon, (1986).
'Replacing asbestos in the handling of hot glass.'
Applon, March, 95.

Anon, (1983).
'Handling of hot glass containers.'
Glass International, March, 40-42.

Ashby M. F. and Jones D. R. H. , (1986).
'Engineering materials 2. An introduction to microstructures, processing and design.'
Pergamon Press, Oxford, UK.

Ashworth D. R. , (1969).
'A method for determining the bulk density of ceramics.'
Journal of the British Ceramic Society, **6**, 70-72.

Bowden F. P. and Tabor D. , (1954).
'The friction and lubrication of solids.'
Clarendon Press, Oxford, UK.

Brearly W. ,Hastilow P. A. P. and Holloway D. G. , (1980).
'The breaking strength of some commercial glasses.'
Physics and Chemistry of Glasses, **3**, 181-188.

Bourne R. , Chowan N. D. and Budd S. M. , (1984).
'Damage to glass surfaces at elevated temperatures: effects of hardness and thermal conductivity of damaging material.'
Glass Technology, **25**, 145-147.

Brungs M. P. , (1988).
'The assessment of a polyurethane coating as a means of maintaining the strength of lightweight containers.
Glass Technology, **29**, 103-105.

Budd S. M. , Cornelius W. P. , (1979).
'Stress corrosion of glass containers and effects of surface treatments.'
Glass Technology, **20**, 170-173.

Budd S. M. , (1980).
'Towards the stronger glass container.'
Glass, April, 170.

Budd S. M. ,Cowan N. D. and Bourne R. , (1980).
'Damage to glass by various materials at elevated temperatures.'
Journal of Non-crystalline Solids, **38-39**, 409-412.

Budd S. M. , (1986, 1987).
Private communication.
United Glass Research Centre, St Albans, UK.

Carslaw H. S. and Jaeger J. C. , (1959).
'Conduction of heat in solids.'
Clarendon Press, Oxford,UK.

Cartwright D. J. and Rooke D. P. , (1976).
'Compendium of stress intensity factors.'
HMSO, London, UK.

Cartwrite D. J. and Rooke D. P. , (1978).
'Evaluation of stress intensity factors, a general introduction to fracture mechanics.'
Burlington Press, Herts, UK.

Congleton J. , (1989).
Private Communication.
University of Newcastle Upon Tyne, UK.

Coulson J. M. and Richardson J. F. , (1985).
'Chemical engineering, Volume 1, Third edition.'
Pergamon Press, Oxford, UK.

Croft D. R. and Lilly D. G. , (1977).
'Heat transfer calculations using finite difference equations.'
Applied Science publishers Ltd., London, UK.

Davidge R. W. , (1979).
'Mechanical behaviour of ceramics.'
Cambridge University Press, Cambridge, UK.

Dorey R. J. and Parker A. G. S. , (1981).
'Cerberite equipment for handling hot glass.'
Glass, January, 12-13.

Dourodo P. , (1990).
'The case against recycling the US's waste.'
New Scientist, **126**, 48.

Dugdale D. S. and Ritz C. , (1971).
'Elasticity for Engineers.'
McGraw-Hill, London, UK.

Edwards I. , (1989).
'Introduction to Carbon science.'
Marsh H. Ed.
Butterworths, Sevenoaks, Kent, UK.

Emery A. F. and Kobayashi A. S. , (1980).
'Transient stress intensity factors for edge and corner cracks in quench test specimens.'
Journal of the American Ceramic Society, **63**, 410-415.

Eschenbacher M. , (1987).
'Acid polishing of crystal glass.'
Glass Technology, **28**, 168-172.

Eshelby J. D. , (1968).
'Fracture toughness. Stress analysis: theory of elasticity.'
The Iron and Steel Institute, London, UK.

Ewalds H. L. and Wanhill R. J. H. ,(1985).
'Fracture mechanics.'
Edward Arnold, London, UK.

Fitzer E. , Kiliani S. W. and Remmele W. , (1988).
'Impregnation of Carbon/Carbon composites with SiC.'
McEnaney B. and Mays T. J. Eds.
Proceedings of the 8^{th} International Conference on Carbon and Graphite, Newcastle Upon Tyne, UK.

Forrest R. A. and Marsh H. , (1977).
'Reflection interference colours in optical microscopy of Carbon.'
Carbon, **15**, 349.

Gilchrist J. D , (1980).
'Extraction Metallurgy 2^{nd} Edition.'
Pergamon Press, Oxford, UK.

Griffel. H. , (1987).
'Lightweighting and manufacturing techniques.'
Glass Technology, **28**, 121-123.

Griffith A. A. , (1920).
'The phenomena of rupture and flow in solids.'
Phil Transactions of the Royal Society of London series A, **221**, 163-198.

Griffith E. and Kaye G. W. C. , (1923).
'The measurement of thermal conductivity.'
Proceedings of the Royal Society A, 104, 71-98.

Hertz H. , (1895).
Gesammelte Werke, bf 1, 155, Leibzig.

Heuttner V. , Weiss R. and Scheifarth J. , (1988).
'Oxidation protection of 2-D carbon composites.'
McEnaney B. and Mays T. J. Eds.
Proceedings of the 8^{th} International Conference on Carbon and Graphite,
Newcastle Upon Tyne, UK.

Ingersol L. R. , (1924).
'Methods of measuring thermal conductivity in solids and liquids.'
Journal of the Optical Society of America, **9**, 495-501.

Inglis C. E. , (1913).
'Stresses in a plate due to the presence of cracks and sharp corners.'
Proceedings of the Institute of Naval Architects, **60**, 219-230.

Irwin G. R. , (1957).
'Analysis of stresses and strain near the end of a crack traversing a plate.'
Journal of Applied Mechanics, **79**, 361-364.

Jacobs I. , (1987).
Private communication.
Set Plastics, Brighton, UK.

Johnson J. , (1987, 1989).
Private communication.
Johnson Radley Limited, Pudsey, UK.

Korb L. M. , Morant C. A. , Colland R. M. and Thatcher C. S. , (1981).
'The shuttle orbiter thermal protection system.'
Ceramic Bulletin, **60**, 1188-1193.

Kroenke W. J. , (1966).
'Mechanical tests for anisotropy failure of aluminoborosilicate glass fibres under combined loadings of tension and torsion.'
Journal of American Ceramic Society, **49**, 508-513.

Lawn B. R. and Wilshaw T. R. , (1975).
'Fracture of brittle solids.'
Cambridge University Press, Cambridge, UK.

LeGood A., (1988, 1987).
Private communication.
Johnson Radley Limited, Pudsey, UK.

Marsh H. , (1989).
'Introduction to carbon science.'
Marsh H. Ed
Butterworths, Sevenoaks ,Kent, UK.

McDermott C. , (1987).
Private communication.
Johnson Radley Limited, Pudsey, UK.

McIvor S. D. , Darby M. I. , Wostenholm G. H. , Yates B. , Banfeild L. , King R. and Webb A. , (1990).
'Thermal conductivity measurements of some glass fibre-reinforced and carbon fibre-reinforced plastics.'
Journal of Material Science, **25**, 3127-3132.

McKee D. W. , (1972).
'Effects of adsorbed phosphorus oxychloride on the oxidation behaviour of graphite.'
Carbon, **10**, 491-497.

McKee D. W. , (1981).
'Chemistry and Physics of Carbon, Volume 1.'
Walker P. L. and Thrower P. A. Eds.
Marcel Dekker, New York, USA.

McKee D. W. , Spiro C. and Lamby E. , (1984).
'The effect of boron additives on the behaviour of Carbons.'
Carbon **22**, 507-511.

McKee D. W. , (1986).
'Borate treatment of Carbon fibres and Carbon/Carbon composites for improved oxidation resistance.'
Carbon **24**, 737-741.

McKee D. W. , (1987).
'Oxidation behaviour and protection of Carbon/Carbon composites.'
Carbon, **25**, 551-557.

Muncaster R. , (1981).
'A Level Physics.'
Stanley Thornes Ltd. , Cheltenham, UK.

Paris P. C. and Sih G. C. , (1965).
'Stress analysis of cracks.'
Fracture Toughness Testing and its Applications, ASTM, STP 381.

Parker A. G. S. , (1982).
'Cerberite 10 and 12 quality.'
United Glass Research, internal report Ref AP/RW.

Proctor B. A. , (1962),
'The effects of hydrofluoric acid etching on the strength of glass.'
Physics and Chemistry of Glasses, **3**, 7-27.

Russel B. , (1988, 1990).
Private communication.
Johnson Radley Limited, Pudsey, UK.

Seidel H. G. ,Williams H. P. and Heather R. P. , (1984).
'Contributions to glass container strength.'
Glass, March, 86-87.

Shugar G. C. ,Shugar R. A. ,Bauman L. and Bauman R. , (1981).
'Chemical Technicians ready reference handbook, second edition.'
McGraw-Hill, New York, USA .

Singer A. , (1989).
'Minerals in soil environments. Chapter 17. Second Edition.'
Dixon J. B. and Weed S. B. , Eds.
Oil Science Society of America, Madison, Winconsin, USA.

Southwick R. D. , (1985).
'A super-lightweight container is feasible.'
Glass Industry, June, 15-17.

Stephens R. C. , (1971).
'Strength of materials, theory and examples.'
Edward Arnold ltd. , London, UK.

Stewart D. R. and Spear B. W. , (1984).
'Developments in asbestos free hot glass handling materials.'
Glass, March, 90-92.

Strife J. R. and Sheeham J. E. , (1988).
'Ceramic coatings for Carbon/Carbon composites.'
Ceramic Bulletin, 67, 369-374.

TPRC Data Series, volume 1, (1970).
'Thermophysical properties of matter. Thermal conductivity, metallic elements and alloys.'
IFI/Plenum, New York, USA.

TPRC Data Series, volume 2, (1970).
'Thermophysical properties of matter. Thermal conductivity, non metallic solids.'
IFI/Plenum, New York, USA.

TPRC Data Series, volume 4, (1970).
'Thermophysical properties of matter. Specific heat capacity, metallic elements and alloys.'
IFI/Plenum, New York, USA.

TPRC Data Series, volume 5, (1970).
'Thermophysical properties of matter. Specific heat capacity, non metallic solids.'
IFI/Plenum, New York, USA.

Vickers T. , (1987, 1988, 1989, 1990).
Private communication.
Johnson Radley Limited. Pudsey, UK.

United Glass research group, (1979).
'Handling hot containers with a polyimide composite material.'
Glass Technology, **20**, 49-50.

Weibull W. , (1951).
'A statistical distribution function of wide applicability.'
Journal of Applied Mechanics, **19**, 293-297.

Williams H. P. , (1985).
'Handling the lightweights.'
Glass Technology, **26**, 248-251.

Zelazny L. W. and Colhoun F. G. , (19).
'Minerals in soil environments. Chapter 13. First Edition.'
Dixon J. B. and Weed S. B. , Eds.
Soil Science Society of America, Madison, Winconsin, USA.

Appendix A

GLOSSARY OF GLASS MAKING TERMS

Blow-and-blow process: The production method for glass containers, where the bottle is produced in two successive blow stages. In both stages the plastic glass is blown onto the mould by compressed air.

Check: A flaw or crack in a glass container which is big enough to cause the bottle to be rejected after production line inspection.

Cold-end: The part of the glass container production line between the exit of the tunnel annealing furnace and the end.

Dead plate: A plate on the production line onto which glass containers are placed after being lifted from the final mould.

Gob: The pre-weighed piece of molten glass which will be formed into the glass container.

Hot-end: The part of the glass container production line between where the bottle is removed from the final mould and the entrance to the tunnel annealing furnace.

Lehr: The tunnel furnace on a glass production line in which the residual stresses from moulding are annealed out.

Parison: The intermediate glass shape which is produced in a two stage process. The parison is formed in the first mould it is then transferred to the bottle mould for the final forming operation.

Press-and-blow Process: The production method for glass containers where the bottle is produced in two moulding stages. In the first stage the parison is formed by the action of a plunger being forced into a mass of plastic glass dropped into a parison mould. The parison is then blown into the shape of the finished container in a second mould by compressed air.

Sweep-out: An 'L' shaped arm which pushes a container from the dead plate onto a conveyer which takes the bottle to the entrance to the tunnel annealing furnace.

Take out tongs: A pair of arms, with inserts shaped to fit around the neck of the container under production, which close around the bottle neck and lift the formed bottle from the mould onto the dead plate.

Appendix B

KEY TO THE LABELS USED TO IDENTIFY MATERIALS IN THIS DOCUMENT

C1: Is a polyimide/graphite/Carbon fibre composite.

C10: Is a Carbon/Carbon composite.

C12: Is a Carbon/Carbon composite.

C22: Is a fine grained graphite.

C25: Is a fine grained graphite with a phosphate based oxidation protection system.

C30: Is a Carbon/Carbon composite with a phosphate based oxidation protection system.

D1: Is an Aluminium bronze.

D2: Is a fine grained carbon.

P1: Is a fine grained carbon with a phosphate based protection system.

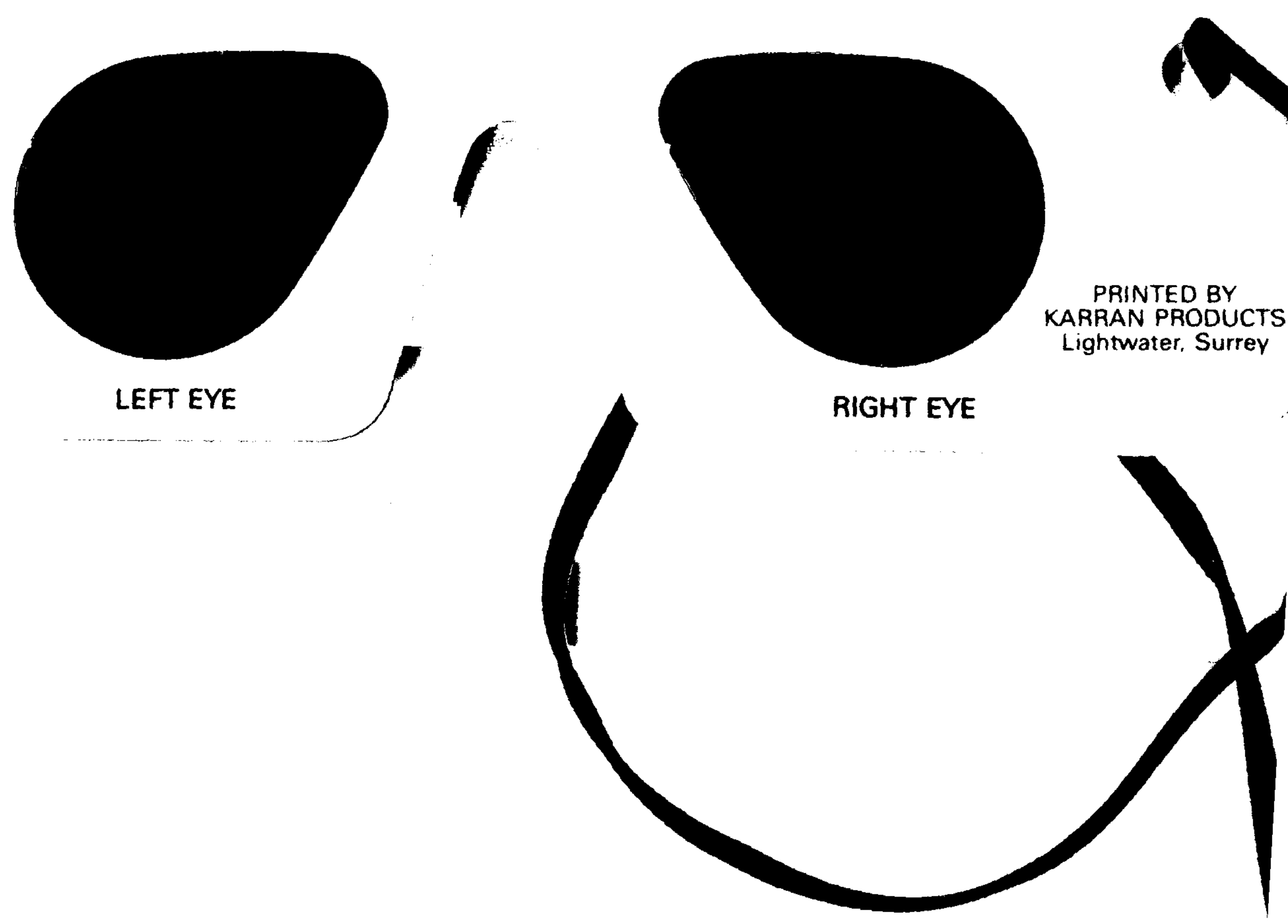
LEFT EYE
RIGHT EYE
PRINTED BY
KARRAN PRODUCTS
Lightwater, Surrey